Spring 5-9-2020

Insights into the Chlamydial Niche: The Dynamic Roles of Inclusion Membrane (Inc) Proteins in Chlamydia trachomatis Development

Macy G. Wood
University of Nebraska Medical Center

INSIGHTS INTO THE CHLAMYDIAL NICHE:

THE DYNAMIC ROLES OF INCLUSION MEMBRANE (INC)

PROTEINS IN CHLAMYDIA TRACHOMATIS DEVELOPMENT

by

Macy G. (Olson) Wood

A DISSERTATION

Presented to the Faculty of the
University of Nebraska Graduate College
in Partial Fulfillment of the Requirements
for the Degree of Doctor of Philosophy

Pathology and Microbiology

Under the Supervision of Professors, Elizabeth A. Rucks and Scot P. Ouellette

University of Nebraska Medical Center
Omaha, Nebraska

May, 2020

Supervisory Committee:

Elizabeth Rucks, Ph.D.	Scot Ouellette, Ph.D.
Paul Fey, Ph.D.	St. Patrick Reid, Ph.D.
Michael Chaussee, Ph.D.	Vinai Thomas, Ph.D.

ACKNOWLEDGMENTS

I am extremely thankful to all that have encouraged me and supported me throughout graduate school.

To my mentors, Lisa and Scot, I feel fortunate to have been able to learn from and work with both of you. You have taught me to question everything, to test a scientific question from all possible angles, to be a better writer, and instilling in me researching because “I want to know”. I appreciate your patience and the time that you have spent teaching me over the last five years. I’d also like to thank the rest of my committee, Dr. Fey, Dr. Thomas, Dr. Reid, and Dr. Chaussee, for providing feedback and advice. You all have supported me and helped me grow as a scientist and as an individual. I also appreciate Dr. Chaussee’s continued support as our lab moved from the University of South Dakota to the University of Nebraska Medical Center. I’d also like to thank Dr. Steve Callister for encouraging me to pursue my Ph.D.

To my lab-mates and colleagues who have essentially become part of my family, thank you for coming to my aid, commiserating with me, supporting me, and keeping me laughing. I have enjoyed scientific conversations, learning life lessons, exploring new places, and always being hungry for good food with you all. I am grateful for the lifelong friendships that have formed.

To my wonderful parents, I am the person I am today because of you and your sacrifices. Your continued love, support, and encouragement have allowed me to try new things and set big goals in life, and I will always be grateful for that. I’d also like to thank my brother, Tyler, for the encouragement and for always lending a listening ear.

Finally, to my husband Nick- you are an amazing partner, confidant, scientist, and role model. I will be forever grateful that you always believe in me, motivate me, make

sacrifices for me. Thank you for making me smile every day and for keeping me laughing. I'm so excited for our future together.

To my family, friends, colleagues, and faculty, you have truly made a lasting impact on my life.

ABSTRACT

INSIGHTS INTO THE CHLAMYDIAL NICHE: THE DYNAMIC ROLES

OF INCLUSION MEMBRANE (INC) PROTEINS IN

CHLAMYDIA TRACHOMATIS DEVELOPMENT

Macy G. (Olson) Wood, Ph.D.

University of Nebraska, 2020

Supervisors: Elizabeth A. Rucks, Ph.D. and Scot P. Ouellette, Ph.D.

Chlamydia trachomatis (Ctr) is the leading cause of bacterial sexually transmitted infections. Ctr, an obligate intracellular bacterium, develops within a membrane-bound vacuole called an inclusion. The inclusion membrane is modified by chlamydial inclusion membrane (Inc) proteins, the functions of which are poorly characterized. Bacterial two-hybrid analyses found some Incs (e.g., IncF) interacted with numerous Incs while others (e.g., IncA) did not. We hypothesize that some Incs organize the inclusion through Inc-Inc interactions whereas other Incs promote chlamydial-host interactions by binding eukaryotic proteins. To test our hypothesis, we implemented the ascorbate peroxidase proximity labeling system (APEX2), which labels proximal proteins with biotin *in vivo*. We transformed Ctr with inducible expression constructs containing *incF-APEX2*, *incA*$_{TM(\text{transmembrane domain})}$*-APEX2*, *incA-APEX2*, and *APEX2* alone. Affinity purification-mass spectrometry (AP-MS) of biotinylated proteins from chlamydial infected monolayers, followed by Significance Analysis of INTeractome (SAINT), was used to identify significant proteins that are proximal to the Inc-APEX2 constructs from five biological replicates. Consistent with our hypothesis, IncF-APEX2 biotinylated more chlamydial Inc proteins, whereas IncA-APEX2 biotinylated more unique eukaryotic proteins. We validated a SAINT significant eukaryotic protein, LRRF1, at the inclusion membrane by immunofluorescence

and determined that the Inc CT226 interacts with LRRF1. Next, we compared our datasets with other AP-MS inclusion studies, finding only seven proteins that were similarly identified, likely a reflection of the different experimental approaches. Importantly, for the first time, we were able to directly compare two Inc-APEX2 studies, which also revealed fewer similarly identified proteins than expected. This led us to hypothesize that the overexpression of certain Incs may alter the organization of the inclusion membrane. Previously, we described defects in inclusion expansion and the production of progeny when IncF-APEX2 was expressed at high levels from transformed Ctr. To further investigate the role of Incs in chlamydial development, we transformed Ctr with inducible expression plasmids containing *FLAG*-tagged *incF*, *ct813*, and *ct226*. The expression of IncF and CT813, but not CT226, altered inclusion development, as observed by smaller inclusions and decreased IncE intensity in the inclusion membrane. These data suggest that coordinated Inc expression and insertion into the inclusion membrane is essential for optimal inclusion development.

TABLE OF CONTENTS

LIST OF FIGURES

LIST OF TABLES

LIST OF SUPPLEMENTARY FIGURES

LIST OF SUPPLEMENTARY TABLES

LIST OF ABBREVIATIONS

aTc	anhydrotetracycline
AP	affinity purification
BACTH	bacterial adenylate cyclase two-hybrid system
C_6-NBD-Cer	N- [7- (4-Nitrobenzo-2-oxa-1,3-diazole)] I aminocaproylsphingosine
DMEM	Dulbecco's modified Eagle medium
DMSO	dimethyl sulfoxide
FBS	fetal bovine serum
hpi	Hours post-infection
H_20_2	hydrogen peroxide
IP	immunoprecipitation
LGV	lymphogranuloma venereum
MS	mass spectrometry
MTOC	microtubule organizing center
STI	sexually transmitted infections
SAINT	Significance Analysis of INTeractome
Y2H	yeast two-hybrid assay

Chapter 1 - Introduction to *Chlamydia*

Chlamydia trachomatis is the leading cause of preventable infectious blindness and bacterial sexually transmitted infections (STI) in the world (1-3). There are an estimated 100-150 million new cases annually worldwide (2, 3). In 2017, 1.7 million cases were reported in the United States, with the highest rate of infection in people ages 15 to 29 (3, 4). The number of reported *C. trachomatis* infections have been steadily increasing since extensive STI surveillance began, with a 22% increase in reported cases since 2013 (3). At this time, there is no effective human vaccine to prevent *C. trachomatis* infections (2, 4). Chlamydial infections in men can cause urethritis, epididymitis, and prostatitis (5). In women, undiagnosed infections can lead to pelvic inflammatory disease, ectopic pregnancy, and infertility (5, 6). In men, about 50% of infections are asymptomatic, and infections in women are estimated to be 70-75%, making the actual number of infected individuals, and the disease burden, much higher than currently reported (1, 3, 5, 7).

Chlamydiaceae

The family *Chlamydiaceae* (order Chlamydiales, class Chlamydiae, phylum Chlamydiae) are Gram-negative, developmentally regulated, obligate intracellular bacteria that reside within a membrane-bound vacuole throughout infection of a host cell (8, 9). *Chlamydiaceae* cause disease in most mammals in a species-dependent manner (10, 11). *Chlamydia caviae* infection results in conjunctivitis and genital tract infections in guinea pigs, and *C. muridarum* causes genital tract infections in mice. Infection of *C. psittaci* can cause respiratory infections in birds, *C. abortus* infects the placenta of sheep and goats, leading to abortions, and *C. pecorum* causes conjunctivitis in cattle, swine, goats, sheep, and koalas (10, 11).

The species of *Chlamydia* that primarily cause disease in humans include *Chlamydia psittaci, C. pneumoniae,* and *C. trachomatis. C. psittaci* is a zoonotic disease spread by parrots and other exotic birds, and the human disease is referred to as psittacosis or parrot fever, (12, 13). Humans infected with *C. psittaci* have atypical pneumonia (12). *C. pneumoniae* causes community-acquired pneumonia, which is likely underdiagnosed as 50-87% of the population, depending on the region, are seropositive for a past *C. pneumoniae* infection (14-17). Three human *C. trachomatis* biovars that comprise 15-19 serovars have been classified based on tissue tropism (4). The trachoma biovar includes serovars A, B, Ba, and C, which primarily cause ocular infections (18). The *C. trachomatis* serovars D, E, F, G, Ia, J, and K are classified within the STI biovar, with a propensity to infect urogenital tissue (19). Finally, the lymphogranuloma venereum (LGV) biovar includes serovars L1, L2, L2b, and L3, which spread to the lymph nodes after sexual transmission resulting in disseminated infection (4, 19). Retrospective studies have not found an association between reported symptomatic and asymptomatic infections with specific *C. trachomatis* serovars (20). Asymptomatic infections likely occur due to the obligate intracellular nature of this pathogen and the manipulation of host cell responses by chlamydial secreted effectors (1, 20).

An Overview of the Developmental Cycle

The *C. trachomatis* genome consists of a 1.04 Mbp chromosome that encodes 894 open reading frames in addition to a 7.5 kbp chlamydial plasmid that encodes eight open reading frames (21). Chlamydiae undergo a biphasic developmental cycle that consists of two morphologically distinct developmental forms. The elementary body, or EB, is the smaller (0.3 µm), with a highly cross-linked outer membrane, and is the infectious developmental form with limited metabolic activity (22, 23). The reticulate body, or RB, is the larger (1 µm), replicative developmental form with a decondensed chromosome and

increased metabolic activity (22). Infection of a host cell begins with attachment of the EB to the host cell in a two-part process: a reversible, electrostatic binding step to heparin-sulfate residues, followed by an irreversible binding step to a currently unknown host cell receptor (24, 25). Evidence that chlamydial proteins initiate entry of the EB into the host cell comes from early studies demonstrating that UV inactivated EBs failed to enter eukaryotic cells (26). Chlamydial effector proteins, including translocated actin recruitment protein (Tarp), are injected into the host cell to initiate rearrangement of the host cytoskeleton to facilitate uptake (27-29).

After host cell entry, the EB resides within a membrane-bound vacuole, and the chlamydiae remain within this vacuole throughout the entirety of the developmental cycle. Early after infection, the inclusion is diverted from the endosomal-lysosomal pathway (30-34) and trafficked to the microtubule organizing center (MTOC), positioning the inclusion near the eukaryotic nucleus and the Golgi apparatus (35). The EB differentiates to an RB approximately 3 hours post-infection (hpi). Following this primary differentiation event at around 8 hpi (depending on the species and strain), the RB begins to divide by a polarized cell division mechanism similar to yeast-like budding (36, 37), giving rise to a large population of RBs. At approximately 18-24 hpi, the RBs begin asynchronous secondary differentiation, in which RBs condense into EBs. At about 48 hpi for *C. trachomatis* serovar L2, the inclusion either lyses to release EBs into the extracellular milieu, or the entire intact inclusion is released from the cell by a process termed extrusion (38, 39).

The C. trachomatis *Inclusion*

The inclusion, derived from eukaryotic membranes, acts as the host-pathogen interface, physically “walling” chlamydiae off from the host cell. Inclusions harboring *Chlamydia* were observed in early electron microscopy studies of inclusions that were purified from host cells (40). Only molecules less than 530 Daltons are freely permeable

to the inclusion (41), meaning most molecules require active transport to cross the membrane. The chlamydial inclusion remains at a near-neutral pH (42), never acquiring the endosomal-lysosomal markers, lysosome-associated membrane protein-1 (LAMP-1), LAMP-2, or Cathepsin D (31, 32) (30, 31). Chlamydial effector proteins that are either inserted into the inclusion, called inclusion (Inc) membrane proteins, or effectors that are secreted into the host cell contribute to the establishment and maintenance of the inclusion (43-45). Active chlamydial protein synthesis is required to evade fusion of the inclusion with the lysosome and for the acquisition of eukaryotic lipids that are important for chlamydial growth and development (30-32).

Lipid acquisition by C. trachomatis *L2*

During the developmental cycle, eukaryotic lipids (e.g., sphingomyelin and cholesterol) acquired from the host cell are trafficked to the inclusion and incorporated both into the inclusion and into the bacteria (30, 46-48). Sphingomyelin acquisition was observed using fluorescent probes such as N-[7-(4-Nitrobenzo-2-oxa-1,3-diazole)] I aminocaproylsphingosine (C_6-NBD-Cer) labeling (30). NBD-C_6-ceramide is metabolized into sphingomyelin and glucosylceramide, and, in the presence of labeled ceramide, fluorescent NBD-C_6-sphingomyelin is observed in the inclusion membrane and chlamydiae (46, 48). The addition of brefeldin A, a fungal metabolite that inhibits Golgi formation, inhibited fluorescent sphingomyelin incorporation into chlamydiae or the inclusion membrane (49). Cholesterol is also incorporated into the inclusion membrane and chlamydiae during infection of a host cell, which can be observed using fluorescent probes and thin-layer chromatography (50-52).

The trafficking or recruitment of these lipids is dependent on chlamydial protein synthesis because the treatment of *C. trachomatis*-infected cell monolayers with chloramphenicol prevents the acquisition of sphingomyelin and cholesterol (50). One

chlamydial inclusion (Inc) membrane protein is directly involved in the recruitment of eukaryotic lipids to the inclusion via recruitment of ceramide transfer protein, CERT (53, 54). Lipids are also trafficked to the inclusion, at least in part, via the recruitment of multivesicular bodies (MVBs) (55, 56). Studies that inhibited MVBs resulted in decreased sphingolipid and cholesterol incorporation and reduced infectious progeny (55, 56). Given the normal trafficking of sphingomyelin to the inclusion during development, sphingomyelin acquisition is often used as a metric for normal development in studies that manipulate chlamydial proteins (57).

Chlamydial Secretion Systems and Substrates

Modification of the inclusion with chlamydial proteins is important for chlamydial development, whereby chloramphenicol treatment early after infection of a host cell halts chlamydial development (58). The halt is due, in part, to the inhibition of a large subset of secreted chlamydial proteins that modify the inclusion and the host cellular environment (58, 59). Chlamydiae encode genes for type II secretion (Sec-dependent) systems, type III secretion systems (T3SS), and type V secretion systems (T5SS) (27, 60-66). The T2SS is a Sec-dependent secretion system, and the T3SS is the non-flagellar, needle-like apparatus. The T5SS is an auto-transporter of polymorphic membrane proteins that are secreted via the Sec-dependent mechanism to the bacterial membrane (66). The chlamydial T3SS and T3SS substrates have been studied more extensively than the T2SS and T5SS in *Chlamydia*.

One well-characterized T2SS substrate is the *Chlamydia* protease/proteasome-like activity factor (CPAF) (60, 67, 68). Secreted into the host cytosol via the T2SS, CPAF has been implicated in the degradation of chlamydial proteins (69), host proteins to evade apoptosis (70), and actin filaments to allow for inclusion expansion during infection (71). CPAF is not inhibited by typical protease inhibitors (72); as such, some CPAF activities

are unclear because the experimental results were confounded by residual CPAF activity after cell lysis, resulting in increased proteolysis of both host and chlamydial proteins (73). Other known Sec-dependent proteases include tail-specific protease (Tsp), chlamydial high-temperature requirement protein A (cHtrA substrate), and CT311, but the precise functions of these proteases are unknown (74, 75).

The C. trachomatis *Type III Secretion System*

In contrast to the small number of characterized T2SS effector proteins, there are 60-80 predicted type III Secretion System (T3SS) effector proteins (76). Highlighting the importance of the T3SS in chlamydial development and survival, the *C. trachomatis* T3SS is required for infection of a host cell (27, 28, 77, 78), inclusion development, immune evasion, and intracellular survival (63). Early electron microscopy studies described small projections that resembled a syringe on EBs and RBs harvested from infected cells (40, 79, 80). The first evidence of a type III secretion system (T3SS) was by Hsia et al. using sequence analysis of a genomic DNA fragment isolated from *C. caviae* (formerly GPIC, *C. psittaci*) (81). The presence of T3SS genes was confirmed upon the sequencing of the *C. trachomatis* serovar D genome (21, 64). T3SS genes are typically clustered on a pathogenicity island with a lower GC content compared to the rest of the genome; however, the chlamydial genome has a low GC content (~40%), which makes it challenging to identify pathogenicity islands (21, 82). Further, chlamydial genes homologous to other bacterial T3SS genes are located dispersed throughout the chlamydial genome in small clusters, rather than on a single pathogenicity island (64, 83, 84). Chlamydiae encode genes for the injectisome (i.e., the needle complex and basal body), the translocon (i.e., the distal membrane proteins that form the pore in the opposing membrane), and the chaperones that are required to maintain an unfolded protein form for the secretion of bacterial effector proteins (83, 85). A preformed functional type III

secretion apparatus on EBs was predicted because Inc proteins that modify the inclusion membrane were transcribed as early as three hours post-infection (hpi), but transcription of T3SS genes was not detected until 12 hpi (58). Additional experiments identified the core T3S apparatus protein, CdsJ, in lysates from both purified EBs and RBs supporting a model where EBs are preloaded with the T3SS for the secretion of early effectors, and RBs produce new T3SS to secrete additional effector proteins (58).

Fields et al. also provided evidence that the chlamydial T3SS secretes Inc proteins, but little was known about the specific secretion mechanism (58, 86-88). The secretion via a chlamydial T3SS had been previously proposed due to the location of Incs in the inclusion membrane (89). To test the possibility of Incs to be type III secreted, the well-characterized *Shigella* and *Yersinia* T3SS were used as surrogate secretion systems. Indeed, IncA and IncC were secreted by the T3SS of *Shigella* (89, 90) and *Yersinia*, respectively (58). Also, *C. trachomatis*-infected cells treated with chloramphenicol resulted in no detectable IncC, which supports the *de novo* synthesis of Incs (58). Incs are only one class of chlamydial T3SS effectors that have been described (76, 91-93). Other non-Inc T3SS effectors have also been observed at the inclusion membrane (94), in the host cell cytosol (e.g., Tarp (28)), plasma membrane (95, 96), nucleus (97), or the Golgi (98). The numerous subcellular locations in which chlamydial effectors have been found suggest that chlamydiae orchestrate the manipulation of multiple host processes to create this specialized niche, the pathogen-specified organelle (59). Moreover, the chlamydial T3SS is essential for growth and development because a T3SS inhibitor significantly reduced the formation of EBs from RBs and also prevented the secretion of Incs (99).

Inclusion Membrane (Inc) Proteins

Chlamydial inclusion membrane proteins (Incs) are a large class of T3SS effectors that stud the inclusion membrane (59, 89, 100). Incs are characterized by the presence of

two or more bi-lobed hydrophobic transmembrane domains that are approximately 40-50 amino acids in length (44, 87, 93). Hydrophobicity plot analyses of the *C. trachomatis* L2 ORFs revealed at least 45 candidate *inc* genes, which make up approximately 7% of the highly reduced chlamydial genome, indicating that these genes are important for chlamydial development (21, 88). To date, there are over 50 putative Incs, which are expressed at different times during the developmental cycle and have been characterized as immediate-early, early, and mid-developmental cycle effectors (101-106). The temporal expression pattern of *inc* genes throughout the developmental cycle likely a reflection of the dynamic needs of *Chlamydia*. Interestingly, not only is there limited conservation of *inc* genes within various *Chlamydia* species, but there is also little homology with other bacterial or eukaryotic genes (83, 104), which makes it difficult to speculate on their role in chlamydial development.

Incs were first described in a series of experiments using serum from guinea pigs that had recovered from guinea pig inclusion conjunctivitis, GPIC (i.e., *C. caviae*). By western blot, proteins were identified from GPIC infected HeLa cell lysates that were not observed in the lysates from purified EBs. To further examine the unknown proteins from the western blot, the guinea pig serum was adsorbed using EBs and then used for immunofluorescence assays. This led to the identification of chlamydial proteins that localize to the inclusion membrane during infection (107). Subsequent studies using a bacteriophage library harboring GPIC cDNA identified clones that were reactive with the guinea pig serum but not with inactivated EBs (i.e., formalin-fixed) (43). Expression of those putative ORFs from *E. coli* also reacted with convalescent sera but not EBs (43). Anti-sera generated against the ORF, termed *incA* (inclusion membrane protein A), confirmed the localization of IncA in the inclusion membrane (43, 108). IncA was predicted to encode two large hydrophobic regions, a unique characteristic that led to the detection

of 50 putative *C. trachomatis inc* genes that encode these domains (101, 104). Additional experiments evaluating GPIC infected HeLa cell lysates identified changes in IncA expression over time (43) and that the host cell could phosphorylate IncA during infection (108). IncA also contains a eukaryotic SNARE-like domain, which is important for the fusion of two or more inclusions within the same host cell (92, 109-113). These early experiments set the stage for the identification of additional Incs that modified the inclusion membrane and began speculation that Incs are involved in mediating various interactions with the host cell.

Further characterization of Incs identified an T3S signal in the N-terminus, although the exact signal peptide sequence remains unknown (91). In support, truncating the first 30 amino acids of IncD prevented the secretion and localization of IncD to the inclusion membrane (91). Both the N- and C-termini of Incs are presumed to be exposed to the host cytosolic face of the inclusion (43, 59, 92, 108), which is supported by experiments that used genetic tags, adenylate cyclase (CyaA) and glycogen synthase kinase (GSK), as well as microinjection of anti-Inc antibodies (91). Incs have been observed to localize in either microdomains (i.e., puncta) or a uniform, ring-like pattern around the inclusion membrane (44, 114). For example, IncF, IncA, CT226, and CT813, have been shown to uniformly surround the inclusion while CT101, IncB, CT222, CT223, and CT850 are observed in microdomains in the inclusion membrane (44, 87, 114). The Incs found in microdomains are associated with localized increased cholesterol concentration and have been shown to co-localize with Src-kinases, which are hypothesized to play a role in the modification of host cell signaling during infection (114). Furthermore, Incs vary in length of the cytosolic C-terminus, which is predicted to contribute to the function of Incs in the inclusion membrane (57, 59, 115). For example, some Incs have short C-terminal cytosolic termini (i.e.,14 amino acids) such as IncF, while other Incs have large cytosolic C-termini,

such as IncA (i.e., 191 amino acids) (87). Both the localization of Incs in the inclusion membrane as well as the length of the C-termini are likely important to the function of Incs, but the functions of only a few Incs are well characterized to date.

Genetic tools to examine C. trachomatis *serovar L2 Inc protein-protein interactions*

Although Incs are presumed to be vital for chlamydial development due to the large percent of *inc* genes and the localization of Incs at the host-pathogen interface, the specific roles for most Incs in the inclusion membrane remain unknown. Progress has been impeded partially due to the inability to genetically modify *Chlamydia* (116). Recent advances in the *C. trachomatis* L2 genetic toolbox have now expanded studies of Incs via the use of overexpression models (91, 93) and knockouts via TargeTron (i.e., targeted intron insertion) mutants (109, 117). More recently, allelic exchange has been described for *C. trachomatis* serovar L2 which enables a clean deletion of chlamydial genes (118-120), and conditional CRISPRi mediated knockdown allows the study of essential genes (121). These tools add flexibility and control in experimental design to examine the role of Incs on a molecular level.

Another major hurdle is related to the inherent hydrophobic makeup of Inc proteins, which makes them difficult to purify from the inclusion membrane using traditional purification methods. Affinity purification experiments to identify protein binding partners are often used as an initial strategy to understand the role of unknown proteins since they may fit into known cellular pathways. However, the large hydrophobic transmembrane domain regions of Incs makes them refractory to purification using these methods because the harsh lysis conditions required to solubilize Incs do not preserve protein-protein interactions. A strategy that has been employed to circumvent purifying full-length Incs

has been to use only the cytosolic C-terminal regions as bait to identify eukaryotic binding partners of Inc proteins. This is done either by ectopically expressing truncated Incs in eukaryotic cells followed by affinity purification methods (122), or screening for interactions using a yeast-two hybrid (Y2H) assay (123). These methods have identified a few Inc-eukaryotic protein interactions yielding information about chlamydial manipulation of host pathways. Still, these methods may not be sufficient to identify transient or weak interactions that are occurring at the inclusion membrane.

C. trachomatis *serovar L2 manipulation of host cell pathways*

C. trachomatis appears to be a master manipulator of major cellular pathways, siphoning amino acids from the lysosome (124), recruiting vesicles (i.e., MVBs) (56) and specific proteins to acquire essential lipids (54, 125, 126), and dampening the host response to infection (127). Inc proteins, anchored in the inclusion membrane and have N- and C-termini in the host cytosol, are hypothesized to mediate interactions with the host that are necessary for survival. To date, a few eukaryotic proteins are known to be recruited to the inclusion membrane via their interaction with Incs. However, the difficulties in purifying inclusion membrane proteins and the lack of genetic tools have hindered the identification of specific Inc-protein interactions. To this end, there are numerous reports of eukaryotic proteins that are recruited to, or co-localize with the inclusion, but do not have an identified Inc protein-binding partner (Table 1-1). Previously published Inc-eukaryotic protein-protein interactions are broadly involved in the re-organization of the host cytoskeleton and the manipulation of host signaling and vesicular trafficking (Table 1-2). The Inc-eukaryotic protein interactions that have been defined and their contribution to chlamydial development is described in the following sections.

Table 1-1. Eukaryotic proteins associated with the inclusion membrane

Eukaryotic Protein	Reference
Ci-MPR	Aeberhard et al. 2015
Fis1	Aeberhard et al. 2015
HSPB1	Aeberhard et al. 2015
ILK	Aeberhard et al. 2015
ORCL1	Moorehead et al 2010
OSBP	Moorehead et al 2010
PI4PkII α	Moorehead et al 2010
PKM2	Aeberhard et al. 2015
Rab1	Rzomp et al. 2003
Rab6	Lipinski et al. 2009
Rab8	Faris et al. 2019
Rab10	Faris et al. 2019
Rab11	Rzomp et al. 2003; Lipinski et al. 2009; Leiva 2013; Ouellette et al. 2010
Rab14	Capmany et al. 2011
Rab32	Faris et al. 2019
Rab34	Faris et al. 2019
Rab35	Faris et al. 2019
Rab39	Garbarte-Tuleda et al. 2015
Rac1	Aeberhard et al. 2015
Sec22b	Aeberhard et al. 2015
SNX1	Aeberhard et al. 2015
SNX2	Aeberhard et al. 2015
Src/Fyn family	Mital et al. 2010
STIM1	Agaisse et al. 2015; Nguyen, Lutter et al 2018; Aeberhard et al.
STIM2	Aeberhard et al. 2015
STX4	Aeberhard et al. 2015
STX6	Moore et al 2011; Kabeisman 2013
STX10	Lucas et al. 2015
SYNGR2	Aeberhard et al. 2015
TFR	Aeberhard et al. 2015

UBXN6	Aeberhard et al. 2015
VAMP3	Delevoye et al. 2008
VAMP4	Kabeisman et al. 2013; Delevoye et al. 2008
VAMP7	Delevoye et al. 2008
VAMP8	Delevoye et al. 2008
VCP	Aeberhard et al. 2015
VPS35	Aeberhard et al. 2015

Table 1-2. Eukaryotic proteins recruited to the inclusion by *C. trachomatis* Inc proteins

Inc[a]	Inc effector class	Eukaryotic binding partner(s)	Experimental method	Role of Inc-Eukaryotic process/pathway
CT005	mid	VAPA, VAPB	ectopic expression	tether inclusion via MCS to ER
CT101	mid	ITPR3	Y2H	regulate Ca2+ levels and inclusion extrusion
IncD (CT115)	early	CERT	RNAi	transport ceramide to inclusion
IncE (CT116)	early	SNX5, SNX6	ectopic expression	interfere with retromer trafficking
IncG (CT118)	early	14-3-3 β	Y2H	prevent apoptosis
CT223	mid	CEP170	AP-MS	cytoskeleton rearrangement
CT228	early	MYPT1	Y2H	inclusion extrusion from host
CT229	early	Rab4	Y2H	intercept receptor recycling of EE; inhibit STING response
CT288	early	CCDC146	Y2H	cytoskeleton rearrangement
CT813	mid	Arf1, Arf4	EMS/ectopic expression	PTM microtubules; reposition Golgi around inclusion
CT850	early	DYNLT1	Y2H/ectopic expression	traffic inclusion to the MTOC

[a] serovar D naming convention used

C. trachomatis *manipulation of the host cytoskeleton*

The eukaryotic cytoskeleton is manipulated throughout the developmental cycle, which has implications on vesicular trafficking and nutrient acquisition for chlamydiae (128, 129). The chlamydial inclusion is surrounded by a “cage” consisting of actin filaments and microtubules (35, 71, 130-132). The rearrangement of the cytoskeleton is initiated by a multitude of T3SS effectors, including Tarp and TepP which re-organize actin to induce uptake of the EB into the host cell (27, 28, 61, 77, 78). Inc proteins interact with dynein light chain 1, to control inclusion trafficking along the cytoskeleton (123), bind centrosomal proteins to direct inclusion localization (133, 134), and bind Arf1 and Arf4 GTPases to control microtubule stability to facilitate nutrient acquisition (128).

CT850 and dynein light chain 1 (DYNLT1)

The chlamydial inclusion is trafficked to the microtubule organizing center (MTOC) early after infection of a host cell (35) in a dynein-dependent manner (131). The overexpression of p50 dynamitin (dynein motor complex) interfered with vesicular trafficking toward the MTOC in uninfected cells but did not impact the trafficking of the *C. trachomatis* L2 inclusion, suggesting that a chlamydial protein might replace p50 dynamitin (35). Y2H assays using the C-terminus of CT850 determined that migration is mediated by the interaction of CT850 with dynein light chain 1 (DYNLT1) (123). CT850 is found in microdomains in the inclusion and co-localizes with the centrosome during infection (114). Overexpression studies determined that CT850 hijacks the dynein motor complex by replacing the function of p50 dynamitin, a protein that links cargo to the dynein motor complex. Further analyses of CT850 identified a KKARR motif within the C-terminus, which is known to bind DYNLT1 and direct cargo to the MTOC. This interaction was also shown by co-immunoprecipitation (Co-IP) from the lysates of uninfected HeLa cells transfected with mCherry-CT850 and GFP-DYNLT1 (123). Although this interaction was

required for the inclusion reach the MTOC, knockdown of DYNLT1 did not affect the production of infectious progeny (123).

CT288 and Coiled-Coil Domain Containing protein 146 (CCDC146)

Another Inc protein, CT288 has been shown to bind a centrosomal protein, CCDC146, located near the MTOC. A Y2H assay using a HeLa cDNA library and truncated CT288 that lacked both the N-terminus and hydrophobic domains yielded a positive interaction with CCDC146 (133). The function of CCDC146 isn't known, but one study reported that CCDC146 co-sedimented with the microtubule fraction and observed CCDC146 co-localization with γ-tubulin (i.e., centrosome marker) (135) suggesting it may play a role in microtubule organization. CT288 and CCDC146 co-immunoprecipitated using lysates from cells that had been transfected with the C-terminus of CCDC146-EGFP and infected with *C. trachomatis* L2 transformed with a plasmid expressing CT288-2HA. In uninfected HeLa cells, transfected EGFP-CCDC146 co-localized with the centrosome. When HeLa cells were infected with wild-type *C. trachomatis* L2 or the *C. trachomatis* L2 CT288-HA strain, transfected EGFP-CCDC146 was re-directed as a ring around the inclusion. CCDC146 was still observed around the inclusion after infecting HeLa cells with *C. trachomatis* L2 *CT288::aadA* (TargeTron mutant of CT288)(133). As the function of CCDC146 is not well defined in eukaryotic cells, this interaction with an Inc during *C. trachomatis* L2 infection remains unclear.

CT813 (InaC) and ADP-ribosylation factors (Arf) Arf1 and Arf4

In addition to hijacking dynein machinery to traffic along microtubules to the MTOC, chlamydial Incs also mediate post-translational modifications of microtubules to increase microtubule stability and to re-position the Golgi around the inclusion (128, 129). A chemical mutagenesis screen identified an interaction between CT813 (also referred to as InaC) and ADP-ribosylation factor 1 (Arf1) (130). These data were expanded to include

both Arf1 and Arf4, which co-immunoprecipitated with CT813-FLAG in co-transfected cells and eukaryotic cells infected with *C. trachomatis* L2 transformed with a plasmid expressing CT813-FLAG (128). Transfected Arf1-HA and Arf4-HA co-localize with wild-type *C. trachomatis* L2 inclusions in HeLa cells, and recruitment is inhibited in *C. trachomatis* L2 CT813::*bla* mutants that lack CT813 (128). The interaction between CT813 and GTP-Arf1 and Arf4 increases de-tyrosinated and acetylated tubulin to stabilize microtubules around the inclusion, which re-positions the Golgi around the inclusion (128, 129). Fragmentation of the Golgi during *C. trachomatis* infection is important for nutrient acquisition (136).

CT223 (IPAM) and Centrosomal Protein 170 (CEP170)

Another chlamydial Inc, CT223 (also referred to as Inclusion Protein Acting on MTs, IPAM), plays a role in the re-arrangement of the cytoskeleton. Similar to CT850 and CT288, CT223 is also observed in microdomains around the inclusion membrane and is often observed near the centrosome (134). CT223 was examined for its role in chlamydial development based on a BLAST search that indicated sequence similarity with centrosome-associated proteins (134). Using recombinant CT223 incubated with eukaryotic cell lysates followed by affinity purification-mass spectrometry, centrosomal protein 170 (CEP170) was identified as a putative binding partner. CEP170 had been previously shown to bind microtubules. siRNA experiments were performed to investigate the role of CEP170 during *C. trachomatis* infection, and, interestingly, in uninfected cells, there was no detectable effect on microtubules, but in *C. trachomatis* L2 infected cells a host cell rounding phenotype was observed (134). These data suggest that the interaction between CT223 and CEP170 may re-organize the microtubule cage around the inclusion to maintain host cell shape during infection (134).

While the role of some Inc-eukaryotic protein-protein interactions with the host cytoskeleton are more defined than others, the positioning of the inclusion near the MTOC

is hypothesized to benefit *Chlamydia* because of the localization proximal to the endoplasmic reticulum and Golgi apparatus which may aid in the acquisition of nutrients. In addition, other Inc proteins have been shown to interact with proteins that reside in the ER or Golgi that aid in lipid acquisition (53, 54, 137). Furthermore, stabilization of the cytoskeleton is important for manipulating vesicular trafficking events (138).

C. trachomatis *manipulation of eukaryotic signaling pathways*

To promote intracellular survival, bacteria manipulate major host cell signaling pathways (139). *C. trachomatis* does this through interactions with protein kinases (114), phosphatases (38, 117), calcium channel regulators (140), and via sequestration of proteins to prevent apoptosis. More specifically, signaling events are associated with non-receptor tyrosine kinases (i.e., Src kinases, Src and Fyn) that have been observed at the inclusion membrane (114). Of note, non-phosphorylated Src-kinases are uniformly distributed around the inclusion, whereby phosphorylated Src and Fyn (Tyr419) are associated with at least four Inc proteins (IncB, CT101, CT222, and CT850) found in microdomains (114). It is not known if Src kinases are recruited by Inc proteins, but their localization at the inclusion likely plays an important role during chlamydial infection since eukaryotic proteins that are known to be recruited by Incs are phosphorylated in regions that co-localize with these Src-kinases (38).

CT228 and Myosin Phosphatase Subunit Target 1 (MYPT1)

Myosin phosphatase subunit target 1 (MYPT1) is recruited to the inclusion by CT228, an Inc that localizes uniformly around the inclusion. The inactive form of MYPT1 (phosphorylated at threonine 853 and 696;) is found in microdomains associated with Src-kinases. The cytosolic C-terminus of CT228 was found to interact with (MYPT1) by Y2H assay (38). This was validated by Co-IP of endogenous MYPT1 with anti-CT228

antibodies from *C. trachomatis* L2 infected HeLa cell lysates (38). MYPT1, among other myosin kinase pathway proteins, myosin IIA, myosin IIB, myosin light-chain kinase (MLCK) and myosin regulatory light polypeptide 9 (MLC2), were also found co-localize with the inclusion throughout the developmental cycle. The current model proposed for CT228 and MYPT1 interaction is to maintain a balance between extrusion from the host cells and host cell lysis. In this model phospho-MYPT1 prevents MYPT1 phosphatase activity on its substrates, myosin II and MLCK, which allow for their activation to signal inclusion extrusion from the host cell late in the developmental cycle (~ 42 hpi)(38). siRNA knockdown of myosin kinase pathway genes moderately reduced the number of extrusions detected (38). Importantly, knockdown of the myosin kinase pathway genes did not impact the number of infectious progeny produced (38), suggesting that the role of CT228 and MYPT1 interaction does not impact chlamydial development or nutrient acquisition.

After the initial studies of CT228 and MYPT1, a targeted intron insertional inactivation system (TargeTron) was developed in *C. trachomatis* L2 (109). Using this system, the group II intron was re-targeted to the C-terminus of CT228 (117). The L2 CT228::*aadA* (Spectinomycin^r) mutant had no defects in the production of infectious progeny but there was a significant increase in the number of extrusions (117). By immunofluorescence assay, MYPT1 was no longer recruited to the inclusions of *C. trachomatis* L2 CT228::*aadA* mutants. However, other myosin kinase pathway machinery, including myosin IIa/b, MLCK, and MCL2 remained associated with the inclusion (117), which may suggest that other Incs recruit the other myosin kinase pathway proteins. CT228 appears to function to suppress extrusion events early after infection to stabilize the intracellular niche until late in the developmental cycle.

CT101 (MrcA) and type 3 inositol-1,4,5-trisphosphate receptor (ITPR3)

CT101 (also referred to as myosin regulatory complex subunit A, MrcA), (114), interacts with the type 3 inositol-1,4,5-trisphosphate receptor (ITPR3) calcium channel releases calcium when cellular inositol triphosphate levels decrease (140). A Y2H assay to investigate the role of CT101 found that the C-terminus of CT101 (amino acids 53-101) interacted with the C-terminus of ITPR3 (140). By immunofluorescence assay, ITPR3 co-localized with active Src-kinases in inclusion microdomains, consistent with the localization described for CT101. CT101-FLAG also immunoprecipitated with ITPR3 in lysates from cells infected with *C. trachomatis* L2 transformed with a plasmid that expresses CT101-FLAG (140). TargeTron disruption of CT101 (*C. trachomatis* L2 CT101::*bla*) resulted in the loss of ITPR3 recruitment to the inclusion, which could be rescued by complementation with pBOMB4-CT101-FLAG (140).

Additional studies revealed fewer extrusions upon infection with *C. trachomatis* L2 CT101::*bla* mutants (140), indicating a potential link with MYPT1 directed inclusion extrusion events (38, 117), so the effect of CT101::*bla* and siRNA knockdown of ITPR3 on recruitment of myosin kinase pathway proteins (e.g., MLCK, MCL2, Src, and MYPT1) was evaluated (140). *C. trachomatis* L2 CT101::*bla* infected cells and siRNA knockdown of ITPR3 in wild-type *C. trachomatis* L2 infected cells resulted in a loss of phosphorylated MYPT1 (pT853; inactive) and MLC2 (pS19; active) at the inclusion but did not impact Src-kinase activity or MLCK (140). Because ITPR3 is a calcium channel and STIM1 is a calcium sensor that has been previously shown to localize with the inclusion (141), the role of calcium levels on inclusion extrusion was also investigated. The addition of the calcium chelator, 1,2-bis (2-aminophenoxy) ethane-N,N,N',N' tetraacetate-acetoxymethyl ester (BAPTA-AM), to *C. trachomatis* L2 infected cells blocked extrusion events but did not impact infectious progeny production. These studies implicate calcium levels and

MYPT1 phosphorylation states in the final stages of the *C. trachomatis* L2 developmental cycle, whereby the presence of calcium tips the balance toward extrusion and the absence of calcium toward inclusion lysis from the host cell (140).

IncG and 14-3-3 β

Incs also function to sequester eukaryotic proteins to prevent the initiation of apoptosis in *C. trachomatis* infected host cells (142). Y2H experiments using the recombinant C-terminus of IncG against a HeLa cDNA library identified an interaction with 14-3-3 β (142). IncG is phosphorylated (at the RxSxSpP motif within IncG) by the eukaryotic cell during infection, and phosphorylation of IncG was required for the interaction with 14-3-3 β (142). The interaction between IncG and 14-3-3 β was later shown to sequester BAD, a binding partner of 14-3-3 β, to block apoptosis by preventing translocation of BAD to the mitochondria (143).

C. trachomatis *manipulation of eukaryotic vesicular and non-vesicular trafficking pathways*

Chlamydiae manipulate both vesicular and non-vesicular trafficking events to obtain essential lipids and other nutrients from the host cell by the recruitment of proteins responsible for vesicle fusion events (e.g., SNARE proteins) and direct vesicle trafficking (e.g., Rab proteins). Chlamydiae manipulate vesicular trafficking via molecular mimicry of eukaryotic soluble N-ethylmaleimide-sensitive factor attachment protein receptor (SNARE) domains that mediate vesicle fusion events to target membranes (144, 145). Several eukaryotic SNARE proteins are targeted to the inclusion and some chlamydial Incs, such as IncA, contain eukaryotic SNARE-like domains, which might be one avenue by which chlamydiae direct vesicle fusion events with the inclusion membrane (113, 144-148). One eukaryotic protein syntaxin 6 (STX6), a trans-Golgi network SNARE protein, is

recruited via its YGRL signal sequence to the inclusion (149). VAMP4 was found to be required for STX6 recruitment to the inclusion and knockdown of VAMP4, but not STX6, results in decreased sphingomyelin acquisition (148). Another SNARE protein, syntaxin 10 (STX10), localizes to the early inclusion membrane, and siRNA knockdown of STX10 decreased infectious progeny production and increased sphingomyelin acquisition (146). Importantly, chloramphenicol treatment did not abolish STX10 localization to the inclusion membrane, which may indicate that an immediately-early chlamydial effector is responsible for recruitment (146). To determine if other eukaryotic SNARE proteins localized to the inclusion, Delevoye et al. screened VAMP proteins by immunofluorescence and determined that VAMP3, VAMP4, VAMP7, and VAMP8 localized to the inclusion of *C. trachomatis* serovar D infected eukaryotic cells (145). Ectopically expressed GFP-tagged VAMP proteins were able to interact with 6xHis-tagged IncA, a chlamydial Inc containing a eukaryotic SNARE-like domain, by co-IP (145). The recruitment of VAMP proteins is hypothesized to be involved in the inclusion fusion with lipid-containing vesicles. siRNA knockdown of VAMP3, 4, 7, or 8 did not impact the development of *C. trachomatis* serovar D, but VAMP proteins have been shown to compensate for one another. This can make it difficult to define the contribution of individual VAMP proteins during chlamydial development.

Vesicular trafficking is also manipulated by *C. trachomatis* via the recruitment of numerous Rab proteins, which are GTPases (i.e., molecular switches) that are involved in vesicle formation and vesicle trafficking in the host cell, (150-154). For example, the recruitment of Rab6 and Rab11 to the inclusion membrane results in fragmentation of the Golgi, which is important for sphingomyelin acquisition (136). Also, Rab14, normally found in the Golgi (154), and Rab39a, on multi-vesicular bodies that are tightly associated with the inclusion, are also involved in sphingomyelin acquisition (155). Although many Rab

proteins are associated with the inclusion, the recruitment of a Rab protein by an Inc protein has only been defined for CT229 and Rab4 (151, 156, 157).

CT229 and Rab4

One of the first interactions between an Inc and a Rab protein was identified based on previous immunofluorescence assays, which showed that Rab4A localized to the inclusion membrane in *C. trachomatis* L2 infected cells. A Y2H assay was used to screen for Rab4A interactions with the C-terminal regions of 27 different Incs and identified a positive interaction between Rab4A and the C-terminus of CT229 (151). Only GTP-bound Rab4A was recruited to the inclusion (151). Additional studies confirmed the interaction of GFP-CT229 with GST-Rab4A from lysates of co-transfected HeLa cells. More recent studies expand on speculation by Rzomp et al., suggesting that the interaction between CT229 and Rab4, among other Rab proteins, supports the utilization of the clathrin-coated vesicle (CCV) pathway during infection (157). The CCV pathway is involved in trafficking transferrin, or EGFR, etc., from the plasma membrane to endosomes (157).

CT229 and Stimulator of Interferon Genes Protein (STING)

In a separate study, CT229 (also referred to as *Chlamydia* promoter of Survival (CpoS)) was linked to preventing host cell death via interactions with the STING pathway (127). Increased host cell death was detected in cells infected with a chemically mutagenized *C. trachomatis* L2 strain harboring a mutation in *CT229* (130). Both HeLa (human cervical epithelial) and THP1 (monocyte cell line) cells infected with the *C. trachomatis* L2 CT229 mutant demonstrated increased propidium iodide staining (i.e., indicative of apoptosis), which could be rescued by trans-complementation (127). Affinity purification-mass spectrometry from cells infected with *C. trachomatis* L2 transformed with a plasmid that expresses CT229-FLAG identified Rab 1A, Rab 1B, and Rab35 as potential binding partners of CT229 (127). *C. trachomatis* L2 CT229::*bla* mutants did not recruit

Rab1A-EGFP in transfected cells. Rab1A-EGFP recruitment was rescued after the trans-complementation of *C. trachomatis* L2 CT229::*bla* mutants with pBOMB CT229-FLAG (127).

To determine if CT229 was involved in preventing the host immune response, RNA-sequencing was performed using *C. trachomatis* L2 wild-type and L2 CT229::*bla* infected cells. Over 50 percent of the transcripts with greater than a 2-fold increase were associated with the Type I and III interferon pathway (127). siRNA knockdown of stimulator of interferon genes protein (STING), a cytosolic DNA sensor of bacterial cyclic di-GMP or cyclic di-AMP, but not cyclic GMP-AMP synthase (cGAS; double-stranded DNA sensor) or IRF3 (double-stranded RNA sensor) moderately rescued cell death in eukaryotic cells infected with the *C. trachomatis* L2 CT229 mutant. This suggests that CT229 prevents the activation of the Type I interferon pathway. These data support a role for CT229 blocking the ability of eukaryotic cells to respond to infection, thereby allowing *C. trachomatis* L2 growth. The exact mechanism by which *C. trachomatis* CT229 prevents activation of STING has not been defined. A *Shigella* T3SS effector, IpaJ, prevents activation of STING, an ER-associated transmembrane protein, by blocking ER exit (158). The interaction between CT229 and various Rab proteins may modify the trafficking or stability of STING (158, 159).

IncD and Ceramide Transfer Protein (CERT)

Perhaps the best-understood interaction between a chlamydial Inc and its eukaryotic binding partner is the interaction between IncD and Ceramide Transfer Protein (CERT) (54, 126). CERT was identified in an RNAi screen for host factors that were important for chlamydial development (54). CERT is involved in the transport of ceramide and for maintaining contact sites between the endoplasmic reticulum and the Golgi (54). CERT localization at the inclusion membrane was confirmed by immunofluorescence

assays using ectopically expressed epitope-tagged CERT and with endogenous anti-CERT antibodies. IncD was identified by affinity purification-mass spectrometry experiments using HEK293T cells transfected with FLAG-tagged CERT and infected with *C. trachomatis* L2. In affinity-purified eluates, a 15 kDa band corresponding to IncD, an Inc expressed early after infection of a host cell (44) was identified (54). This interaction was validated by co-transfecting HEK293T cells with epitope-tagged CERT and IncD, whereby IncD bound the Pleckstrin homology domain (PH domain) of CERT. This interaction maintains inclusion proximity via contact sites with the ER and with CERT binding partners, vesicle-associated membrane protein-associated protein A and B (VAPA and VAPB) (54). The depletion of either CERT, VAPA, or VAPB moderately decreased infectious progeny (about 4-fold). The interaction of IncD with CERT and maintaining contact sites with the ER plays a role, at least in part, in the recruitment of ceramide to the inclusion (54), which is a precursor for sphingomyelin, a lipid required for chlamydial development (30).

CT005 (IncV) and Vesicle-associated membrane protein-associated protein (VAP) A

Maintaining multiple contact sites with the ER is likely important for *C. trachomatis* development as another Inc, CT005, binds VAPA and VAPB. Mirrashidi et al. detected an interaction between CT005 (also referred to as IncV) and VAPA/B by transfecting uninfected eukaryotic cells with Strep-tagged Incs followed by AP-MS identification of interacting partners (122). Co-IP validated the interaction between CT005 and VAPA and VAPB using lysates from uninfected HEK293T cells that had been co-transfected with CT005-FLAG and GFP-VAPA or GFP-VAPB (137). CT005 contains two FFAT motifs (i.e., two phenylalanine's in an acid tract), which creates multiple contact sites with the ER via the interaction with ER-resident proteins, VAPA and VAPB. VAPA and VAPB are also known to interact with two lipid transfer proteins that had been previously shown to localize

with the inclusion, CERT (54) and oxysterol binding protein (OSBP) (160). Mutating the FFAT motifs of CT005 moderately decreased the association of the inclusion with VAPA and VAPB, but neither siRNA depletion of VAPA or targeted disruption of CT005 negatively impacted *C. trachomatis* growth (45, 137). This may support the concept of redundant roles for Incs in the inclusion membrane.

IncE and Sorting Nexins (SNX) 5 and 6

The ectopic expression and purification of strep-tagged C-terminus of IncE revealed novel interactions between IncE and Sorting Nexin (SNX) 5 and SNX6 (122). SNX proteins contain a Phox-homology (PX) domain, which is involved in the endosomal trafficking of BAR proteins. Histidine tagged-SNX5 and SNX6 co-immunoprecipitated with Strep-tagged IncE from the lysates of transfected HEK293Tcells. Using truncated IncE, SNX5 and SNX6 were shown to affinity purify with IncE when the C-terminus containing the PX domain was present (122). SNX5 and SNX6 also co-localize with IncE positive fibers (122, 161). The interaction of IncE with SNX5 and SNX6 is believed to be important for *C. trachomatis* to interfere with retromer trafficking because transient transfection of HEK293T cells with the C-terminus of IncE (AA 101-132) resulted in co-localization of a retromer cargo protein, cation-independent mannose-6-phosphate receptor (CI-MPR), with IncE. In contrast, in non-transfected cells, CI-MPR (162) remained associated with the Golgi (122). siRNA knockdown of SNX5 and SNX6 decreased tubule production, but increased the number of infectious progeny produced by 10-fold (122), which makes the function of IncE binding SNX5/6 unclear. Based on the known Inc-eukaryotic protein-protein interactions, Incs are clearly involved in the manipulation of numerous host cellular pathways, but these data are also confounded as the knockdown of a single eukaryotic protein often does not substantially impact chlamydial development.

Inc-Inc interactions and the role of Incs in inclusion stability

Although Incs are involved in host-pathogen interactions that are important for the growth and development of *Chlamydia*, the organization of Incs and the Inc-Inc interactions that occur in the inclusion membrane are not well understood. Incs are known to exhibit different localization patterns within the inclusion (i.e., microdomain or uniform, ring-like formation), which likely reflects their different roles in the inclusion. There are only a handful of studies of Inc-Inc interactions and the contribution of Incs to inclusion stability (45, 57, 105). The Bacterial Adenylate Cyclase Two-Hybrid (BACTH) assay is one tool that has been used to assess Inc protein-protein interactions in *E. coli* (105, 115, 163-165). The premise of the BACTH system and a detailed protocol are in Chapter 2. By BACTH assay, some Incs, such as IncF, were found to interact with multiple Inc proteins. In contrast, other Incs had very few or no heterotypic interactions, such as IncA and CT813, respectively (105). These data led to the hypothesis that Incs broadly function to organize the inclusion membrane and to bind eukaryotic proteins to acquire nutrients (59). More specifically, IncF interacted with several Incs and has a short C-terminus, which may indicate that IncF is involved in Inc-Inc interactions, supporting the hypothesis that IncF may play an organizational role in the inclusion membrane (105). IncA, which did not interact with many other Incs (105), contains a eukaryotic SNARE-like domain that is involved in inclusion fusion (92, 112, 144, 166) and by which IncA may interact with eukaryotic proteins.

To test this hypothesis, Rucks et al. compared the impact of the overexpression of IncF and IncA on chlamydial development using *C. trachomatis* L2 transformed with either IncF, or the transmembrane(TM) domain of IncA (i.e., $IncA_{TM}$) fused to a proximity labeling enzyme (APEX2) (57). The exogenous overexpression of IncF-APEX2 from *C. trachomatis* L2 resulted in smaller inclusions and IncF-APEX2 puncta outside of the

inclusion membrane, which may suggest that the organization of the inclusion is disrupted by IncF overexpression (57). The deleterious effects on inclusion diameter were abrogated by reducing IncF expression levels (57). Moreover, the plasmid encoding IncF was not retained during secondary infection (progeny assays), indicating that high levels of overexpression of IncF was not well tolerated by chlamydiae (57). Finally, using sphingomyelin acquisition as a metric for normal inclusion development, the overexpression of IncF, but not $IncA_{TM}$, from *C. trachomatis* L2 resulted in decreased sphingomyelin acquisition (57). These data support a role for IncF in the organization of the inclusion membrane.

Another study evaluated the loss of Incs on chlamydial development (45) by creating *inc* mutants using a targeted group II intron insertion (i.e., TargeTron) system (109). *C. trachomatis* L2 TargeTron mutants were created with disrupted *CT005, CT179, CT224, CT229, IncC* (e.g., *CT233*), *CT288, CT383, CT449, CT813, CT850*, or *IncA* genes and evaluated for growth defects (45). Five of the 11 mutants, *C. trachomatis* L2 *CT229::bla*, *IncC::bla*, *CT288::bla*, *CT383::bla*, and *CT449::bla* resulted in premature inclusion lysis and reduced infectivity in mice (45). Further analysis of these mutant strains indicated initiation of intrinsic apoptosis as observed by increased bromodeoxyuridine (BrdU), propidium iodide, and Annexin V staining. By western blot, lysates from eukaryotic cells infected with either *C. trachomatis* L2 CT229, CT383, or IncC mutants resulted in cytochrome C release and cleavage of caspase-7 and 9, all indicators of intrinsic apoptosis (45). The ruptured inclusions of *C. trachomatis* L2 CT229, CT383, and IncC knockout strains were positive for LAMP1 and STING, indicating that these inclusions had fused with the lysosome. Interestingly, the premature lysis of inclusions from the *C. trachomatis* L2 CT229 mutant, but not CT383 or IncC, infected cells could be blocked by inhibiting eukaryotic protein synthesis with cycloheximide or by disrupting the ER-Golgi

trafficking (e.g., with Brefeldin A). This suggests that the role of CT229 in inclusion stability is likely more related to the recruitment of certain eukaryotic proteins that are necessary for chlamydial development. On the other hand, CT383 and IncC are likely directly contributing to inclusion stability (45).

Summary of Inc protein-protein interactions

The ability to genetically modify *C. trachomatis* L2 has contributed to the increase in Inc protein-protein interactions described in recent years (Table 2; Fig. 1-1). However, there are still relatively few known binding partners for Inc proteins (i.e., 11 out of 50+ predicted Incs). More importantly, the function of many of the known Inc-eukaryotic protein interactions remains unclear as the targeted disruption of some Incs (i.e., CT005 (137), CT101 (140), CT288 (133), or their eukaryotic binding partners, did not impact chlamydial development. The few Incs for which a eukaryotic protein binding partner has been identified, bind eukaryotic proteins via molecular mimicry (i.e., IncG (142), IncE (122, 161), CT005 (137), CT228 (38).

While the cytosolic C-terminal regions of Incs used in yeast two-hybrid assays, affinity purification, or ectopic expression of Incs in uninfected host cells did successfully identify Inc protein binding partners for a few Incs (54, 122), experimental limitations likely impede the ability to identify binding partners for all Incs using only these methods. The most prominent limitations include the inability of the truncated protein to fold appropriately, which may be required to facilitate protein-protein interactions. Also, under transient transfection conditions, Incs are not anchored in a membrane but instead aggregate together, resulting in an incorrect subcellular localization within the host cell, which may facilitate false protein interactions. It is also possible that experiments using a single Inc prevents an understanding of the complex role of Incs in the inclusion membrane.

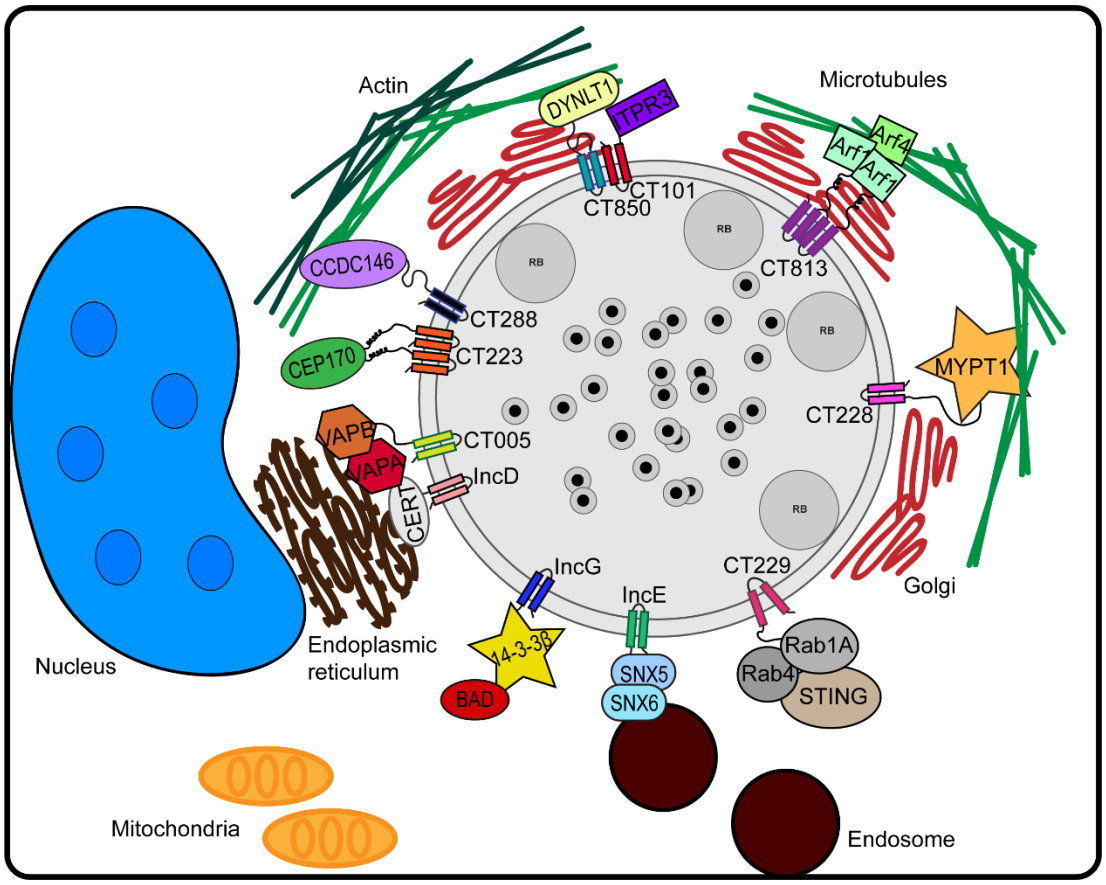

Figure 1-1. Summary of defined Inc-eukaryotic protein-protein interactions.

Chlamydial Inc proteins manipulate numerous host cell pathways via interactions with eukaryotic proteins. These interactions are important for the chlamydial inclusion to be trafficked to the microtubule organizing center, to obtain lipids from the ER and Golgi, and to prevent apoptosis and type I interferon pathway activation.

To better address these issues, a comprehensive system to identify interacting partners for Incs *in vivo,* in the context of *C. trachomatis* infection is needed. An *in vivo* system will help to understand the cooperative role of Incs in a manner not limited by transfection with a single Inc, or partial (C-terminus) Inc, or by the limitations of purifying hydrophobic proteins and maintaining protein-protein interactions. Recently described proximity labeling tools yield a significant advantage, particularly for Incs, to detect protein-protein interactions *in vivo*.

Proximity labeling systems as a molecular tool to identify protein-protein interactions at the C. trachomatis *L2 inclusion membrane in vivo*

Proximity labeling systems are based on the principles of a promiscuous enzyme that covalently modifies proximal proteins, which is genetically fused to a gene that encodes a protein of interest (167-169). In contrast to Y2H and ectopic expression experimental systems, proximity labeling systems allow for the identification of proximal interactions between two or more Incs as well as eukaryotic proteins because they are labeled *in vivo*, in the context of infection. In addition, the expression of Inc-APEX2 fusion proteins from *C. trachomatis* L2 promotes the appropriate protein folding and localization of the fusion proteins in the inclusion membrane (57, 115, 170). This is expected to facilitate accurate protein-protein interactions that are occurring proximal to the inclusion membrane. Furthermore, proximity labeling systems circumvent the issues related to the solubility of Incs because of the covalent modification (e.g., with a biotin molecule) *in vivo,* so there is no need to maintain protein-protein interactions. In this fashion, the biotin modified proteins are affinity-purified, then identified by mass spectrometry.

We hypothesize that some Incs organize the inclusion through Inc-Inc interactions, whereas other Incs promote chlamydial-host interactions by binding eukaryotic proteins. To test our hypothesis, we adapted the APEX2 ascorbate peroxidase proximity labeling

system for use in *C. trachomatis* serovar L2 to label proximal interactions *in vivo* (Detailed protocol in Chapter 2)(57) (115, 169). We used IncF, which interacted with numerous other Incs by BACTH, thus may support an organizational role, compared to IncA, which demonstrated fewer interactions (105) and contains a eukaryotic SNARE-like domain (87, 108, 110, 111, 144)(Chapter 3). Because proximity labeling systems label proximal proteins, to distinguish significant proteins from false positives, it is crucial to include the appropriate controls and data analysis tools.

It is also important to understand how our *in vivo* proximity labeling AP-MS datasets studies fit with previous studies of protein-protein interactions at the inclusion membrane (Chapter 4). Before the development of APEX2 for use in *C. trachomatis* L2, two large-scale AP-MS studies that aimed to understand the inclusion “interactome” via ectopic expression and inclusion purification (122, 171). In addition, a second APEX2 proximity labeling study was recently published (170), which allowed a direct comparison between two APEX2 studies that evaluated Inc protein-protein interactions at the inclusion membrane. These studies provide insight into the *in vivo* interactions at the inclusion membrane, highlight differences in experimental design and analysis on the outcome of the statistically significant proteins identified. These studies also highlight the impact Inc overexpression models on chlamydial development and host cell interactions.

Chapter 2 – Methods: Proximity Labeling of the *Chlamydia trachomatis* Inclusion Membrane

*Chapter 2 is reused with the permission of the following published book chapter of which I am a first author:

Macy G. Olson[1], Lisa M. Jorgenson[1], Ray E. Widner, and Elizabeth A. Rucks. 2019. Proximity Labeling of the *Chlamydia trachomatis* Inclusion Membrane. 2042 p 245-278. Methods in Molecular Biology.

[1]Equally contributing first authors

Abstract

Within the field of intracellular bacteria that reside within a membrane-bound vacuole, there are many questions related to how prokaryotic or eukaryotic transmembrane or membrane-associated proteins are organized and protein function within the membranes of these pathogen-containing vacuoles. Yet, this host-pathogen interaction interface has proven difficult to experimentally resolve. For example, one method to begin to understand protein function is to determine the protein-binding partners; however, examining protein-protein interactions of hydrophobic transmembrane proteins is not widely successful using standard immunoprecipitation or co-immunoprecipitation techniques. In these scenarios, the lysis conditions that maintain protein-protein interactions are not compatible with solubilizing hydrophobic membrane proteins. In this chapter, we outline two proximity labeling systems to circumvent these issues to study (1) eukaryotic proteins that localize to the membrane-bound inclusion formed by *Chlamydia trachomatis* using BioID, and (2) chlamydial proteins that are inserted into the inclusion membrane using APEX2. BioID is a promiscuous biotin ligase to tag proximal proteins with biotin. APEX2 is an ascorbate peroxidase that creates biotin-phenoxyl radicals to label proximal proteins with biotin, or 3,3'-diaminobenzidine intermediates for examination of APEX2 labeling using electron microscopy. We present how these methods were originally conceptualized and developed, so that the user can understand the strengths and limitations of each proximity labeling system. We discuss important considerations regarding experimental design, which include careful consideration of background conditions and statistical analysis of mass spectrometry results. When applied in the appropriate context with adequate controls, these methods can be powerful tools towards understanding membrane interfaces between intracellular pathogens and their hosts.

1. Introduction

1.1 Overview

Members of *Chlamydiae* are obligate intracellular pathogens and the entirety of their characteristic and unique biphasic developmental cycle is completed within a vacuole, called the chlamydial inclusion. *Chlamydia* manipulate the host cell in order to create and maintain the inclusion as a stable specialized niche to promote chlamydial growth and development. Although *Chlamydia* has undergone significant genomic reduction, they have maintained a significant portion of their coding capacity towards a type III secretion system and associated effector proteins (21). The chlamydial type III secretion system is essential (172), which highlights the importance of this system in modulating chlamydial-host interactions. A significant portion of chlamydial type III effectors have large hydrophobic transmembrane domains and belong to the Inc family of proteins; these effectors reside within the inclusion membrane. Incs are characterized by having two or more hydrophobic transmembrane domains, with the amino-terminal and carboxy-terminal ends of the proteins exposed to the eukaryotic cytosol (91, 92, 108); although, it is conceivable that the N- and C- termini of some Incs may be exposed to the lumen of the chlamydial inclusion. While these proteins are important to the intracellular development of *Chlamydia*, their high hydrophobicity make them difficult proteins to purify and study. This chapter describes methods that allow for the study of protein-protein interactions of chlamydial membrane and host membrane proteins. Ostensibly, these methods will be applicable to any investigator trying to examine the molecular interactions of pathogen and host proteins, particularly within the context of membrane-associated interactions.

1.2 Introduction to Inc studies

Despite the fundamental importance of the inclusion membrane to chlamydial fitness, specific molecular events, including Inc protein function, that are responsible for inclusion membrane composition and integrity are unknown. The lack of mechanistic data concerning Incs and the inclusion membrane is due to two main reasons. Firstly, the inclusion membrane is difficult to biochemically purify (171, 173). A recent study reports the identification of a chlamydial inclusion interactome, this study relied on an extensive purification scheme that only captured 50% of the inclusions from $6x10^7$ infected cells and failed to identify host-chlamydial or Inc-Inc interactions (171). Labor-intensive schemes complicate attempts to characterize the inclusion membrane interactome over the course of the developmental cycle—key requirements in understanding the inclusion and its function. Secondly, Inc proteins are membrane proteins, which are notoriously difficult to study due to their hydrophobicity. Identification of interacting partners for Incs have typically relied on expressing the cytosolic domains of a given large Inc in yeast two-hybrid systems or purifying a recombinant version of this domain for pulldowns (38, 54, 123, 126, 142, 145, 174). A last and final consideration is that addition of molecular tags may prevent Inc-fusion constructs from being properly type III secreted. To address two out of three of these obstacles, we have adapted several proximity labeling systems to understand protein-protein interactions at the chlamydial inclusion membrane. In this chapter, we will outline the origins of these systems, discuss how these methods have already been applied by the field to understand chlamydial-host interactions, and present our methods in adapting these systems to help understand chlamydial-host interactions.

1.3 Origins of BioID

The origins of the BioID proximity dependent labeling began with the examination of the impact of point mutations on the enzymatic activity of BirA, a bacterial biotin ligase.

Biotinylation reactions by BirA occur in two steps: the first being the binding of BirA to biotinyl-5'-ATP (175), and the second is the recognition of the biotin acceptor tag, or BAT, where the biotin intermediate is transferred to a specific lysine (176). Mutation of the arginine at position 118 to a glycine resulted in an alteration in BirA substrate specificity (177). Further characterization of the mutant BirA, recognized that the BirA R118G (BirA*) mutant maintained the ability to transfer biotin moieties to lysine residues of proteins in close proximity to the enzyme, but any specificity towards specific target proteins with known BATs was eliminated (178). Most of these studies had been performed in *Escherichia coli*, but the fact that BirA* promiscuously biotinylated proteins in a proximity-dependent manner made it an attractive tool to adapt for cell biology studies. In the first cell biology-based study, Kyle Roux and colleagues created a molecular fusion between BirA* and a nuclear lamin protein (167). Nuclear lamins are transmembrane proteins and important for the function of the nuclear envelope. Their hydrophobicity made them difficult proteins to study. Given that biotin has a strong affinity for streptavidin (K_D 10^{-13} to 10^{-15} M; (179)), they designed a BirA* construct to biotinylate potential lamin-interacting proteins, and then relied on the high affinity of biotin for streptavidin to purify these binding partners for identification by mass spectrometry (167).

Since its inception, the BioID system has been used in cell biology studies to identify regulators of centriole duplication and structure (180, 181) and understanding proteins involved in the insulin-like growth factor I receptor pathway (182). In the field of cellular microbiology, the BioID system has been useful in determining protein targets of the *Legionella pneumophila* effector protein, PieE, (183), identifying components of the *Toxoplasma* inner membrane complex (184), components of the *Trypanosoma brucei* biolobe (185), and novel proteins on the *Plasmodium* parasitophorous vacuolar membrane (186). Further, several laboratories, are adapting BioID in novel ways to

advance understanding of protein-protein complexes. These include the development of a ‘split BioID’ system, that places the N-terminus or C-terminus of BirA* onto separate proteins. If the proteins interact, then the biotin ligase activity is restored, and biotinylation of surrounding proteins occurs (187). A similar 2C-BioID system has been developed, which also recapitulates a two component or two-hybrid system within a native cellular environment (188). In all cases, utilization of BirA*-protein fusion constructs have helped elucidate difficult to study protein-protein interaction networks.

1.4 Origins of APEX2

Another proximity-dependent biotinylation system to determine difficult to study protein-protein interactions networks is APEX2 (189). APEX is a soybean ascorbate peroxidase, whose activity is similar to horseradish peroxidase (HRP). HRP has been useful in electron microscopy studies because, in the presence of H_2O_2, it can polymerize 3,3’-diaminobenzidine (DAB), which gives a localized contrast in activity when the samples are processed with osmium tetroxide (OsO_4) (190, 191). Attempts to create fusion constructs with various mammalian proteins and HRP failed to create a system to tag neighboring protein networks. HRP has 4 structurally essential disulfide bonds and 2 Ca^{2+} binding sites for activity. The mammalian cytosol is a reducing environment that is also Ca^{2+} poor, which renders HRP inactive (192). APX, the endogenous soybean ascorbate peroxidase and a class I cytosolic plant peroxidase, is 40% smaller in size than HRP, and lacks disulfide bonds and the necessity for Ca^{2+} cofactors for activity. The protein known as APEX, which stands for “enhanced APX”, was molecularly engineered with point mutations within *APX* to increase enzymatic activity, and this original construct was used to label the mitochondria and endoplasmic reticulum with DAB to render greater structural resolution (168). This same group substituted biotinyl-tyramide for DAB as a substrate and demonstrated that they could use APEX-mitochondrial protein constructs to selectively

label, with biotin, other mitochondrial proteins within the inner and outer membranes of the mitochondrial matrix in a proximity dependent manner (193). In these reactions, biotinyl-tyramide or, more commonly used, biotin-phenol is incubated with eukaryotic cells that are expressing APEX-fusion constructs. In the presence of H_2O_2, APEX reacts with the biotin-phenol, producing a biotin phenoxyl radical, that can then covalently attach (or react with) tyrosine, tryptophan, histidine, or cysteine amino acids within adjacent proteins (193). As discussed below, these adjacent proteins include binding partners as well as proximal proteins.

The original APEX molecule was monomeric, and using directed evolution to select for improved activity, APEX2 was created. This new protein contained a point mutation at position 134 that resulted in a proline replacing an alanine, creating APEX2 (APEX,A134P) (189). APEX2 is able to form dimeric complexes (189), which has been shown to increase the stability and activity of ascorbate peroxidases (194). It also requires heme for activity (189), and heme is a molecule that is ubiquitous in eukaryotic cells, as it is required for oxidation-reduction reactions, amongst other metabolic processes (195).

Many APEX2 constructs have been generated and have contributed to studies that have created ‘organelle barcodes’, which reveal the subcellular localization of difficult to study proteins (196), and spatiotemporally resolved protein interaction networks of G-protein coupled receptors (197). The latter study also discussed the resolution of proteins that are directly involved in protein networks or those that are considered ‘bystander’ proteins, which are proteins that are in the area of the interactions but are not directly involved in their function or signaling networks. These studies have exploited the power and the limitations of the proximity-dependent labeling systems to further our understanding of protein-protein interaction dynamics and have increased our understanding of the spatial organization of many proteins within eukaryotic cells.

As it relates to understanding protein-protein interactions within bacteria or host-pathogen interactions, Eric Cascales's group used the APEX2 system to identify novel binding partners for a type VI secretion system protein (T6SS), TssA, which helped illuminate dynamics of T6SS apparatus assembly (198).

Relative to the field of *Chlamydia*, both the BioID and APEX2 systems have been employed. For example, the BioID system has been used to determine if specific eukaryotic proteins are recruited to the chlamydial inclusion. For example, to clarify if a eukaryotic protein, syntaxin 6, and a mutant of syntaxin 6 lacking a signal sequence trafficked to the chlamydial inclusion, a BirA*-syntaxin 6 and its mutant was exogenously expressed in chlamydial infected HeLa cells (199). Syntaxin 6 is a eukaryotic SNARE protein that localizes to the Golgi and traffics between the Golgi and the plasma membrane (200). As the chlamydial inclusion develops within the proximity of the Golgi, localization of Golgi-resident or Golgi-associated proteins can be murky. Wild type BirA*-syntaxin 6, but not the mutant, was recruited and, in the presence of exogenously added biotin, biotinylated the chlamydial inclusion membrane (199). BioID has also been used to identify eukaryotic interacting proteins for a *Chlamydia psittaci* type III effector protein, SINC. In this study, BirA*-SINC exogenously expressed in eukaryotic cells was determined to localize similarly as SINC that is expressed and secreted by *C. psittaci* and used to identify several candidates that might bind SINC during a chlamydial infection (201). In another study, BioID was used to demonstrate that a chlamydial type III effector, TmeA, and a specific eukaryotic protein interacted within the host cytosol (118). In this study, the eukaryotic protein, AHNAK, was fused to BirA* and exogenously expressed in HeLa cells. As a control, a eukaryotic protein, BirA*-Perforin-2, which was known to interact with early inclusions (202), but not TmeA, was also expressed. Five hours post-infection, the chlamydial protein was analyzed for biotinylation, and was found to be biotinylated by

BirA*-AHNAK only, thereby confirming the proteins' interaction (118). To date, BirA*, has not been fused to a chlamydial protein and successfully expressed by *Chlamydia*. It is unknown if BirA* can be type III secreted by the chlamydial type III secretion apparatus. In contrast, it has been demonstrated that chlamydial Inc proteins with C-terminal APEX2 fusions are expressed and type III secreted by *C. trachomatis* (57, 59). As this seminal study demonstrated, it is important to optimize Inc-APEX2 expression levels from *Chlamydia* to replicate, as close as possible, expression levels of endogenously expressed chlamydial proteins, and to limit possible negative effects of Inc overexpression on inclusion development (57). Methods provided in this chapter outline our progress in these areas.

1.5 General Procedure

General considerations.

When embarking on one of these proximity labeling systems that use biotin to tag binding partners or adjacent proteins, there are several considerations that must be factored into experimental design. For each system, one must consider where the greatest source of background will come from, so it can be controlled for accordingly. Second, if expressing these constructs from *C. trachomatis*, how will expression be controlled (i.e. via an inducible promoter, endogenous promoter, from a chlamydial transformation plasmid, or by inserting the construct into the chlamydial chromosome). Further, does addition of APEX2 or BirA* tags prevent normal localization (or secretion) of the protein, which will impact not only the proteins that are targeted by the fusion constructs, but how the resulting data are interpreted.

Biotinylation is a natural post-translational modification in eukaryotes and is also used in prokaryotes to modify protein function. As such, there are several cellular sources

of natural background proteins that will be purified by any streptavidin pulldown of whole eukaryotic cell lysates. Some of these naturally biotinylated eukaryotic proteins include 5 mitochondrial and cytosolic carboxylases (203), mitochondrial proteins (204), mRNA processing proteins (205), and ribosomal proteins (206). Also, given the high homology between conserved bacterial proteins and mitochondrial proteins, careful consideration of how to account for the presence of naturally biotinylated mitochondrial proteins so that false positive and false negative hits are not arbitrarily included or excluded, respectively.

Table 2-1 includes a direct comparison of the BioID and APEX2 proximity labeling systems. Part of the appeal of using BioID, is that you can get a 'roadmap' of where your protein has been over an extended period of time. If using a eukaryotic protein-BirA* fusion, one can also understand how chlamydial infection impacts protein interactions within a specific network/pathway. With the APEX2 system, you will receive a snapshot of protein interactions at specific time intervals. Specifically, after expression of a BirA*-protein construct, one will add biotin to the tissue culture medium for 5-24 hours before using the samples for downstream applications (118, 167). In contrast, the labeling requirements of APEX2-protein constructs happen quickly. Biotin-phenol is added to the medium for 30 minutes, and the labeling reaction is catalyzed by the addition of H_2O_2 for 30 seconds to a minute (193, 197), followed by a quenching reaction that relies on a temperature change, peroxidase inhibitors, and a competitive substrate to reduce APEX2 activity (193).

1.6 Anticipated results and statistical evaluation of mass spectrometry results

In an APEX2 or BioID experiment, a single mass spectrometry data set can yield hundreds to thousands of protein identifications. These data sets are typically a list of peptides or proteins represented with mass-to-charge (m/z) ratios and their corresponding signal intensities, analyzed against a known and annotated protein database, like

Table 2-1. Comparison of BioID and APEX2 proximity-dependent labeling systems

	BioID (BirA*)[1]	APEX2[2]
Enzyme	Promiscuous biotin ligase	Ascorbate peroxidase
Substrate	Biotin	Biotin-phenol
Intermediate	Biotinoyl-5'-AMP	Biotin phenoxyl radical
Target amino acids	Lysine (Lys, K)	Tyrosine (Tyr, Y); Tryptophan (Trp, W); Histidine (His, H); Cysteine (Cys, C)
Half-life	Several minutes	~1 millisecond
Labeling time	5-24 hours[3]	30 minutes
Labeling radius	~40 nanometers	20 nanometers

[1] Roux et al. 2012. J Cell Biol.

[2] Rhee et al. 2013. Science

[3] Roux et al. 2012. J Cell Biol.; Moore and Ouellette. 2014. Front Cell Infect Microbiol.

Table adapted from Olson et al. 2019. MiMB.

the *Homo sapiens* Swiss protein database. Very clearly, not all these proteins are true interacting partners, or even spatially related to the protein of interest. Conversely, the same results analyzed against a *Chlamydia trachomatis* Swiss protein database, will yield at maximum: 895 proteins; however, some of these protein identifications may be proteins that are highly homologous to mitochondrial proteins. Great care must be taken to ensure that proteins are not over- or under- represented in the final results. Statistical evaluation of these data is critical towards obtaining an unbiased and rigorously examined list of significant protein targets. Integral towards having a statistically significant dataset is having a minimum of 5 biological replicate experiments, which include all experimental and control conditions, and are processed identically for mass spectrometry.

Further, the type of statistical analysis used to properly evaluate these data is important. The current trend in the field is to use a statistical analysis program that uses Bayesian statistics (207, 208). For our studies, we have used one such program, known as SAINT for ‘significance analysis of interactome’ (207). With this program, the spectral counts for a given peptide or protein are normalized to the length of the protein and the total number of spectra that were received in the experiment/purification. Further, the statistical output is used to estimate the Bayesian False Discovery Rate (BDFR), which gives the probability of whether a specific protein is likely to be a significant finding or part of background (207). This method is an improvement upon standard *t*-tests of spectral counts between replicates and allows for the inclusion of proteins/peptides that appear weakly in controls (background) and more strongly and definitively in the experimental conditions (208).

2. Materials

2.1 Construction of BioID gene fusions for transfection and expression in eukaryotic cells

1. Tabletop centrifuge with rotors or adaptors for 15 mL and 50 mL conical tubes
2. Microcentrifuge to accommodate 1.5 ml microfuge tubes
3. Standard cloning materials and vectors
4. 37 °C and 42 °C water bath
5. Plasmid Miniprep kit
6. Plasmid Midiprep kit
7. 30 °C or 37 °C incubator for agar plates
8. 30 °C or 37 °C shaking incubator for liquid cultures
9. Standard *E. coli* strain for cloning (10-β or DH5 α)
10. PCR reagents, including a proofreading polymerase
11. Ligation kit e.g. NEBuilder HiFi Assembly Cloning Kit, NEB Cat# E5520S
12. -80 °C freezer
13. -20 °C
14. 4 °C

2.2 Construction of APEX2 gene fusions for transformation and expression from C. trachomatis

1. Tabletop centrifuge with rotors or adaptors for 15 mL and 50 mL conical tubes
2. Microcentrifuge to accommodate 1.5 ml microfuge tubes
3. Standard cloning materials and vectors
4. 37 °C and 42 °C water bath
5. Plasmid Miniprep kit
6. Plasmid Midiprep kit

7. 30 °C or 37 °C incubator for agar plates
8. 30 °C or 37 °C shaking incubator for liquid cultures
9. Standard *E. coli* strain for cloning (10-β or DH5 α)
10. *Dam-/dcm- E. coli* for *Chlamydia* transformation
11. -80 °C freezer
12. -20 °C
13. 4 °C

2.3 Proximity Labeling Using BioID Constructs

1. HeLa 229 cells (ATCC, CCL-2.1) (*see* **Note 1**)
2. Mycoplasma test kit (e.g. 'LookOut Mycoplasma Detection Kit', SigmaAldrich, MP0035) (*see* **Note 2**)
3. Standard tissue culture materials
4. Biosafety cabinet
5. 5% CO_2 37 °C incubator for tissue culture
6. 37 °C water bath
7. Refrigerated microcentrifuge (capable of 10,000 x g; 4 C)
8. 6-well tissue culture plates
9. 24-well tissue culture plates
10. Round 12 mm glass coverslips
11. 1x DMEM without biotin (Hyclone # SH30243.01 or Gibco DMEM #11-965-092)
12. Heat inactivated fetal bovine serum
13. BioID-fusion construct (*see* **Note 3**)
14. Biotin powder suitable for cell culture (stock 1 mM in serum free 1x DMEM, *see* **Note 4**)
15. 1xDMEM supplemented with 1% heat inactivated FBS

16. Transfection reagent (*see* **Note 5**)
17. Antibody against Myc
18. Fluorescent streptavidin conjugate; e.g., Streptavidin-488 Jackson ImmunoResearch Laboratories Inc., 016-540-084
19. Fixative (e.g, methanol or paraformaldehyde) and permeabilization reagent (e.g. 0.1% Triton X-100 or 0.5% saponin) (*see* **Note 6**)

2.4 Proximity labeling using APEX2 constructs

1. HeLa 229 cells (ATCC, CCL-2.1) (*see* **Note 1**)
2. Mycoplasma test kit (e.g. 'LookOut Mycoplasma Detection Kit', SigmaAldrich, MP0035) (*see* **Note 2**)
3. Standard tissue culture materials
4. Biosafety cabinet
5. 5% CO_2 37 °C incubator for tissue culture
6. 37 °C water bath
7. Refrigerated microcentrifuge (capable of 10,000 x g; 4 °C)
8. 6-well tissue culture plates
9. 24-well tissue culture plates
10. Round 12 mm glass coverslips
11. 1x DMEM without biotin (Hyclone, SH30243.01 or Gibco DMEM, 11-965-092)
12. Heat inactivated fetal bovine serum
13. 1x Phosphate buffered saline (PBS)
14. Anhydrous DMSO
15. Antibiotics: cycloheximide, gentamicin, penicillin, or another selective antibiotic
16. A clonal population of *C. trachomatis* transformants
17. Fixative (e.g, methanol or paraformaldehyde)

18. Permeabilization reagent (e.g. 0.1% Triton X-100 or 0.5% saponin)
19. Anhydrotetracycline
20. Biotin phenol (biotinyl-tyramide) (Adipogen; stock 50 mM in anhydrous DMSO (*see* **Note 7**).
21. Hydrogen peroxide
22. Quenching wash solution (10 mM sodium ascorbate, 10 mM sodium azide, 5 mM Trolox in dPBS (*see* **Note 8**)
23. RIPA buffer A (50 mM Tris-HCl, pH 7.4; 150 mM NaCl, 0.1% SDS, 0.5% sodium deoxycholate) buffer modified with:
    a. 150 μM Clastolactacystin β-lactone (*see* **Note 9**)
    b. 10 mM sodium azide
    c. 10 mM sodium ascorbate
    d. 5 mM Trolox (*see* **Note 8**)
    e. 5% Triton X-100
    f. 1% SDS
    g. 1X HALT + 1X EDTA protease inhibitor (ThermoFisher, 87786)
    h. 0.1 μL/mL Universal Nuclease (ThermoFisher, 88701)
24. Sonicator
25. Cell scrapers
26. 15 mL conical tubes (sterile)
27. 1.5 mL microcentrifuge tubes (sterile)
28. Tabletop centrifuge with rotors or adaptors for 15 mL and 50 mL conical tubes

2.5 Affinity Purification of Biotinylated Proteins

1. EZQ Protein Quantification Kit (ThermoFisher, R33200)

2. RIPA buffer (50 mM Tris-HCl, pH 7.4; 150 mM NaCl, 0.1% SDS, 0.5% sodium deoxycholate)
3. Streptavidin magnetic beads (e.g. Pierce streptavidin magnetic beads, 88816) (*see* **Note 10**)
4. Wash buffer A: RIPA buffer (50 mM Tris-HCl, pH 7.4; 150 mM NaCl, 0.1% SDS, 0.5% sodium deoxycholate) modified with:
    a. 500 mM NaCl
    b. 5% Triton X-100
    c. 1% SDS
5. Wash buffer B: 2 M urea in 10 mM Tris-HCl (pH 7.4)
6. 2X Laemmli sample buffer (Use premade/high grade Laemmli sample buffer (e.g., 2X Sample Buffer, BioRad, 1610737) if intended for mass spectrometry.) (*see* **Note 11**)
7. 1.5 mL microcentrifuge tubes (sterile)
8. Magnetic rack and individual magnet (*see* **Note 12**)
9. Tube rotator (1.5 mL tube compatible)

2.6 Confirmation of Protein Biotinylation and Mass Spectrometry Identification

1. Gel electrophoresis apparatus
2. Standard denaturing gel (e.g., BioRad 4-20% gradient Criterion gels, 5671093
3. Western blot transfer apparatus
4. Western blotting reagents: Polyvinylidene membrane (PVDF), blocking reagents (e.g., Bovine serum albumin or Milk), antibodies (e.g., streptavidin conjugate, anti-FLAG antibody), staining trays, wash solution (e.g PBS + 0.1% Tween-20).
5. Streptavidin-680 in 5% Bovine serum albumin in PBS + 0.1% Tween20 (PBST) (*see* **Note 13**)

6. Gel imaging system
7. 2x Sample buffer (both laboratory prepared and mass spectrometry grade) (*see* **Note 11**)
8. β-mercaptoethanol
9. Biotin (3 mM)
10. Coomassie stain (Coomassie G-250, 10% methanol, 5% acetic acid in tissue culture grade water) (*see* **Note 14**)
11. Destain solution (10% methanol, 5% acetic acid in tissue culture grade water)
12. 30% methanol (*see* **Note 15**)
13. Non-autoclaved tubes
14. Scalpel blades or razor for cutting SDS-PAGE protein bands
15. Mass spectrometry core facility (*see* **Note 16**)
16. Significance Analysis of Interactome (SAINT) or similar appropriate statistical analysis program to accurately assess background biotinylated proteins from the proximal proteins identified and prevent bias (*see* **Note 17**)

2.7 DAB Staining for Electron Microscopy

1. Plastic coverslips suitable for electron microscopy. (e.g. Thermo Scientific™ Nunc™ Thermanox™ coverslips, cat. no. 174985).
2. 6-well cell tissue culture plate
3. HeLa 229 cells (*see* **Note 1**)
4. Mycoplasma test kit (e.g. 'LookOut Mycoplasma Detection Kit', SigmaAldrich, MP0035) (*see* **Note 2**)
5. DMEM + 10% FBS
6. Cycloheximide (*see* **Note 18**)

7. Penicillin G (*see* **Note 18**)
8. Enumerated *Chlamydia* strains
9. Anhydrotetracycline
10. Dulbecco's phosphate-buffered saline
11. Fixing solution (2% paraformaldehyde, 2% glutaraldehyde, 0.1 M sodium cacodylate fixative): Combine 8 ml of 25% glutaraldehyde, 12 mL of 16% paraformaldehyde, 50 ml of 0.2 M sodium cacodylate, and 30 mL of distilled H_2O.
12. Wash buffer (0.1 M sodium cacodylate): Combine 100 mL of 0.2 M sodium cacodylate, pH 7.4 with 100 mL of distilled H_2O.
13. Quenching/blocking buffer (20 mM glycine in 0.1 M sodium cacodylate, 2 mM $CaCl_2$ blocking buffer). As described in (209), dissolve 75.1 mg glycine in 50 mL of 0.1 M sodium cacodylate, 2 mM $CaCl_2$. To make 0.1 M sodium cacodylate, 2 mM $CaCl_2$, dissolve 32.103 g of sodium cacodylate trihydrate in 450 mL Milli-Q™ H_2O. Decrease the pH to 7.4 by adding HCl drop by drop. Dissolve 0.441 g of calcium chloride, dihydrate. Bring the solution up to 500 mL with Milli-Q™ H_2O. This is 0.3 M sodium cacodylate, 6 mM $CaCl_2$. Then, combine 167 mL of this solution and 333 mL of Milli-Q™ H_2O to give 0.1 M sodium cacodylate, 2 mM $CaCl_2$.
14. 3,3'-Diaminobenzidine (DAB) stock solution (5 mg/mL). As described in (168, 209), dissolve 50 mg of DAB in 10 mL of 0.1 M HCl. Make 1 mL aliquots, freeze these by placing in dry ice, and store at -80° C.
15. Working DAB solution (0.5 mg/mL DAB, 0.1 M sodium cacodylate, 2 mM $CaCl_2$ solution): As described in Martell et al. 2017 (209), combine 1 mL of 5 mg/mL DAB stock solution, 3.33 mL of 0.3 M sodium cacodylate, 6 mM $CaCl_2$ (see above), and 5.67 mL of Milli-Q™ H_2O.

16. 0.5 mg/mL DAB, 3 mM H_2O_2, 0.1 M sodium cacodylate, 2 mM $CaCl_2$ solution: As described in Martell et al. 2017 (209), mix solutions together as for the previous solution. Add 3 µL 30% (weight/weight) H_2O_2. The concentration of H_2O_2 must be determined empirically. The DAB solutions with and without H_2O_2 should be made fresh just before adding them to the samples. Add H_2O_2 last to avoid beginning the polymerization reaction before the solution has been applied to the samples.
17. Electron Microscopy Facility

3. Methods

Biotinylation is a natural post-translational modification in eukaryotes. As such, there are several cellular sources of natural background proteins that will be purified by any streptavidin pulldown of whole eukaryotic cell lysates. Some of these naturally biotinylated eukaryotic proteins include 5 mitochondrial and cytosolic carboxylases (203), mitochondrial proteins (204), mRNA processing proteins (205), and ribosomal proteins (206). Therefore, during the experimental design steps, several negative controls for background biotinylated should be considered. Table 2- 2 outlines the controls that we use in our experiments.

The methodology for implementing a proximity labeling system in *Chlamydia* can be broken down into three major steps. First, clone the gene of interest in frame with either BioID or APEX2 into the desired vector (e.g., mammalian or *C. trachomatis* vector). Second, transfect or transform the vector encoding the BioID or APEX2 fusions (e.g., gene X-BioID, gene Y-APEX2) into the eukaryotic cells or *Chlamydia*, respectively and then optimize the expression of the fusion protein in your system. Step three, affinity purify the biotinylated proteins from the solubilized lysate and confirm biotinylation by western blotting.

Table 2-2. Negative controls for BioID, APEX2, and DAB labeling

BioID (BirA*) Controls	**Biotin**	**BirA***	**Reason**
Uninfected cells	+	+	For comparison to infected cells to determine if infection with *Ct* causes any changes in protein-protein interactions
WT L2	–	+	Negative control to determine endogenous biotinylation during transfection
WT L2	+	–	Negative control to determine endogenous biotinylation during infection with WT *Ct*
Uninfected cells	+	–	Negative control to determine endogenous biotinylation
APEX2 Controls	**aTc[a]**	**BP[b]**	**Reason**
APEX2 fusion control 1	+	–	Negative control for background biotinylation
WT L2	+	+	Negative control for background biotinylation
Uninfected cells	+	+	Negative control for background biotinylation
DAB Controls	**DAB[c]**	**H_2O_2**	**Reason**
WT L2	+	+	Negative control to check for background DAB labeling
APEX2 expressing strain	–	–	Negative control to make sure there is no DAB labeling in the absence of DAB and H_2O_2

[a] anhydrotetracycline (aTc)

[b] Biotin-phenol (BP)

[c] 3,3'-Diaminobenzidine (DAB)

Table adapted from Olson et al. 2019. MiMB.

3.1 Construction of BioID gene fusions for transfection and expression in eukaryotic cells

This section will briefly describe the steps involved in constructing BioID gene fusions and assumes that the scientist is proficient in standard cloning techniques.

1. Design primers to amplify your gene of interest, and perform PCR using standard methodologies and a proofreading polymerase.
2. Purify PCR products using a commercial PCR purification or gel extraction kit.
3. Clone in frame into the BioID plasmid, pcDNA3.1 mycBioID, (Addgene plasmid #35700) (167) using standard cloning methods (*see* **Note 3**).
4. Transform into a standard *E. coli* cloning strain, isolate the plasmid, and verify the DNA sequence. The isolated plasmid will be used to transfect HeLa cells to allow for biotin labeling of proteins proximal to your protein of interest with the addition of exogenous biotin.

3.2 Construction of APEX2 gene fusions for transformation and expression from C. trachomatis

This section will briefly describe the steps involved in constructing APEX2 gene fusions and assumes that the scientist is proficient in standard cloning techniques.

1. Amplify the gene of interest from *Chlamydia* genomic DNA (or other template as needed), and *APEX2* from pcDNA3 APEX2-NES (Addgene cat#49386) (189).
2. Purify PCR products using a commercial PCR purification or gel extraction kit
3. Clone in frame into the desired chlamydial expression vector (e.g., pASK-mKate (210), or pBomb4 (91)) followed by *APEX2* (*see* **Note 19**)**.**
4. Transform into standard *E. coli* cloning strains.

5. Isolate plasmids and confirm by DNA sequencing analysis.

6. Transform sequence verified clones into *dam*$^{-}$/*dcm*$^{-}$ *E. coli* (116, 211), purify plasmids.

7. Transform demethylated plasmids into *C. trachomatis* following the chlamydial transformation protocol as previously published (116, 211). In brief: Approximately 24 hours prior to transformation, seed McCoy cells in a 6-well tissue culture plate. Plate enough wells for one well per sample intended for transformation. The next day resuspend purified *C. trachomatis* elementary bodies that lack the endogenous plasmid (-pL2) in calcium chloride ($CaCl_2$) and add 2 µg of demethylated plasmid DNA. Incubate the mixture at room temperature for 30 minutes. Rinse the 6-well plate of McCoy cells with Hanks Buffered Salt Saline (HBSS) and replace with 2 mL of HBSS. After incubation, add the EB/pDNA mixture dropwise to a single well of a 6-well tissue culture plate per condition. Centrifuge the plates at 400 x g for 15 minutes at room temperature then incubate at 37 °C + 5% CO_2 for 15 minutes. Replace the HBSS with DMEM + 10 % FBS and place the 6-well plate back at 37 °C + 5% CO_2 incubator. At 8 hpi, aspirate the media and replace with DMEM + 10 % FBS containing the appropriate antibiotic and cycloheximide. Passage samples every 48 hours by scraping and infecting onto a fresh monolayer of McCoy cells until mature inclusions are observed.

8. Finally, test the *C. trachomatis* transformed with a plasmid that expresses the construct of interest for the appropriate localization of the constructs containing APEX2 by indirect immunofluorescence microscopy, and optimize the expression of each construct. For example, infect HeLa cell monolayers with *C. trachomatis* L2 transformed with a plasmid that expresses the construct of interest and induce with variable amounts of anhydrotetracycline. Fix and stain for indirect immunofluorescence to determine induction conditions that yield localization that

most closely matches endogenous protein localization according to the literature. In addition, it is best to perform subsequent biotinylation experiments with a clonal population of *C. trachomatis*. This can be done by plaque purification (see Chapter 12, 'Mutagenesis of *Chlamydia trachomatis* using TargeTron', section 3.4) or by limiting dilution.

3.3 Proximity Labeling Using BioID Constructs (see Note 5)

1. Seed HeLa 229 cells (*see* **Note 1** and **Note 2**) in a 6-well plate at the appropriate cell density determined from troubleshooting in 3 mL per well of 1x DMEM supplemented with 10% heat inactivated FBS.
    a. Place one round 12 mm glass coverslip in 2 separate wells of the 6-well plate to monitor transfection and biotin-labeling efficiency via immunofluorescence.
2. Approximately 24 hours after seeding cells and before transfecting, wash the cells twice with 1 mL per well of prewarmed 1X DMEM supplemented with 1% FBS *(we use 1% FBS to limit exogenous biotin contamination from the FBS)* and replace media with 2 mL of 1X DMEM containing 1% heat inactivated FBS.
3. Transfect with the BioID-fusion construct using preferred transfection method in 500 µL and allow to incubate at 37°C and 5% CO_2 for 4 hours.
4. Aspirate transfection medium and replace with 2 mL of DMEM + 1% FBS + 50 µM Biotin (*see* **Note 4**) per well (or not as a control) to begin the labeling. See Table 2- 2 for the appropriate negative controls.
    a. Make sure to use separate pipet tips and Pasteur pipettes between samples to prevent cross-contamination.
5. Allow the cells to recover for 2 hours.

6. Infect the cells with wild-type *Chlamydia* 6 hours post transfection (4-hour transfection + 2-hour recovery) by centrifugation at 400 x g for 15 minutes at room temperature, then incubate 37 °C 5% CO_2.
7. At the timepoint post-infection you are interested in, remove glass coverslips from the two wells and place them into a new 24-well plate containing 500 µL of appropriate fixative and permeabilization with appropriate permeabilization reagent (e.g. 0.1% Triton X-100 or 0.5% saponin), *see* **Note 6**. Process the coverslips by indirect immunofluorescence assay (212) to monitor transfection efficiency (use an antibody against Myc) and biotin labeling (use a fluorescent streptavidin conjugate; e.g., Streptavidin-488 Jackson ImmunoResearch Laboratories Inc., 016-540-084).
    a. If the transfection efficiency is too low or biotinylation is not sufficient, discard the samples and repeat.
    b. It is also important to monitor localization of the BirA*-protein fusion in uninfected cells to ensure the addition of BirA* is not disrupting the protein's normal localization.
    c. See Fig. 2-1A for an example of an indirect immunofluorescence assay of a BioID labeling experiment using a host protein normally found within the Golgi, syntaxin 10, which has been previously shown to localize to the chlamydial inclusion (146) with a C-terminal BirA* fusion. In infected cells, the exogenously expressed syntaxin 10–BirA* can be seen around the inclusion, while in mock infected cells the syntaxin 10-BirA* is found in the Golgi. Biotinylated proteins are co-localized with syntaxin 10-BirA* in both infected and uninfected cells.
8. Continue with sample collection and affinity purification, see protocol 3.4.8. (The processing for BioID and APEX2 cell lysate converges at this step).

3.4 Proximity labeling using APEX2 constructs

1. Seed HeLa 229 cells (*see* **Note 1** and **Note 2**) in a 6-well plate (1 x 10^6 cells/well) in biotin-free media (DMEM) supplemented with 1% heat inactivated FBS. *We decreased the FBS to deplete biotin levels in HeLa cells.* Seed one 6-well plate per condition/control sample. Place one glass coverslip in two separate wells of the 6-well plate to determine the expression level of the APEX2 construct and biotin labeling efficiency by immunofluorescence. It is important to include the appropriate negative controls for endogenous biotinylated proteins in both the host cell and *Chlamydia* (See Table 2- 2).
2. After the biotin limiting step (~24 hours), aspirate the media and infect the HeLa cells with the appropriate *C. trachomatis* L2 APEX2 strain or negative controls in DMEM +10% FBS (1 µg/mL cycloheximide, 10 µg/mL gentamicin, and the appropriate selective antibiotic). *We have found more robust biotinylation using 10 % FBS than with 1 % FBS with limited additional background biotinylation.*
3. Infect the HeLa cells by rocking, or by centrifugation at 400 x g for 15 min at room temperature, then transfer the plates to an incubator at 37 °C + 5% CO_2.
4. Induce expression of constructs at a pre-determined time post-infection (e.g., 7-10 hpi), by adding an optimized concentration of anhydrotetracycline (aTc) directly to the tissue culture media. *Ensure that induction conditions allow for the appropriate localization of the APEX2 fusion construct as over-expression can cause mislocalization.*
5. Add biotin-phenol (1.5 mM final concentration) to each well 30 minutes before the desired reaction time (e.g., 23.5 hpi for 24 hpi biotinylation time) and incubate for 30 min at 37 °C + 5% CO_2. Keep the biotin-phenol stock solution ≤ 50 mM in anhydrous DMSO for optimal solubility (*see* **Note 7**).

6. To catalyze the biotin labeling reaction, aspirate the media and add 2 mL/well of 3 mM H_2O_2 in PBS. Incubate the samples at room temperature for 1 minute, with rocking. *We have found that labeling two to four plates at a time is manageable. If there are greater than five 6-well plates in the experiment, stagger the infection times.*
7. After the labeling step, aspirate the H_2O_2 solution. Quench the labeling reaction with 3 x 1 mL/well washes using the quenching wash solution (10 mM sodium ascorbate, 10 mM sodium azide, 5 mM Trolox in dPBS (*see* **Note 8**)). Use gentle rocking during washes (approximately 15-30 seconds). After the washes, add 2 mL/well of PBS and then remove the coverslips for fixation to confirm construct expression via indirect immunofluorescence microscopy. This can be done using a fluorescent streptavidin conjugate, anti-FLAG antibody (FLAG is in N-terminus of APEX2), and other appropriate cell markers using the methods described above (**See section 3.3.7**) (*see* **Note 6**). An example is provided in Fig. 2-1B of biotinylation at the inclusion membrane using an Inc fused to APEX2 compared to APEX2 only which lacks the type III secretion signal and thus biotinylation appears to localize with the individual *Chlamydiae*.
8. Immediately after the coverslips are removed, scrape the remaining cells and pipet into a 15 mL conical tube on ice (12 mL total volume per 6-well plate). Pellet the cells by centrifugation at 900 x g for 10 minutes at 4 °C. *Keep these steps at 4 °C and move quickly to limit protease activity.*
9. Aspirate the supernatant and re-suspend the pellet in 1 mL of modified RIPA buffer per sample (The modified RIPA contains a protease inhibitor cocktail and Clastolactacystin β-lactone, which specifically inhibits the chlamydial protease-like activity factor (CPAF) (68) (*see* **Note 9**). Transfer the lysate to a 1.5 mL tube for

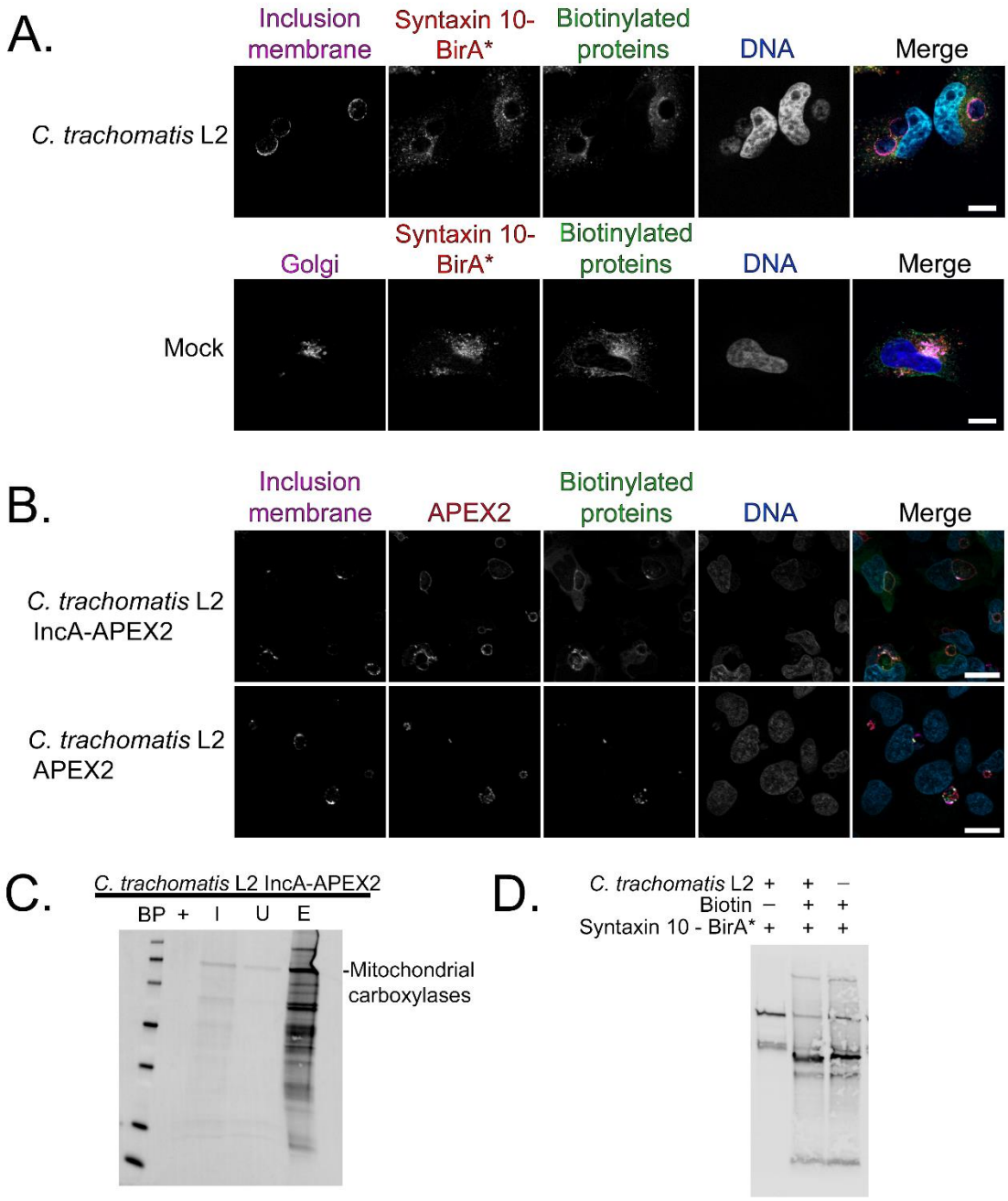

Figure 2-1. Confirmation of BioID and APEX2 specific biotinylation using indirect immunofluorescence assays and western blotting.

(continued on the next page)

Figure 2-1. Confirmation of BioID and APEX2 specific biotinylation using indirect immunofluorescence assays and western blotting.

A) HeLa cells transfected with Syntaxin10-BirA* were mock-infected or infected with *C. trachomatis* L2 in media supplemented with 50 µM biotin to catalyze the labeling of proximal proteins with biotin. Cells were fixed at 23 hours post infection and processed for immunofluorescence to visualize the inclusion membrane in infected cells (anti-IncA, pink) or the Golgi in uninfected cells (anti-Giantin, pink), expression of Syntaxin10-BirA* (anti-Myc, red), biotinylated proteins (streptavidin-488 conjugate, green) and DNA (DAPI, blue). Images were taken at 100x magnification using a Zeiss Apotome 2.1. Scale bar = 10 µm.

B) HeLa cells infected with *C. trachomatis* L2 transformed with IncA-APEX2 or APEX2 only and induced with anhydrotetracycline (aTc) at 7 hpi. Biotin-phenol was added 30 min prior to the biotin labeling step at 24 hpi. Biotinylation was catalyzed by the addition of 3 mM H_2O_2 for 1 min and washed with a quenching solution. Coverslips were fixed and processed for immunofluorescence to visualize the inclusion membrane (anti-CT223, pink) expression of the construct (anti-Flag, red), biotinylated proteins (streptavidin-488 conjugate, green), and DNA (DAPI, blue). Coverslips were imaged using a Zeiss with Apotome 2.1 63x Scale bar = 20 µm.

C) Lysates were collected from *C. trachomatis* L2 IncA-APEX2 infected HeLa cells treated with biotin phenol and the biotinylation reaction was catalyzed to label proximal proteins. The total solubilized lysate (input; I), unbound fraction (U), and eluate fraction (E) from the streptavidin affinity purification were separated by SDS-PAGE and transferred to a PVDF membrane. To determine if biotinylated proteins were affinity purified, membranes were blotted with a streptavidin-680 conjugate. Images were taking using an Azure c600.

D) Lysates were collected from HeLa cells transfected with Syntaxin10–BirA* and infected with wild-type *C. trachomatis* L2 (or not), in the presence (or not) of 50 µM Biotin to induce biotin-labeling of proteins proximal to syntaxin 10 with BirA* (as shown in part A). Lysates were affinity purified using streptavidin magnetic beads and eluates were resolved by SDS-PAGE, transferred to a PVDF membrane, and were blotted for biotinylated proteins using a streptavidin-680 conjugate. Images were taking using an Azure c600.

Figure modified from Olson et al. 2019. MiMB.

sonication. *These tubes work well for the sonication step to prevent excessive foaming of the sample.*

10. To solubilize the lysate, sonicate samples 3 times for 20 seconds at 20% amplitude. *Keep the microtip near the bottom of the 1.5 mL tube to prevent foaming.*
11. After sonication, incubate the samples on ice for 90 minutes. Vortex the samples every 30 minutes.
12. Clarify the lysate by centrifuging at 14,000 x g for 10 minutes at 4 °C. Transfer the supernatant (soluble protein fraction) into a fresh tube and re-suspend the pellet (insoluble protein fraction) in 400 µL modified RIPA. *If a large pellet remains, sonicate the samples (step 11) again. Using the above described conditions, the pellet is almost non-existent.* Save each fraction and make a small aliquot (e.g., 50 µL). Store samples at - 80 °C until protein quantification, western blot confirmation of protein biotinylation, and affinity purification steps are performed.

3.5 Affinity Purification of Biotinylated Proteins

1. Using the small aliquot, quantify the protein from each sample condition collected. *We use the EZQ Protein Quantification Kit (ThermoFisher) as it is compatible with high detergent levels in the modified RIPA lysis buffer and only requires on a few microliters of sample (< 5 µL).*
2. Normalize the solubilized lysate prior to SDS-PAGE and western blot analysis (e.g., 1 mg/mL).
3. Analyze the solubilized lysate by standard denaturing gel and western blot techniques, See Chapter 5 Western Blotting: An Introduction (213); for gel electrophoresis and western blotting conditions, in brief: Load the normalized lysate mixed with sample buffer into a 4-20% gradient polyacrylamide gel and

electrophorese at 200 volts for 30 minutes, or as desired. To transfer for western blotting, soak the polyvinylidene (PVDF) membrane in methanol, then place in transfer buffer. Assemble the gel sandwich by placing one blotting pad at the base of the transfer cassette. Then place the polyacrylamide gel on the blotting pad, followed by the membrane. Place a second blotting pad on top of the membrane and close the cassette and load it into the wet transfer system, with the membrane closest to the positive electrode and transfer as desired (e.g., 100 V for 48 min with cold pack).

   a. Confirm that biotinylated proteins are present in the soluble fraction and not in the insoluble fraction by blotting the membrane with using a streptavidin conjugate (e.g., streptavidin-680 conjugate; Li-Cor Biosciences) in blocking buffer (e.g., 5% BSA in PBST (PBS + 0.1% Tween-20)) (*see* **Note 13**). After incubating with the streptavidin conjugate, wash the membrane with PBST three times for five minutes at room temperature with rocking. Then perform a final wash step in PBS only (five minutes) and image using the preferred imaging system.

4. Affinity purify the biotinylated proteins from solubilized lysate using streptavidin beads, (*see* **Note 10**). Vortex the beads to re-suspend them, then aliquot 100 µL of the streptavidin magnetic beads (10 mg/mL stock) per sample condition into a 1.5 mL tube for affinity-purification.
5. To equilibrate the streptavidin magnetic beads, add 1 mL of RIPA (modified with 5% Triton X-100 and 1% SDS) to each tube.
6. Rotate the beads for 5 minutes at room temperature using a tube rotator.
7. Pellet the beads using a magnetic rack or handheld magnet and remove the supernatant.

8. Repeat once more for a total of two washes. Remove the liquid immediately before adding soluble lysate to prevent the beads from drying out, (*see* **Note 12**).
9. After the beads are equilibrated, add the solubilized lysate (1 mg/mL; 1 mL total volume/tube) and rotate the samples for 1.5 to 2 hours at room temperature or overnight at 4 °C.
10. After the affinity-purification incubation step, pellet the beads using the magnetic rack and SAVE the unbound fraction. By western blot, confirm that the biotinylated proteins were affinity purified from the solubilized lysate and do not remain in the unbound fraction (Fig. 2-1C).
11. Perform the following washes to remove non-specific proteins from the streptavidin beads. Incubate in the indicated wash buffer for 5 minutes at room temperature on a rotator. Pellet the beads between each wash using the magnetic rack (*see* **Note 12**):
    i. 2 washes x wash buffer A (1 mL RIPA buffer (plus 1% SDS, 5% Triton X-100, 500 mM NaCl)
    ii. 1 wash x wash buffer B (1 mL 2 M urea in 10 mM Tris-HCl (pH 7.4))
    iii. 2 washes x 1 mL RIPA buffer (unmodified)
12. After the final wash, remove all residual liquid and elute the biotinylated proteins directly in 2X Laemmli sample buffer (containing 5 % β-mercaptoethanol, 3 mM biotin), (*see* **Note 11**). Elute the biotinylated proteins from the streptavidin magnetic beads with 40 µL of sample buffer per tube.
13. Rotate the beads for 5 minutes with the elution buffer, then boil at 95 °C for 4 minutes, (*see* **Note 20**).
14. Pellet the beads using the magnet and transfer the eluate to a new tube. Save the leftover beads in case they are needed to test/troubleshoot elution conditions, (*see* **Note 10**).

3.6.1 Confirmation of Protein Biotinylation and Mass Spectrometry Identification.

(see **Note 21**)

1. Electrophorese until the desired separation is reached (e.g., 200 Volts ~50 min for a midi gel).
2. Transfer to membrane for blotting following typical transfer methods, in brief: Soak the PVDF membrane in methanol, then place in transfer buffer. Assemble the gel sandwich by placing one blotting pad at the base of the transfer cassette. Then place the polyacrylamide gel on the blotting pad, followed by the membrane. Place a blotting pad on top of the membrane and close the cassette and load it into the wet transfer system. Place the side with the membrane closest to the positive electrode and transfer as desired (e.g., 100 V for 48 min with cold pack).
3. Blot for biotinylated proteins using a streptavidin conjugate (Fig. 2-1C, D) (e.g., streptavidin-680 in 5% BSA in PBST for 2 hours at room temperature or overnight), (*see* **Note 13**).

3.6.2 Gel electrophoresis for mass spectrometry identification of biotinylated proteins

1. Use pre-cast gels to reduce keratin contamination (e.g., 4-20% gradient midi Criterion gels, BioRad, 5671093) for samples intended for mass spectrometry analysis.
2. Electrophorese the samples for 10-15 min, or about ~5.0 cm into the gel. *This reduces the area of gel sections which helps the efficiency of the digestion in downstream processing steps for mass spectrometry.*
    a. While the gel is running, use 30% methanol (*see* **Note 15**) to remove keratin and other contaminants to clean the Coomassie gel staining container.

3. Remove gel from the cassette and add the Coomassie stain solution; incubate for one hour at room temperature, (*see* **Note 14**).
4. Destain the Coomassie gel overnight at 4 °C with gentle rocking using the destain solution. Perform additional wash steps as needed to remove excess Coomassie, leaving as little stain remaining as possible.
5. Cut the gel pieces in a biosafety cabinet (or area with dead space, away from vents which are a major source for keratin contamination) and place in tubes that have not been autoclaved, (*see* **Note 15)**.
6. Submit the gel samples to the mass spectrometry core facility for processing and mass spectrometry identification of affinity purified biotinylated proteins (*see* **Note 16**).
7. Use the appropriate statistical analysis program to accurately assess background biotinylated proteins from the proximal proteins identified and prevent bias. For example, Significance Analysis of Interactome (SAINT; (207)) uses Bayesian statistics to calculate the probability that a protein is real in test samples compared to designated control samples, (*see* **Note 17**).

3.7 DAB Staining for Electron Microscopy

Day 1: Seed Cells. Place 25 mm plastic coverslips in the wells of a 6-well cell tissue culture plate. Seed 1.0 x 10^6 HeLa 229 cells per well in DMEM + 10% FBS (*see* Note 1 and Note 2). Incubate in a CO_2 incubator set at 37° C and 5% CO_2 for approximately one day.

Day 2: Infect and Induce. The next day, verify that the number of cells doubled using a light microscope. Aspirate the old cell culture growth media from the wells. Immediately replace the old media with fresh DMEM + 10% FBS supplemented with 1 µg/mL cycloheximide and 1-2 U/mL penicillin G for wells to be infected with transformed *Chlamydia* strains and 1 µg/mL cycloheximide only for wells to be infected with wild type

Chlamydia (*see* Note 18). Replacing the media immediately after aspiration is important to ensure cells do not dry out and become stressed.

1. Thaw *Chlamydia* strains to be used for infection on ice (*see* **Note 22**) using controls indicated in Table 2- 2.
2. Infect with a multiplicity of infection of 0.75 *Chlamydia* cells per host cell for transformed strains and 0.4 for the wild type strain. The transformed *Chlamydia* strains are used at a higher multiplicity of infection than the wild type strain because they may not infect as efficiently.
3. Tilt the plate back and forth and side to side to distribute the *Chlamydia* organisms throughout the cell layer. Centrifuge the plate at 400 x g for 15 minutes. The plate is centrifuged to aid attachment to and infection of the host cells by the *Chlamydia* cells. Incubate the plate at 37° C and 5% CO_2 for 7 hours.
4. At 7 hours post infection (hpi), pipette anhydrotetracycline into the wells to induce expression of APEX2 constructs. The optimal concentration must be determined empirically. In one example, APEX2 expression is induced at 7 hpi to maximize construct expression. The final concentration of anhydrotetracycline we used was 5.0 nM for some constructs and lower concentrations for one of the constructs (57).
5. Tilt the plate back and forth and side to side to distribute the anhydrotetracycline throughout the wells.
6. Incubate the plate at 37° C and 5% CO_2 until 24 hpi.

Day 3: Process for TEM (*see* **Note 23** and **Note 24**)

7. At 24 hpi, aspirate the media from the wells.

8. Wash the wells once with DPBS that has been prewarmed in a 37° C water bath.
9. Aspirate the DPBS.
10. Fix the samples by applying a solution of room temperature 2% paraformaldehyde, 2% glutaraldehyde, 0.1 M sodium cacodylate buffer to the wells.
11. Place the plate on ice for 1 hour to fix the cells.
12. Aspirate the fixative from the wells.
13. Wash the wells five times for 2 minutes each time with cold 0.1 M sodium cacodylate. Keep the plate on ice during the washes.
14. Block the samples by applying a solution of cold 20 mM glycine in 0.1 M sodium cacodylate, 2 mM $CaCl_2$ for 5 minutes. Keep the plate on ice.
15. Wash the wells five times for 2 minutes each time with cold 0.1 M sodium cacodylate. Keep the plate on ice during the washes.
16. Pretreat the samples with a solution of DAB that does not contain H_2O_2 by applying a solution of cold 0.5 mg/mL DAB, 0.1 M sodium cacodylate, 2 mM $CaCl_2$ for 30 minutes (*see* **Note 25**). Keep the plate on ice. As a negative control, do not apply this solution to one of the samples infected with a *Chlamydia* strain transformed with an APEX2 construct. Rather, apply a solution of cold 0.1 M sodium cacodylate instead.
17. Aspirate the solutions from the wells.
18. Treat the samples with a solution containing both DAB and H_2O_2 by applying a solution of cold 0.5 mg/mL DAB, 3 mM H_2O_2, 0.1 M sodium cacodylate, 2 mM $CaCl_2$ for 30 minutes. Keep the plate on ice. For the negative control that is not supposed to receive DAB or H_2O_2, apply a solution of cold 0.1 M sodium cacodylate instead.

19. Aspirate the solutions from the wells. Wash the wells five times for 2 minutes each time with cold 0.1 M sodium cacodylate. Keep the plate on ice.
20. The samples are then processed by an EM Facility. Briefly, the cells are post-fixed with osmium tetroxide, stained with Toluidine Blue (to see the cells during processing), dehydrated with a series of increasing ethanol concentrations, embedded, sectioned, stained with uranyl acetate, stained with Reynold's lead citrate, and visualized via TEM using an FEI Tecani G2 Spirit transmission electron microscope. See Fig. 2-2 for TEM images of DAB staining in HeLa cells infected with APEX2 fusion constructs.

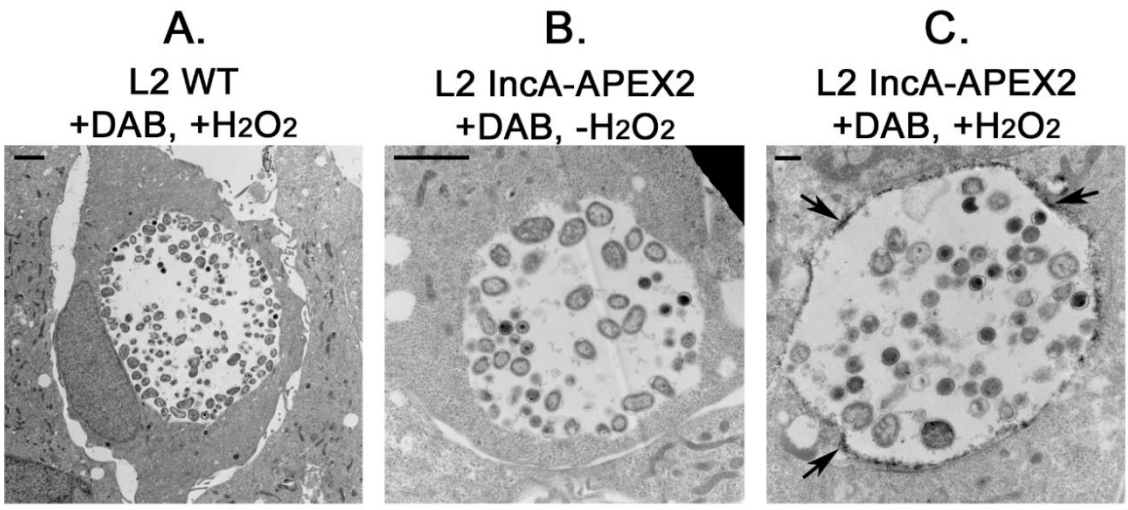

Figure 2-2. DAB staining of the inclusion membrane by *C. trachomatis* serovar L2 IncA-APEX2

Wild type *C. trachomatis* serovar L2 (L2 WT)-infected HeLa 229 cells treated with DAB and H_2O_2 (A) and *C. trachomatis* serovar L2 *IncA-APEX2* (L2 IncA-APEX2) -infected HeLa 229 cells not treated with DAB or H_2O_2 (B) do not demonstrate DAB staining of the inclusion membrane. L2 IncA-APEX2 -infected HeLa 229 cells treated with DAB and H_2O_2 (C) demonstrate DAB staining at the inclusion membrane as evidenced by the presence of the black polymer. Arrows point to examples of the DAB polymer. Scale bars (upper left corner) represent 2 µm in (A) and (B) and 0.5 µm in (C).

Figure modified from Olson et al. 2019. MiMB

4. Notes

1. HeLa cells at higher passage numbers tend to demonstrate decreased biotinylation compared to lower passage number HeLa cells. For best results, use HeLa cells between passage 3 and passage 16 after cells are cultured from frozen stocks. In addition, when transfecting HeLa cells with exogenous DNA (i.e. BioID constructs), all media should be antibiotic free as addition of antibiotics to tissue culture medium can negatively affect the transfection efficiency. If HeLa cells are routinely passaged in media containing antibiotics, passage the cells in medium without antibiotics at least twice before starting the BioID labeling experiments.
2. Routinely test your cells for *Mycoplasma* contamination using a *Mycoplasma* test kit. We test our cells with each fresh vial and/or once a month.
3. When creating BioID (BirA*) fusions, consideration must be made when choosing to position BirA* on either the N or C termini of your protein of interest. Thus, it is important to know the domains of your protein of interest and understand that the addition of BirA* could disrupt its function/localization. For example, we have created a construct containing *BirA** fused to the N-terminus of *syntaxin 6* (199), a host *trans*-Golgi network (TGN) protein, since it contains an C-terminal transmembrane domain. This positioning would help ensure the addition of BirA* would not disrupt its normal transmembrane localization within TGN-derived membranes.
4. The stock of 1mM biotin in serum free 1X DMEM for BioID labeling experiments is stable for 8 weeks stored at 2-8°C. Dilutions to 50 µM in 1XDMEM + 1% FBS should be made the day of the biotin-labeling experiment for best results.
5. Prior to affinity purification experiments using BioID constructs, it is critical to troubleshoot transfection conditions using your preferred transfection reagent

(amount of DNA, amount of transfection reagent, and cell density) in a 6-well tissue culture plate following the recommendations from the manufacturer. Different constructs will have different parameters for transfection, so it is important to troubleshoot each construct individually to maximize transfection efficiency. Each experimental condition uses a full 6-well plate to ensure proteins are at a high enough concentration for affinity purification and identification via mass spectrometry.

6. Use consideration when determining what type of fixation solution and permeabilization reagent for immunofluorescence assays to use that will best capture the proteins you are interested. We use a 4% paraformaldehyde solution for 15 minutes at room temperature followed by permeabilization with 0.1% Triton X-100 in 1X PBS for 5 minutes at room temperature since the proteins we are interested in are normally localized within the Golgi and we want to preserve organelle/Golgi structure. Other techniques using methanol as a fixative can disrupt the structure of lipid membranes/organelles. Furthermore, cell components have been shown to be inside the inclusion after fixation when they are not present during live-cell imaging (214).
7. Both the solubilization reagent used and the stock concentration of biotin-phenol is important to obtain efficient biotinylation during the labeling reaction step. We have observed the most efficient biotinylation using anhydrous DMSO (AnDMSO) to solubilize biotin-phenol immediately prior to the experiment (or ≤3 months at -20 °C). We also observe the best results when our stock biotin-phenol kept at 50 mM in AnDMSO rather than higher concentrations, which may affect the solubility of biotin-phenol.
8. Trolox can be difficult to make as it requires several steps and has limited solubility (max solubility 100 mM). To make 100 mM Trolox: In a 15 mL conical tube mix

0.1 g Trolox with 0.43 mL of methanol and vortex vigorously until Trolox is in solution. After Trolox is in solution, add 3.2 mL of water and the sample will change color accompanied by an expansion in volume (it will have a cement like consistency). To get the Trolox back into solution, add 0.36 mL of 1 M sodium hydroxide and mix well by vortexing; adding more in small amounts as necessary. When the solution reaches pH 9.0-9.5, the Trolox will go into solution and should be slightly yellow. Store at -20 °C until use. Scale up as desired for larger volumes of 100 mM Trolox. We routinely make 45 mL of 100 mM Trolox at a time.

9. Clastolactacystin β-lactone is soluble in methyl acetate and anhydrous DMSO (AnDMSO). Methyl acetate can be harmful to the cells. If purchased in methyl acetate, evaporate the methyl acetate with nitrogen gas and resuspend Clastolactacystin β-lactone in AnDMSO. Be aware that high DMSO concentrations can affect eukaryotic cell viability. To reduce this possibility, we resuspend Clastolactacystin β-lactone at 23 mM in AnDMSO. In an aqueous solution, Clastolactacystin β-lactone is only stable for one day, so dilute in RIPA buffer the day of sample collection, but it is stable in AnDMSO at -20°C.

10. We prefer to use Pierce streptavidin magnetic beads (cat# 88816) as they have a high binding capacity. Other brands will likely work, but you will have to optimize the input concentration and elution conditions. In most cases boiled beads cannot be re-used for affinity purification experiments.

11. Use premade/high grade Laemmli sample buffer (e.g., 2X Sample Buffer, BioRad, 1610737) if intended for mass spectrometry.

12. To minimize the loss of beads during the pipetting steps, hold a strong magnet directly next to the tube while removing supernatant (e.g., washes/unbound fraction).

13. We have found that 5 % milk in PBST greatly reduces background for visualization of most antibodies; however, streptavidin conjugates work best using 5% BSA in PBST.

14. Do not exceed one hour for the Coomassie staining. Over-staining the gel can interfere with the downstream processing steps prior to the mass spectrometry analysis.

15. Autoclaving is significant source for keratin contamination; rinse empty the tubes with 30% methanol as an extra wash step to remove contaminants.

16. Work with your preferred core facility to design a digestion and mass spectrometry protocol. We have found a double digestion with Trypsin and AspN proteases improves the detection of membrane proteins. We also use a more sensitive mass spectrometer (Orbitrap Fusion ™ Lumos™; Thermo Scientific) the to increase the resolution of peptides detected.

17. SAINT is freely available and uses output files from Scaffold (Scaffold, http://www.proteomesoftware.com/products/free-viewer) to construct the SAINT files for statistical analysis.

18. Cycloheximide inhibits host cell protein synthesis; the media is supplemented with it to aid the growth of transformed *Chlamydia* strains. Penicillin G is added to select for the *Chlamydia* harboring the plasmid as the plasmid used for transformation contains the gene for beta-lactamase. Consequently, untransformed *Chlamydia* organisms will present as large, aberrant cells in the presence of penicillin G while transformed organisms will show normal morphology. For this reason, penicillin G is not added to the media of the wild type-infected sample. The concentration of penicillin G must be determined empirically.

19. *APEX2* can either be positioned at the N-terminus or the C-terminus of the gene of interest based on functions of the expressed proteins. For example, inclusion

membrane proteins (Incs) have an N-terminal type III secretion signal (58), so *APEX2* was placed at the C-terminus to avoid interfering with secretion.

20. Perform a quick centrifugation step before loading the eluate sample into a polyacrylamide gel.

21. This section describes gel electrophoresis and western blotting methods to confirm sample biotinylation and preparation of samples for mass spectrometry analysis. After confirming biotinylation by western blot, to identify the biotinylated proteins, we recommend separating the sample briefly by electrophoresis and cutting the Coomassie stained gel into sections. This is preferred over digesting the biotinylated proteins directly off the beads or sending the entire eluate for mass spectrometry analysis; both can cause significant streptavidin background. Sectioning the gel enhances the resolution of peptide identification during mass spectrometry analysis. This is especially important when looking for chlamydial proteins in complex eukaryotic cell background.

22. Be sure to have one cell sample infected with wild type, untransformed *Chlamydia* as a negative control, one cell sample infected with a strain of *Chlamydia* transformed with an APEX2 construct that will not receive DAB or H_2O_2 treatment later as another negative control, and one or more strains of *Chlamydia* transformed with APEX2 constructs as the experimental samples.

23. The TEM protocol is adapted from Martell et al. 2017 (71).

24. Every time a solution is placed in the wells, lift the coverslips slightly using a sharp object, such as a needle, to allow that solution to flow underneath the coverslips.

25. Pretreatment with a solution containing DAB but not H_2O_2 may not be necessary depending on the situation. In our experience, we have seen better DAB labeling when samples are pretreated in comparison to samples that are not. Pretreatment allows the DAB molecules to diffuse into the cells (209).

5. Acknowledgments

We would like to thank Scot Ouellette for critical reading of the manuscript. We would also like to thank Tom Bargar and Nicholas Conoan of the Electron Microscopy Core Facility (EMCF) at the University of Nebraska Medical Center for technical assistance. The EMCF is supported by state funds from the Nebraska Research Initiative (NRI) and the University of Nebraska Foundation, and institutionally by the Office of the Vice Chancellor for Research. This work is supported by NIH/NIAID R01 AI114670 (E. Rucks) and UNMC Department of Pathology and Microbiology start-up funds (E. Rucks).

Chapter 3 - Proximity Labeling to Map Host-Pathogen Interactions at the Membrane of a Bacterium-Containing Vacuole in *Chlamydia trachomatis*-Infected Human Cells

Macy G. Olson, Ray E. Widner, Lisa M. Jorgenson, Alyssa Lawrence, Dragana Lagundzin, Nicholas T. Woods, Scot P. Ouellette, and Elizabeth A. Rucks. 2019. Proximity Labeling to Map Host-Pathogen Interactions at the Membrane of a Bacterium-Containing Vacuole in *Chlamydia trachomatis*-Infected Human Cells. Infection and Immunity.

Abstract

Many intracellular bacteria, including the obligate intracellular pathogen *Chlamydia trachomatis*, grow within a membrane-bound “bacteria containing vacuole” (BCV). Secreted cytosolic effectors modulate host activity, but an understanding of the host-pathogen interactions that occur at the BCV membrane is limited by the difficulty in purifying membrane fractions from infected host cells. We used the ascorbate peroxidase proximity labeling system (APEX2), which labels proximal proteins with biotin *in vivo*, to study the protein-protein interactions that occur at the chlamydial vacuolar, or inclusion, membrane. An *in vivo* understanding of the secreted chlamydial inclusion membrane protein (Inc) interactions (e.g., Inc-Inc and Inc-eukaryotic protein) and how these contribute to overall host-chlamydial interactions at this unique membrane is lacking. We hypothesize some Incs organize the inclusion membrane whereas other Incs bind eukaryotic proteins to promote chlamydial-host interactions. To study this, Incs fused to APEX2 were expressed in *C. trachomatis* L2. Affinity purification-mass spectrometry (AP-MS) identified biotinylated proteins, which were analyzed for statistical significance using Significance Analysis of INTeractome (SAINT). Broadly supporting both Inc-Inc and Inc-host interactions, our Inc-APEX2 constructs labeled Incs as well as known and previously unreported eukaryotic proteins localizing to the inclusion. We demonstrate that endogenous LRRFIP1 (LRRF1) is recruited to the inclusion by the Inc, CT226, using bacterial two-hybrid and co-immunoprecipitation assays. We further demonstrate interactions between CT226 and the Incs used in our study to reveal a model for inclusion membrane organization. Combined, our data highlight the utility of APEX2 to capture the complex *in vivo* protein-protein interactions at the chlamydial inclusion.

Introduction

To capture dyanamic *in vivo* protein-protein interactions, including Inc-Inc interactions at the chlamydial inclusion, we were the first to use and characterize the feasibility, including important caveats, of using the ascorbate peroxidase proximity labeling system (APEX2) to identify Inc binding partners in the context of *C. trachomatis* infection (57). APEX2 has also recently been utilized by others in the field (with noted differences described in Discussion, (170)). APEX2, a mutated soybean peroxidase (168, 193), can be fused to a protein of interest and activated during a short (one minute) reaction to covalently modify proximal proteins with a biotin molecule (193). This system can be used to capture *in vivo* “snapshots” of the dynamic protein-protein interactions that occur at the chlamydial inclusion during development. Incs fused to APEX2 are secreted by *C. trachomatis* and inserted in the inclusion membrane (57). Proteins proximal to the expressed Inc-APEX2 fusion protein are covalently modified with biotin after the addition of biotin-phenol and hydrogen peroxide to catalyze the APEX2 biotinylation reaction (57). An additional advantage of using APEX2 to identify Inc protein binding partners is the ability to use high concentrations of detergent to solubilize hydrophobic membrane proteins, like Incs, because there is no need to maintain binding partners after the covalent addition of biotin to neighboring proteins (57). Subsequently, the cells are lysed, and the biotinylated proteins are affinity purified using streptavidin beads and identified using mass spectrometry (AP-MS).

We applied APEX2 to test our hypothesis using two Incs, IncF and IncA. IncF may be primarily involved in organizing the inclusion because it has been shown to interact extensively with other Incs via BACTH studies (105) and is expressed early after infection (102). IncA may primarily interact with eukaryotic proteins as it contains a eukaryotic SNARE-like domain (145) and has been shown to bind fewer Incs by the same BACTH

studies (105). We also created a truncated IncA ($IncA_{TM}$) to interrogate if removal of the C-terminal domain of IncA would alter the specificity of proteins labeled by this construct (57). Using the APEX2 proximity labeling system, we tested these interactions *in vivo* by transforming *C. trachomatis* serovar L2 with Inc-APEX2 fusion constructs that localize to the inclusion membrane when expressed (57). These experiments have helped define novel Inc-protein binding partners and whether Incs collaborate to support chlamydial development within the inclusion.

We carefully designed our experiments to (i) inducibly express Incs which localize in a pattern that resembles their endogenous form in an effort to detect protein-protein interactions in the most “natural” conditions, (ii) control for background contaminant proteins, and (iii) statistically analyze the mass spectrometry interaction data in an unbiased manner to determine the probability of a “true” protein interaction. In regards to the latter point, our AP-MS data were analyzed for statistical significance using a Bayesian-based statistical analysis tool, Significance Analysis of INTeractome (SAINT) (207). In each Inc-APEX2 dataset, we identified chlamydial Inc proteins that were statistically significant, and we also identified eukaryotic proteins that had been previously shown to localize with the chlamydial inclusion. Importantly, we identified previously undescribed eukaryotic proteins at the inclusion membrane. Leucine-Rich Repeat Flightless-Interacting Protein 1 (LRRF1) was identified in all of our Inc-APEX2 datasets and has been identified in other AP-MS studies (122, 170, 171). We also identified a LRRF1 binding partner, Protein Flightless 1 homolog (FLII), in our IncA-APEX2 dataset, indicating that we were also identifying partial signaling pathways.

The presence of LRRF1 in our datasets gave us the opportunity to ask why this is a prominently identified protein in ours and others’ AP-MS studies. We were skeptical that one protein was a true interactor with every single one of our Inc-APEX2 constructs.

Therefore, we designed a series of experiments to help us understand how LRRF1 was identified, either through direct interaction with one of our Inc-APEX2 constructs or interaction with an adjacent Inc, but within the labeling radius of our Inc-APEX2 constructs. For the first time, we demonstrate that endogenous LRRF1 and FLII localize with the chlamydial inclusion. LRRF1 localization with the inclusion was conserved between closely related *C. trachomatis* serovars and strains. By bacterial two-hybrid assay, LRRF1 was found to interact with the Inc, CT226, which is consistent with a previous study which identified LRRF1 and FLII by transfecting Strep-tagged CT226 into uninfected eukaryotic cells (122). We also performed a co-immunoprecipitation using CT226-FLAG expressed from *C. trachomatis* and identified LRRF1 in the eluate. Overall, our proximity labeling system has identified both known and previously unreported proteins at the inclusion membrane and highlights the utility of an *in vivo* proximity labeling system to identify protein-protein interactions and how they are recruited to the chlamydial inclusion membrane.

Methods

Antibodies and reagents

Primary antibodies used: mouse anti-FLAG (Sigma), rabbit anti-FLAG (Sigma), mouse anti-Giantin (Enzo), mouse anti-GAPDH (EMD Millipore), goat anti-MOMP (Meridian), rabbit anti-LRRF1 (Bethyl), rabbit anti-FLII (Thermo Fisher), rabbit anti-IncA (Kind gift from Ted Hackstadt, NIAID, Rocky Mountain Laboratories, Hamilton, MT), mouse anti-CT223 (Kind gift from R. Suchland, University of Washington, WA;, D. Rockey, Oregon State University, OR), mouse anti-*C. trachomatis* Hsp60 (a kind gift from Rick Morrison, University of Arkansas for Medical Sciences, Little Rock, AR), rabbit anti-*C. burnetii* (Elizabeth A. Rucks), mouse anti-*C. pneumoniae* AR39 (a kind gift from H. Caldwell, NIAID, Bethesda, MD). Secondary antibodies used for immunofluorescence

were each donkey anti-647, 594, 488, and 405, or streptavidin-488 conjugate. DRAQ5 and DAPI were used to visualize DNA as indicated. Western blots were visualized using the appropriate secondary antibodies conjugated to IRDye 680LT, or IRDye 800 CW (LiCor Biosciences, Lincoln, NE), and membranes were imaged using Azure c600 (Azure Biosystems, Dublin, CA) and processed using Adobe photoshop creative cloud (Adobe).

Organisms and cell culture

HeLa 229 cells [American Type Culture Collection (ATCC); Manassas, VA; CCL-2.1] were cultured at 37°C with 5% CO_2 in biotin-free DMEM (Gibco; Grand Island, NY) that was supplemented with 10% heat-inactivated fetal bovine serum (FBS; HyClone, Logan, UT), for routine tissue culture, or with 1% FBS, for experiments involving biotinylation as previously described (57) with 10 µg/mL gentamicin (Gibco-BRL/Life Technologies; Grand Island, NY). HeLa cells were used to propagate *Chlamydia trachomatis* serovar L2 (LGV 434) for purification using established protocols (215, 216). Chlamydial titers were determined using conventional protocols to establish multiplicities of infection (m.o.i.), based on inclusion forming units (i.f.u.) and determined in HeLa cells as previously described (216, 217). McCoy cells (ATCC; Manassas, VA; CRL-1696) were cultured at 37°C with 5% CO_2 in biotin-free DMEM (Gibco; Grand Island, NY) that was supplemented with 10% fetal bovine serum (FBS; HyClone, Logan, UT) used for *C. trachomatis* L2 (LGV 434) transformation experiments. HeLa cells, McCoy cells, and density-gradient purified *C. trachomatis* strains are routinely tested for *Mycoplasma* spp (Lookout Mycoplasma PCR Detection Kit, Sigma; St. Louis, MO). For some experiments, *C. trachomatis* serovar D (UW3-CX), *C. muridarum*, *C. caviae*, *C. pneumoniae* AR39, and *Coxiella burnetii* avirulent Nine Mile Phase II (provided by Bob Heinzen, Rocky Mountain Laboratories, Hamilton, MT) were used (48).

Creation of Inc fusion constructs for transformation into *C. trachomatis* L2

All primers used in this study are listed in Table S3-5. All plasmids and *E. coli* strains used in cloning projects are listed in Table S3-6. The Inc-APEX2 fusion constructs were made as previously described (57). pcDNA3 APEX2-NES was a gift from Alice Ting (Addgene plasmid # 49386) (189). APEX2 contains a single N-terminal FLAG tag. For the construction of IncF-FLAG, IncF with the C-terminal FLAG epitope was amplified from pTLR2 IncF-APEX2 (57) and cloned into pTLR2. CT226 was amplified from *C. trachomatis* L2 genomic DNA with primers containing a C-terminal FLAG tag and inserted into the mCherry site pBOMB4-Tet (EagI/KpnI) (a gift from Dr. T. Hackstadt, NIAID, Rocky Mountain Laboratories, Hamilton, MT) using NEBuilder HiFi Assembly Cloning Kit (NEBuilder). The final constructs were transformed into *dam*$^{-}$*/dcm*$^{-}$ *E. coli*. All constructs were confirmed by sequencing (Eurofins MWG Operon; Huntsville, AL).

Transformation of *C. trachomatis* L2

C. trachomatis L2 transformations were performed as described previously (116, 211). *C. trachomatis* L2 transformed with a plasmid that expresses the Inc-APEX2 constructs (57) were plaque purified as described elsewhere (116, 218) and density gradient purified. Both pTLR2-IncF-FLAG and pBOMB4-Tet-CT226-FLAG were transformed as above in the presence of 1 U/mL penicillin and 1 µg/mL cycloheximide.

Electron microscopy determination of APEX2 activity and localization

HeLa cells were seeded at 1.0 x 10^6 cells/well in a 6-well plate containing 25 mm Thermanox cell culture treated coverslips for electron microscopy (Nunc; Rochester, NY). To confirm construct expression using indirect immunofluorescence, glass coverslips were included in duplicate wells of a 24-well plate. Wells were infected with *C. trachomatis* L2 wild-type, or L2 transformed with a plasmid that expresses IncF-APEX2, $IncA_{TM}$-APEX2, IncA-APEX2, or APEX2 only. *C. trachomatis* L2 IncF-APEX2, $IncA_{TM}$-APEX2 (m.o.i. 0.75) were infected by centrifugation in DMEM + 10% FBS containing 2 U/mL

penicillin and 1 µg/mL cycloheximide. *C. trachomatis* L2 IncA-APEX2 and APEX2 only (m.o.i. 0.75) infected wells received 1 U/mL penicillin and 1 µg/mL cycloheximide. *C. trachomatis* L2 wild-type was infected (m.o.i. of 0.4) in DMEM + 10% FBS containing 1 µg/mL cycloheximide. At 7 hpi, the *C. trachomatis* L2 strains were induced with 0.3 nM aTc for the expression of IncF-APEX2, and 5 nM for all other strains and *C. trachomatis* L2 wild-type respectively. At 24 hpi, glass coverslips were fixed in 4% paraformaldehyde for 15 min at room temperature (RT) and methanol permeabilized for 5 min, then processed for immunofluorescence confirmation of construct expression as above.

The wells intended for electron microscopy were prepared using a protocol adapted from Martell et al. 2017 (209). Briefly, cells were washed with dPBS and fixing solution (2% glutaraldehyde, 2% paraformaldehyde in 0.1 M sodium cacodylate) was added to the wells and incubated on ice for 1 hour. All subsequent steps were performed on ice. The expressed APEX2 remains functional after fixing (using conditions below 4% formaldehyde). After 1 hour, the wells were washed 5 x 2 min with cold buffer A solution (0.1 M sodium cacodylate). To quench unreacted aldehyde groups, cold 20 mM glycine containing 2 mM $CaCl_2$ in wash buffer A was incubated with the cells for 5 min. The wells were washed 5 x 2 min with cold buffer A. To enhance diffusion of the large molecule, 3,3′-Diaminobenzidine (DAB), the cells were pre-treated with 0.5 mg/mL DAB in buffer A containing 2 mM $CaCl_2$ for 30 min prior to the polymerization step. The pre-treatment step allows the DAB to uniformly diffuse into the cells without being converted to the polymer (no H_2O_2 present). To catalyze the polymerization of DAB (regions proximal to APEX2) 0.5 mg/mL DAB and 3 mM H_2O_2 in buffer A containing 2 mM $CaCl_2$ was added to cells and incubated for 30 min. Negative controls to determine background activity included *C. trachomatis* L2 wild-type with DAB treatment and *C. trachomatis* L2 IncA-APEX2, induced, without DAB. Polymerized DAB is unable to diffuse from the subcellular compartment.

Finally, the wells were washed 5 x 2 min with cold buffer A and delivered to the University of Nebraska Medical Center electron microscopy core to be processed. In brief, the samples were post-fixed with 1% osmium tetroxide, stained with Toluidine Blue, dehydrated with a series of increasing ethanol concentrations, embedded and sectioned. Sections were placed on 200 mesh uncoated copper grids (Ted Pella Inc.), stained with uranyl acetate and Reynold's lead citrate, and examined using a Tecnai G2 Spirit (FEI) transmission electron microscope (TEM) operated at 80 Kv. Representative electron micrographs are shown.

FLAG affinity purification of APEX2 fusion constructs

HeLa cells were seeded in a 6-well plate in DMEM + 10% FBS and allowed to grow overnight. The cells were infected with *C. trachomatis* L2 IncF-APEX2, $IncA_{TM}$-APEX2, IncA-APEX2, or APEX2 only (m.o.i. 0.75) with DMEM + 10% FBS containing 1 µg/mL cycloheximide, plus appropriate antibiotics (2 U/mL penicillin for *C. trachomatis* L2 IncF-APEX2 and $IncA_{TM}$-APEX2, 1 U/mL penicillin for *C. trachomatis* L2 IncA-APEX2 and APEX2) and induced at 7 hpi with 0.3 nM aTc (IncF-APEX2 only; see (57) regarding lower induction levels), and 5 nM aTc (all other *C. trachomatis* L2 strains). The cell collection, lysis procedure, and FLAG affinity purification were performed essentially as previously described (219). Briefly, at 24 hpi, coverslips were removed from the respective wells, methanol fixed for 5 min at RT, and the remaining cells were scraped into dPBS and centrifuged at 900 × g for 10 min at 4°C. The pellets were resuspended in cell lysis buffer [50 mM Tris-HCl, pH 7.4, 150 mM NaCl, 0.5% sodium deoxycholate, 0.1% sodium dodecyl sulfate (SDS), 1% Triton X-100 (Sigma; St. Louis, MO), 1X HALT protease inhibitor cocktail (Thermo; Waltham, MA), universal nuclease (Pierce; Rockford, IL), and 150 µM Clastolactacystin-β-lactone (Santa Cruz Biotechnology, Dallas, TX)]. Equal volumes (EZQ protein quantification; Life Technologies, Carlsbad, CA) of clarified lysates were prepared

for FLAG affinity purification with FLAG magnetic beads (Sigma; St. Louis, MO) and rotated for 2 hours at 4° C. The affinity purified proteins were eluted in 30 µL of lysis buffer (above) containing FLAG peptide (200 µg/mL). The eluates from each sample were combined with an equal volume of 4x Laemmli sample buffer containing 5% β-mercaptoethanol and then loaded into a Criterion Midi 4-20% gradient SDS-PAGE (BioRad; Hercules, CA). The gel was transferred to PVDF (0.45 µm, Thermo Scientific; Waltham, MA) and blotted using anti-FLAG antibody to detect construct expression. Clarified lysate (used as the input for the FLAG affinity purification) was electrophoresed and transferred to PVDF to blot for chlamydial Hsp60 as a loading control.

Labeling with biotin-phenol and affinity purification of biotinylated proteins

To identify proteins that were biotinylated using *C. trachomatis* L2 IncF-APEX2, $IncA_{TM}$-APEX2, IncA-APEX2, and APEX2, HeLa cells were seeded into a 6-well plate in DMEM + 1% FBS for 1, 6-well plate per condition (e.g., one plate for L2 IncF-APEX2 for induced and one plate for uninduced etc.). To monitor construct expression and biotinylation, coverslips were placed in 2 of the wells of the 6-well plate. The biotinylation assays were performed essentially as previously described (57, 168, 193). The cells were infected with *C. trachomatis* L2 IncF-APEX2, $IncA_{TM}$-APEX2, IncA-APEX2, or APEX2 only (m.o.i. 0.75) with DMEM + 10% FBS containing 1 µg/mL cycloheximide, plus appropriate antibiotics (2 U/mL penicillin for *C. trachomatis* L2 IncF-APEX2 and $IncA_{TM}$-APEX2, 1 U/mL penicillin for *C. trachomatis* L2 IncA-APEX2 and APEX2), and centrifuged 400 × g at RT for 15 min. Penicillin and cycloheximide were present for all biotinylation experiments to preserve the integrity of our *C. trachomatis* L2 strains that were transformed with a plasmid and to minimize host cell background, respectively. The samples were induced for construct expression at 7 hpi with 0.3 nM aTc (IncF-APEX2 only; see (57) regarding lower induction levels) or 4 nM aTc (all other strains). At 23.5 hpi,

the cell monolayers were incubated with 1.5 mM biotinyl-tyramide (biotin-phenol) (AdipoGen, San Diego, CA) for 30 min at 37°C + 5% CO_2. At 24 hpi, the labeling process was catalyzed, quenched, and the lysate was collected as previously described (57). Normalized lysates (1 mg/mL) were added to equilibrated streptavidin magnetic beads (Pierce; Rockford, IL) and rotated for 90 min at RT. Proteins were eluted from streptavidin magnetic beads by 4 min incubation at 95 °C in 2x Laemmli sample buffer containing 0.5 mM biotin. The eluates were loaded into Criterion Midi 4-20% gradient denaturing gels (BioRad; Hercules, CA) in duplicate. The gel intended for Coomassie staining was resolved briefly (~2-3 cm), then stained (10% methanol, 5% acetic acid, Coomassie blue G). The duplicate gel, for western blot confirmation of affinity purification was resolved completely, transferred to PVDF (0.45 µm, Thermo Scientific; Waltham, MA) and blotted using the indicated primary antibodies, a streptavidin-488 conjugate (immunofluorescence) or streptavidin-680 conjugate (western blot), and appropriate secondary antibodies conjugated to IRDye 680LT, IRDye CW, or a streptavidin-IRDye 680LT conjugate (LiCor Biosciences, Lincoln, NE). The PVDF membranes were imaged using an Azure c600 (Azure Biosystems, Dublin, CA) and processed using Adobe photoshop creative cloud (Adobe).

Identification of biotinylated proteins using mass spectrometry

Coomassie-stained gels were imaged, then each lane was cut into six gel fractions to enhance the resolution of lower abundance proteins. The UNMC proteomics core facility performed in-gel digestion, preparation, and analysis of gel fractions. Protein fractions excised from the SDS-PAGE were destained, reduced with tris-carboxyethyl phosphine, alkylated with iodoacetamide, and were digested overnight with sequencing-grade trypsin (Promega; Madison, WI) and Asp-N (Promega; Madison, WI). Trypsin (cleaves Lys and Arg) and Asp-N endoproteinase (cleaves Asp and Cys residues). Peptides were eluted

from the gel and concentrated to 20 µL by vacuum centrifugation and analyzed using a high-resolution mass spectrometry nano-LC-MS/MS Tribrid system, Orbitrap Fusion™ Lumos™ coupled with UltiMate 3000 HPLC system (Thermo Scientific; Waltham, MA). Approximately 500 ng of peptides were run by the pre-column (Acclaim PepMap™ 100, 75µm × 2cm, nanoViper, Thermo Scientific; Waltham, MA) and the analytical column (Acclaim PepMap™ RSCL, 75 µm × 50 cm, nanoViper, Thermo Scientific; Waltham, MA). The samples were eluted using a 100-min linear gradient of Acetonitrile (2.5-45 %) in 0.1% Formic acid.

All MS/MS samples were analyzed using Mascot (Matrix Sciences, London, UK, vs. 2.6.). Mascot was set up to search the SwissProt database (selected for Homo sapiens, 2017_02, 20286 entries and *C. trachomatis* 434/Bu entries) assuming the digestion enzymes trypsin and AspN. Parameters on MASCOT were set as follows: Enzyme: Trypsin and Asp-N for biological replicates n=5, Max missed cleavage: 2, Peptide charge: 1+, 2+ and 3+, Peptide tolerance: ± 0.8 Da, Fixed modifications: carbamidomethyl (C), Variable modifications: oxidation (M) and biotin-phenol (C, Y, W, H). MS/MS tolerance: ± 0.6 Da, Instrument: ESI-TRAP. Proteins identified by Mascot search were uploaded into Scaffold for visualization of the identified proteins (Scaffold, Proteome Software, Inc. Portland, Oregon).

Statistical analysis of mass spectrometry samples using Significance Analysis of INTeractome (SAINT)

Significance Analysis of INTeractome (SAINT) was performed to assign statistical significance (Bayesian false discovery rate; BFDR) to our mass spectrometry data (207). SAINT calculates the probability that a protein identified in the test sample is a true interacting protein based on average hits in the test samples compared to the control in an unbiased fashion. Scaffold files containing each replicate (n=5) were set to 95% protein

threshold, 1 peptide minimum, and 95% peptide threshold, and the sample report was exported to an excel file. The sample report file was used to make three files required for SAINT analysis: bait, prey, and interaction (Table S3-1 and S3-3). The bait file corresponds to the sample condition (e.g., IncF-APEX2, replicate 1, Test condition) and assigns samples as either a test or control. For our dataset, the Inc-APEX2 biotinylated proteins via IncF-APEX2, $IncA_{TM}$-APEX2, IncA-APEX2 are the test, “T”, and the controls “C” were assigned to APEX2, L2 wild-type, and mock-infected HeLa cells. The prey file is the list of all the proteins from the Scaffold sample reports file using their gene names and amino acid length (obtained from UniProt). The last file required for SAINT is the interaction file which assigns the biological replicate number and spectral counts for each protein identified in the test subjects and the control samples. These files are input to calculate the Bayesian False Discovery Rate (BFDR) and were used to prioritize which proteins were statistically significant (207). We then input high confidence data (BFDR ≤0.05) into the pipeline to visualize interaction networks created using the STRING database (interaction confidence 0.7 STRING). The defined STRING networks were exported and analyzed using Cytoscape v 3.7.1 (220) with ClueGo to determine globally enriched biological processes and molecular functions within each dataset.

Transfection of LRRF1-GFP and FLII-GFP

LRRF1 detected by mass spectrometry corresponded to LRRF1 variant 3. To assess LRRF1 and FLII localization during *C. trachomatis* L2 infection, we obtained pCMV6-AC-LRRF1-GFP (LRRF1 variant 3; origene #RG226542; Rockville, MD) and pCMV6-AC-FLII-GFP (Origene # RG206863; Rockville, MD) respectively. For DNA transfections, 8×10^4 HeLa cells per well were seeded in a 24-well plate onto 12 mm glass coverslips. Approximately 24 hours later fresh DMEM + 10 % FBS (antibiotic free) was added to the cells. Transfection efficiency was first optimized using varying nanogram

amounts of pDNA and volumes of jetPRIME® transfection reagent (Polyplus; Illkirch, France). Optimal efficiency was determined at 100 ng of pCMV-LRRF1-GFP or 500 ng pCMV6-AC-FLII-GFP added to 50 µL of jetPRIME® buffer and 1.0 µL of transfection reagent (Polyplus; Illkirch, France). Samples were vortexed for 10 sec, centrifuged briefly, and incubated at RT for 10 min. The plasmid/transfection reagent mixture was added dropwise to individual wells. After four hours post-transfection, the media was changed and two hours later (6 hours post-transfection), HeLa cells were infected with *C. trachomatis* L2 wild-type (m.o.i. 0.8) by centrifugation at 400 x g for 15 min at RT. At 24 hpi, cells were fixed in 4% paraformaldehyde, permeabilized with 0.5 % Triton X-100 for 5 min at RT and stained for immunofluorescence to visualize the inclusion membrane (anti-CT223), LRRF1-GFP or FLII-GFP, and DNA (DAPI). The coverslips were imaged using Zeiss with Apotome.2 at 100x. Scale bar = 10 µm. Inclusion area measurements were also taken for LRRF1-GFP transfected HeLa cells infected with *C. trachomatis* L2 wild-type and compared to the inclusion area for non-transfected cells. The inclusion area is reported LRRF1-GFP Total (the inclusions from both high and low LRRF1-GFP expressing cells) and individually for LRRF1-GFP high and low expression only (see inset). A minimum of 100 inclusions were measured for non-transfected samples, and a minimum of 100 inclusions were measured for each HeLa cells with high LRRF1-GFP expression and low LRRF1-GFP expression of (see inset). Two independent experiments were performed. Inclusion area was graphed in GraphPad Prism 7 and a one-way ANOVA with Tukey's multiple comparisons post-hoc test was performed to determine statistical significance.

siRNA knockdown of LRRF1 to determine the effect on infectious progeny production

siRNA knockdown experiments were performed following the manufacturer's protocol (Polyplus; Illkirch, France). Non-targeting siRNA (Origene #: SR30004; Rockville,

MD), GAPDH siRNA (Ambion cat #4390849), and pooled LRRF1 siRNA (Ambion Life Technologies siRNA cat #43450, s229968, and s17599) were used in knockdown experiments. siRNA experiments were set up in quadruplicate to confirm LRRF1 knockdown efficiency by western blot (one well), to detect LRRF1 (unpublished) or FLII localization by immunofluorescence (one well), and to quantify infectious progeny (two wells). Briefly, 20 nM of the non-targeting (NT), GAPDH, single LRRF1 siRNA, or pooled LRRF1 siRNA was added to serum free Opti-MEM (100 µL/well), and 2 µL of INTERFERin reagent (Polyplus; Illkirch, France) was added to each well. The wells were incubated for 15 min at RT with gentle rocking. Then 2.5 x 10^4 HeLa cells were added to each well on top of the siRNA/transfection reagent mixture and incubated at 37 °C + 5% CO_2. The media was replaced with fresh DMEM + 10% FBS after 24 hours. At 48 hours post-siRNA transfection, HeLa cells were infected with *C. trachomatis* L2 wild-type (m.o.i. 0.8) by centrifugation at 400 x g 15 min at RT.

At 30 hpi, to confirm knockdown efficiency, *C. trachomatis* L2 infected HeLa cells were trypsinized, centrifuged and resuspended in 2x Laemmli sample buffer. The lysate was loaded, electrophoresed, and transferred to PVDF, then blotted to detect the presence of LRRF1 and GAPDH. To measure infectious progeny, experiments were performed essentially as previously described (146, 148). Briefly, duplicate wells for each sample were lysed at 30 hpi by scraping and then centrifuged at 17,000 × g for 30 min at 4 °C. The pellet was resuspended in sucrose phosphate buffer (2SP), serially diluted, and infected in duplicate onto a fresh monolayer of HeLa cells by centrifugation at 400 × g for 15 min at RT. Cells were incubated at 37°C + 5% CO_2 for 15 min, then the 2SP buffer was replaced with DMEM + 10 % FBS containing 1 µg/mL cycloheximide. To quantify infectious progeny, at 24-30 hours post-secondary infection, the cells were fixed in methanol for 5 min at RT and processed for indirect immunofluorescence to visualize the

inclusion using anti-MOMP antibodies (Meridian Biosciences; Memphis, TN). The average inclusion forming units (IFU/mL) from three biological replicates is reported.

Validation of LRRF1 at the chlamydial inclusion and time course experiments

HeLa cells infected with *C. trachomatis* L2 (m.o.i 0.75) in DMEM + 10% FBS without antibiotics were fixed at 24 hpi in 4% paraformaldehyde, permeabilized with 0.5 % Triton X-100 for 5 min at RT and stained for immunofluorescence to visualize the inclusion membrane (anti-CT223), LRRF1, and DNA (DAPI). The coverslips were imaged using Zeiss with Apotome.2 at 100x. Scale bar = 10 µm.

For the time course experiments, HeLa cells infected with *C. trachomatis* L2 (m.o.i 0.75) or mock-infected in DMEM + 10% FBS without antibiotics were fixed at 8, 12, 16, 24, and 36 hpi in methanol for 5 min at RT. One sample was treated with 34 µg/mL chloramphenicol at 8 hpi and then methanol fixed at 36 hpi. Fixed coverslips were stained for immunofluorescence to visualize the inclusion membrane (anti-CT223), LRRF1, *Chlamydiae* (MOMP), and DNA (DAPI) and imaged using Zeiss with Apotome.2 at 100x. Scale bar = 10 µm.

Assessing LRRF1 localization during infection of *C. trachomatis* serovars, *Chlamydia* species and *Coxiella burnetii*

HeLa cells infected with *C. trachomatis* L2 (m.o.i 0.75), *C. trachomatis* serovar D (m.o.i 1), *C. muridarum* (m.o.i 0.25), *C. caviae* (m.o.i 0.25), *C. pneumoniae* (m.o.i 1), and *Coxiella burnetii* avirulent Nine Mile Phase II were used. DMEM + 10% FBS media did not contain antibiotics (penicillin or cycloheximide) for these experiments. *C. trachomatis* serovar D was pre-treated with DEAE-Dextran prior to infection. All *Chlamydia*-infected HeLa cells were centrifuged at 400 x g 15 min at RT. *C. burnetii* Nine Mile Phase II infected HeLa cells were centrifuged for 1 hr at 2000 rpm at RT. At 24 hpi, *C. trachomatis* L2, *C.*

trachomatis serovar D, *C. muridarum*, and *C. caviae* infected HeLa cells were methanol fixed and stained for immunofluorescence. At 96 hpi, *C. pneumoniae* infected HeLa cells were fixed in 4% paraformaldehyde, permeabilized with 0.5% Triton X-100 and stained for immunofluorescence. At 3 days post infection, *C. burnetii* Nine Mile Phase II infected HeLa cells were methanol fixed for 5 min at RT and stained. Coverslips were stained using organism-specific and LRRF1 antibodies listed in to examine LRRF1 localization and DRAQ5 or DAPI to visualize DNA.

Bacterial adenylate cyclase two-hybrid (BACTH) assays

To screen for LRRF1 interacting partners, *LRRF1* was amplified from the pCMV-LRRF1-GFP vector (Origene; Rockville, MD), and *Incs* were amplified from *C. trachomatis* L2 genomic DNA using primers with overlapping sequences for each pST25 and pUT18C vectors (Table S3-5, Table S3-6). *LRRF1*, *CT288, CT226, CT223, IncA, IncF*, and *IncE* were amplified using the primers listed in Table S3-6 were cloned into each either pST25 or pUT18C using the NEbuilder HiFi Assembly Cloning Kit (NEBuilder) and transformed into DH5α lacI^{q} *E. coli*. Individual clones were cultured overnight, pDNA was isolated (Qiagen; Germantown, MD), verified by restriction digest, and the final clones were verified by DNA sequencing. pUT18C-IncF (Gateway®) (serovar D) was made as previously described (105). To screen for interactions, assays were performed as described previously (105, 165, 221-223). Briefly, plasmids were co-transformed into DHT1 (Δ*cyaA*) *E. coli* (Table S3-6) and prior to plating, *E. coli* cells were pelleted, washed and resuspended in 1x M63 minimal media. The resuspended DHT1 *E. coli* were then plated on 1x M63 minimal media plates containing, 0.2% Maltose, Isopropyl β-D-1-thiogalactopyranoside (IPTG; 0.5 mM), 5-bromo-4-chloro-3-indolyl-β-D-galactopyranoside (X-gal; 0.04 mg/mL), casamino acids (0.04%), spectinomycin (25 µg/mL), and ampicillin (50 µg/mL) and incubated at 30 °C for 3-5 days. To quantify

interactions by β-galactosidase assay, eight colonies (or streaks from negative plates) were set up for overnight culture in minimal media (1x M63 containing 0.2% maltose, IPTG 0.5 mM, 0.04 mg/mL X-gal, 0.01% casamino acids, spectinomycin (25 µg/mL), and ampicillin (50 µg/mL). After 20-24 hours, the cultures were diluted, and the OD600 was measured. A duplicate set of samples were permeabilized with SDS (0.05 %) and chloroform. After permeabilization, the supernatant was transferred to an optical plate containing 0.4% ONPG in PM2 buffer with 100 mM 2-mercaptoethanol. After 20 minutes, the enzymatic reaction was stopped with 1 M Na_2CO_3 stop solution and the absorbance at 405 nm was measured. The OD405 was normalized to bacterial growth (OD600) and reported as relative units (RU). A positive interaction is defined as greater than five times the negative control (164). Three independent experiments were analyzed for each interaction and graphed using GraphPad Prism 7 and reported as the mean with standard deviation.

Super resolution microscopy to assess LRRF localization with Incs

HeLa cells seeded on glass coverslips were infected with *C. trachomatis* L2 wild-type, or *C. trachomatis* L2 strains containing plasmids that express IncF-APEX2, $IncA_{TM}$-APEX2, IncA-APEX2, or CT226-FLAG and induced for expression at 20 hpi (5 nM aTc for all strains except IncF-APEX2 was induced with 1 nM aTc). At 24 hpi, coverslips were rinsed once with dPBS and then fixed with ice cold methanol and stained for immunofluorescence to visualize construct expression (FLAG) or CT223 (red), LRRF1 (green), *Chlamydiae* and DNA (blue). Coverslips were imaged using Zeiss ELYRA PS.1 Super Resolution Microscope Zeiss with Structured Illumination Microscopy (SIM). Scale bar = 5 µm. Using Zen Blue (Zeiss), 3D snapshots from *C. trachomatis* L2 CT226-FLAG infected HeLa cells and *C. trachomatis* L2 IncA-APEX2 infected HeLa cells with IncA fibers were generated and exported for visualization.

Overexpression of CT226-FLAG from *C. trachomatis* L2 CT226-FLAG results in increased LRRF1 and FLII at the inclusion membrane

HeLa cells seeded on glass coverslips were infected with *C. trachomatis* L2 transformed with a plasmid that expresses CT226-FLAG and either not induced or induced for expression at 7 hpi using 5 nM or 20 nM aTc. At 24 hpi, coverslips were fixed with 3% formaldehyde and 0.022% glutaraldehyde in dPBS, permeabilized with methanol, and stained for immunofluorescence to visualize construct expression (FLAG; red), *Chlamydiae* (MOMP; gray), DNA (DAPI; blue), and either LRRF1 (green) or FLII (green). Coverslips were imaged using a Zeiss confocal LSM 800 with 63x magnification and 2x zoom. Scale bar = 5 µm. Images were captured using the same exposure time (set for 20 nM aTc images) for uninduced and 5 nM aTc samples.

To examine LRRF1 recruitment using normal exposure time HeLa cells seeded on glass coverslips were infected with *C. trachomatis* L2 CT226-FLAG and either not induced or induced for expression at 7 hpi using 5 nM. At 24 hpi, coverslips were fixed with 4% paraformaldehyde, permeabilized with 0.5% triton X-100, and stained for immunofluorescence to visualize construct expression (FLAG; red), LRRF1 (green), GFP expressing *Chlamydiae* (pseudo-color blue), and DNA (DAPI; blue). Coverslips were imaged using a Zeiss with Apotome 2.1 with 100x magnification. Scale bar = 10 µm.

Co-immunoprecipitation of CT226-FLAG with endogenous LRRF1

HeLa cells were seeded in a 6-well plate in DMEM + 10% FBS and allowed to grow overnight. A coverslip was placed in two wells of each 6-well plate to monitor construct expression and localization by indirect immunofluorescence for each experiment. The cells were infected with *C. trachomatis* L2 CT226-FLAG and IncF-FLAG (m.o.i. 0.8) with DMEM + 10% FBS containing 1 U/mL penicillin (no cycloheximide) and not induced or induced with 5 nM (CT226-FLAG) or 1 nM aTc (IncF-FLAG) at 7 hpi. At 24 hpi, coverslips

were removed, fixed in 4% paraformaldehyde, triton-X permeabilized (0.5%) and stained for immunofluorescence to detect construct expression (FLAG), the inclusion membrane (IncA), DNA and *Chlamydiae*. The cells were lysed and affinity purified using FLAG magnetic beads as described above and previously (219). The eluates were mixed with an equal volume of 4x Laemmli sample buffer containing 5% β-mercaptoethanol and then loaded into a Criterion Midi 4-20% gradient SDS-PAGE (BioRad; Hercules, CA). The gel was transferred to PVDF (0.45 µm, Thermo Scientific; Waltham, MA) and blotted using anti-FLAG antibody to detect construct expression and anti-LRRF1 antibody. Three biological replicates were analyzed by co-immunoprecipitation.

Results

Biotinylation of proximal proteins at the inclusion membrane using C. trachomatis L2 strains that express IncF-APEX2, IncA$_{TM}$-APEX2, or IncA-APEX2

To examine our hypothesis that some Incs preferentially interact with other Inc proteins whereas other Incs primarily interact with eukaryotic proteins, we used the ascorbate peroxidase proximity labeling system (APEX2) to determine chlamydial Inc binding partners *in vivo* (57). To do this, we transformed *C. trachomatis* serovar L2 with a plasmid encoding IncF-APEX2, IncA$_{\text{Transmembrane Domain}}$-APEX2 (IncA$_{TM}$-APEX2), IncA-APEX2, or APEX2 only controlled by an anhydrotetracycline (aTc) inducible promoter system. IncF has previously been shown to interact with several Incs (105) and contains a short cytosolic domain, which could limit its ability to interact with eukaryotic proteins. In the same study, IncA interacted with fewer Incs (105) and has a large cytosolic domain with a eukaryotic SNARE-like domain (110-112, 145), suggesting that IncA might preferentially interact with eukaryotic proteins. IncA$_{TM}$-APEX2 is truncated to have a short cytosolic domain like IncF-APEX2 and is to determine if the C-terminus of IncA confers specificity towards determining protein binding partners (57). APEX2 only is a negative

control included in each experiment and, when expressed in transformed *C. trachomatis* L2, remains in the bacterial cytosol because it lacks the type III secretion signal (Fig. 3-1) (57). All proximity labeling experiments were performed using a plaque-cloned population of *C. trachomatis* L2 strains. HeLa 229 cells were infected with *C. trachomatis* L2 IncF-APEX2, $IncA_{TM}$-APEX2, IncA-APEX2, or APEX2 strains and induced with anhydrotetracycline (aTc). As previously determined, this resulted in the expression and localization of each construct that matches endogenous IncA and IncF (44, 57, 88). An epitope tag (FLAG) is located at the N-terminus of APEX2 and is used to visualize the localization of the various APEX2 constructs expressed from *C. trachomatis* L2.

For each biotinylation experiment, coverslips were placed in two wells of a six-well plate to confirm the presence of biotinylated proteins at the inclusion membrane by indirect immunofluorescence microscopy. This was performed for each of the test conditions and controls. HeLa cells were infected with *C. trachomatis* L2 IncF-APEX2, $IncA_{TM}$-APEX2, IncA-APEX2, or APEX2 and construct expression was induced at 7 hpi (0.3 nM aTc for IncF-APEX2 and 4 nM aTc for all other strains). Biotin-phenol was added to each well at 23.5 hpi, and at 24 hpi hydrogen peroxide (H_2O_2) was added to the wells to catalyze the biotinylation reaction during a one-minute incubation. After biotinylation, the enzymatic APEX2 activity was quenched. Coverslips were removed from the wells, fixed, then stained for immunofluorescence to confirm appropriate biotinylation. Separately, the lysate was collected as indicated in the *Methods* and processed after confirming biotinylation by indirect immunofluorescence. Expression of each construct containing APEX2 and biotinylation at the inclusion membrane was observed using each of the *C. trachomatis* Inc-APEX2 strains (Fig. 3-1). For *C. trachomatis* L2 APEX2, which lacks a type III secretion signal, biotinylation was co-localized with the bacterial cytosol (Fig. 3-1). For *C. trachomatis* L2 wild-type (i.e., untransformed) infected and mock-infected HeLa

cells (i.e., no APEX2), faint biotinylation was observed in subcellular structures consistent with mitochondria, but no biotinylation was detected at the inclusion of *C. trachomatis* L2 wild-type (Fig. 3-1). This confirmed that proteins proximal to the inclusion were biotinylated using the Inc-APEX2 constructs.

Verification of Inc-APEX2 labeling activity on the cytosolic face of the inclusion membrane by electron microscopy

C. trachomatis L2 transformed with IncF-APEX2, $IncA_{TM}$-APEX2, and IncA-APEX2 target the constructs to the inclusion membrane with the C-terminus (that contains APEX2) exposed to the host cytosol (91). We used electron microscopy to further support that the *C. trachomatis* L2 Inc-APEX2 strains were labeling the cytosolic face of the chlamydial inclusion (209). For these studies, HeLa cells were infected with wild-type (i.e., non-transformed) or *C. trachomatis* L2 Inc-APEX2 strains, and the monolayers were treated with aTc to induce APEX2 fusion protein expression. Then, cells were fixed with a glutaraldehyde and paraformaldehyde solution, which maintains APEX2 activity (209), and labeled with or without 3,3'-Diaminobenzidine (DAB). DAB and hydrogen peroxide (H_2O_2) diffuse into non-permeabilized cells, and, in the proximity of APEX2, DAB polymerizes (168, 189, 209). Upon polymerization, DAB becomes membrane impermeable and remains closely associated with the site of polymerization (209). DAB reacts with the heavy metal staining procedure (osmium tetroxide) to create a contrast that can be observed by electron microscopy (209).

As seen in Fig. 3-2A, no DAB polymerization is observed at the inclusion membrane in HeLa cells infected with wild-type *C. trachomatis* L2. To control for background activity, HeLa cells were infected with *C. trachomatis* L2 IncA-APEX2, induced for expression, but not treated with DAB (Fig. 3-2B). In these samples, no DAB staining was observed at the inclusion membrane (Fig. 3-2B). There was no detectable

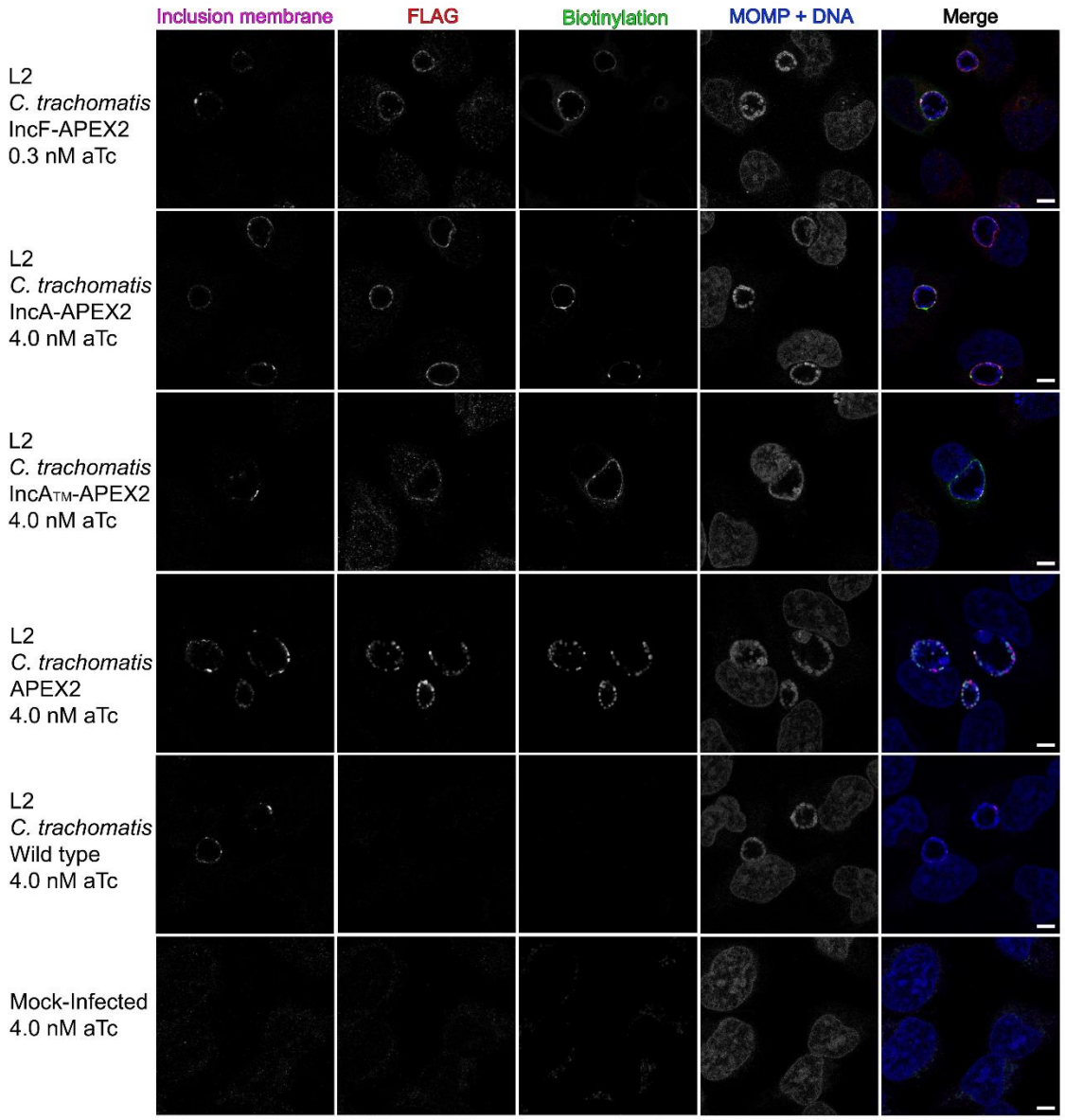

Figure 3-1. Localization and biotinylation of proteins proximal to the inclusion membrane in HeLa cells infected with *C. trachomatis* L2 transformed strains expressing Inc-APEX2 constructs.

Coverslips were placed in two wells of a 6-well tissue culture plate to ensure appropriate biotinylation. HeLa cells infected with *C. trachomatis* serovar L2 transformed with the indicated APEX2 constructs, *C. trachomatis* L2 wild-type (WT), or mock-infected were induced for construct expression with the indicated concentrations of anhydrotetracycline (aTc) at 7 hpi. Biotin-phenol was added at 23.5 hpi, biotinylation was catalyzed at 24 hpi by the addition of 3 mM H_2O_2 for 1 min, after which the reaction was quenched. Coverslips were removed from the 6-well plate and processed for immunofluorescence to visualize biotinylated proteins (streptavidin-488 conjugate), expression of the construct

(continued on the next page)

(anti-Flag, red), *Chlamydiae* (MOMP) and DNA (DAPI; blue), and the inclusion membrane (anti-CT223, pink). Coverslips were imaged using a Zeiss confocal LSM 800 with 63x magnification and 2x zoom. Scale bar = 5 µm.

Figure modified from Olson et al. 2019. IAI.

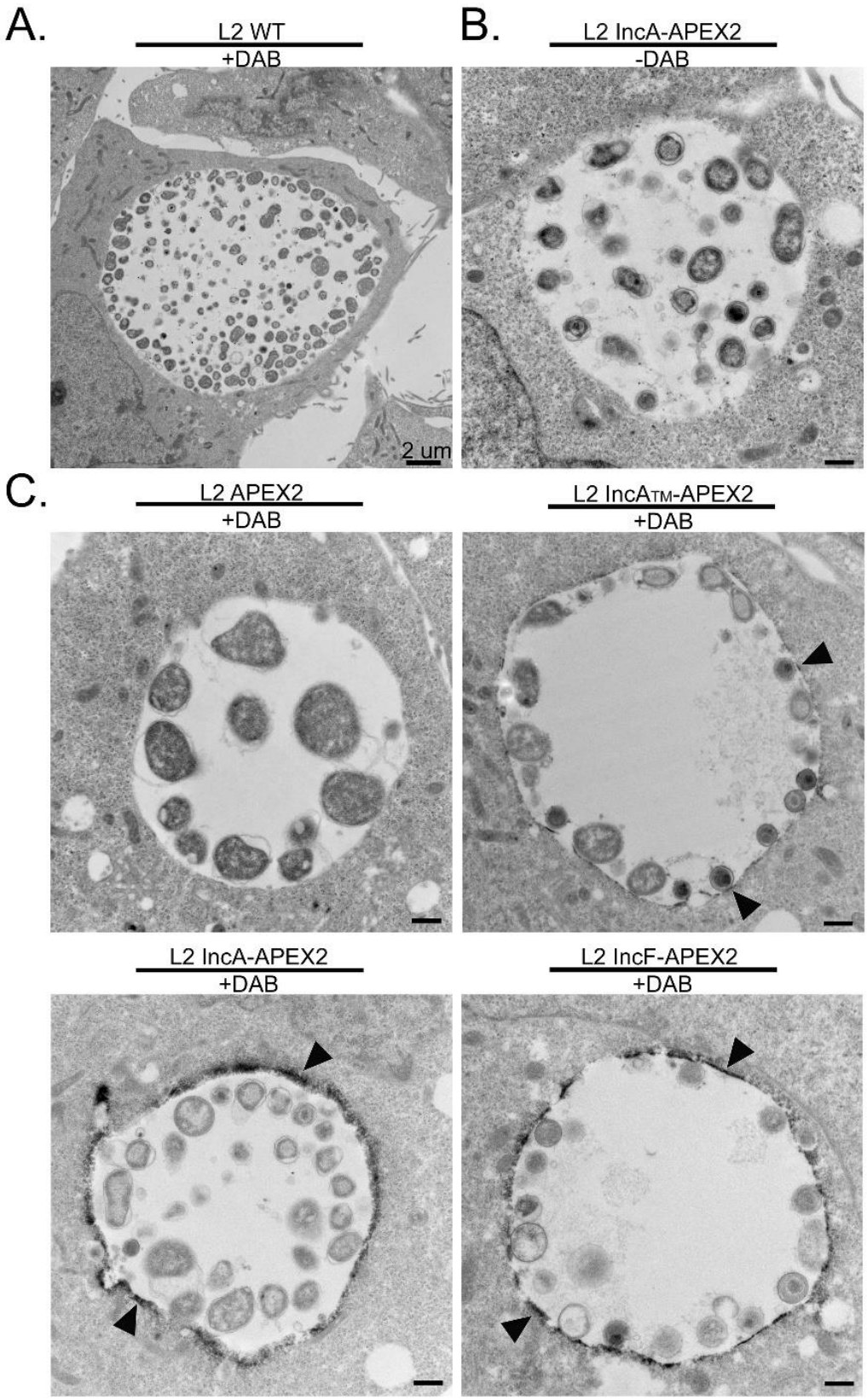

(continued on the next page)

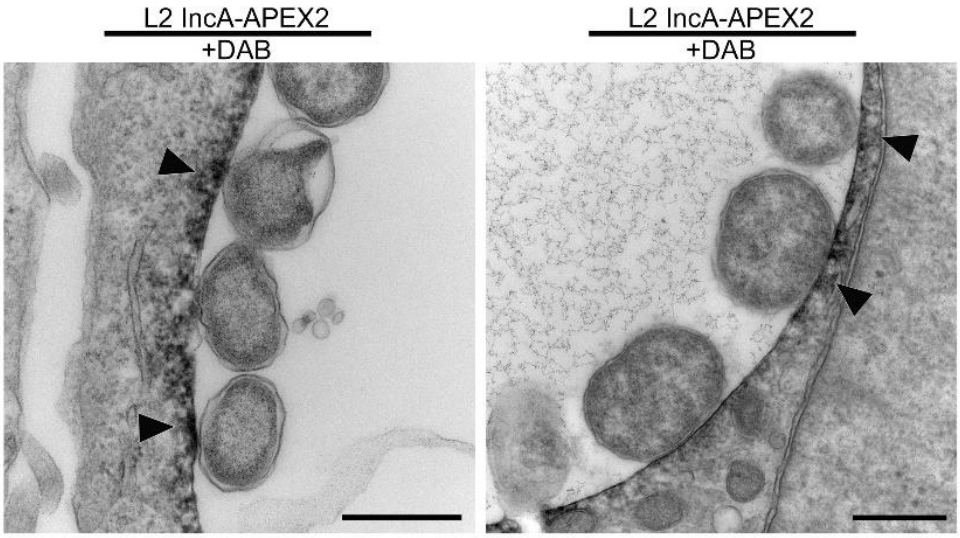

Figure 3-2. Ultrastructural localization of APEX2 activity to the cytosolic face of the inclusion membrane in HeLa cells infected with *C. trachomatis* L2 transformed strains expressing Inc-APEX2 constructs as determined by electron microscopy.

HeLa cells seeded onto electron microscopy grade, cell culture treated coverslips were infected with *C. trachomatis* serovar L2 transformed with the indicated constructs, or *C. trachomatis* serovar L2 wild-type (WT) were induced with anhydrotetracycline (aTc) at 7 hpi (IncF-APEX2 0.3 nM aTc, all others 5 nM aTc). At 24 hpi, a glutaraldehyde and paraformaldehyde fixing solution was added to each sample and incubated on ice. Next, samples were pre-treated with DAB (or not, as indicated) 30 min prior to labeling by the addition of H_2O_2 solution (also containing DAB) to catalyze DAB polymerization. The reaction was quenched with glycine and processed for electron microscopy as indicated in *Methods*. (A) *C. trachomatis* L2 wild-type (WT) treated with DAB; scale bar= 2 µm, (B) *C. trachomatis* L2 IncA-APEX2 without DAB; scale bar= 500 nm, (C) *C. trachomatis* L2 Inc-APEX2 infected cells treated with DAB; DAB polymer staining around the inclusion is indicated by arrows; scale bar= 500 nm.

Figure modified from Olson et al. 2019. IAI.

DAB labeling at the inclusion membrane in HeLa cells infected with *C. trachomatis* L2 APEX2, but we did not observe strong DAB polymerization within individual organisms (Fig. 3-2C). In HeLa cells infected with *C. trachomatis* L2 IncF-APEX2, $IncA_{TM}$-APEX2, or IncA-APEX2 strains, DAB polymerization was observed at the inclusion membrane (Fig. 3-2C, arrows). However, there appeared to be less DAB labeling with $IncA_{TM}$-APEX2 compared to IncF-APEX2 and IncA-APEX2. Overall, by electron microscopy, we observed Inc-APEX2 directed DAB labeling at the inclusion membrane, and this labeling appeared on the cytosolic face of the inclusion membrane.

Western blot detection of APEX2 containing constructs expressed from C. trachomatis L2 Inc-APEX2 strains

To confirm the correct expression of each construct containing APEX2, HeLa cells were infected with the *C. trachomatis* L2 APEX2, IncF-APEX2, $IncA_{TM}$-APEX2, or IncA-APEX2 strains and either not induced or induced at 7 hpi (0.3 nM aTc for IncF-APEX2 and 5 nM for all other strains). Cell lysates were collected at 24 hpi and prepared for affinity purification using FLAG magnetic beads essentially as previously described (219). The eluates were blotted for the presence of each APEX2 containing construct using anti-FLAG antibody (the FLAG epitope tag is located at the N-terminus of APEX2). Lower levels of IncF-APEX2 (39.7 kDa) were detected compared to $IncA_{TM}$-APEX2 (40.7 kDa), IncA-APEX2 (59.3 kDa), and APEX2 (30.3 kDa) (Fig. S3-1). We detected some leaky expression of IncF-APEX2, $IncA_{TM}$-APEX2, and IncA-APEX2 in our uninduced samples (Fig. S3-1). As a loading control, the solubilized lysate was blotted for the presence of chlamydial Heat shock protein 60 (cHsp60) (Fig. S3-1; Input, lower panel; cHsp60 antibody kind gift from Rick Morrison, University of Arkansas for Medical Sciences, Little Rock, AR). These data confirmed that each APEX2 containing construct was expressed from the *C. trachomatis* L2 strains at the expected molecular weight.

Affinity purification of biotinylated proteins

After confirming the correct construct localization, labeling activity at the inclusion membrane, and molecular weight of the proteins expressed from *C. trachomatis* L2, the lysates from *C. trachomatis* L2 IncF-APEX2, $IncA_{TM}$-APEX2, IncA-APEX2 strains, and the negative control infected HeLa cells from the biotinylation experiments described above (Fig. 3-1) were affinity purified to isolate biotinylated proteins. The negative controls, mock-infected, *C. trachomatis* L2 wild-type infected, and *C. trachomatis* L2 APEX2 infected HeLa cells treated with biotin-phenol and hydrogen peroxide (to catalyze labeling) served to control for background, endogenous biotinylated proteins. As described previously, the major background endogenous biotinylated proteins include eukaryotic mitochondrial carboxylases (75 and 125 kDa) (57, 224), and, in *C. trachomatis* L2 infected HeLa cells, the chlamydial biotin ligase (21 kDa), which uses biotin as a co-factor (57, 225). We did not include uninduced *C. trachomatis* L2 strains in our analysis because we observed some leaky construct expression and were concerned that using this as a negative control would subtract true interacting proteins during the analysis step (Fig. S3-1).

Biotinylated proteins were affinity-purified using streptavidin beads and visualized by western blotting using a fluorescent streptavidin-conjugate (Fig. 3-3; streptavidin panel). Biotinylated proteins were detected from each of the *C. trachomatis* L2 IncF-APEX2, IncA-APEX2, and $IncA_{TM}$-APEX2 infected cells that received both biotin-phenol and H_2O_2 (Fig. 3-3; streptavidin panel). Without the addition of biotin-phenol to the *C. trachomatis* L2 Inc-APEX2 strains, only endogenous biotinylated proteins were detected. Similarly, in each of the negative controls, *C. trachomatis* L2 APEX2, *C. trachomatis* L2 wild-type (not transformed) and mock-infected HeLa cells, only background endogenous biotinylated proteins were detected (Fig. 3-3; streptavidin panel).

To determine if the expressed constructs containing APEX2 were biotinylated *in vivo* and affinity purified, we blotted the eluates using an anti-FLAG antibody (APEX2 contains the FLAG epitope in the N-terminus). We detected biotinylated $IncA_{TM}$-APEX2 (40.7 kDa), IncA-APEX2 (59.3 kDa), and APEX2 (30.3 kDa) (Fig. 3-3; FLAG panel). We did not observe biotinylated IncF-APEX2 (40.7 kDa) in the eluate fraction, which is likely a result of the lower expression necessary to preserve its correct localization ((57) and Fig. S3-1). In addition, to determine if we could detect solubilized endogenous chlamydial Incs, we used an anti-IncA antibody (a gift from Dr. T. Hackstadt, NIAID, Rocky Mountain Laboratories, Hamilton, MT) and an anti-CT223 antibody (a gift from R. Suchland, University of Washington, WA and Dr. D. Rockey, Oregon State University, OR) to blot the eluates from the streptavidin affinity purification. We detected endogenous IncA in the eluate from *C. trachomatis* L2 IncF-APEX2 and IncA-APEX2 (Fig. 3-3; IncA panel). The IncA antibody is specific for the C-terminus, so it detects IncA-APEX2 (59.3 kDa band) containing full-length IncA and not the truncated $IncA_{TM}$-APEX2 expressed construct, which lacks the epitope that is recognized by the antibody. We also detected CT223 (29.3 kDa) in the streptavidin affinity purified eluate from each of the *C. trachomatis* L2 Inc-APEX2 samples but not in the negative controls (Fig. 3-3C; CT223 panel). These western blot data provide an initial validation of our proximity labeling system because IncA homotypic interactions have been described (105, 110, 111, 145, 166) (e.g., IncA-APEX2 interacts with endogenous IncA in the inclusion membrane). These data are also consistent with previously published *in vivo* protein-protein interaction data using the BACTH system that identified IncF and IncA interactions (105).

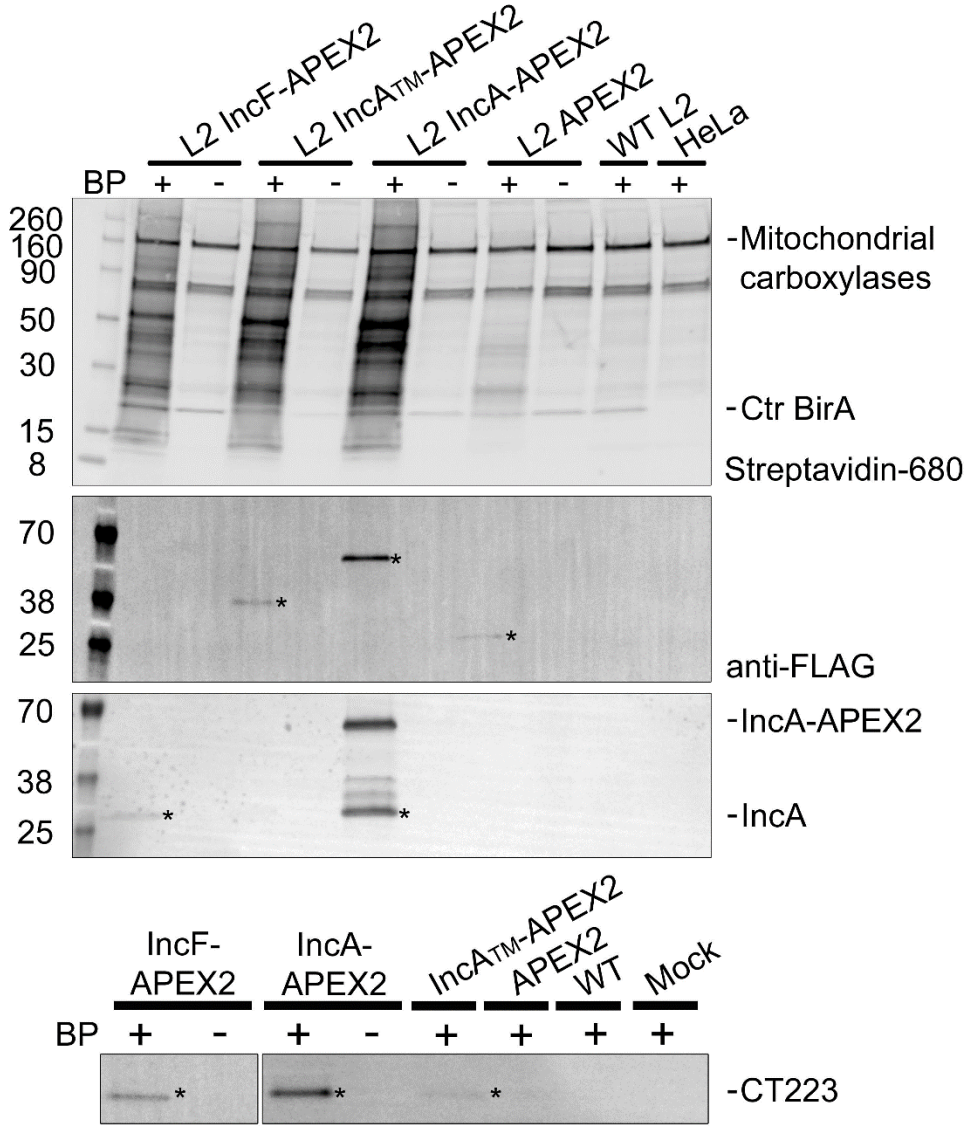

Figure 3-3. Western blot detection of affinity purified biotinylated proteins.

HeLa cells infected with *C. trachomatis* L2 Inc-APEX2 transformed strains, wild-type (WT), or mock-infected were induced with anhydrotetracycline (aTc) at 7 hpi (0.3 nM for IncF-APEX2, and 4 nM for all others). Biotin-phenol (BP) was added 30 min prior to the biotinylation reaction at 24 hpi. Biotinylation was catalyzed by the addition of 3 mM H_2O_2 for 1 min and stopped with a quenching wash solution. Biotinylated proteins were affinity purified from solubilized lysates using streptavidin beads, eluted in sample buffer, separated by SDS-PAGE and transferred to PVDF for western blotting. The eluate fraction was probed for biotinylated proteins (streptavidin-680 conjugate), construct expression (anti-FLAG antibody), IncA (anti-IncA antibody), CT223 (anti-CT223 antibody), and imaged using Azure c600. Asterisks indicate detected proteins. See Supplementary Figure 1.

Figure modified from Olson et al. 2019. IAI.

Mass spectrometry identification of streptavidin affinity purified biotinylated C. trachomatis L2 and eukaryotic proteins

To identify the proteins proximal to or interacting with the inclusion membrane that were biotinylated *in vivo* using the APEX2 proximity labeling system, the eluates from streptavidin affinity purification were briefly electrophoresed, sectioned, and then processed for mass spectrometry identification. To enhance mass spectrometry peptide identification, individual gel sections were digested with two enzymes, trypsin and AspN (226), and then processed as indicated in the *Methods*. Five biological replicates for each condition were analyzed by tandem mass spectrometry (MS/MS) and individual peptides were identified by performing Mascot searches against the *C. trachomatis* L2 (434/Bu) database and the *Homo sapiens* database. Our analysis detected 810 *C. trachomatis* L2 proteins (Table S3-1) and over 5,000 eukaryotic proteins (Table S3-2) in total from the combined datasets. To analyze our mass spectrometry data for statistical significance and to remove non-specific or background biotinylated proteins, we used Significance Analysis of INTeractome (SAINT) (207). SAINT uses quantitative data embedded in the raw mass spectrometry data from label-free quantification methods to filter out background peptides (207). The peptide spectra for a protein (i.e. prey) identified in the sample of interest (i.e. bait) is normalized to both the protein length and the total number of spectra compared to the negative controls. Bayesian statistics are used to calculate the probability of an interaction between each bait-prey interaction identified. The calculated probability is expressed as Bayesian False Discovery Rate (BFDR). We used a BFDR less than or equal to 0.05 as a cut-off for our analysis parameters, which indicates the probability that the interaction is "true" (i.e., at BFDR=0.05, we are 95% confident in the protein associations described).

When we analyzed the *C. trachomatis* L2 proteins for statistical significance, several Inc proteins were among the top SAINT identified significant hits using our Inc-APEX2 constructs (Table 3-1; Table S3-1). Using our BFDR cut-off (BFDR≤0.05), we identified three statistically significant chlamydial proteins using *C. trachomatis* L2 IncF-APEX2 and IncA-APEX2, and two significant proteins using *C. trachomatis* L2 $IncA_{TM}$-APEX2. CT223 was the only chlamydial protein that was identified as statistically significant using each *C. trachomatis* L2 Inc-APEX2 strain. IncA was detected using *C. trachomatis* L2 IncA-APEX2 and $IncA_{TM}$-APEX2. The identification of CT223 and IncA by mass spectrometry using IncA-APEX2 is supported by the detection of proteins eluted from the streptavidin affinity purified lysate (Fig. 3-3). Statistically significant chlamydial proteins that were unique to the individual *C. trachomatis* L2 Inc-APEX2 strains included IncD and IncF which were identified using *C. trachomatis* L2 IncF-APEX2 and outer membrane complex B (OmcB) which was identified using *C. trachomatis* L2 IncA-APEX2 (Table 3-1; Table S3-1). Additional chlamydial Inc proteins that were detected by mass spectrometry but did not make the BFDR (BFDR≤0.05) cut-off using *C. trachomatis* L2 IncA-APEX2 include IncC (BFDR=0.09), CT813 (BFDR=0.1), IncD (BFDR=0.11), and IncE (BFDR=0.2) (Table S3-1). In contrast, there were no additional Incs identified using *C. trachomatis* L2 $IncA_{TM}$-APEX2 with a less stringent cut-off (BFDR ≤0.2). Using *C. trachomatis* L2 IncF-APEX2, IncA (BFDR= 0.12), CT228 (BFDR= 0.15), and IncE (BFDR=0.18) were detected (Table S3-1). Although IncA was not statistically significant using IncF-APEX2, IncA was detected in the affinity-purified eluate of IncF-APEX2 by western blot (Fig. 3-3; Table S3-1). These data are also supported by previously observed IncF-IncA interactions by BACTH (105) and IncA-IncA interactions that have been previously described (105, 110). Importantly, our AP-MS data analyzed against the *C. trachomatis* L2 (434/Bu) database were supported by our western blot data.

Table 3-1. Significant *C. trachomatis* L2 proteins

Sample	Protein (Uniprot ID)	Gene name	Protein name [a]	BFDR [b]
IncF-APEX2	A0A0H3MKT3_CHLT2	CTL0476	CT223	0
	INCD_CHLT2	CTL0370	IncD	0.02
	INCF_CHLT2	CTL0372	IncF	0.03
$IncA_{TM}$-APEX2	A0A0H3MD02_CHLT2	CTL0374	IncA	0
	A0A0H3MKT3_CHLT2	CTL0476	CT223	0.02
IncA-APEX2	OMCB_CHLT2	CTL0702	OmcB	0
	A0A0H3MKT3_CHLT2	CTL0476	CT223	0
	A0A0H3MD02_CHLT2	CTL0374	IncA	0

[a] Protein name indicated using *C. trachomatis* serovar D naming convention

[b] SAINT Bayesian False Discovery Rate

Table adapted from Olson et al. 2019. IAI.

When we applied SAINT to our *Homo sapiens* AP-MS data, 13 statistically significant eukaryotic proteins (BFDR ≤0.05) were identified using *C. trachomatis* L2 IncF-APEX2, 18 statistically significant proteins using $IncA_{TM}$-APEX2, and 192 statistically significant proteins using IncA-APEX2 (Table S3-2 and S4-3). To visualize common pathways for eukaryotic protein biological processes and molecular functions, the significant eukaryotic proteins (BFDR ≤0.05) from each SAINT analyzed Inc-APEX2 dataset were evaluated by ClueGO (Cytoscape (220)) (Fig. 3-4). For IncF-APEX2 (Fig. 3-4A; Fig. 3-S2A) the 13 significant eukaryotic proteins identified were associated with transport and the negative regulation of biological processes. For $IncA_{TM}$-APEX2, the 18 statistically significant proteins were associated with regulation of metabolic processes and biological processes (Fig. 3-4B; Fig. S3-2B). Finally, the pathway analysis of the 192 significant eukaryotic proteins for IncA-APEX2 yielded globally enriched pathways including regulation of cellular protein metabolic processes, vesicle-mediated transport, actin cytoskeleton organization, regulation of cellular component organization, and translation (Fig. 3-4C; Fig. S3-2C).

Individual datasets were also analyzed using STRING (Cytoscape (220)) to visualize the protein binding partner network for statistically significant (BFDR ≤0.05) eukaryotic proteins within each IncF-APEX2 (Fig. S3-3A), $IncA_{TM}$-APEX2 (Fig. S3-3B), and IncA-APEX2 (Fig. S3-3C) dataset. Four statistically significant eukaryotic proteins were common to all Inc-APEX2 datasets: Leucine-Rich Repeat Flightless-Interacting Protein 1 (LRRF1 or LRRFIP1), microtubule-associated protein 1B (MAP1B), Cystatin-B (CYTB), and brain acid soluble protein 1 (BASP1) (Table S3-2). Twelve proteins were shared between *C. trachomatis* L2 IncA-APEX2 and $IncA_{TM}$-APEX2 including myosin phosphatase target subunit 1 (MYPT1 or PPP1R12A), transitional endoplasmic reticulum ATPase (TERA, VCP), microtubule-associated protein 4 (MAP4), multifunctional protein

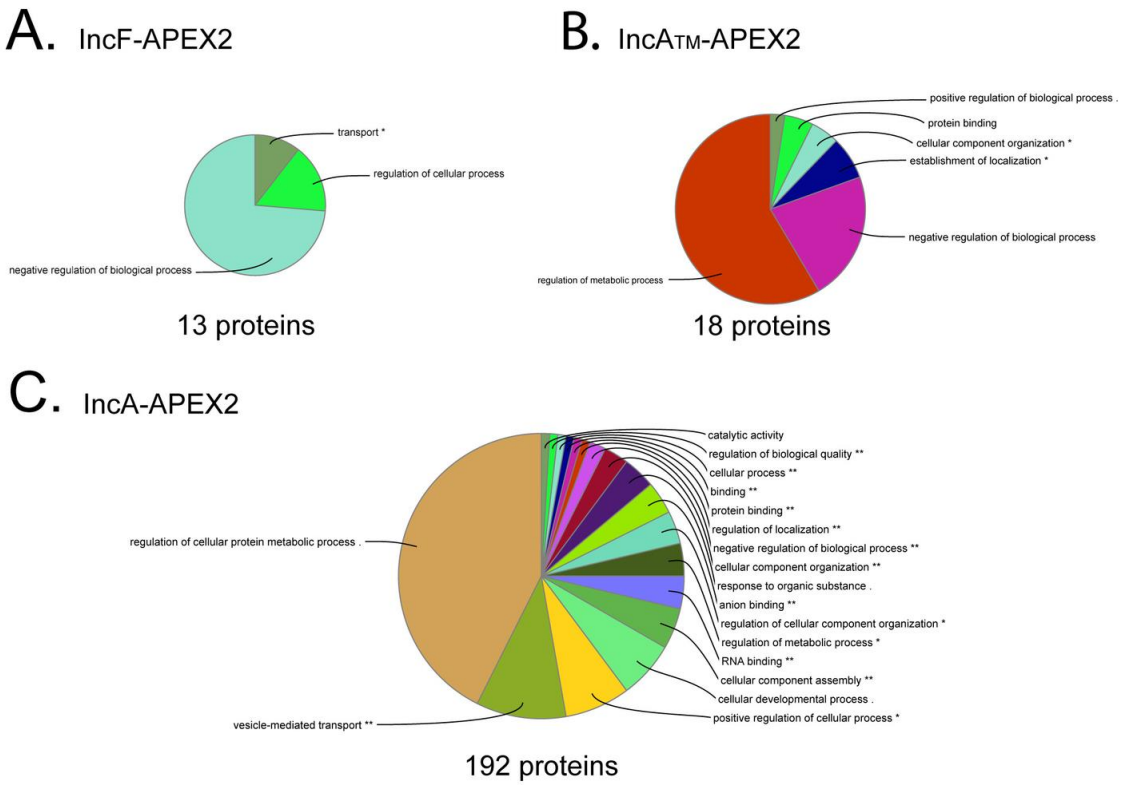

Figure 3-4. Visualization of global biological functions of AP-MS identified and statistically significant eukaryotic proteins from Inc-APEX2 pulldowns.

ClueGO global network visualization of eukaryotic proteins identified by mass spectrometry (SAINT BFDR ≤ 0.05) from *C. trachomatis* L2 (A) IncF-APEX2, (B) IncA$_{TM}$-APEX2, and **(**C) IncA-APEX2. See Supplementary Figure 2 and 3.

Figure modified from Olson et al. 2019. IAI.

ADE2 (PUR6), sorting nexin-1 (SNX1), src substrate cortactin (SRC8, CTTN), methylosome protein 50 (MEP50), sorting nexin 6 (SNX6), perilipin-3 (PLIN3), eukaryotic translation initiation factor 4B (IF4B), nucleoside diphosphate kinase A (NDKA), and nucleoside diphosphate kinase B (NDKB) (Table S3-2). In both the IncF-APEX2 and IncA-APEX2 datasets, four eukaryotic proteins were statistically significant: 14-3-3-η (YWHAH), myristoylated alanine-rich C-kinase substrate (MARCKS), 14-3-3-β (YWHAB), and keratin type I cytoskeletal 20 (K1C20) (Table S3-2). These data included statistically significant eukaryotic proteins that have been previously shown to be recruited to the inclusion by Inc proteins. For example, in our IncA-APEX2 and IncF-APEX2 dataset, we identified 14-3-3-β, which is known to bind IncG (142). In addition, the eukaryotic proteins, SNX5 and SNX6, which bind IncE (122), and MYPT1, which binds CT228 (38, 117), were identified in both the IncA-APEX2 and $IncA_{TM}$-APEX2 datasets (Table S3-2). Furthermore, the known chlamydial Inc binding partners for the eukaryotic proteins listed above (IncG, IncE, and CT228) were also identified in the AP-MS *C. trachomatis* L2 protein analyzed datasets (Table S3-1). We also identified eukaryotic proteins that are known to localize at the inclusion but for which an Inc binding partner has not been identified, including microtubule-associated protein 1B (MAP1B) (227) and Src-substrate cortactin (SRC8, CTTN) (114). A full summary of our data set compared to Aeberhard et al 2015 (171) can be found in Table S3-4. Importantly, besides identifying eukaryotic proteins that are known to localize at the inclusion membrane, our Inc-APEX2 data identified several eukaryotic proteins that have not been previously examined for localization to the chlamydial inclusion.

Co-localization of LRRF1 with the C. trachomatis L2 inclusion membrane

One of the high confidence AP-MS identified eukaryotic proteins (significant in each Inc-APEX2 dataset (BFDR=0)), Leucine-Rich Repeat in Flightless Interacting Protein 1 (LRRF1), has been reported to be involved in activating a type 1 interferon response (228-232), which plays a role in host cell clearance of intracellular bacteria during infection and the development of adaptive immunity (233). Also, a known LRRF1 binding partner called Protein Flightless-1 homolog (FLII) (BFDR=0.02) (230, 234) was identified as significant by SAINT analysis in the IncA-APEX2 dataset (Table S3-2). FLII has been reported to associate with β-catenin to regulate its activity (235). In support, LRRF1 (122, 170, 171) and FLII (122, 171) were also identified in previous AP-MS experiments and ectopically expressed FLII was shown to localize with the inclusion (171). Neither endogenous LRRF1 nor FLII has been examined for localization to the chlamydial inclusion.

LRRF1 was first confirmed by western blot (dimer 160 kDa) in the eluate from streptavidin affinity purified lysate from each of the *C. trachomatis* L2 Inc-APEX2 infected HeLa cells but not in the *C. trachomatis* L2 Inc-APEX2 samples that did not receive biotin-phenol, in the *C. trachomatis* L2 wild-type, or in mock-infected negative control samples (Fig. 3-5A). These data confirm the identification of LRRF1 by mass spectrometry. To assess if LRRF1 and FLII localized to the chlamydial inclusion, HeLa cells were infected with *C. trachomatis* L2 wild-type, fixed at 24 hpi, and stained for immunofluorescence. LRRF1 (Fig. 3-5B) and FLII (Fig. 3-5C) were observed to localize to the inclusion membrane at 24 hpi. Subsequently, we transfected HeLa cells with a vector encoding LRRF1-GFP or FLII-GFP and then infected or not with *C. trachomatis* L2 wild-type. At 24 hpi, cells were fixed and processed for immunofluorescence. In *C. trachomatis* L2 infected

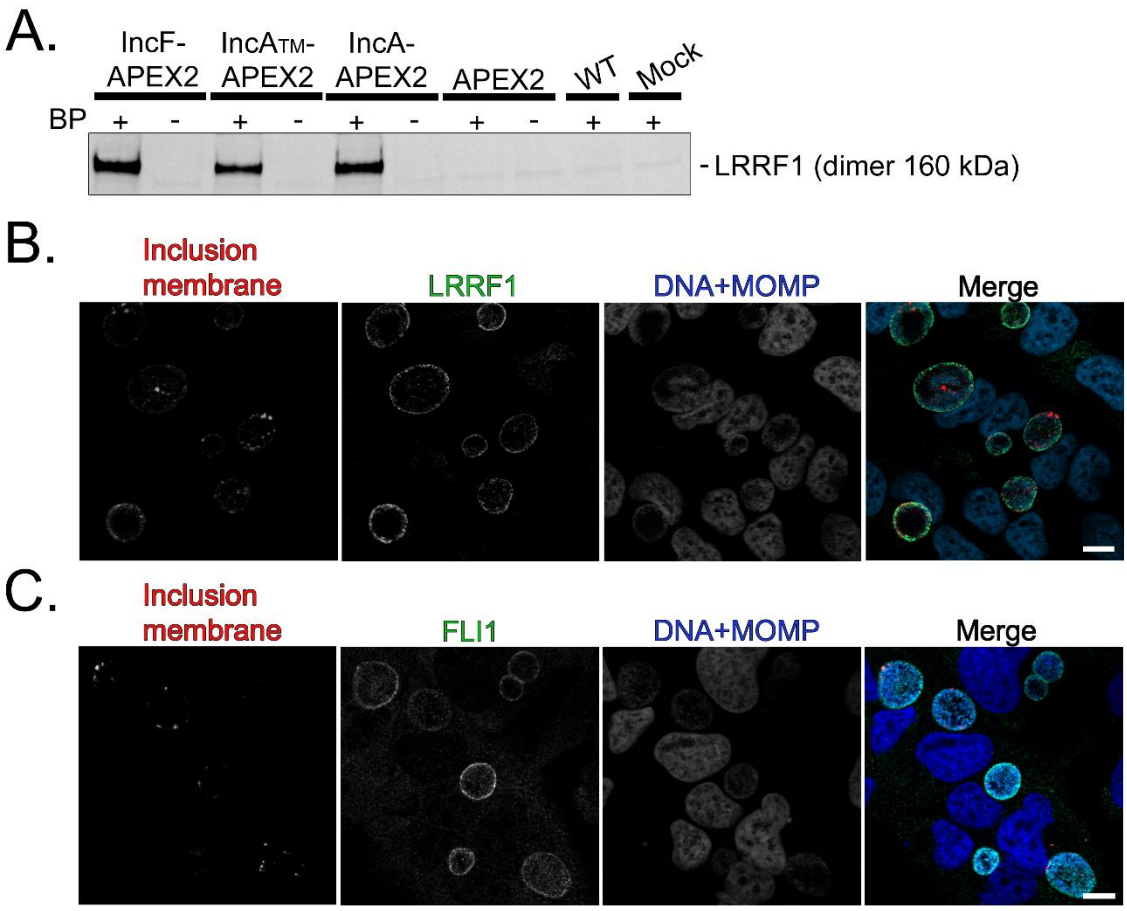

Figure 3-5. Confirmation of LRRF1 biotinylation by Inc-APEX2 proteins and localization of LRRF1 and FLII to the chlamydial inclusion.

(A) Western blot confirmation of LRRF1 in the eluates from streptavidin affinity purified biotinylated lysate from *C. trachomatis* L2 IncF-APEX2, $IncA_{TM}$-APEX2, and IncA-APEX2 strains at 24 hpi (BP= biotin-phenol). (B) Confirmation of LRRF1 co-localization with the inclusion of *C. trachomatis* L2 wild-type infected HeLa cells. Cells were fixed at 24 hpi in 4% paraformaldehyde and permeabilized with 0.5% Triton X-100 then stained for indirect immunofluorescence to visualize the inclusion membrane (CT223; red), LRRF1 (green), DNA and *Chlamydiae* (DRAQ5 and MOMP; blue). (C) Confirmation of FLII co-localization with the inclusion of *C. trachomatis* L2 wild-type infected HeLa cells. Cells were fixed at 24 hpi in 4% paraformaldehyde, permeabilized with 0.5% Triton X-100, then stained for indirect immunofluorescence to visualize the inclusion membrane (CT223; red), FLII (green), and DNA and *Chlamydiae* (DAPI and MOMP; blue). Coverslips were imaged using Zeiss Apotome.2 with 100x magnification. Scale bar= 10 µm. See Supplementary Figure 4.

Figure modified from Olson et al. 2019. IAI.

HeLa cells, LRRF1-GFP (Fig. S3-4A) and FLII-GFP (Fig. S3-4B) were each observed at the inclusion membrane. In support, ectopically expressed HA epitope-tagged FLII was previously reported to localize to the *C. trachomatis* L2 inclusion (171). In mock-infected HeLa cells, LRRF1-GFP and FLII-GFP both appeared diffusely in the host cytosol (Fig. S3-4A and S4-4B, respectively). There was no significant difference in the inclusion area of *C. trachomatis* L2 wild-type infected HeLa cells when LRRF1 was overexpressed (LRRF1-GFP transfected) compared to non-transfected HeLa cells (Fig. S3-4C). When we knocked down LRRF1 expression in HeLa cells, we did not observe a biologically significant change in the production of infectious progeny (Fig. S3-4D; Non-targeting siRNA= 2.73 x 10^6 IFU/mL; GAPDH siRNA=4.46 x 10^6 IFU/mL; Single LRRF1 siRNA= 2.3 x 10^6 IFU/mL; Pooled LRRF1 siRNA= 4.09 x 10^6 IFU/mL).

LRRF1 co-localizes with the C. trachomatis inclusion from mid to late developmental cycle

To determine if LRRF1 stably or transiently localized to the inclusion during the developmental cycle, we infected HeLa cells with *C. trachomatis* L2 wild-type, fixed cells at intervals between 8 hpi and 36 hpi, and then stained for immunofluorescence to observe LRRF1 localization. Using CT223 as an inclusion membrane marker, LRRF1 could be observed at the inclusion as early as 12 hpi (Fig. 3-6; arrows) and remained at the inclusion up to 36 hpi (Fig. 3-6). Chloramphenicol (Cm) was added at 8 hpi to inhibit bacterial translation, and this treatment abolished the localization of LRRF1 to the inclusion (Fig. 3-6; Cm treated panel), suggesting that LRRF1 recruitment is dependent on active chlamydial protein expression. These data indicate that LRRF1 is stably localized to the inclusion membrane from mid to late time points in the *C. trachomatis* L2 developmental cycle and that a chlamydial protein may recruit LRRF1 to the inclusion.

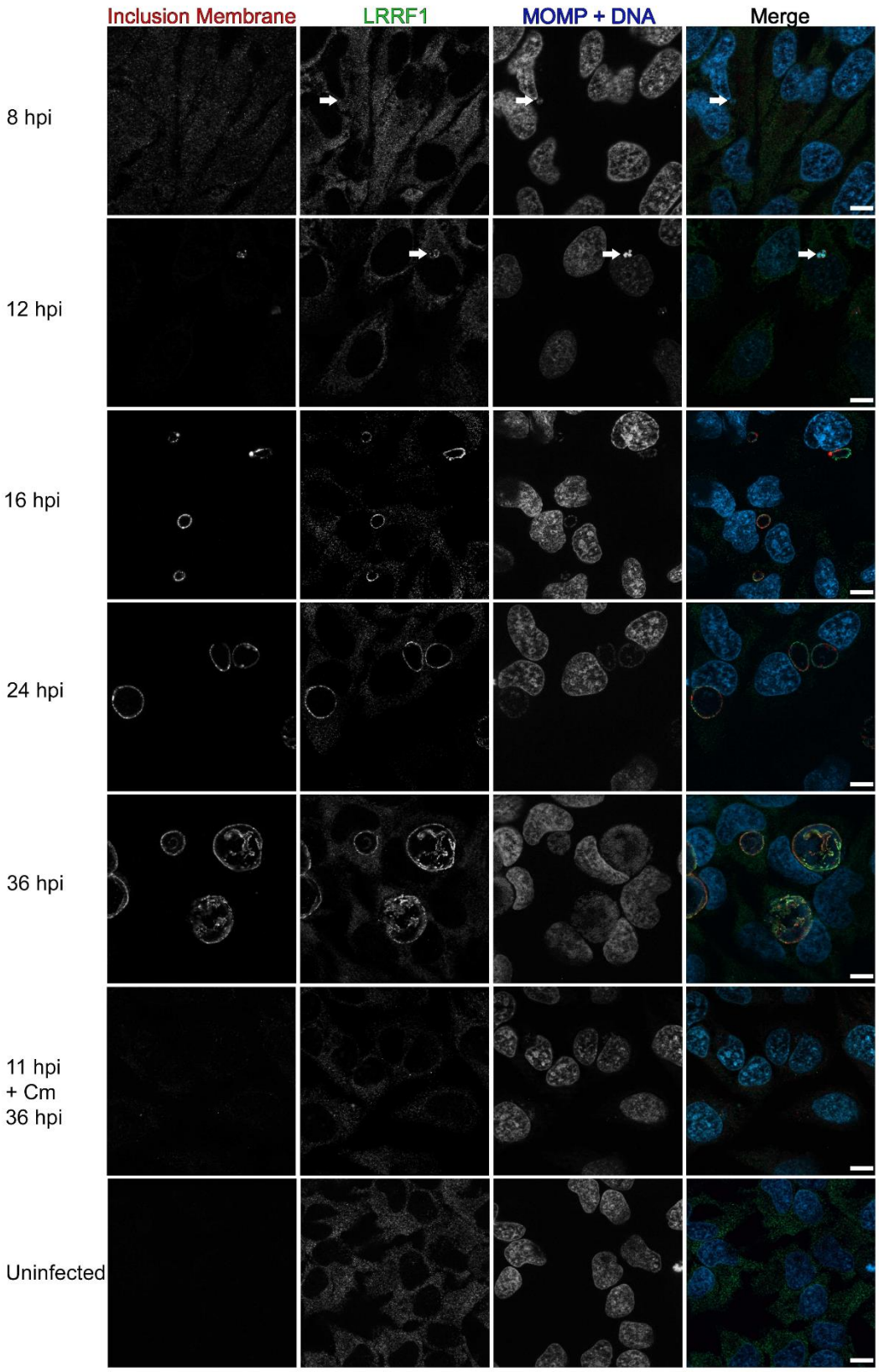

(continued on the next page)

Figure 3-6. Recruitment of LRRF1 to the inclusion of *C. trachomatis* L2 during the developmental cycle and after chloramphenicol treatment.

HeLa cells seeded on glass coverslips were infected with *C. trachomatis* L2 wild-type or mock infected. Wells were methanol fixed at 8, 12, 16, 24, and 36 hpi. One sample was treated with 34 µg/mL chloramphenicol (Cm) at 8 hpi and fixed at 36 hpi. Fixed coverslips were stained for indirect immunofluorescence to visualize LRRF1 (green), the inclusion membrane (CT223; red), and DNA and *Chlamydiae* (DAPI and MOMP; blue). Coverslips were imaged using a Zeiss ApoTome.2 with 100x magnification. Scale bar = 10 µm. Arrows indicate early inclusions at 8 hpi and LRRF1 co-localization with the inclusion at 12 hpi, respectively.

Figure modified from Olson et al. 2019. IAI.

LRRF1 co-localization with the inclusion is conserved among several Chlamydia trachomatis serovars and Chlamydia species

LRRF1 contains a coiled-coil domain as well as a cytosolic nucleic acid binding domain (229, 231), indicating two possible modes of LRRF1 recruitment to the inclusion membrane. To test if LRRF1 recruitment was mediated by a bacterial protein or as part of an innate response to infection by an intracellular bacterium, HeLa cells were infected, fixed, and processed as indicated in the *Methods* with various *Chlamydia trachomatis* serovars and *Chlamydia* species. The avirulent strain of *Coxiella burnetii* (Nine Mile Phase 2) was also included, which interacts with different eukaryotic pathways than *Chlamydia* (31). Our analysis of LRRF1 localization during infection of different *Chlamydia* species and *C. trachomatis* serovars revealed that LRRF1 co-localized with the inclusion of *C. trachomatis* serovar L2 (as observed above (Fig. 3-6)), *C. trachomatis* serovar D, and the closely related *Chlamydia muridarum* (Fig. 3-7A). LRRF1 did not co-localize with the inclusion of *Chlamydia pneumoniae*, *Chlamydia caviae*, or to the *Coxiella*-containing vacuole of *Coxiella burnetii* (Fig. 3-7B). We conclude from these data that an Inc protein conserved between *C. trachomatis* serovar L2, serovar D, and *C. muridarum* recruits LRRF1 to the inclusion membrane.

BACTH assay to screen for LRRF1-Inc interacting partners

To determine if IncF and IncA used in the proximity labeling experiments can bind LRRF1, we used the bacterial adenylate cyclase two-hybrid (BACTH) system to screen for protein-protein interactions (105, 223, 236). Here, two plasmids encoding proteins of interest genetically fused to the catalytic fragments (i.e., T25 and T18) of the *Bordetella pertussis* adenylate cyclase are co-transformed into *E. coli* (Δ*cyaA*) (163-165, 236). An interaction between two proteins of interest brings the catalytic fragments in close proximity, restoring adenylate cyclase activity (165, 236, 237). Adenylate cyclase

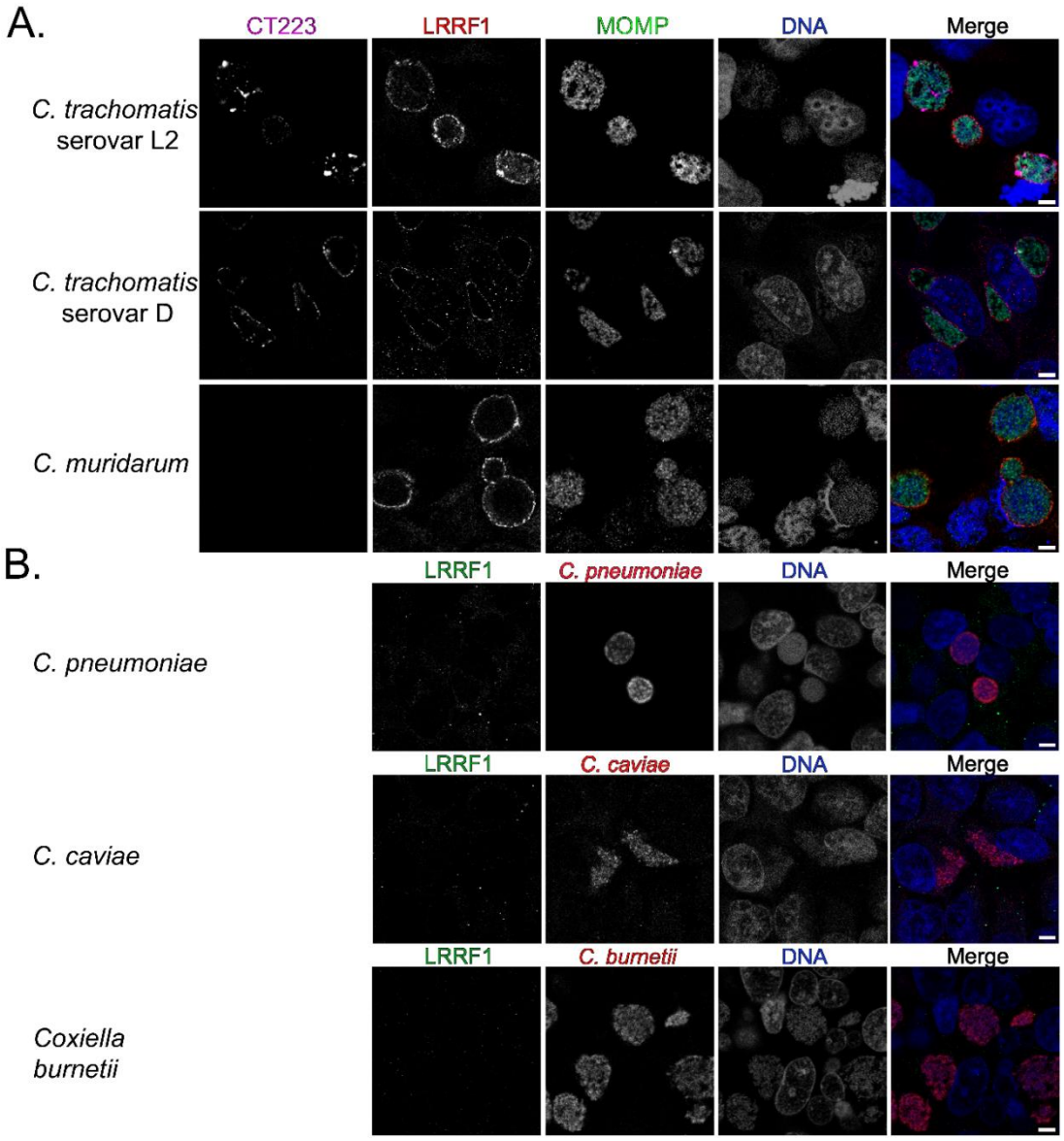

Figure 3-7. Examination of recruitment of LRRF1 to the inclusions of different chlamydial species and to the parasitophorous vacuole of the *Coxiella burnetii* Nine Mile Phase II.

(A) HeLa cells were infected with *C. trachomatis* serovar L2, *C. trachomatis* serovar D, or *C. muridarum*, fixed with methanol at 24 hpi and stained for immunofluorescence to visualize the inclusion membrane (CT223; pink), LRRF1 (red), *Chlamydiae* (MOMP; green), and DNA (DAPI; blue). (B) HeLa cells were infected with either *C. pneumoniae* and fixed in 4% paraformaldehyde at 96 hpi, with *C. caviae* and methanol fixed at 24 hpi, or with *C. burnetii* Nine Mile Phase II and fixed with methanol at 3 days post-infection. Coverslips were stained for immunofluorescence to visualize LRRF1 (green), bacteria (red), and DNA (DRAQ5; blue) and imaged using a Zeiss confocal LSM 800 with 63x magnification and 2x zoom. Scale bar = 5 µm.

Figure modified from Olson et al. 2019. IAI.

activity results in the production of cAMP and activates the expression of β-galactosidase via regulation of the chromosomally encoded *lac* operon in *E. coli* (163-165, 236). Positive interactions, indicated by the presence of blue colonies, are detected on minimal media (supplemented with Isopropyl β-D-1-thiogalactopyranoside (IPTG) and 5-Bromo-4-chloro-3-indolyl-β-D-galactopyranoside (X-gal), and interactions are quantified by β-galactosidase assay (163-165, 236).

A targeted screen was performed using IncF and IncA, CT223, CT813, CT288, and CT226. These Incs were either detected in our proximity labeling experiments or are Incs that are conserved between *C. trachomatis* serovar L2, serovar D, and *C. muridarum* (104). Of interest, LRRF1 contains a coiled-coil domain (231), which is a feature shared by several chlamydial Incs (103, 110, 111). Homotypic interactions have been previously described for IncA (105), which was used as a positive control. All interactions tested were quantified by β-galactosidase assay (105, 221). No interaction was observed between LRRF1 and IncF, IncA, CT288, CT223, or CT813 (Fig. 3-8A). A positive interaction was detected between CT226 and LRRF1 (Fig. 3-8A) and is consistent with previously reported data (122). CT226, like LRRF1, contains a coiled-coil domain (103). The interaction between LRRF1 and CT226 appeared specific because no other Incs tested, even Incs with coiled-coil domains, yielded a positive interaction (Fig. 3-8A). In addition, CT226 and LRRF1 interactions were positive in both BACTH plasmid conformations (e.g., T25-LRRF1 vs. T18-CT226; T25-CT226 vs. T18-LRRF1).

We did not detect a positive interaction between LRRF1 and IncA or LRRF1 and IncF, our original Inc-APEX2 constructs. Instead, it is possible that LRRF1 may be proximal to, but not directly binding, IncA and IncF at the inclusion membrane. To address this, we tested by BACTH the interactions of IncF and IncA with CT226, and both were found to interact with CT226 (Fig. 3-8B). CT226 also demonstrated homotypic

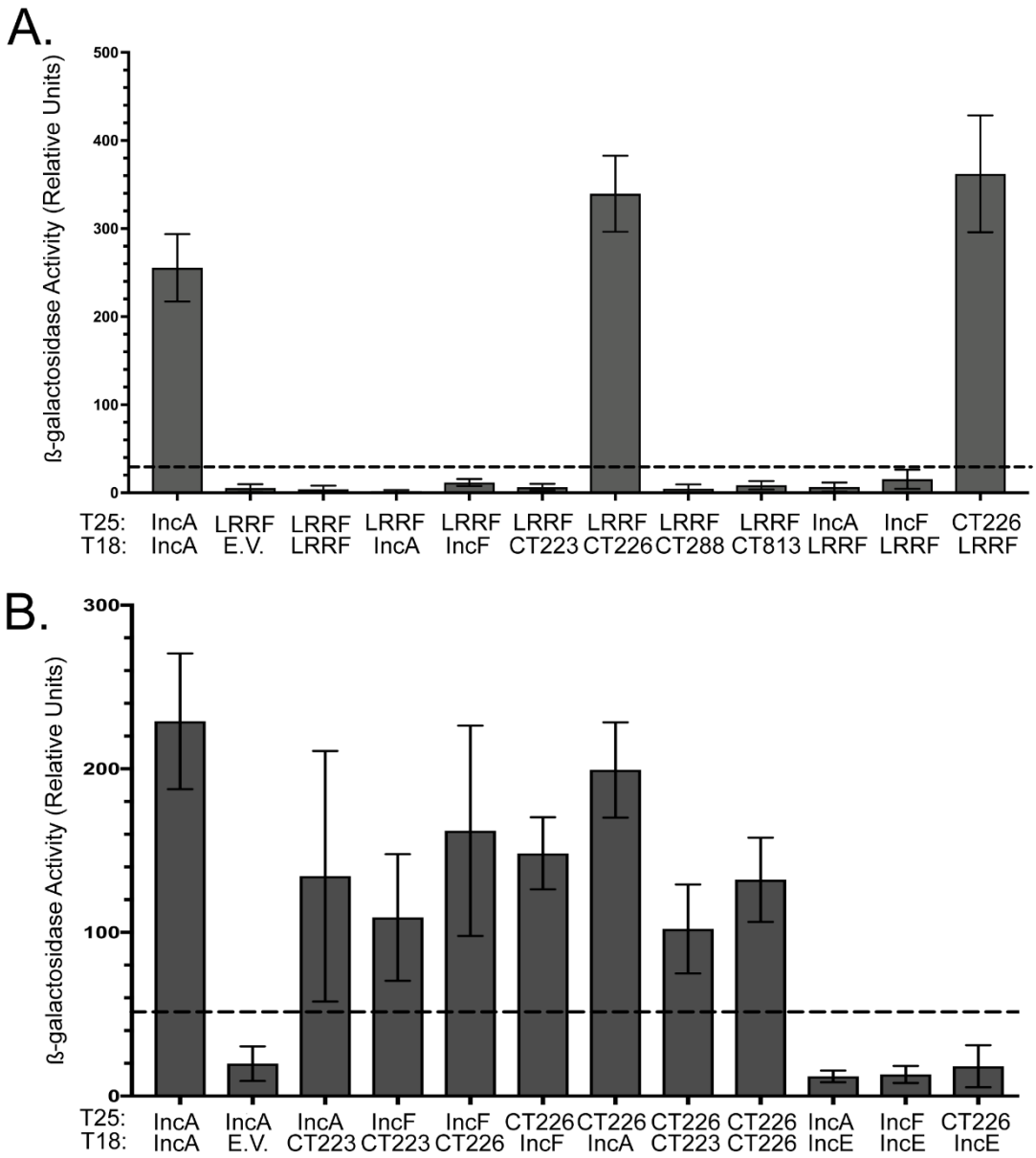

Figure 3-8. Bacterial Adenylate Cyclase Two-Hybrid (BACTH) assay to screen for LRRF1-Inc and Inc-Inc protein interactions.

pST25 and pUT18 fused to chlamydial *Incs* or *LRRF1* as indicated were co-transformed into DHT1 *E. coli* (Δ *cyaA*), plated on minimal media containing IPTG and X-gal and grown for 3-5 days at 30 °C. Colonies were picked for overnight culture, and the interaction was quantified by β-galactosidase assay and reported at relative units (RU). (A) Quantitative analysis of LRRF1-Inc interactions, (B) Quantitative analysis of Inc-Inc interactions. Greater than five times the negative control is considered a positive interaction (indicated by the dotted line). Data shown are the mean and standard deviation from three biological replicates, except for IncE interactions which are representative of two biological replicates.

Figure modified from Olson et al. 2019. IAI.

interactions (Fig. 3-8B). Finally, we tested the ability of IncF and IncA to interact with CT223 (SAINT BFDR=0), the statistically significant Inc identified from each IncF-APEX2, $IncA_{TM}$-APEX2, and IncA-APEX2 dataset. IncF and IncA each interacted with CT223 by BACTH (Fig. 3-8B). CT223 also interacted with CT226 by BACTH (Fig. 3-8B). In contrast, neither IncF nor IncA positively interacted with IncE (SAINT BFDR=0.18 and 0.2, respectively), indicating specificity for the BACTH interactions between the Incs tested (Fig. 3-8B), and not due to the lack of sufficient IncE expression (Fig. S3-5). These data support the likelihood that CT223 and CT226 are proximal to IncF and IncA in the inclusion membrane. The identification of CT226-LRRF1 interaction by BACTH assay corresponds to both the immunofluorescence data (Fig. 3-7) and bioinformatic predictions because CT226 is conserved between *C. trachomatis* and *C. muridarum* but not *C. pneumoniae* or *C. caviae* (104).

Assessment of LRRF1 co-localization with chlamydial Incs in C. trachomatis L2 infected HeLa cells by super-resolution microscopy

To assess the spatial localization and proximity of LRRF1 with respect to IncA and IncF, we used structured illumination (SIM) super-resolution microscopy. We also examined the localization of CT226, which was identified by BACTH as a potential interacting partner with LRRF1. Our IncA and IncF antibodies are both rabbit antibodies, as are the LRRF1 and FLII antibodies, precluding our ability to test endogenous IncF and IncA co-localization in *C. trachomatis* L2 infected eukaryotic cells. There are also no antibodies currently available to test if endogenous CT226 co-localizes with LRRF1 during *C. trachomatis* L2 infection. To assess co-localization of LRRF1 with IncF and IncA, we used our *C. trachomatis* L2 IncF-APEX2, $IncA_{TM}$-APEX2, and IncA-APEX2 strains. In addition, we created *C. trachomatis* L2 transformed with a plasmid encoding CT226 fused

to a FLAG tag (CT226-FLAG) to test localization between CT226 and endogenous LRRF1.

HeLa cells were infected with *C. trachomatis* L2 wild-type (i.e., non-transformed) or the *C. trachomatis* L2 Inc-APEX2 or CT226-FLAG strains and induced for construct expression at 20 hpi (1 nM aTc for IncF-APEX2 and 5 nM for all other strains). At 24 hpi, cells were fixed in ice cold methanol and processed for immunofluorescence as in *Methods* to detect the localization of IncF-APEX2, $IncA_{TM}$-APEX2, IncA-APEX2, and CT226-FLAG with endogenous LRRF1. We assessed LRRF1 localization with endogenous CT223, the statistically significant chlamydial protein identified in each Inc-APEX2 dataset (Fig. 3-9). Endogenous CT223 appeared in puncta as previously observed (87, 238), and LRRF1 appeared to uniformly localize around the inclusion, consistent with our earlier localization data for LRRF1 (Fig. 3-5B). By SIM super-resolution microscopy, LRRF1 co-localized with each Inc-APEX2 construct, supporting the identification of LRRF1 using each construct (Fig. 3-9). The expressed CT226-FLAG also co-localized with endogenous LRRF1 (Fig. 3-9). Interestingly, the expression of CT226-FLAG resulted in fibers staining for CT226 extending from the inclusion, similar in appearance to IncA-fibers (239). LRRF1 was also observed to co-localize with CT226 fibers (Fig. 3-9B; arrows indicate fibers). In contrast, LRRF1 did not co-localize with fibers of IncA-APEX2 constructs (Fig. 3-9C).

Overexpression of CT226-FLAG from C. trachomatis L2 CT226-FLAG results in increased LRRF1 and FLII at the inclusion membrane

Next, we determined the effect of variable expression levels of CT226-FLAG from *C. trachomatis* L2 CT226-FLAG on the recruitment of LRRF1 and FLII. HeLa cells were infected with *C. trachomatis* L2 CT226-FLAG and either not induced or induced for

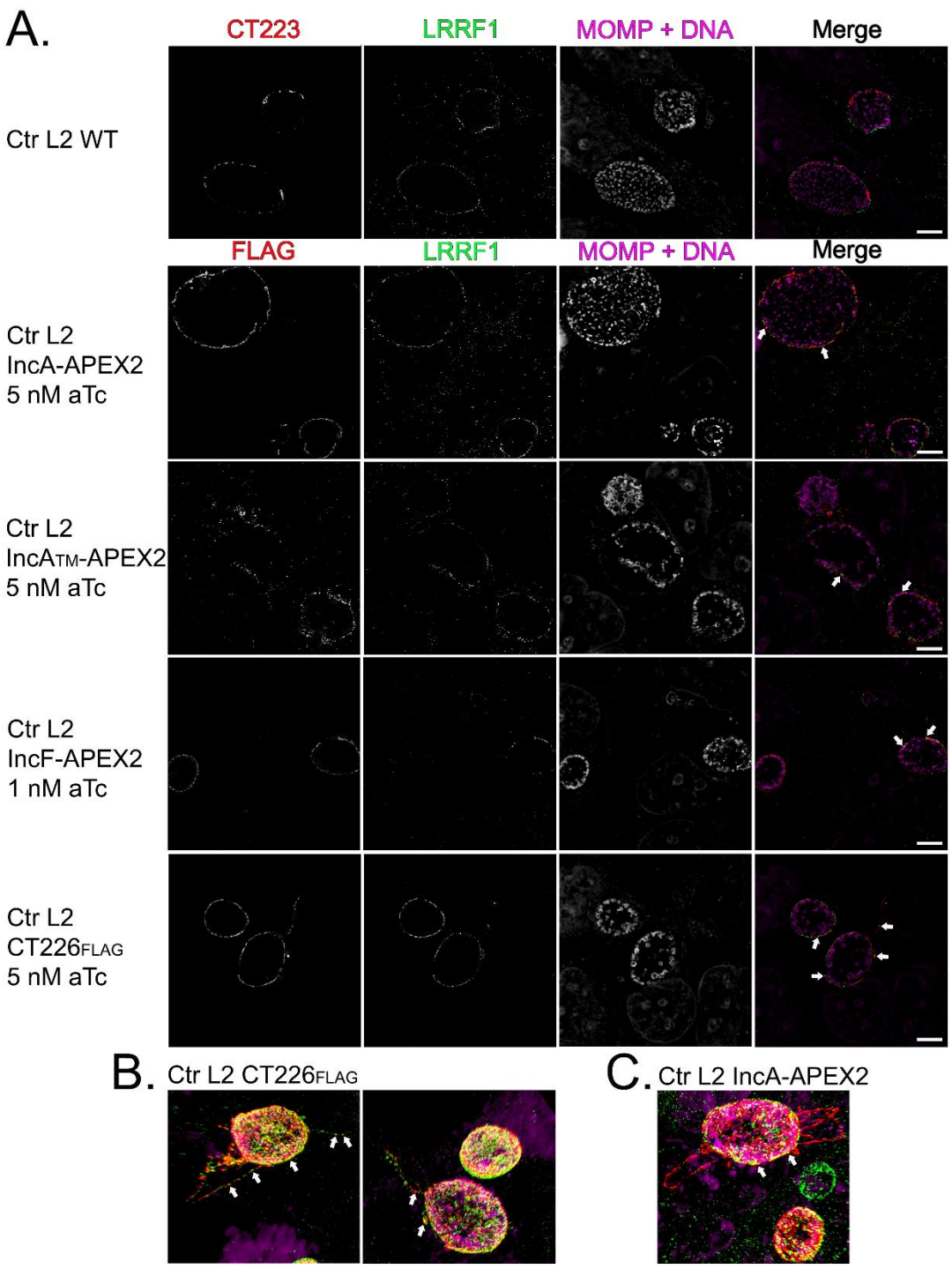

Figure 3-9. Assessment of LRRF1 co-localization with Incs using *C. trachomatis* L2 transformed strains in infected HeLa cells with super-resolution microscopy.

(A) Hela cells seeded on glass coverslips were infected with the *C. trachomatis* L2 Inc-APEX2 strains or the CT226-FLAG strain and induced for expression at 20 hpi (IncF-APEX2 was induced with 1 nM aTc; 5 nM aTc for all other strains).

(continued on the next page)

At 24 hpi, coverslips were fixed with ice cold methanol and stained for immunofluorescence to visualize construct expression (FLAG) or CT223 (red), LRRF1 (green), *Chlamydiae* and DNA (DRAQ5 and MOMP; pink). Coverslips were imaged by Zeiss Elyra super-resolution microscopy 63x2x with structural illumination (SIM). Scale bar = 5 µm. (B) SIM 3D snapshot of *C. trachomatis* L2 CT226-FLAG infected HeLa cells with CT226-FLAG and LRRF1 positive fibers. (C) SIM 3D snapshot of *C. trachomatis* L2 IncA-APEX2 infected HeLa cells with IncA fibers. Arrows indicate co-localization between the indicated expressed construct and LRRF1.

Figure modified from Olson et al. 2019. IAI.

construct expression at 7 hpi using 5 nM aTc and 20 nM aTc. The coverslips were fixed at 24 hpi with a formaldehyde/glutaraldehyde solution as indicated in *Methods* and stained to visualize LRRF1, FLII, and CT226-FLAG. All images were obtained using the same exposure (set to the 20 nM aTc samples) on a confocal LSM 800 with 63x2x magnification. Increased LRRF1 and FLII is detected at the inclusion membrane upon increased expression of CT226-FLAG (Fig. S3-6). Note that LRRF1 is observed at the inclusion of *C. trachomatis* L2 CT226-FLAG infected cells not induced for expression of CT226 using normal exposure levels (Fig. S3-7). These data support the recruitment of LRRF1 to the inclusion membrane by CT226 during *C. trachomatis* infection of HeLa cells.

Co-immunoprecipitation of endogenous LRRF1 with C. trachomatis L2 CT226-FLAG

To test if LRRF1 was directly binding to CT226, we performed co-immunoprecipitation assays with CT226-FLAG expressed from *C. trachomatis* transformed with CT226-FLAG in infected HeLa cells. HeLa cells were plated in 6-well plates containing glass coverslips to confirm construct expression and localization. HeLa cells were infected with *C. trachomatis* L2 CT226-FLAG or with *C. trachomatis* L2 IncF-FLAG as a negative control. At 7 hpi, the constructs were either not induced or induced for expression using 5 nM aTc for *C. trachomatis* L2 CT226-FLAG and 1 nM aTc for IncF-FLAG (see (57) regarding IncF induction conditions). At 24 hpi, glass coverslips were removed, paraformaldehyde fixed, processed for immunofluorescence, and then cell lysates were collected and prepared for affinity purification using FLAG beads essentially as previously described (219). Both the clarified lysates (soluble fraction) and the eluates were blotted to detect each construct containing FLAG using an anti-FLAG antibody, and LRRF1 using an anti-LRRF1 antibody. Construct expression was observed for each *C. trachomatis* L2 CT226-FLAG or IncF-FLAG infected cells by immunofluorescence

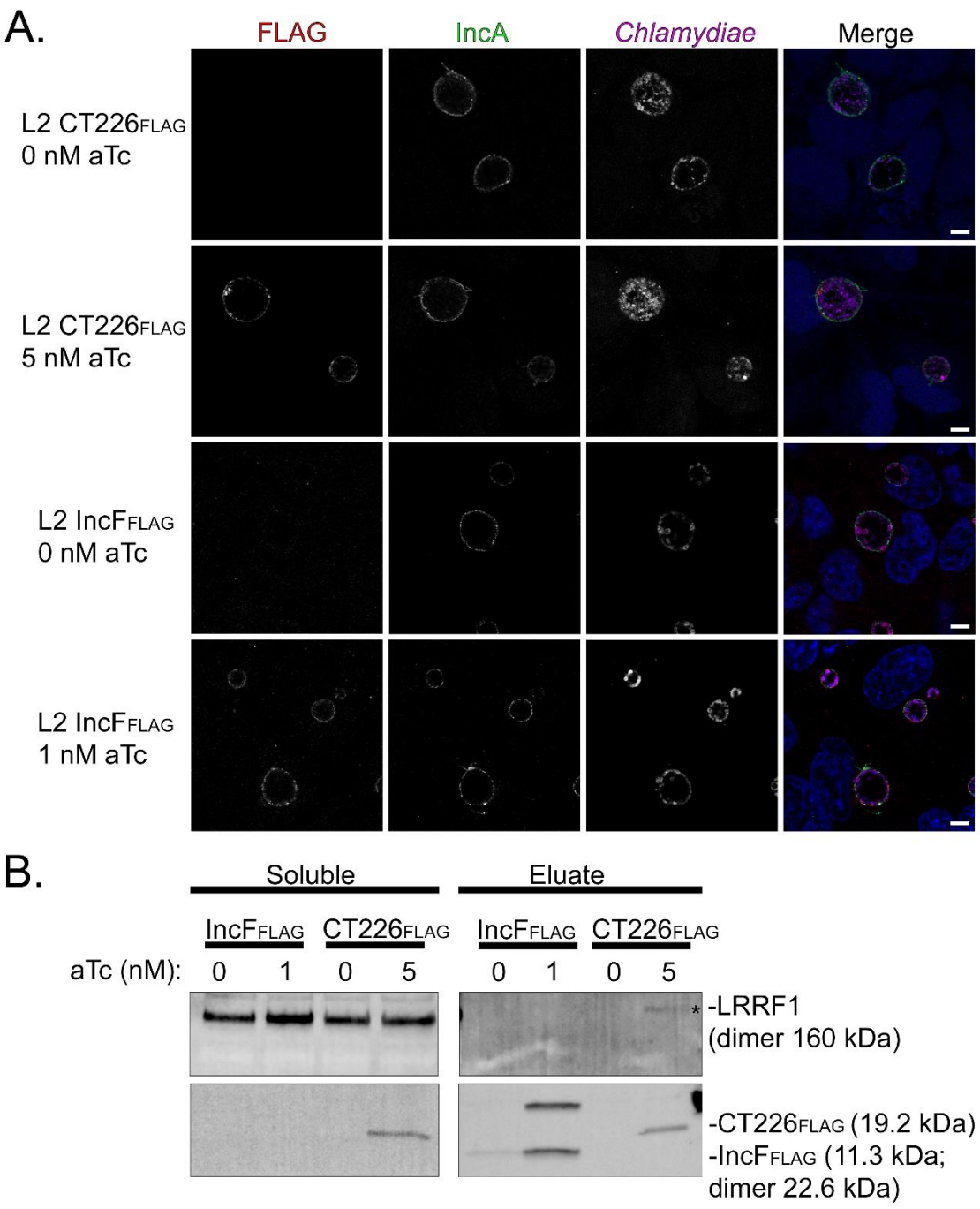

Figure 3-10. Co-immunoprecipitation of endogenous LRRF1 with *C. trachomatis* L2 transformed strain expressing CT226-FLAG.

HeLa cells seeded in a 6-well plate with glass coverslips were infected with *C. trachomatis* L2 CT226-FLAG or IncF-FLAG and either not induced or induced for expression at 7 hpi with 5 nM aTc (CT226-FLAG) or 1 nM aTc (IncF-FLAG).

(continued on the next page)

(A) At 24 hpi, coverslips were removed, fixed in 4% paraformaldehyde (L2 CT226-FLAG) or methanol (L2 IncF-FLAG), and stained to visualize FLAG (red), inclusion membrane marker (IncA; green), chlamydiae (MOMP; pink), and DNA (DAPI; blue) and imaged using a Zeiss confocal LSM 800 with 63x magnification and 2x zoom. Scale bar = 5 μm. (B) The remaining cells were collected, solubilized, normalized, and affinity purified using FLAG beads. The clarified lysates (soluble fraction) and eluate fractions were probed for construct expression (FLAG; CT226-FLAG 19.2 kDa and IncF-FLAG 11.3 kDa), and LRRF1 (dimer 160 kDa). Three independent experiments were performed (see supplementary figure 6 for additional replicates).

Figure modified from Olson et al. 2019. IAI.

co-localized with the inclusion membrane marker, IncA (Fig. 3-10A). The FLAG affinity purified constructs were also detected by western blot (Fig. 3-10B, CT226-FLAG 19.2 kDa, IncF-FLAG 11.3 kDa (monomer) and 22.6 kDa (dimer); Fig. S3-8). However, LRRF1 (dimer 160 kDa) was only detected in the eluate fraction from the *C. trachomatis* L2 strain induced for the expression of CT226-FLAG and not IncF-FLAG. These data further support our BACTH data, suggesting that LRRF1 can bind CT226-FLAG during *C. trachomatis* infection of eukaryotic cells. However, we cannot exclude that CT226-FLAG binds a third protein *in vivo* that recruits LRRF1, which results in the co-immunoprecipitation with CT226-FLAG.

Discussion

We previously reported the feasibility of using the ascorbate peroxidase proximity labeling system (APEX2) in *C. trachomatis* L2 to detect protein-protein interactions at the inclusion *in vivo* (57). This tool improves upon past techniques to understand protein-protein interactions by maintaining the spatial organization of Inc proteins in the inclusion membrane (57). Proteins proximal to and within the inclusion membrane can be biotinylated and identified by affinity purification-mass spectrometry (AP-MS). Here, we used *C. trachomatis* L2 transformed with APEX2 fused to IncF and IncA, two Incs that, based on preliminary data, may represent distinct functional groups: Inc-Inc interactions to promote inclusion membrane organization and integrity or Inc-host protein interactions to facilitate chlamydial-host interactions and nutrient acquisition. As a control, we also created a *C. trachomatis* L2 $IncA_{TM}$-APEX2 strain that lacks the C-terminal SNARE-like domain of IncA and more closely resembles IncF in size.

As a field, we are at the early stages of understanding how the expression of various Inc constructs in the inclusion membrane can alter inclusion membrane organization and host-protein recruitment. We focused on expressing our Inc-APEX2

constructs under conditions similar to endogenous expression levels. This is an important consideration as overexpression of certain Incs can have deleterious effects on inclusion development and Inc localization (57) or can recruit a greater abundance of eukaryotic proteins (Fig. S3-6) that may or may not reflect *in vivo* conditions. This in contrast to a recent study where the authors over-expressed IncB-APEX2 (170), which did not result in localization of IncB-APEX2 to microdomains within the inclusion membrane, as endogenous IncB does (114, 240). The goal of this study may have been to identify all possible inclusion proximal proteins, regardless of specificity. Here, we have sought to understand the context for why a specific protein was prominent in ours and others' datasets, which ultimately revealed important information for how the inclusion membrane may be organized (Fig. 3-11).

To assign statistical significance and eliminate background contaminant proteins from the AP-MS data in an unbiased fashion, the identified proteins from *H. sapiens* and *C. trachomatis* L2 were analyzed by Significance Analysis of INTeractome (SAINT) (207) (Table 3-1; Table S3-1 to S3-3). This type of analysis is an improvement over the previously described statistical analyses used for similar datasets (170) because the *t*-test and G-test to determine whether to include a protein in the dataset is not sufficient to estimate the False Discovery Rate (FDR). Newer methods, such as PepC, use a matrix of *t*-test and G-test confidence intervals to detect differentially expressed proteins (241). The SAINT method constructs separate distributions for true and false interactions to derive the probability of the observed bait-prey interaction. The probability model for the bait-prey interaction pair is used to estimate measurement errors in a transparent manner. SAINT generates a Bayesian False Discovery Rate (BFDR) calculation for each potential interaction detected in the dataset. SAINT also normalizes spectral counts based on protein length, which affects the potential availability of peptides that can be analyzed by

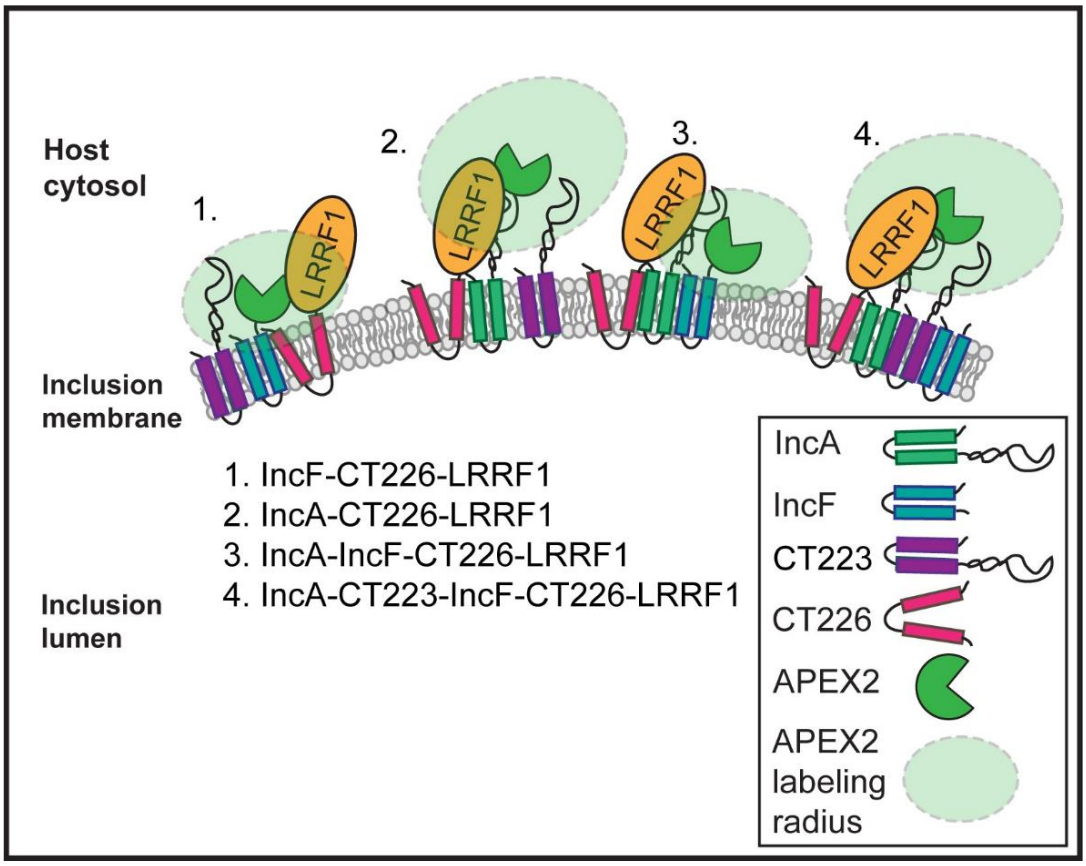

Figure 3-11. Model of Inc-Inc organization in the inclusion membrane and Inc-APEX2 proximity labeling.

Proposed model of Inc organization based on mass spectrometry identified chlamydial Inc proteins using IncA-APEX2 and IncF-APEX2 proximity labeling constructs and bacterial two-hybrid assays (BACTH) to test protein-protein interactions. Based on these data we propose four possible scenarios for the spatial organization of Incs and how these Incs were detected using the APEX2 proximity labeling system: (1) IncF interacts with CT226 which binds LRRF1. (2) IncA interacts with CT226 which binds LRRF1. (3) IncA binds IncF and CT226 which binds LRRF1. (4) IncA, CT223, IncF, and CT226 (which binds LRRF1) all interact with each other. CT223 was statistically significant by SAINT analysis from mass spectrometry data and was able to interact with IncF and IncA by BACTH.

Figure modified from Olson et al. 2019. IAI.

MS/MS. These are more rigorous statistical tests than the independent *t*-test and G-test analyses (207, 242, 243).

We applied STRING interaction and ClueGo pathway analysis tools to our SAINT significant (BFDR≤0.05) eukaryotic proteins identified using the Inc-APEX2 constructs to detect globally enriched pathways. Consistent with our original hypothesis that IncA may preferentially interact with eukaryotic proteins compared to IncF, we detected a larger number of statistically significant eukaryotic proteins with our IncA-APEX2 (192 total) construct than with IncF-APEX2 (13 total), albeit with the caveats related to labeling radius noted below. For $IncA_{TM}$-APEX2, there was more than a log reduction in the number of proteins identified when compared to full-length IncA-APEX2, suggesting specificity for interactions at the C-terminus of IncA. Given the presence of a SNARE-like domain in the C-terminus of IncA, it is possible that the large number of proteins identified with IncA-APEX2 reflects its interactions with other SNARE proteins on vesicles carrying diverse cargo. For instance, vesicle-mediated transport (e.g., ANXA1, AP1M1, CAV1, GOLGA2, PDCD6, PDCD6IP, RAB34, RAB5B, SEC16A, SEC24C, SEC31A, SNX1, SNX2, SNX3, SNX5, SNX6, TFG, TSG101, USO1) has been described in the context of *C. trachomatis* L2 acquisition of specific lipids from Golgi apparatus-derived exocytic vesicles (30, 48, 50). Statistically significant hits involved in SNX-retromer pathway disruption during chlamydial infection include SNX1, SNX2, SNX3, SNX5, SNX6, and SNX27 (122). Additional globally enriched biological processes and molecular functions involving cytoskeleton organization and translation align with previously published data. Cytoskeleton organization (e.g., ACTN1, ACTN4, CDC42, DPYSL3, DYNLL1, MARCKS, PLS3, RAC1, RHOA, SHTN1) corresponds with the literature as the inclusion is surrounded by an F-actin cage (71, 244, 245). One of the four statistically significant eukaryotic proteins identified using each Inc-APEX2 construct, microtubule-associated

protein 1B (MAP1B) (Table S3-2) would be expected because microtubules are known to surround the inclusion (35, 123, 227) and thus would be proximal to both IncF and IncA, which uniformly label the inclusion (88). This interpretation is consistent with the findings of another study using APEX2 (170).

Our AP-MS data also identified multiple statistically significant Inc proteins. Again, IncF-APEX2 labeled three different Incs compared to only two for each of the IncA-APEX2 constructs (one of which was IncA itself). Consistent with our hypothesis, these data, taken together with the few eukaryotic proteins identified, suggest IncF may preferentially interact with other Inc proteins. Importantly, $IncA_{TM}$-APEX2 did not label more Incs than full-length IncA, even if we lowered the BFDR threshold. These data indicate specificity to the IncF-APEX2 identified Incs. Although we identified chlamydial Incs with our Inc-APEX2 proximity labeling system, the majority of Incs detected were not statistically significant by SAINT (Table 3-1; Table S3-1). Some of this may reflect the residues that APEX2 covalently modifies during the biotinylation reaction (cysteine, histidine, tryptophan, and tyrosine residues) (168, 189, 193). The Incs that were significant (e.g., CT223 and IncA) have 11-20 cytosolically exposed target amino acids, whereas Incs that were not found to be statistically significant have fewer than 5-6 exposed target amino acids, in general. Therefore, proteins containing fewer APEX2-modifiable amino acids will not be efficiently tagged with biotin and subsequently not enriched as efficiently in the streptavidin affinity purification. Secondly, there are also inherent difficulties in identifying hydrophobic proteins by mass spectrometry. To counter this difficulty, we included two enzymes to digest purified proteins into peptides, but these efforts, in combination with limited modifiable amino acids, may not have allowed for enough enrichment of APEX2-targeted Inc proteins. To compensate for this limitation, a lower BFDR significance threshold could be considered when analyzing chlamydial Inc proteins. For example, when we lowered

the BFDR threshold to 0.2, we identified eight Incs from our AP-MS data, including IncA in the IncF-APEX2 dataset that was detected by western blot (Fig. 3-3). Further experimentation and analysis of Inc-Inc APEX2 data are required to identify an appropriate cut-off.

Using chlamydial expressed Inc-APEX2 constructs, we identified several chlamydial Incs and their known interacting eukaryotic protein partners including IncG and 14-3-3β (142), IncD and CERT (54, 126), CT228 and myosin phosphatase target protein subunit 1 (MYPT1) (38), and IncE and sorting nexin 5 (SNX5) and SNX6 (122) (Table 3-1; Table S3-1 to S4-3). In addition, we identified eukaryotic proteins that were unique to each IncF-APEX2 and IncA-APEX2 datasets that have not been demonstrated to localize to the chlamydial inclusion, and, thus, require further validation (Table 3-2). In support of our hypothesis that IncA might preferentially interact with eukaryotic proteins compared to IncF, more eukaryotic proteins were identified using IncA-APEX2 than with IncF-APEX2 as noted above (Table S3-2). We expanded on the current knowledge of proteins recruited to the inclusion membrane with the validation of two eukaryotic proteins not previously reported at the inclusion: LRRF1, which was statistically significant in each Inc-APEX2 dataset, and its known binding partner FLII, which was statistically significant in the IncA-APEX2 dataset (Table S3-2; Fig. 3-5 through Fig. 3-7). We also identified a potential chlamydial protein interacting partner for LRRF1 by BACTH: CT226 (Fig. 3-8A). These data are consistent with a previous report of LRRF1 and CT226 potential interactions identified by transfecting host cells with epitope-tagged CT226 followed by AP-MS (122).

We detected LRRF1 at the inclusion membrane, but LRRF1 knockdown does not negatively impact chlamydial progeny production in HeLa cells (Fig. S3-4C). One explanation for this may be that *C. trachomatis* already prevents the normal function of LRRF1 by sequestering it at the inclusion membrane. In this context, knockdown would

not affect the production of infectious progeny. Alternatively, LRRF1 has been implicated in the production of a type 1 interferon response (229, 230) so a more relevant tissue culture model may be required, such as human macrophages (246), which produce a robust interferon-mediated immune response. As no phenotype for LRRF1 knockdown was apparent, we chose to examine the nature of how LRRF1 was biotinylated by our constructs and ultimately identified in our dataset, as it has also been found in previous AP-MS datasets (122, 170, 171). The BACTH assays (Fig. 3-8A) provide evidence for an interaction between LRRF1 and CT226. Further, the SIM super-resolution data indicated co-localization between LRRF1 and overexpressed CT226-FLAG (*C. trachomatis* L2 CT226-FLAG strain) at the inclusion membrane as well as with CT226-FLAG positive fibers emanating from the inclusion (Fig. 3-9). Lastly, we identified LRRF1 in CT226-FLAG co-immunoprecipitations, indicating that these proteins are true binding partners during chlamydial infection. We conclude that LRRF1 was likely labeled by APEX2 because CT226 is adjacent to, and likely interacting with, IncA and IncF in the inclusion membrane, which would position it within the labeling radius of our APEX2 constructs (Fig. 3-11). We attempted to make a CT226 knockout by allelic exchange but have been unsuccessful thus far. This may suggest that CT226 is essential or that possible overexpression of CT225 and CT227 in the homology regions of the allelic exchange vector is deleterious. Alternatively, other genetic tools such as TargeTron (109), or a conditional knockdown by CRISPRi (121), may successfully disrupt CT226 expression.

Our study has also revealed potential limitations of the APEX2 proximity labeling system to distinguish differences between Inc-protein binding partners and proteins that are in spatial proximity to the Incs at the inclusion membrane, as summarized in Fig. 3-11. For instance, the labeling radius of APEX2, at least in our hands, may be larger than originally described (189). This would explain the identification of proteins proximal to IncF

and IncA and not only specific protein binding partners at the inclusion (Fig. 3-11). For example, although we identified strong LRRF1 recruitment to the inclusion (Fig. 3-5), IncF and IncA, our bait proteins, were not identified as interacting partners of LRRF1 by BACTH or using IncF-FLAG co-immunoprecipitations (Fig. 3-8A). In addition, the spatial organization of Incs in the inclusion membrane is not currently well understood, but IncA and IncF uniformly decorate the inclusion membrane as opposed to CT223, which localizes in discrete regions. *In vivo* two-hybrid experiments have shown that IncA and IncF interact (105), which might support the labeling of similar proximal proteins, and we identified IncA in IncF-APEX2 labeled eluates (Fig. 3-3). Another possible explanation for a larger labeling radius is related to the diffusion rate and half-life of biotin-phenol, which is approximately one millisecond (193). Diffusion of biotin-phenol would contribute to a greater labeling radius and a larger pool of proteins identified. In support of the diffusion of biotin-phenoxyl radicals with our Inc-APEX2 constructs, we identified Outer Membrane Complex B (OmcB) and Major Outer Membrane Protein (MOMP) in the AP-MS data (Table 3-1, Table S3-1). It is possible that during labeling with the Inc-APEX2 strains, biotin-phenoxyl diffuses across the inclusion membrane and labels the bacteria (intra-inclusion) before the quenching step, and OmcB and MOMP are amongst the most abundant outer membrane chlamydial proteins. Shorter labeling times may decrease the labeling radius and increase labeling specificity (197). Also, BACTH assays are a useful tool to determine protein-protein interactions *in vivo* using *E. coli*. In this study, using the BACTH assay to test chlamydial Inc-Inc protein interactions, we observed CT223-IncF and CT223-IncA interactions (Fig. 3-8B), which supports the identification of CT223 as a statistically significant Inc using each Inc-APEX2 construct (Table 3-1). However, we might miss some interactions with the BACTH system if eukaryotic post-translational modifications are required for the protein interactions to occur (e.g., phosphorylation; (247)). Therefore, other validation methods such as super-resolution microscopy or

Duolink® PLA technology, provided antibodies are available, are required. Alternatively, overexpression models could be used to detect interactions with epitope-tagged Incs (with the caveats previously noted). Importantly, these data highlight the necessity of using adequate controls and statistical analyses to eliminate false positives and other proteins that may be transiently near the inclusion during the labeling period.

Our data highlight the utility of the ascorbate peroxidase proximity labeling system to detect novel protein interactions at the *C. trachomatis* inclusion membrane *in vivo*. This tool improves upon past techniques by maintaining the spatial organization of Incs in the inclusion membrane and biotinylating proximal proteins *in vivo*. Our goal was to determine if there is a preference for certain Incs toward Inc-Inc interactions or Inc-eukaryotic interactions in the inclusion membrane using the AP-MS SAINT data as the foundation for further study. Determining the complex types of interactions that Incs orchestrate in the inclusion membrane will lead to a better understanding of how *Chlamydiae* survive in their intracellular niche. Importantly, this technique is broadly applicable, when properly controlled, to other intracellular bacteria or parasites residing within a membrane-bound vacuole.

Acknowledgments

This work was supported by UNMC start-up funds for E.A. Rucks and S.P. Ouellette and partially supported by both an R01AI114670-01A1 awarded to E.A. Rucks and an R35GM124798-01 awarded to S.P. Ouellette. N.T. Woods is supported by P20 GM121316. A. Lawrence is supported by The Sherwood Foundation.

We would like to thank R. Suchland (University of Washington, WA) and Dr. D. Rockey (Oregon State University, OR) for the anti-CT223 antibody, Dr. T. Hackstadt (NIAID, Rocky Mountain Laboratories, Hamilton, MT) for the anti-IncA antibody, Dr. R.

Morrison (University of Arkansas for Medical Sciences, Little Rock, AR) for the anti-chlamydial Hsp60 antibody, and Dr. H. Caldwell (NIAID, Bethesda, MD) for the *C. pneumoniae* anti-MOMP antibody. We would also like to thank Dr. Bob Heinzen (NIAID, Rocky Mountain Laboratories, Hamilton, MT) for avirulent *Coxiella burnetii* Nine Mile Phase II strains.

The authors would also like to thank Eric Troudt and Vikas Kumar for processing samples for mass spectrometry and their technical expertise, and Tom Bargar for processing samples for electron microscopy. The transmission electron microscope is supported by NIH Shared Instrument grant (NIH 1 S10 RR024650 01A1). This work was also supported by the UNMC Center Advanced Microscopy Core Facility and the UNMC Advanced Proteomics Core Facility, and the UNMC Electron Microscopy Core Facility. The University of Nebraska Medical Center Advanced Microscopy Core Facility receives partial support from the National Institute for General Medical Science (NIGMS) INBRE - P20 GM103427 and COBRE - P30 GM106397 grants, as well as support from the National Cancer Institute (NCI) for The Fred & Pamela Buffett Cancer Center Support Grant- P30 CA036727, and the Nebraska Research Initiative. This publication's contents and interpretations are the sole responsibility of the authors.

Appendix A - Supplementary Figures

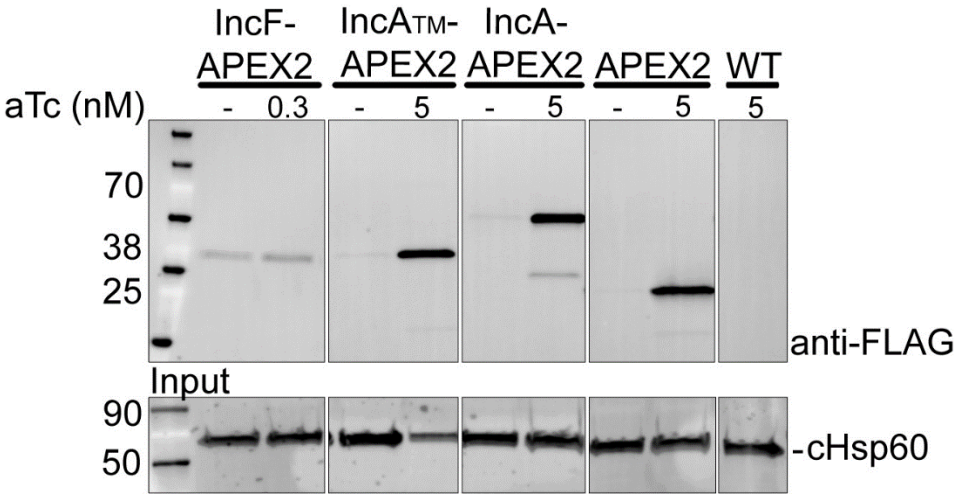

Figure S3-1. Western blot detection of the expressed APEX2 constructs.

HeLa cells infected with *C. trachomatis* L2 Inc-APEX2, APEX2 only, or wild-type (WT) strains were induced with anhydrotetracycline (aTc) at 7 hpi (0.3 nM for IncF-APEX2; all other samples 5 nM), or not induced as indicated. Lysates were collected at 24 hpi, solubilized, and affinity purified using FLAG beads. The eluates were separated by electrophoresis, transferred to PVDF membrane, and blotted for APEX2 containing constructs using anti-FLAG antibody. The total lysate (input) was probed with anti- *C. trachomatis* Hsp60 (cHsp60) antibody as a loading control.

Figure modified from Olson et al. 2019. IAI.

A. IncF-APEX2

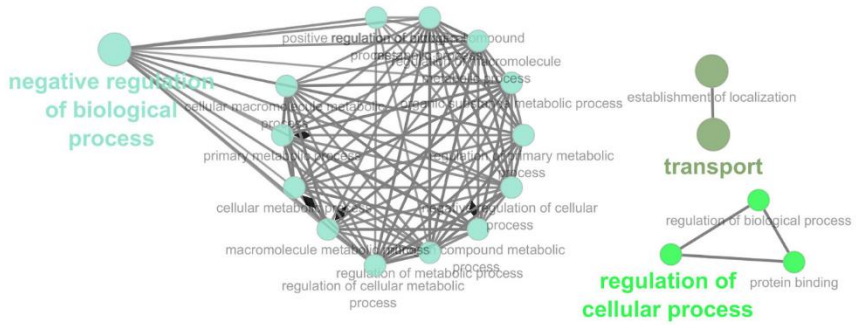

B. IncA$_{TM}$-APEX2

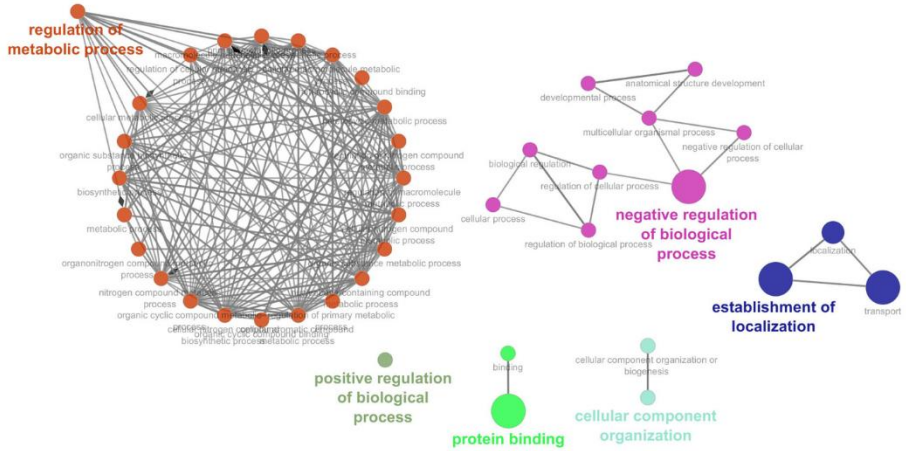

C. IncA-APEX2

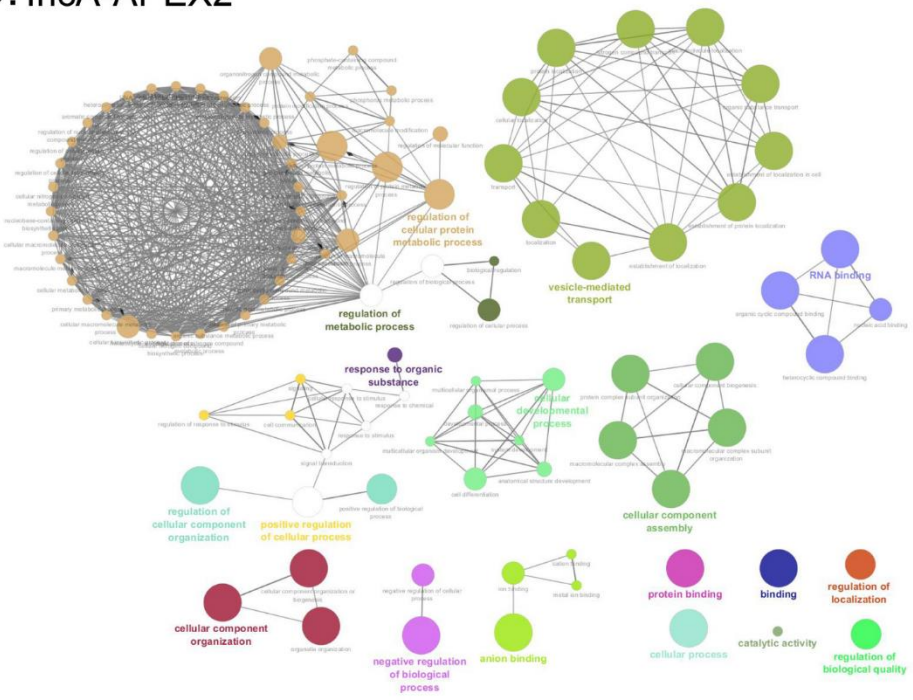

(continued on next page)

Figure S3-2. Visualization of global biological processes and molecular function of AP-MS identified statistically significant eukaryotic proteins using *C. trachomatis* L2 Inc-APEX2 strains.

Affinity purified-mass spectrometry (AP-MS) identified spectra were compared to the Homo sapiens database using Mascot and then Significance Analysis of INTeractome (SAINT) was applied to identify statistically significant proteins (BFDR ≤ 0.05) from each dataset. Global networks identified using each *C. trachomatis* L2 transformed with (A) IncF-APEX2, (B) $IncA_{TM}$-APEX2, and (C) IncA-APEX2 are shown.

Figure modified from Olson et al. 2019. IAI.

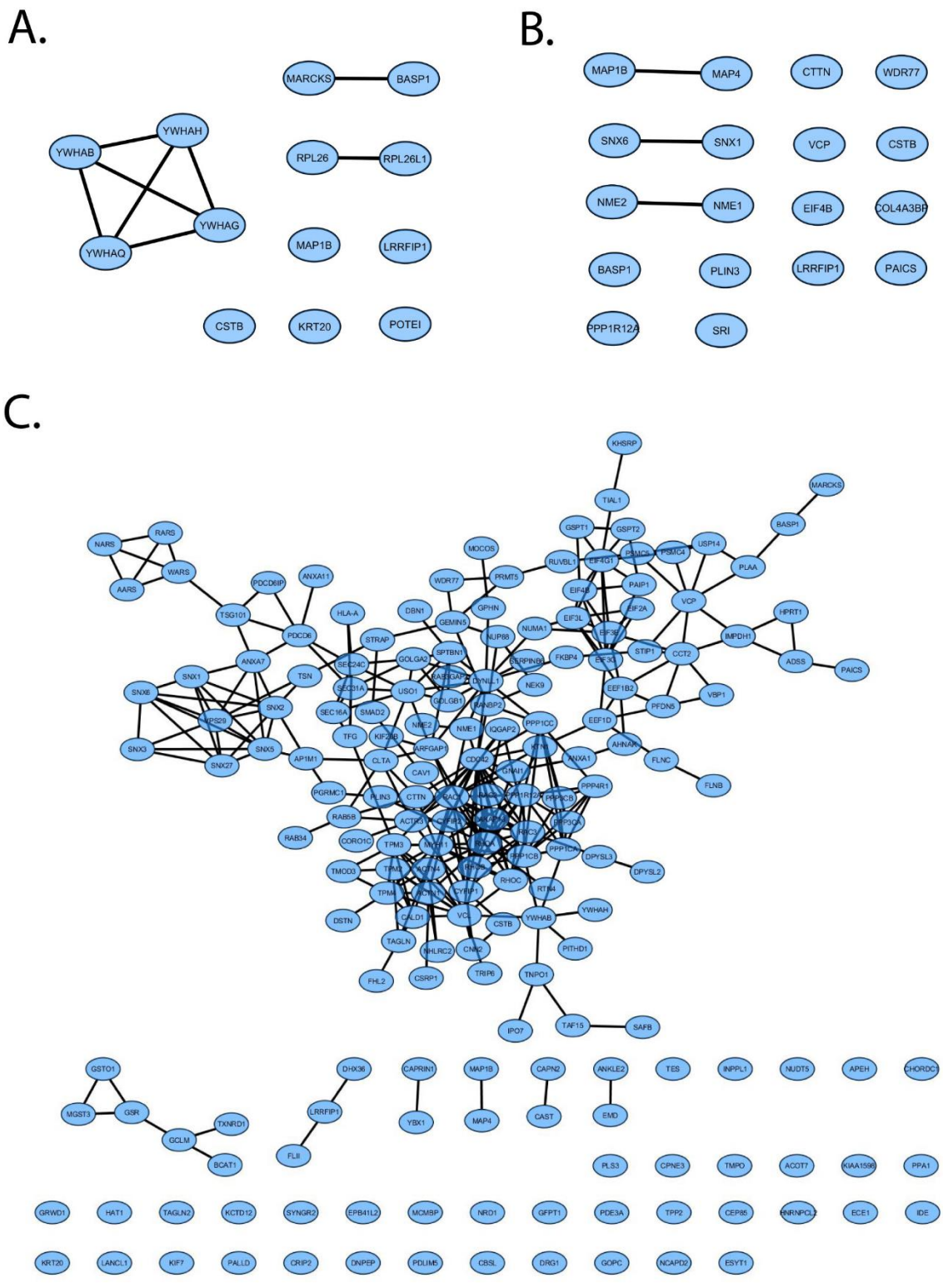

(continued on next page)

Figure S3-3. STRING network analysis of statistically significant eukaryotic proteins.

Significance Analysis of INTeractome (SAINT) was applied to identify statistically significant AP-MS identified eukaryotic proteins using *C. trachomatis* L2 IncF-APEX2, $IncA_{TM}$-APEX2, and IncA-APEX2. STRING network (0.7 high confidence) visualization of eukaryotic proteins identified by mass spectrometry (SAINT BFDR ≤ 0.05) from each *C. trachomatis* L2 (A) IncF-APEX2, (B) $IncA_{TM}$-APEX2, and (C) IncA-APEX2.

Figure modified from Olson et al. 2019. IAI.

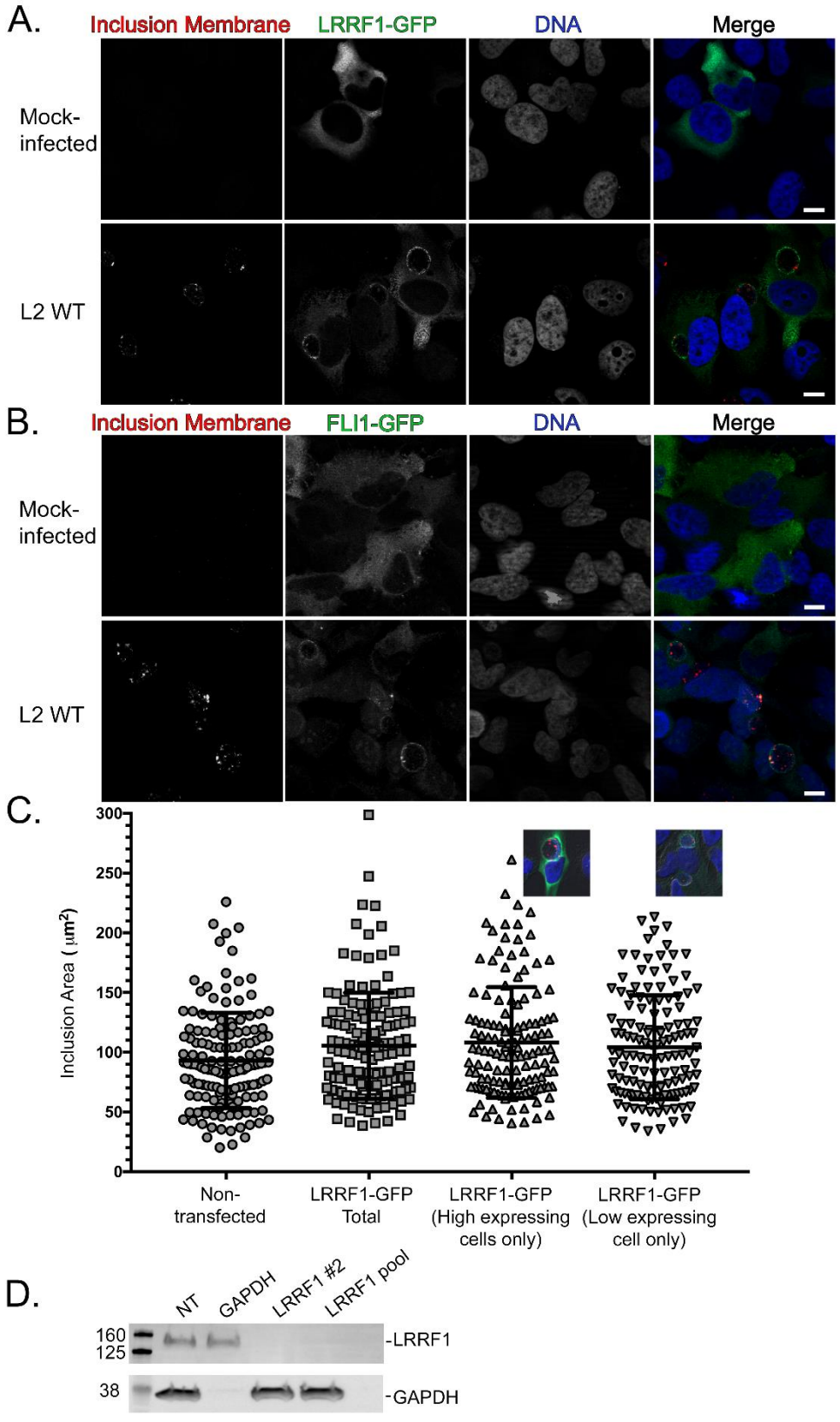

(continued on next page)

Figure S3-4. The effect of LRRF1-GFP and FLII-GFP overexpression and LRRF1 knockdown on *C. trachomatis* progeny production.

HeLa cells seeded onto coverslips were transfected with (A) 100 ng pCMV6-AC-LRRF1-GFP or (B) 500 ng pCMV6-AC-FLII-GFP. Transfected cells were either mock-infected or infected with *C. trachomatis* L2 wild-type at 6 hours post-transfection. At 24 hpi, HeLa cells were paraformaldehyde fixed, 0.5 % Triton X-100 permeabilized, and stained for immunofluorescence to visualize the inclusion membrane (CT223; red), DNA (DRAQ5; blue) and (A) LRRF1-GFP or (B) FLII-GFP. Coverslips were imaged using a Zeiss with ApoTome.2 at 100x. Scale bar = 10 µm. (C) Inclusion area measurements from HeLa cells transfected with pCMV6-AC-LRRF1-GFP and infected with *C. trachomatis* L2 wildtype (as above) were compared to non-transfected HeLa cells infected with *C. trachomatis* L2 wild-type. Inclusion area is reported for non-transfected, LRRF1-GFP Total (the inclusions from both high and low LRRF1-GFP expressing cells) and broken into LRRF1-GFP high and low expression only (see inset). Two independent experiments were performed. Inclusion area was graphed in GraphPad Prism 7 and a one-way ANOVA with Tukey's multiple comparisons post-hoc test was performed to determine statistical significance. There was no significant difference in inclusion area. (D) siRNA knockdown of LRRF1 in HeLa cells. 20 nM of non-targeting (NT), GAPDH, LRRF1 single siRNA or 3 pooled siRNAs were reverse transfected as indicated into HeLa cells that were then infected with *C. trachomatis* L2 wild-type at 48 hours post-transfection and collected 24 hours later. Lysates from siRNA treated, *C. trachomatis* L2 wild-type infected cells were collected in 2x Laemmli sample buffer, electrophoresed, transferred to PVDF and blotted to confirm siRNA knockdown efficiency of LRRF1 and GAPDH.

Figure modified from Olson et al. 2019. IAI.

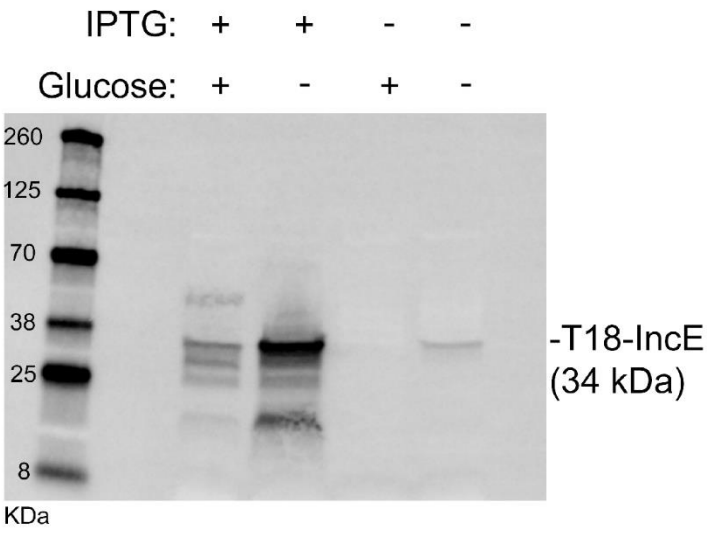

Figure S3-5. T18-IncE is expressed in *E. coli*.

DH5α lacIq E. coli were transformed with pUT18C-IncE and grown overnight. Expression of T18-IncE was induced or not using 0.5 mM IPTG and with or without the presence of 0.4% glucose, then grown for 4 hours at 30°C. Bacterial lysates were collected, separated by SDS-PAGE and transferred to a PVDF membrane. The membrane was blotted for expression of T18-IncE using an antibody against T18 (T18-IncE 34 kDa).

Figure modified from Olson et al. 2019. IAI.

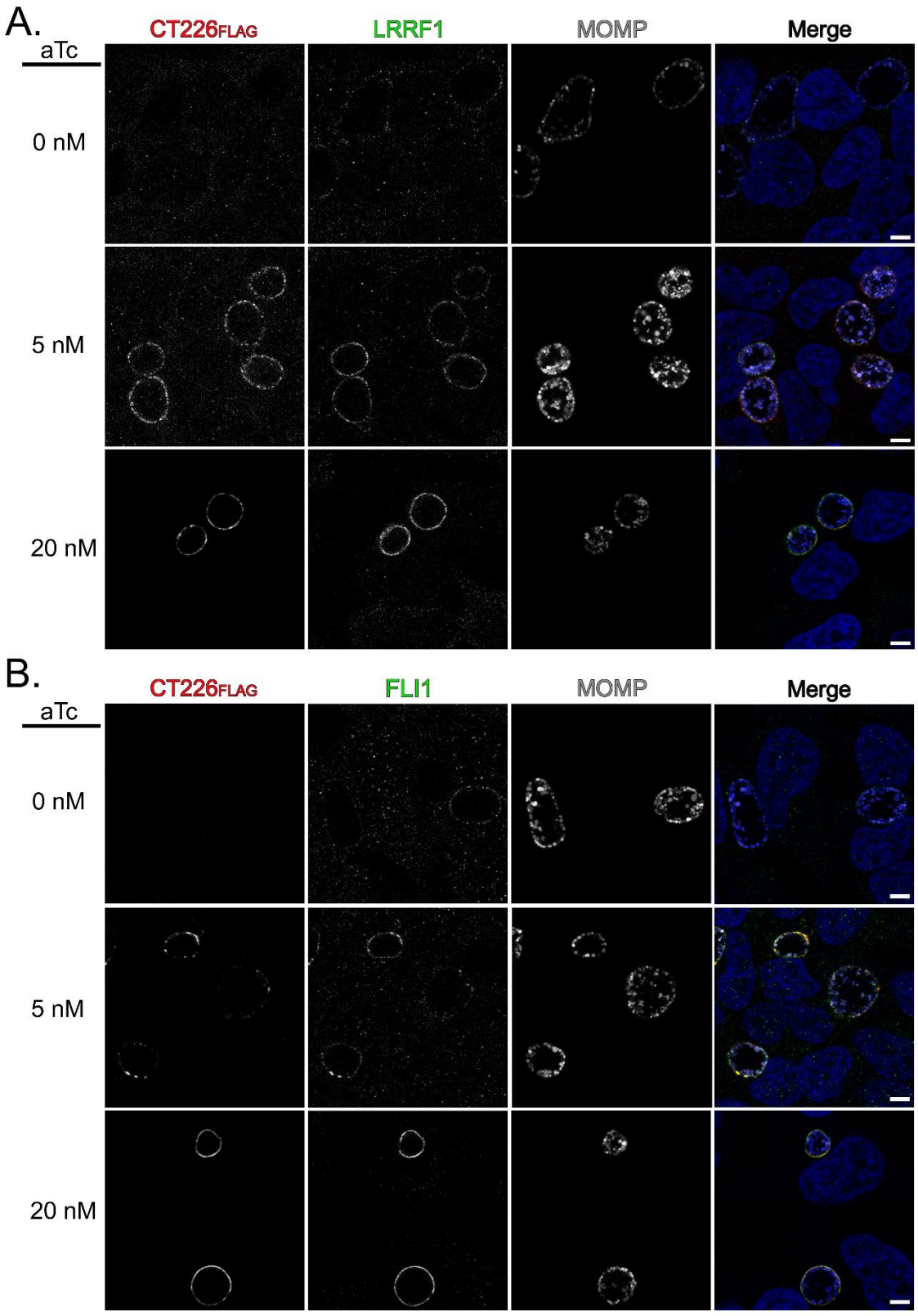

(continued on next page)

Figure S3-6. Overexpression of CT226-FLAG from *C. trachomatis* L2 CT226-FLAG results in increased LRRF1 and FLII at the inclusion membrane.

HeLa cells seeded on glass coverslips were infected with *C. trachomatis* L2 CT226-FLAG and either not induced or induced for expression at 7 hpi using 5 nM or 20nM aTc. At 24 hpi, coverslips were fixed with 3% formaldehyde and 0.022% glutaraldehyde, permeabilized with methanol, and stained for immunofluorescence to visualize construct expression (FLAG; red), chlamydiae (MOMP; gray), DNA (DAPI; blue), and A) LRRF1 (green) or B) FLII (green). Coverslips were imaged using a Zeiss confocal LSM 800 with 63x magnification and 2x zoom. Scale bar = 5 μm. Images were captured using the same exposure time (set for 20 nM aTc images) for uninduced and 5 nM aTc samples.

Figure modified from Olson et al. 2019. IAI.

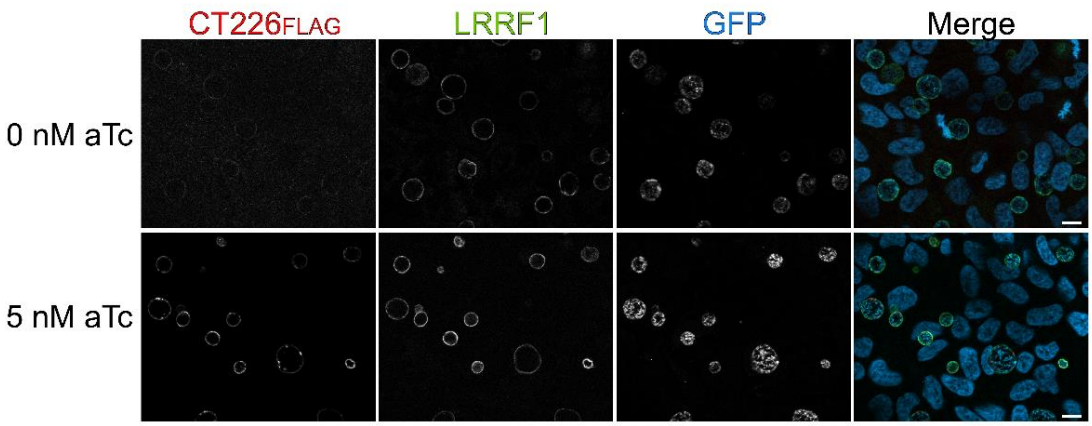

Figure S3-7. Assessment of CT226-FLAG expression on LRRF1 localization using *C. trachomatis* L2 CT226-FLAG infected HeLa cells using normal exposure levels.

HeLa cells seeded on glass coverslips were infected with *C. trachomatis* L2 CT226-FLAG and either not induced or induced for expression at 7 hpi using 5 nM. At 24 hpi, coverslips were fixed with 4% paraformaldehyde, permeabilized with 0.5% triton X100, and stained for immunofluorescence to visualize construct expression (FLAG; red), LRRF1 (green), GFP expressing chlamydiae (pseudo-color blue), and DNA (DAPI; blue). Coverslips were imaged using a Zeiss with Apotome 2.1 with 100x magnification. Scale bar = 10 μm.

Figure modified from Olson et al. 2019. IAI.

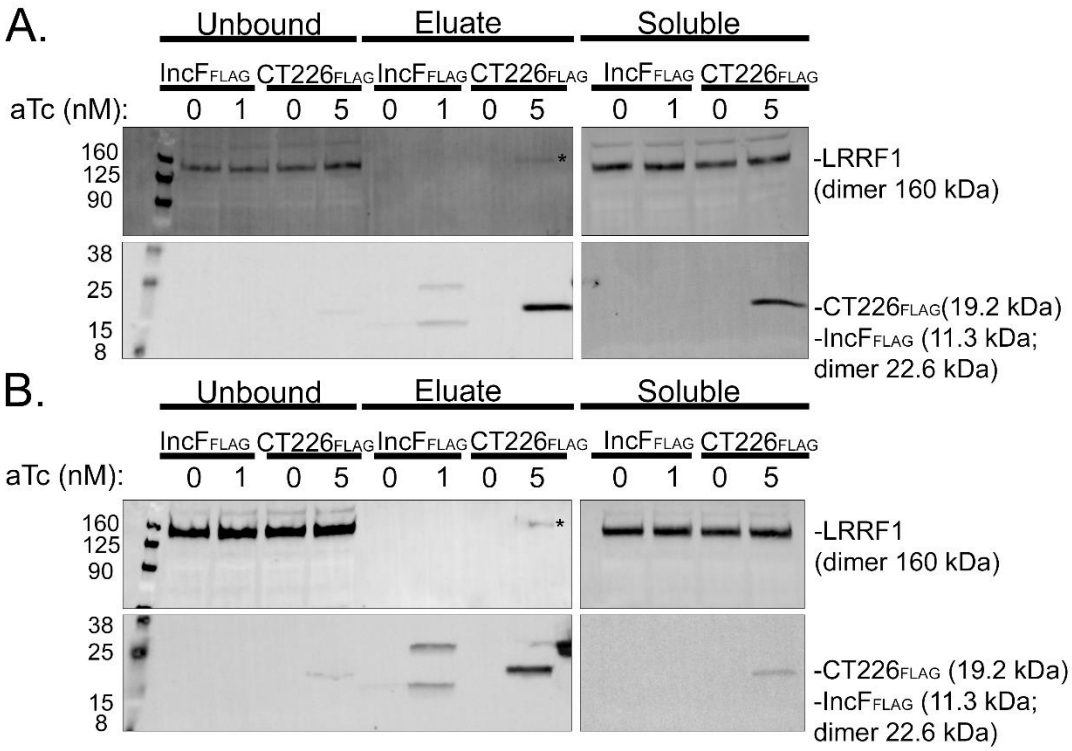

Figure S3-8. Co-immunoprecipitation of endogenous LRRF1 with *C. trachomatis* L2 CT226-FLAG.

HeLa cells seeded in a 6-well plate with glass coverslips were infected with *C. trachomatis* L2 CT226-FLAG or IncF-FLAG and either not induced or induced for expression at 7 hpi with 5 nM aTc (CT226-FLAG) or 1 nM aTc (IncF-FLAG). At 24 hpi, cells were collected, solubilized, normalized, and affinity purified using FLAG beads. The clarified lysates (soluble), unbound fractions and eluates were probed for construct expression (FLAG; CT226-FLAG 19.2 kDa; IncF-FLAG 11.3 kDa monomer and 22.6 kDa dimer) and LRRF1 (dimer 160 kDa). (A) and (B) are representative of two biological replicates. A total of three independent experiments were performed.

Figure modified from Olson et al. 2019. IAI.

Appendix B- Supplementary Tables

Table S3-1. Complete SAINT analysis of *C. trachomatis* L2 proteins identified by mass spectrometry. IAI.00537-19-sd002.xlsx

Table S3-2. SAINT significant eukaryotic proteins identified by mass spectrometry. IAI.00537-19-sd003.xlsx

Table S3-3. Complete SAINT analysis of eukaryotic proteins identified by mass spectrometry. IAI.00537-19-sd004.xlsx

Table S3-4. Proteins that associate with the inclusion of *C. trachomatis* at 24 hpi. IAI.00537-19-sd005.xlsx

Table S3-5. Primers used for construction of plasmids. IAI.00537-19-sd006.xlsx

Table S3-6. *E. coli* strains and plasmids. IAI.00537-19-sd007.xlsx

Chapter 4 - A Meta-Analysis of Affinity Purification-Mass Spectrometry Experimental Systems Used to Identify Eukaryotic and Chlamydial Proteins at the *Chlamydia trachomatis* Inclusion Membrane

*Chapter 4 is reused and edited with permission from the Journal of Proteomics:

Macy G. Olson, Scot P. Ouellette, and Elizabeth A. Rucks. 2020. A Meta-Analysis of Affinity Purification-Mass Spectrometry Experimental Systems Used to Identify Eukaryotic and Chlamydial Proteins at the *Chlamydia trachomatis* Inclusion Membrane. Journal of Proteomics.

Abstract

The obligate intracellular bacterial pathogen, *Chlamydia trachomatis*, develops within a membrane-bound vacuole termed the inclusion. Affinity purification-mass spectrometry (AP-MS) experiments to study the interactions that occur at the chlamydial inclusion membrane have been performed and, more recently, combined with advances in *C. trachomatis* genetics. However, each of the four AP-MS published reports used either different experimental approaches or statistical tools to identify proteins that localize at the inclusion. We critically analyzed each experimental approach and performed a meta-analysis of the reported statistically significant proteins for each study, finding that only a few eukaryotic proteins were commonly identified between all four experimental approaches. The two similarly conducted *in vivo* labeling studies were compared using the same statistical analysis tool, Significance Analysis of INTeractome (SAINT), which revealed a disparity in the number of significant proteins identified by the original analysis. We further examined methods to identify potential background contaminant proteins that remain after statistical analysis. Overall, this meta-analysis highlights the importance of carefully controlling and analyzing the AP-MS data so that pertinent information can be obtained from these various AP-MS experimental approaches. This study provides important guidelines and considerations for using this methodology to study intracellular pathogens residing within a membrane-bound compartment.

Significance

Chlamydia trachomatis, an obligate intracellular pathogen, grows within a membrane-bound vacuole termed the inclusion. The inclusion is studded with bacterial membrane proteins that likely orchestrate numerous interactions with the host cell. Although maintenance of the intracellular niche is vital, an understanding of the host-pathogen interactions that occur at the inclusion membrane is limited by the difficulty in purifying membrane protein fractions from infected host cells. The experimental procedures necessary to solubilize hydrophobic proteins fail to maintain transient protein-protein interactions. Advances in *C. trachomatis* genetics has allowed us and others to use various experimental approaches in combination with affinity purification mass spectrometry (AP-MS) to study the interactions that occur at the chlamydial vacuolar, or inclusion, membrane. For the first time, two groups have published AP-MS studies using the same tool, the ascorbate peroxidase proximity labeling system (APEX2), which overcomes past experimental limitations because membrane protein interactions are labeled in vivo in the context of infection. The utility of this system is highlighted by its ability to study chlamydial type III secreted inclusion membrane protein (Inc) interactions. Incs act as the mediators of host-pathogen interactions at the inclusion during *C. trachomatis* infection. When carefully controlled and analyzed, the data obtained can yield copious amounts of useful information. Here, we critically analyzed four previously published studies, including statistical analysis of AP-MS datasets related to *Chlamydia*-host interactions, to contextualize the data and to identify the best practices in interpreting these types of complex outputs**.**

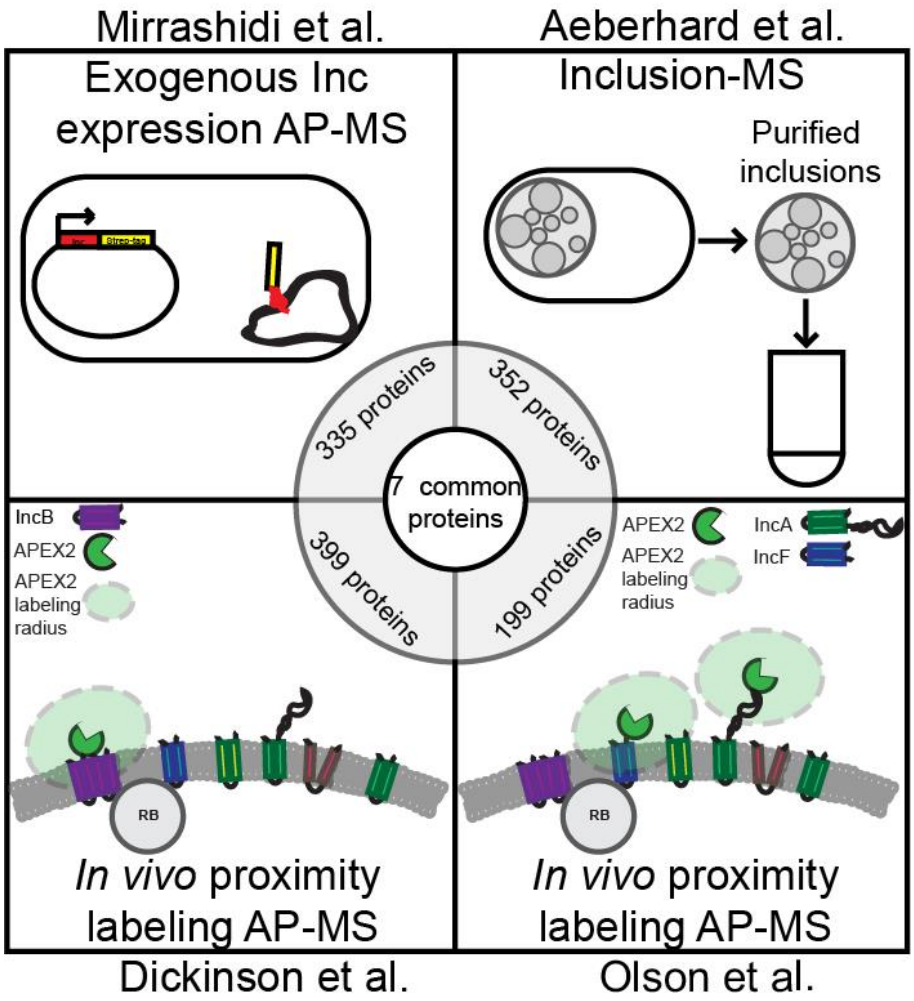

Graphical abstract: A Meta-Analysis of Affinity Purification-Mass Spectrometry Experimental Systems Used to Identify Eukaryotic and Chlamydial Proteins at the *Chlamydia trachomatis* Inclusion Membrane.

Graphical abstract adapted from Olson et al. 2020. JProt.

1. Introduction

Recently, four large-scale proteomics experiments to identify inclusion-associated proteins at the *C. trachomatis* inclusion membrane have been published, with two 2019 studies leveraging advances in genetic manipulation of *C. trachomatis* (115, 116, 122, 170, 171). This has allowed more direct experimental approaches to be implemented to identify chlamydial Inc-binding partners or inclusion-associated proteins. Each approach affinity-purified tagged proteins or whole inclusions and then the purified proteins were identified by mass spectrometry. However, each of these AP-MS studies featured different experimental approaches and/or utilized different statistical analysis tools to assign significance to the identified proteins (115, 122, 170, 171). We compare these experimental approaches, critically analyzing the limitations of each.

We first compared the statistically significant proteins reported in the four AP-MS *C. trachomatis* inclusion membrane interaction studies to identify common proteins, while noting the differences in processing and identification. Next, we directly compared the two proteomics experiments that used the APEX2 proximity labeling system (115, 170). We processed the Mascot data reported by Dickinson et al. (170) using the SAINT statistical analysis tool (207) described in Olson et al. (115) to determine the effect of statistical analysis tools on the identification of significant proteins. We found that there were notable differences in the number of significant proteins found using SAINT compared to the G- and *t*-test as reported by Dickinson et al. (170). Finally, we examined our Inc-APEX2 AP-MS datasets (115) using a more rigorous minimum peptide threshold to determine how these parameters affected the SAINT statistically significant eukaryotic and chlamydial proteins. The results suggest that a rigorous statistical analysis is critical to eliminate likely false-positive hits from these datasets.

2. Materials and Methods

2.1 Source of AP-MS data and how these data were used

The statistically significant proteins reported by Mirrashidi et al. (122), Aeberhard et al. (171), Dickinson et al. (170), and Olson et al. (115) with data source are listed in Table 4-1. The statistically significant protein identifiers from each source (listed in Table 4-1) were uploaded into UniProt (www.uniprot.org) using the "retrieve/mapping" tool to obtain the most current UniProt KB annotation. These UniProt KB protein annotations (listed in Table S4-1) were used for the Venny (248) comparison of these experimental datasets. The complete UniProt mapped input list of proteins from each of the experimental datasets are found in Table S4-1. Using the current version of UniProt, some entries mapped to more than one identifier (Table S4-1). Venny 2.0 (248), a Venn diagram tool (https://bioinfogp.cnb.csic.es/tools/venny/index.html), was used to compare the proteins identified in Mirrashidi et al. (122), Aeberhard et al. (171), Olson et al. (115), and Dickinson et al. (170).

2.2 SAINT analysis of Dickinson et al. (170)

To analyze the results of Dickinson et al. (170) using Significance Analysis of INTeractome (SAINT), the Mascot results files were downloaded from the PRIDE consortium (PRIDE via ProteomeXchange; PXD012494). These results files were input into Scaffold Viewer (http://www.proteomesoftware.com/products/free-viewer) to visualize spectral count data for each protein. In Scaffold, the parameters were set to 95% protein threshold, one-peptide minimum threshold, and 95% peptide threshold. The generated "samples report" file was exported as an excel file, which contains the protein identification and spectral counts for each biological replicate and bait protein (e.g., IncB-APEX2) at 8, 16, and 24 hours post-infection, and used to create the SAINT input files (i.e., bait, prey,

interaction files) (Table S4-2). The SAINT input files were analyzed using the GUI Significance Analysis of INTeractome (SAINT) interface available via the APOSTL Galaxy Server (http://apostl.moffitt.org/) (Table S4-2). SAINT is a statistical tool which accounts for protein length and uses Bayesian statistics to calculate a Bayesian False Discovery Rate (BFDR) for each prey-bait interaction indicated (207, 242). A Venny comparison of the SAINT data with Dickinson et al. reported data is provided in Table S4-3 and Table S4-4.

2.3 Analysis of Dickinson et al. statistically significant proteins using the CRAPome (249)

The Contaminant Repository for Affinity Purification (CRAPome; www.crapome.org) (249), was used to further analyze the reported data from Dickinson et al. for potential contamination with background proteins. The list of statistically significant proteins reported by Dickinson et al. was input into the CRAPome and the results for each prey identified are reported in Table S4-5. Each sample was normalized by dividing the average spectral counts (out of the 411 experiments available in the CRAPome) by the amino acid length. The “percent of experiments identified” column was calculated by dividing the average spectral counts by the 411 total AP-MS experiments in the CRAPome that contain the spectral count information.

2.4 Identification of mitochondrial proteins that have homology to C. trachomatis proteins

AP-MS peptide samples from uninfected HeLa cells supplemented with biotin, which were prepared as previously described (115), were analyzed using the Mascot server, which searched the Swiss-Prot database selected for *C. trachomatis* strain 434/Bu. Proteins with spectral counts in three or more out of six total replicates were then BLAST searched against *Homo sapiens* using NCBI Protein BLAST. The resulting human proteins

were then identified by UniProtKB. Subcellular localization, query cover, Expect value and percent identity from the BLAST search are provided (Table S4-6).

2.5 Analysis of two-peptide minimum threshold on Olson et al. SAINT significant eukaryotic and C. trachomatis L2 proteins

To determine the SAINT significant proteins using a two-peptide minimum threshold in Scaffold, the filtering parameters reported by Olson et al. (115) for the eukaryotic (PRIDE accession number: PXD015890) and *C. trachomatis* L2 proteins (PRIDE accession number: PXD015883) identified were changed to a two-peptide minimum, and the generated "samples report" file was exported as an excel file. The SAINT input files were created from this output (207) and analyzed using SAINT v3.6.1 through the APOSTL Galaxy Server (http://apostl.moffitt.org/). The samples report and SAINT results for eukaryotic proteins are in Table S4-8 and *C. trachomatis* L2 proteins in Table S4-9.

3. Results and Discussion

3.1 A Meta-Analysis of C. trachomatis AP-MS and Inclusion-MS Experiments to Identify Protein-Protein Interactions at the Chlamydial Inclusion Membrane

Given the complex nature of the protein-protein interactions (PPIs) that occur at the *C. trachomatis* L2 inclusion membrane, we sought to compare previously identified inclusion-associated proteins from four AP-MS datasets. Briefly, Mirrashidi et al. (122) transfected uninfected HEK293T cells with tagged Incs, which were purified by AP-MS; Aeberhard et al. (171) purified *C. trachomatis* L2 inclusions from eukaryotic cells; both Dickinson et al. (170) and Olson et al. (115) used the APEX2 proximity labeling system to tag interacting proteins *in vivo*, followed by AP-MS to identify interacting or proximal proteins. To compare the proteins that were identified using each of these experimental

approaches, we analyzed the statistically significant proteins that were reported from each experiment (summarized in Table 4-1). Aeberhard et al. identified 350 ($p \leq 0.05$) statistically significant proteins for purified inclusions (171), Mirrashidi et al. identified 331 (MiST score (1 = perfect score)) statistically significant proteins by transfecting uninfected cells with epitope-tagged Incs (122), Dickinson et al. (24 hpi time point only) identified 396 ($p \leq 0.05$) statistically significant proteins using *C. trachomatis* L2 IncB-APEX2 (170), and Olson et al. identified 199 ($p \leq 0.05$) statistically significant proteins combined from *C. trachomatis* L2 IncF-APEX2, IncA-APEX2, and $IncA_{TM}$-APEX2 strains(115). We used Venny (248), to compare these lists with Venn diagrams (http://bioinfogp.cnb.csic.es/tools/venny/) to detect the commonly identified, statistically significant proteins from each AP-MS and inclusion-MS experimental dataset (Fig. 4-1; Table S4-1) (115, 122, 170, 171).

Highlighting the numerous differences in each of these experimental protocols, only 0.7% (7 proteins) of the total input for Venny were commonly identified as statistically significant in all four inclusion-MS or AP-MS experimental datasets (Table 4-Table 4-1, Table S4-1; Fig. 4-1). These proteins were: Leucine-Rich Repeat Flightless-Interacting Protein 1 (LRRF1, LRRFIP1), Myosin Phosphatase-Targeting Subunit 1 (MYPT1, PPP1R12A), Reticulon-4 (RTN4), Sorting Nexin-1 (SNX1), Tropomodulin-3 (TMOD3), 14-3-3 protein beta (YWHAB), and 14-3-3 protein eta (YWHAH)(Table S4-1). In agreement with the current literature, several of the statistically significant eukaryotic proteins identified by all four studies have been reported to localize at the inclusion membrane (Table S4-1). These include 14-3-3 β (142), MYPT1 (38, 117), SNX1 (171), and LRRF1 (115). This highlights the potential for the three other commonly identified proteins, Reticulon-4, Tropomodulin-3, and 14-3-3 η, to localize at the chlamydial inclusion during infection of a host cell.

Table 4-1 Comparison of large-scale AP-MS *C. trachomatis* L2 studies

Experimental procedure	Source of data used in this study	Statistical test used for data analysis	Statistical significance cut-off reported	Statistically significant proteins[#]
Strep-Tag® AP-MS[a]	Table S1; "prey.entry.name" column	CompPASS and MiST	Top 1% ComPASS; MiST ≥ 0.7	335 (N=3)
Inclusion-MS[b]	Table S1; “Protein ID” column	SILAC/Two-sided Wilcoxon test with Benjamini-Hochberg	p≤ 0.05	352 (N=3)
IncB-APEX2 [c]	S1 Table; Complete proteomic data	G-test and *t*-test	p≤ 0.05	399 (N=6)
IncF-APEX2, IncA-APEX2, $IncA_{TM}$-APEX2[d]	Table 1, Table S1. Significant *C. trachomatis* L2 proteins; Table S2. statistically significant eukaryotic proteins	Significance Analysis of INTeractome (SAINT)	BFDR ≤ 0.05	199 (N=5)

[#] The statistically significant proteins at 24 hpi for all but the Strep-tag experiments by Mirrashidi et al. which transiently transfected (uninfected) HEK293T cells

[a] Mirrashidi et al.; 331 protein entries reported by Mirrashidi et al. mapped to 335 proteins (Uniprot)

[b] Aeberhard et al.; 350 protein entries reported by Aeberhard et al. mapped to 352 proteins (Uniprot)

[c] Dickinson et al.; 396 protein entries reported by Dickinson et al. mapped to 399 proteins (Uniprot)

[d] Olson et al.; 199 unique protein entries combined using each IncF-APEX2, IncA-APEX2, and $IncA_{TM}$-APEX2

Table adapted from Olson et al. 2020. JProt.

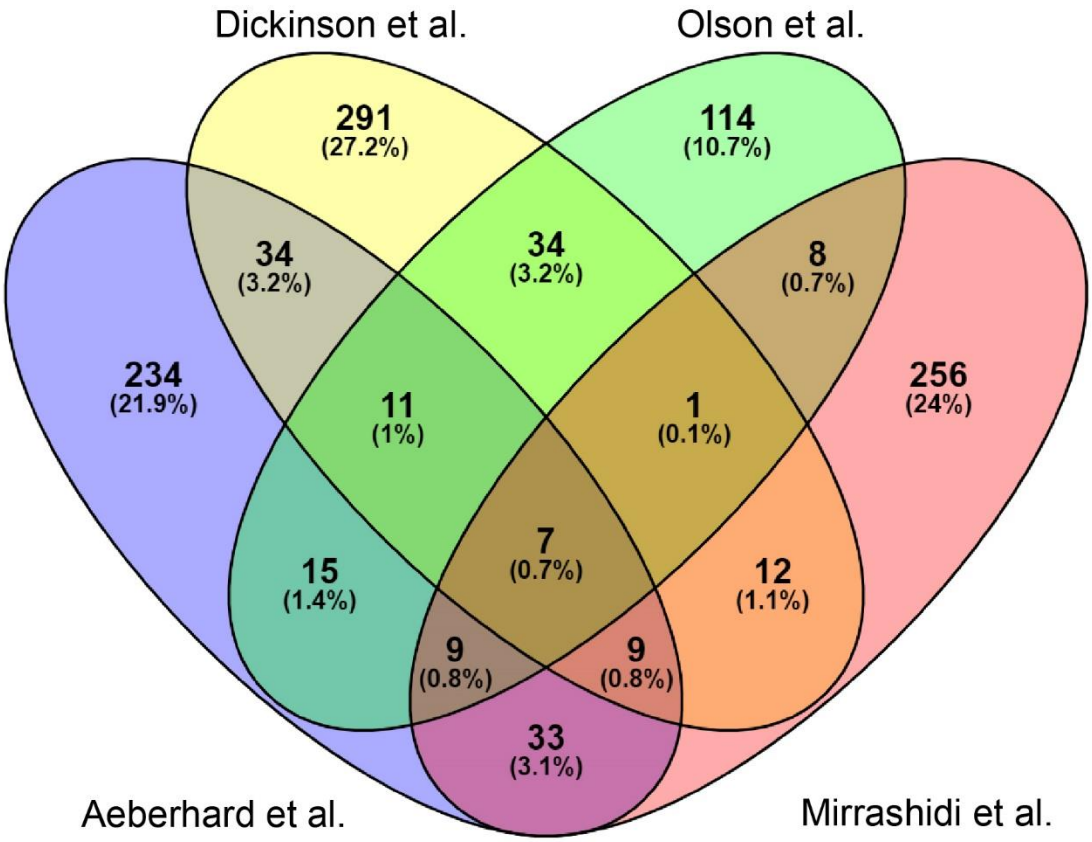

Figure 4-1. Venny comparison of eukaryotic proteins at the *C. trachomatis* inclusion reported by Olson et al., Aeberhard et al., Mirrashidi et al., and Dickinson et al.

The significant proteins reported from each study were input into Venny to determine commonly identified proteins. The total number of proteins as well as the percentage of total is indicated within each overlapping section.

Figure modified from Olson et al. 2020. JProt.

3.2 Comparison of Aeberhard et al. (171), Dickinson et al. (170), and Olson et al. (115) reported statistically significant eukaryotic proteins

We next compared the reported significant proteins from each of the three studies that were performed using chlamydial infected cells and found that 18 proteins or 2.2% of the total proteins are common between these three experiments (Fig. 4-2, Table S4-1). In addition to the seven commonly identified proteins from all four AP-MS experiments indicated above, there were 11 additional commonly identified proteins from the Aeberhard et al., Dickinson et al., and Olson et al. studies. The 11 additional commonly identified proteins were: Alpha-actinin-4 **(**ACTN4_HUMAN), Brain acid soluble protein 1 (BASP1_HUMAN), Caprin-1 (CAPR1_HUMAN), Elongation factor 1-delta, EF-1-delta (EF1D_HUMAN), Membrane-associated progesterone receptor component 1 (PGRC1_HUMAN), Stress-induced-phosphoprotein 1, (STIP1_HUMAN), Tropomyosin alpha-3 chain (TPM3_HUMAN), Tropomyosin alpha-4 chain (TPM4_HUMAN), Vinculin (VINC_HUMAN), Nuclease-sensitive element-binding protein 1 (YBOX1_HUMAN), and 14-3-3 protein theta (1433T_HUMAN). This may represent a small but biologically relevant increase due to these experiments being carried out in the context of *C. trachomatis* infection (115, 170, 171), rather than ectopically expressing Incs in uninfected host cells (122). Fewer of these proteins have been validated for their localization thus far, but the inclusion has been shown to be surrounded by actin and intermediate filaments (e.g., vinculin) cytoskeleton network (71). This would explain the identification of such factors as TPM3 and TPM4, for example (250, 251).

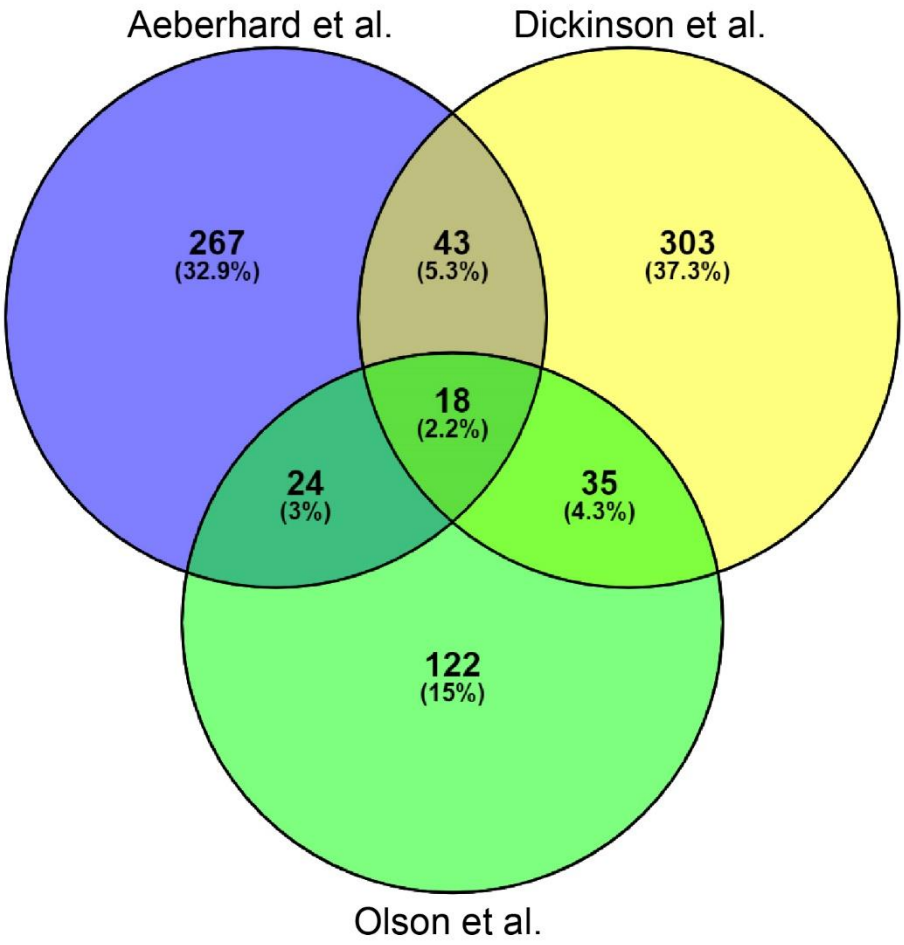

Figure 4-2. Venny comparison of eukaryotic proteins identified at 24 hours post-infection in Olson et al. compared to Dickinson et al. and Aeberhard et al. experimental approaches.

The reported significant proteins from each study using *C. trachomatis* L2 infected eukaryotic cells were input into Venny to determine commonly identified proteins. The total number of proteins as well as the percentage of total is indicated within each overlapping section.

Figure modified from Olson et al. 2020. JProt.

3.3. Comparison of Dickinson et al. and Olson et al. reported statistically significant eukaryotic proteins

Finally, we directly compared the statistically significant proteins reported from the published *C. trachomatis* L2 APEX2 proximity labeling system experiments (115, 170).This is the first time that two large-scale AP-MS experiments using the same APEX2 proximity labeling system tool to identify interactions at the *C. trachomatis* inclusion membrane have been reported (115, 170). A comparison of the experimental parameters used in each APEX2 experiment is summarized in Table 4-Table 4-2. Both experiments fused *APEX2* to the C-terminus of an *Inc* to detect protein-protein interactions at the inclusion membrane *in vivo*.

The major differences between these studies include the specific Inc(s) used for each of the Inc-APEX2 constructs, the protein digestion enzymes used in mass spectrometry sample preparation, and statistical analysis of mass spectrometry data. The specifics of each study are listed in Table 4-2. Of note, Dickinson et al. used *C. trachomatis* L2 transformed with IncB-APEX2 that uniformly decorated the inclusion (170) (Table 4-2). The localization of IncB in this context is different than the reports of endogenous IncB, which has been shown to localize in microdomains within the inclusion membrane (114). Olson et al. used *C. trachomatis* L2 transformed with IncA-APEX2, IncF-APEX2, or $IncA_{TM}$-APEX2 (a truncated IncA construct), all of which uniformly decorated the inclusion similar to endogenous IncA or IncF, respectively (44, 87, 88).

Venny (248) was used to compare the statistically significant proteins reported at 24 hpi by both Dickinson et al. (170) and Olson et al. (115). At 24 hpi, 399 statistically significant proteins were reported by Dickinson et al. using the G and *t*-test (170), while 199 statistically significant proteins were reported by Olson et al. using Significance Analysis of INTeractome (SAINT) (115) (Fig. 4-3, Table S4-1). Fifty-three proteins (9.7%

Table 4-2. Affinity purification-mass spectrometry experimental parameters reported in Dickinson et al. * and Olson et al. &

	Dickinson et al.*	Olson et al.&
Tissue type	HeLa 229 cells	HeLa 229 cells
Inc-APEX2 construct	IncB-APEX2	IncF-APEX2, IncA-APEX2, $IncA_{TM}$-APEX2
Affinity Purification	Streptavidin-agarose resin	Streptavidin Magnetic beads
Elution	On resin trypsin digestion	SDS-PAGE and sectioned
Digestion Enzyme(s)	Trypsin	Trypsin and AspN
Mass Spectrometer	Thermo Fisher Velos Orbitrap	Thermo Fisher Orbitrap Lumos
Software	MS-GF+ Release (v2016.10.24)	Mascot and Scaffold
Protein modifications	Carbamidomethyl and Oxidation	Carbamidomethyl and Oxidation
Fasta search *Homo sapiens*	UniProt SPROT accessed 20170412	UniProt Human accessed 20180927
Fasta search *C. trachomatis*	*C. trachomatis* L2 434/Bu pL2 Plasmid accessed 20180105	*C. trachomatis* L2 434/Bu accessed 20180330
Peptide/protein Filtering	False Discovery Rate ≤ 1%, Unique peptides, requiring a minimum of six amino acids in length, were filtered using an MS-GF threshold of ≤ 1×10^{-9}, corresponding to an estimated false-discovery rate (FDR) <1% at a peptide level.	Scaffold filtering: 95% protein threshold, 1-peptide minimum, 95% peptide threshold
Additional data processing	Relative peptide abundances were log-transformed. Elimination of statistical outliers was confirmed using a standard Pearson correlation at a sample level	
Statistical Test	G-test and *t*-test	SAINT#

*previously published in Dickinson et al., PLoS Pathog. 2019 15(4):e1007698, doi: 10.1371/journal.ppat.1007698

& previously published in Olson et al., Infection and Immunity. 2019

Significance Analysis of INTeractome (SAINT)

Table adapted from Olson et al. 2020. JProt

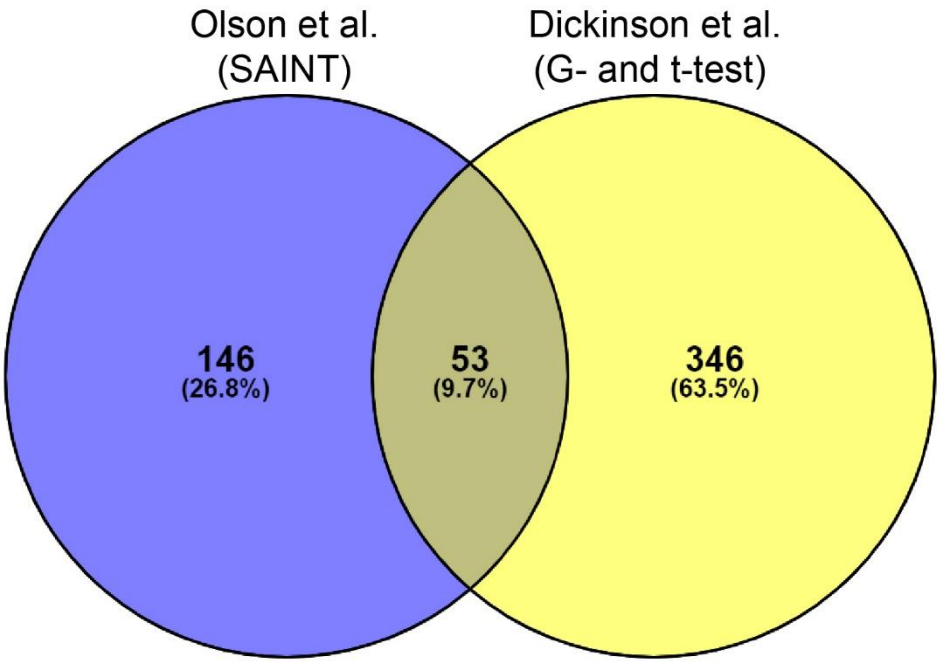

Figure 4-3. Venny comparison of reported eukaryotic proteins at 24 hours post-infection by Olson et al. (SAINT analysis) and Dickinson et al. (G- and *t*-test analysis) using the *in vivo* ascorbate peroxidase proximity labeling system (APEX2) combined with AP-MS

The reported significant proteins from each study were input into Venny to determine commonly identified proteins. The total number of proteins as well as the percentage of total is indicated within each overlapping section.

Figure modified from Olson et al. 2020. JProt.

of the total protein input) were commonly identified in both studies; given that different Inc proteins were used for these proximity labeling experiments, some differences may be expected. However, each Inc-APEX2 construct, IncB-APEX2 used by Dickinson et al. (170) and IncF-APEX2, IncA-APEX2, and $IncA_{TM}$-APEX2 used by Olson et al. (115), uniformly labeled the inclusion when the expression of the constructs was induced. Therefore, it is surprising that at 24 hpi, only approximately 13% of the statistically significant proteins reported by Dickinson et al. (using the G and *t*-test) (170) were commonly identified by Olson et al. (using SAINT) (115) (Fig. 4-3, Table S4-1). In addition, greater than 88% of Dickinson et al. (170) and 72% of Olson et al. (115) datasets contained unique proteins (i.e., proteins not commonly identified by both studies) (Fig. 4-3, Table S4-1).

3.4 SAINT analysis of Dickinson et al. identified eukaryotic proteins from APEX2 proximity labeling AP-MS data

One possible explanation for the differences in the reported significant proteins is the statistical analysis tools used for each experiment. For example, Olson et al. (115) used SAINT, which takes into account the protein length when calculating the probability that a protein is a true interacting protein and not a false-positive (207). The probability is reported as Bayesian False Discovery Rate (BFDR) (207). Dickinson et al. used an unspecified G- or *t*-test to assign significance to their mass spectrometry data. Because both Dickinson et al. and Olson et al. used the APEX2 proximity labeling system, it is possible for the first time to directly compare the proteins identified in these experiments. Although it is not possible to change the experimental conditions prior to mass spectrometry (Table 4-2), the raw mass spectrometry data can be re-analyzed. To directly compare the results from Dickinson et al. (170) with the SAINT statistically significant proteins reported by Olson et al. (115) and to minimize differences in the AP-MS data

processing between these two datasets, we analyzed the Dickinson et al. datasets (170) using SAINT as described in the Materials and Methods. By the SAINT analysis tool, at 24 hpi, 76 eukaryotic proteins were found to be statistically significant (Table 4-3, Table S4-2 and S4-3). To determine if these SAINT analyzed data appeared more similar to the data reported by Olson et al., we compared the 24 hpi SAINT analyzed Dickinson et al. datasets with the 24 hpi SAINT analyzed Olson et al. datasets. When the same tool was used to calculate statistical significance, the number of commonly identified statistically significant proteins increased from 9.7% (Fig. 4-3) to 14.1% (Fig. 4-4). In addition, 45% (34 of 76 proteins) of the Dickinson et al. SAINT significant proteins were commonly identified by Olson et al. Furthermore, now only 55% (42 of 76 proteins) of the Dickinson et al. SAINT significant proteins were unique (Fig. 4-4), compared to 88% (354 of 399 proteins) of proteins from the G-test and *t*-test results (Fig. 4-3). The different Inc-APEX2 (IncB vs. IncA and IncF) constructs and overexpression of each construct used to identify proximal or interacting proteins likely contribute to the remaining proteins that are unique in each dataset.

While the specific implications for the mislocalization of Incs and “flooding” the inclusion membrane with additional Incs is not well understood at this time (59), the phenotypic changes in IncF-APEX2 localization upon overexpression support the concept that overexpression may impact the organization of the inclusion membrane (57). It is also likely that overexpression of other Inc proteins will subsequently influence or change the recruitment of certain host proteins to the inclusion. In support, Rucks et al. showed that reducing the expression levels of IncF-APEX2 rescued normal inclusion development (57), indicating that carefully assessing induction time and amount of the inducing agent used (i.e., overexpression levels) will influence the interaction data. It is important to note, that while IncB-APEX2 did not localize in the inclusion in a manner that is consistent with

Table 4-3. Comparison of Dickinson et al. results relative to the indicated statistical tests

Time (hours post-infection)	Number of statistically significant[&] proteins		Number of proteins identified by both statistical tests
	G/*t*-test*	SAINT[#]	
8 hpi	90	0	n/a
16 hpi	180	17	13
24 hpi	399	76	70

*previously published in Dickinson et al., PLoS Pathog. 2019

[#]Analyzed for this study (BFDR ≤0.05)

[&]p ≤0.05

Table adapted from Olson et al. 2020. JProt

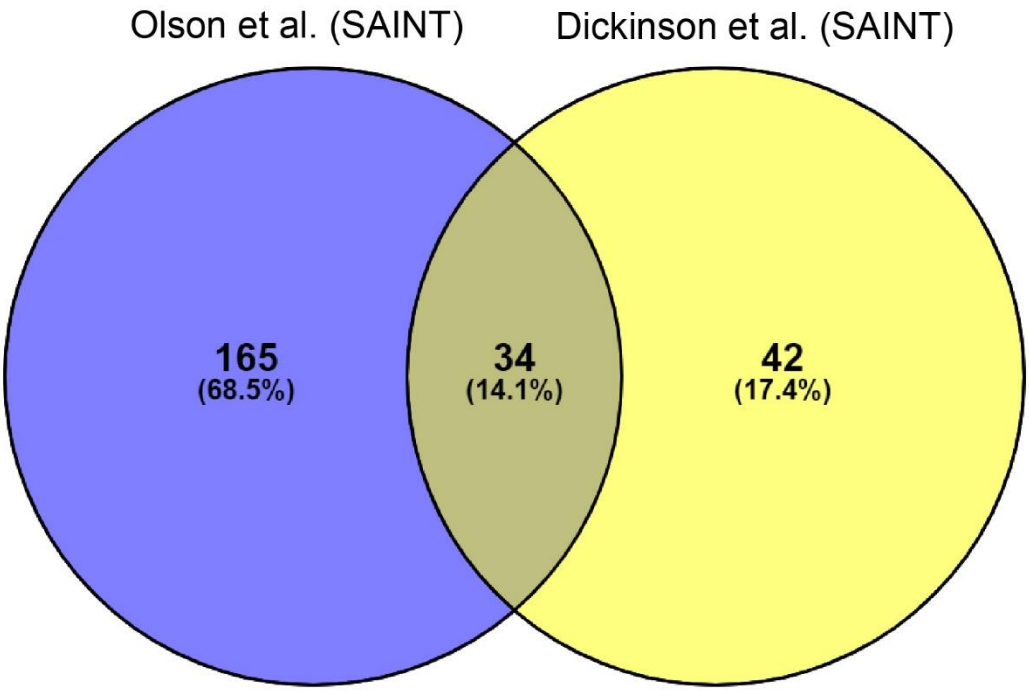

Figure 4-4. Venny comparison of SAINT analyzed Dickinson et al. eukaryotic proteins at 24 hpi.

The raw data reported by Dickinson et al. at 24 hpi were analyzed by SAINT then compared to Olson et al. reported 24 hpi SAINT significant proteins. The total number of proteins as well as the percentage of total is indicated within each overlapping section.

Figure modified from Olson et al. 2020. JProt.

reports of endogenous IncB (114), Dickinson et al. did not report any abnormalities in inclusion size or bacterial morphology upon IncB-APEX2 overexpression (170).

3.5 Comparison of SAINT significant Dickinson et al. eukaryotic protein datasets with the previously reported G- and t-test significant proteins at 24 hpi

Because the SAINT analyzed Dickinson et al. datasets drastically decreased the overall number of statistically significant proteins compared to those reported by Dickinson et al. using the G- and *t*-test at 24 hpi, we further examined which proteins were statistically significant using each analysis tool. The statistically significant proteins reported by Dickinson et al. using the G- and *t*-test ($p \leq 0.05$) [25] were compared to the SAINT analyzed significant proteins (BFDR ≤ 0.05) (Table 4-3, Table S4-2 to S4-3). At 24 hpi, the 399 statistically significant eukaryotic proteins were identified using the G-test and *t*-test compared to only 76 statistically significant eukaryotic proteins identified by SAINT (Table 4-3; Table S4-5). We used Venny (248) to determine which proteins were commonly identified by each statistical analysis tool (i.e., SAINT and the G-and *t*-test). Most SAINT significant proteins (70 of 76 proteins) were also identified as significant using the G- and *t*-test (Table 4-3; Table S4-3). Six proteins were unique to the SAINT statistical analysis tool (i.e., not determined to be statistically significant by G- and *t*-test) at 24 hpi: Hsc70-interacting protein, Hip (F10A1_HUMAN), Protein transport protein Sec16A (SC16A_HUMAN), Src substrate cortactin (SRC8_HUMAN), Tropomyosin beta chain (TPM2_HUMAN), HLA class I histocompatibility antigen (1A30_HUMAN), and Ataxin-2-like protein (ATX2L_HUMAN) (Table 4-3, Table S4-3). In support of these SAINT data, cortactin has been previously shown to localize with the chlamydial inclusion (252).

These results indicate that despite using permissive Scaffold parameters (95% protein, 1-peptide minimum, 95% peptide identification), SAINT provides a more rigorous analysis than the G-test and *t*-test alone (Table 4-3, Table S4-3). Most of the proteins

identified by SAINT were also identified by the G-test and *t*-test which indicates that SAINT has more stringent parameters to calculate statistical significance (Table 4-3) and that amino acid length of each prey protein is an important aspect in these statistical calculations.

3.6 Comparison of SAINT statistically significant Dickinson et al. eukaryotic protein datasets with the reported G- and t-test significant proteins at 16 and 8 hpi

A stated goal of the Dickinson et al. study was to use the APEX2 system to understand how the proteome around the chlamydial inclusion changes over the course of the developmental cycle, and AP-MS data were taken from 8 hpi (early developmental cycle), 16 hpi (mid-developmental cycle), and 24 hpi (mid-late developmental cycle). As we have already re-analyzed the 24 hpi dataset above, we performed a similar re-analysis of the 16 and 8 hpi datasets and again compared SAINT significant proteins with the G- and *t*-test reported statistically significant proteins.

At 16 hpi, Dickinson et al. reported 180 statistically significant proteins using the G- and *t*-test method, while only 17 statistically significant proteins were identified by SAINT (Table 4-3, Table S4-3). Consistent with the re-analysis of the 24 hpi dataset, at 16 hpi, most of the G- and *t*-test significant proteins were also detected using SAINT (13 of 17 total proteins) (Table S4-3). The four unique proteins identified only by the SAINT analysis included: Caprin-1 (CAPR1_HUMAN), Microtubule-associated protein 4 (MAP4_HUMAN), Src substrate cortactin (SRC8_HUMAN), and Vimentin (VIME_HUMAN) (Table 4-3, Table S4-3). Consistent with previous studies, cortactin has been shown to be associated with the inclusion (252), and both vimentin (71) and microtubules (35) have been extensively studied for their roles near the inclusion during infection.

Finally, the SAINT analysis was applied to the 8 hpi Dickinson et al. dataset (170). At 8 hpi, using the G-test and *t*-test, Dickinson et al. reported 90 statistically significant proteins (170). In contrast, the SAINT analyzed Dickinson et al. dataset did not identify any statistically significant proteins (Table 4-3). These SAINT data are further supported by the findings published by Dickinson et al. in which they used RNAi specific for the genes corresponding to 64 of the 90 statistically significant proteins at 8 hpi to validate eukaryotic proteins that were recruited to the inclusion (170). Of the 64 proteins that underwent further testing by RNAi, only silencing of two genes (Stress-induced-phosphoprotein 1 (STIP1) and Myosin light polypeptide 6 (MYL6) yielded a 2-fold decrease in the production of infectious progeny (170). By the G- and *t*-test, STIP1, and MYL6 were also statistically significant at 16 and 24 hpi, but only SAINT significant at 24 hpi (Table S4-3, Table S4-4). The proteins that were silenced by RNAi in Dickinson et al. (170) are also directly compared to the SAINT calculated BFDR in Table S4-4.

3.7 Analysis of Dickinson et al. and Olson et al. reported statistically significant eukaryotic proteins using the CRAPome (249)

The most striking difference between the original dataset reported by Dickinson et al. and the SAINT analyzed datasets was with the 8 hpi samples, where, by SAINT, no proteins were identified as statistically significant. We asked if there was another metric of eliminating background proteins from a list of statistically significant proteins. Hence, we analyzed the G- and *t*-test reported statistically significant Dickinson et al. datasets using the CRAPome (249) to determine if their original list of statistically significant proteins was contaminated with background proteins. The CRAPome is a repository for background, contaminant proteins identified from AP-MS experiments (249). A list of eukaryotic proteins is queried, and the CRAPome reports the number of experiments that identified the protein including the average spectral counts for each experiment that identified the

queried protein. The Dickinson et al. G- and *t*-test reported statistically significant proteins from each 8, 16, and 24 hpi were queried into the CRAPome. The CRAPome reported average spectral count data for each queried protein was normalized to the queried protein length. We then used a two-pronged approach to defining contaminant proteins as those with spectral counts in greater than 30% of the experiments (i.e., 411 total AP-MS experiments uploaded to the CRAPome) and being above an arbitrary cut-off of greater than 0.02 for the average spectral counts normalized to protein length (Table S4-5).

Using these two criteria, at 8 hpi, 15 of the 90 (16.7%) reported statistically significant (by G- and *t*-test) proteins are potentially background contaminant proteins (Table 4-4; Table S4-5). At 16 hpi, 19 of 180 (10.6%) significant proteins (by G- and *t*-test), and at 24 hpi 33 of 399 (8.3%) significant proteins (by the G- and *t*-test) are potential background proteins. We then queried the SAINT analyzed Dickinson et al. datasets at each timepoint into the CRAPome to determine if the SAINT analysis reduced the number of contaminant proteins. While SAINT decreased the number of statistically significant proteins detected (Table 4-3), a similar percentage of the SAINT significant proteins identified fit the criteria for probable contaminant proteins except for 8 hpi, where no proteins were identified as SAINT significant (Table 4-4). The proteins that were flagged as potential contaminants from the SAINT analysis were also common to the G- and *t*-test CRAPome analysis, indicating that regardless of the statistical tool used, some contaminant proteins will be identified as statistically significant (Table 4-4).

We also ran our 24 hpi SAINT analyzed AP-MS data (115) through the CRAPome to identify potential contaminant proteins for our datasets. At 24 hpi, 13 of 199 (6.5%) proteins were identified as potential contaminants using a one-peptide minimum threshold as reported by Olson et al. (115). When the threshold was increased to the two-peptides minimum (see “Intra-experimental analysis of Olson et al. AP-MS” section below), then 7 of 101 (6.9%) statistically significant proteins were identified as contaminants (Table 4-4

Table 4-4. CRAPome analysis of Dickinson et al. reported G- and t-test datasets, SAINT analyzed Dickinson et al. and Olson et al. SAINT datasets

Dickinson et al. datasets	Statistical analysis tool used	Statistically significant proteins queried	Identified contaminant proteins	Commonly identified proteins	Proteins identified as contaminants (%)
8 hpi	G- and *t*-test	90	15		16.67
8 hpi	SAINT[#]	0	n/a	n/a	n/a
16 hpi	G- and *t*-test	180	19		10.56
16 hpi	SAINT[#]	17	3	(2)[*]	17.65
24 hpi	G- and *t*-test	399	33		8.27
24 hpi	SAINT[#]	76	11	(11)[*]	14.47

Olson et al. datasets	Statistical analysis tool	Total proteins input	Identified contaminant proteins	Commonly identified proteins	Proteins identified as contaminants (%)
24 hpi 1-peptide	SAINT	199	13		6.53
24 hpi 2-peptide	SAINT	101	7	(7)[&]	6.93

[#] SAINT statistical significance calculated using 1-peptide minimum threshold in Scaffold

* denotes the commonly identified proteins using G- and *t*-test and SAINT

[&] denotes commonly identified proteins using SAINT 1-peptide and 2-peptide

Table adapted from Olson et al. 2020. JProt

and Table S4-5). The same seven proteins identified as contaminants from the two-peptide minimum dataset were also identified as contaminants in the one-peptide dataset (Table 4-4 and Table S4-5), indicating that some contaminant proteins will be identified regardless of the stringency of the minimum peptide threshold. Overall, to reduce the number of contaminant proteins in future AP-MS studies and to identify potential contaminant proteins, it is important to evaluate statistically significant proteins using the CRAPome. We have compiled a list of the eukaryotic proteins that were commonly identified as contaminants in these APEX2 studies (Table S4-5).

To help further distinguish contaminant proteins from true positive interacting partners, we have also compiled a list of eukaryotic proteins that were identified in uninfected cells that share sequence homology with chlamydial proteins (Table S4-6). At 8 hpi, *C. trachomatis* is in the early stages of the developmental cycle, the inclusions are very small, and chlamydial protein content will be orders of magnitude less than the eukaryotic host background. Further, the host cell produces naturally biotinylated host proteins, some of which have high homology to bacterial proteins, including *C. trachomatis* proteins. These facts can lead to false identification of chlamydial proteins by mass spectrometry at early time points post-infection. For these early time points a secondary method of labeling chlamydial proteins to differentiate from host proteins may be necessary. The use of both the CRAPome (249) and Table S4-6 containing chlamydial proteins with homology to eukaryotic cells may provide the best insight into background proteins.

3.8 Analysis of temporal recruitment of eukaryotic proteins identified by Dickinson et al. at the inclusion membrane

An enticing utility of the APEX2 proximity labeling system is the possibility of identifying “snapshots” of interactions or chlamydial inclusion proteomes throughout the

developmental cycle. As noted above, Dickinson et al. obtained AP-MS data at each 8, 16, and 24 hpi to identify temporal changes in eukaryotic protein recruitment to the *C. trachomatis* L2 inclusion. We used Venny to examine which SAINT-identified statistically significant proteins remained associated with the inclusion from 16 to 24 hpi to distinguish the eukaryotic proteins that are potentially temporally recruited to the inclusion membrane from those proteins that remain associated with the inclusion throughout the developmental cycle.

We first compared the commonly identified statistically significant proteins as originally reported by Dickinson et al. using the G- and *t*-test. From these analyses, 85.5% (154 of 180) of Dickinson et al. 16hpi protein hits (i.e., G-test and *t*-test significant proteins) were commonly detected at 24 hpi (Table 4-3 and Table S4-3) (170). Consistent with the G- and *t*-test datasets results, the SAINT analyzed Dickinson et al. datasets have a high percent of commonly identified proteins at 16 and 24 hpi. 94.1% (16 of 17 proteins) of the statistically significant proteins at 16 hpi were also significant at 24 hpi (Table 4-3 and Table S4-3). The unique protein at 16 hpi (i.e., not significant at 24 hpi) was aspartyl/asparaginyl beta-hydroxylase (ASPH_HUMAN). These results are not unexpected because both 16 hpi and 24 hpi are mid-developmental cycle, and the requirements for *C. trachomatis* L2 development at these times are likely not very different. This analysis also suggests the chlamydial inclusion proteome may be quite stable during the mid-developmental cycle period.

3.9 SAINT analysis of Dickinson et al. chlamydial proteins identified by APEX2 proximity labeling AP-MS

In contrast to the experiments in Mirrashidi et al. (122) and Aeberhard et al. (171), the APEX2 *in vivo* proximity labeling system allows for the detection of proximal or interacting *C. trachomatis* L2 Inc proteins (115, 170). Again, to minimize differences

in the datasets, we analyzed the chlamydial protein datasets from Dickinson et al. using SAINT (see Materials and Methods) (Table S4-2). We then compared the statistically significant proteins detected in the Dickinson et al. and Olson et al. APEX2 proximity labeling experiments. Both APEX2 studies identified four statistically significant *C. trachomatis* L2 inclusion membrane proteins (Incs) with the Inc, CT223, being identified in both studies (Table 4-5) (115, 170).

Unique to individual experimental datasets, the SAINT analyzed Dickinson et al. dataset identified IncG, CT228, and CT813 as statistically significant at 24 hpi (Table 4-5; Table S4-2). However, only IncG was SAINT significant at 16 hpi, and no Incs were significant at 8 hpi (Table 4-5; Table S4-2) (170). The lack of statistically significant Incs identified at the 8hpi is consistent with the smaller inclusions and few early Inc proteins being localized to the inclusion membrane at this time (102). In contrast, the Olson et al. study identified IncD, IncF, and IncA as SAINT statistically significant (Table 4-5). The differences in statistically significant Incs identified in each dataset may reflect the use of different Inc-APEX2 fusion proteins in each study, but the organization of Incs in the inclusion membrane is currently not well defined (59).

3.10 Intra-experimental analysis of Olson et al. AP-MS identified eukaryotic and C. trachomatis L2 proteins

After comparing the two APEX2 proximity labeling studies, we aimed to further examine how various parameters such as minimum peptide threshold would impact our own APEX2 AP-MS datasets. We have previously published the SAINT statistically significant proteins identified using a one-peptide minimum threshold (115). A two-peptide minimum (e.g., two unique peptides per parent protein) is generally accepted in the proteomics field as more rigorous than a one-peptide minimum threshold for mass

Table 4-5. Comparison of SAINT statistically significant *C. trachomatis* L2 proteins[a] identified in two APEX2 proximity labeling studies

Dickinson et al. (SAINT)				
IncB-APEX2	24 hpi	BFDR*	16 hpi	BFDR*
	IncG	0	IncG	0
	CT223	0.01		
	CT228	0.01		
	CT813	0.02		
Olson et al. (SAINT)				
	24 hpi	BFDR*		
IncF-APEX2	CT223	0		
	IncD	0.02		
	IncF	0.03		
IncAtm-APEX2	IncA	0		
	CT223	0.02		
IncA-APEX2	OmcB	0		
	CT223	0		
	IncA	0		

[a] Protein name indicated using *C. trachomatis* serovar D naming convention
* SAINT calculated Bayesian False Discovery Rate (BFDR)

Table adapted from Olson et al. 2020. JProt

spectrometry data. However, conflicting reports in the field suggest that the two-peptide minimum may not significantly change the overall number of proteins identified (253). We decided to examine how the proposed, more rigorous, peptide threshold cut-off would affect the SAINT identified statistically significant eukaryotic and *C. trachomatis* L2 proteins within our own data set (115). As reported by Olson et al. (115), the one-peptide minimum threshold identified 199 SAINT statistically significant proteins. To re-analyze these data under the new parameters, we applied the two-peptide minimum threshold filtering parameters in Scaffold to each of the eukaryotic (Table S4-7) and *C. trachomatis* L2 (Table S4-8) protein datasets (see Materials and Methods). After applying the two-peptide minimum (i.e., including hits from each IncF-APEX2, $IncA_{TM}$-APEX2, and IncA-APEX2), 101 unique eukaryotic proteins were identified by SAINT as statistically significant (Table S4-7; Fig. 4-5). All but two of the proteins from the two-peptide minimum analysis were also identified in the one-peptide minimum dataset. For the eukaryotic protein datasets, the increased stringency of using a two-peptide minimum may be beneficial to decrease the overall false-discovery rate and reduce potential false-positive identifications. This is speculation as only the localization of some of these SAINT significant eukaryotic proteins have been validated thus far.

Next, to determine if the minimum number of peptides would affect statistically significant chlamydial proteins identified, SAINT was applied to spectral count data obtained from the two-peptide minimum threshold (Table S4-8). We thought the two-peptide minimum might negatively impact the identification of *C. trachomatis* L2 Inc proteins because proteomics studies have found that hydrophobic proteins are often underrepresented in mass spectrometry experiments (254). For example, proteins that contain large transmembrane regions (e.g., Incs) typically have fewer tryptic peptides, thus are less frequently detected by the mass spectrometer. Surprisingly, the two-peptide

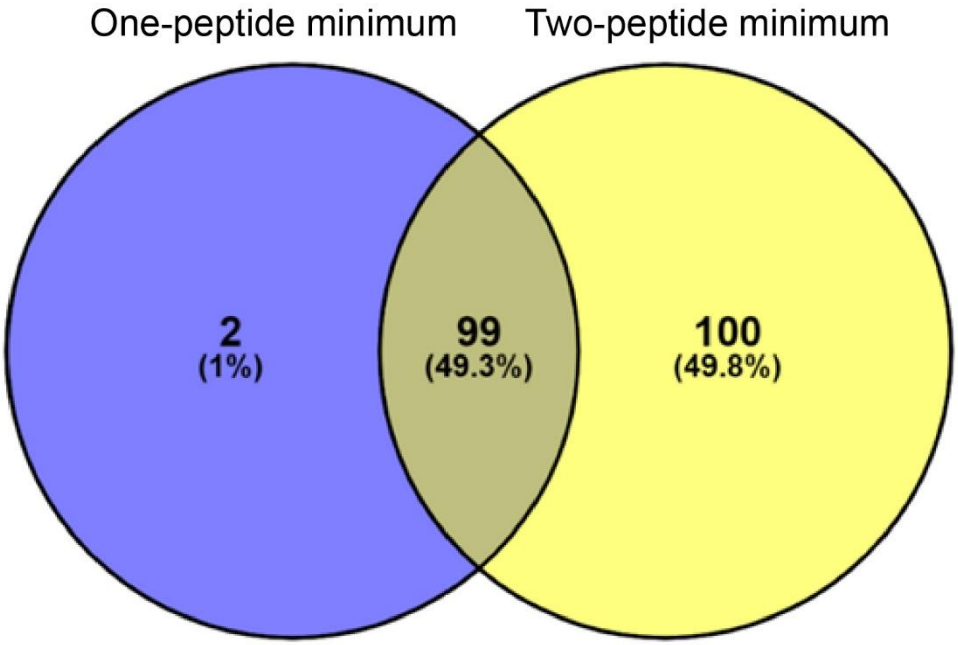

Figure 4-5. The effect of minimum peptide threshold on identification of SAINT significant proteins from Olson et al.

The SAINT significant eukaryotic proteins were calculated using a two-peptide minimum threshold and compared to a one-peptide minimum threshold as reported in Olson et al. The total number of proteins as well as the percentage of total is indicated within each overlapping section.

Figure modified from Olson et al. 2020. JProt.

minimum did not affect the number of SAINT statistically significant chlamydial Inc proteins in our dataset (Table 4-6). In fact, the same proteins were found to be statistically significant, with minimal change in BFDR, regardless of a one-peptide or two-peptide minimum (Table 4-6). These data suggest that, for identifying chlamydial proteins, a one-peptide threshold is sufficient.

3.11 Determination of availability of APEX2 amino acid targets of chlamydial Inc proteins

After determining the peptide threshold had a minimal effect on the identification of chlamydial Inc proteins, we aimed to better understand the ability of APEX2 to covalently tag different proteins. This is because the use of both AspN and trypsin for protein digestion to enhance peptide sequence coverage and identification (115, 226) resulted in the identification of only four Inc proteins as significant by SAINT analysis.

These results were surprising as there are 50+ predicted Incs expressed on the inclusion membrane (93), and a previous study indicated that both IncF and IncA could potentially interact with at least 8 and 4 additional Inc proteins, respectively (105). The specific amino acid residues that APEX2 covalently modifies with a biotin molecule are cysteine, tyrosine, tryptophan, and histidine (57, 189, 209), but we have not mapped how prevalent these amino acids are outside of the large hydrophobic transmembrane regions (254). It is plausible that Incs that have fewer APEX2 modifiable residues will have decreased total biotinylation and may not be as efficiently enriched during the affinity purification steps as the proteins that have numerous biotin modifiable residues. Overall, this would result in these proteins being more difficult to detect by mass spectrometry. We analyzed our chlamydial datasets (115) to understand how these intrinsic differences in the amino acid composition of Inc proteins might influence our analysis (Table 4-7; Fig. S4-1). We found in general that chlamydial Inc proteins with 11 or more biotin modifiable residues are identified with statistical significance (BFDR ≤0.05) (115).

Table 4-6. Comparison of minimum peptide threshold on SAINT calculated statistically significant *C. trachomatis* L2 proteins

Sample	Protein (Uniprot ID)	Protein[a]	1 peptide minimum BFDR [b]	2 peptide minimum BFDR [b]
IncF-APEX2	A0A0H3MKT3_CHLT2	CT223	0	0
	INCD_CHLT2	IncD	0.02	0.01
	INCF_CHLT2	IncF	0.03	0.02
$IncA_{TM}$-APEX2	A0A0H3MD02_CHLT2	IncA	0	0
	A0A0H3MKT3_CHLT2	CT223	0.02	0
IncA-APEX2	OMCB_CHLT2	OmcB	0	0
	A0A0H3MKT3_CHLT2	CT223	0	0
	A0A0H3MD02_CHLT2	IncA	0	0
	MOMP_CHLT2	MOMP	ns	0.05

[a] Protein name indicated using *C. trachomatis* serovar D naming convention

[b] Bayesian False Discovery Rate (SAINT)

ns; not significant

Table adapted from Olson et al. 2020. JProt.

Table 4-7. Analysis of APEX2 modifiable amino acid targets of various Inc proteins

Inc protein Serovar D naming convention	Targets (#[a])	Length (AA[b])	Modifiable residues[c] (%)
CT101[d]	18	153	11.76
CT249	9	116	7.76
CT058	25	367	6.81
CT222[d]	8	128	6.25
IncE	7	132	5.3
CT223[d]	14	268	5.22
IncB[d]	6	115	5.22
CT850[d]	21	405	5.19
CT813	13	264	4.92
CT005	16	363	4.41
IncD	6	146	4.11
IncA	11	273	4.03
IncF	4	104	3.85
IncG	6	167	3.59
CT226	6	176	3.41
CT228	6	196	3.06

[a] number of amino acid targets for APEX2

[b] amino acid (AA)

[c] number of AA targets divided by Inc length

[d] endogenous protein localizes in microdomains

Table adapted from Olson et al. 2020. JProt.

In contrast, Inc proteins with fewer than five modifiable residues were less frequently detected by mass spectrometry and were not statistically significant. For example, IncA (serovar L2) has 11 modifiable residues (not in the transmembrane domain region), where CT226 has only six residues (not in the transmembrane domain region) with three of those biotin-modifiable residues in the N-terminal type three secretion signal region. In contrast, IncA contains only one residue in the N-terminal T3SS region of the 11 biotin-modifiable residues. IncA was statistically significant for IncA-APEX2 and $IncA_{TM}$-APEX2 and was detected by western blot in the eluates from the streptavidin affinity purification (115). Another statistically significant Inc detected in our dataset, CT223, has 17 modifiable residues (115). One important note is that because the organization of Incs in the inclusion is not understood (59), we cannot exclude the impact of the proximity of Incs (Inc-APEX2 constructs) to other Incs in the inclusion membrane on the labeling efficiency. We also identified chlamydial outer membrane proteins, OmcB and MOMP, as significant for our *Chlamydia* dataset (115). Both proteins have numerous APEX2 targets with OmcB containing 49 APEX2 biotin-modifiable residues and MOMP containing 29 APEX2 modifiable residues, respectively. It is possible that during the short biotinylation reaction step the small biotin-phenoxyl radicals diffuse across the inclusion membrane and label the outer membranes of chlamydial developmental forms (168, 189).

4. Conclusion

With the recent advances in genetic tools for the manipulation of *C. trachomatis* L2, there has also been an expansion in the acquisition of large-scale AP-MS data to determine protein-protein interactions at the inclusion membrane. Four large-scale AP-MS experiments have been published in the last five years, each of which each aims to either identify eukaryotic proteins recruited to the chlamydial inclusion (171) or to understand the role of Incs in the inclusion, beginning with the identification of protein-

protein interaction partners (115, 122, 170). Each experiment was approached in a different fashion (e.g., Inc fused to a Strep-tag, inclusion purification, or proximity labeling), yielding over approximately 200 statistically significant eukaryotic proteins at the inclusion membrane. Large-scale proteomics studies, regardless of the software used in the analysis, frequently generate lists of hundreds of proteins detected in the sample. It is necessary to validate the localization and interaction by independent means to discern true interactions from these protein lists. This is highlighted in this meta-analysis as only seven of over 1,000 proteins were commonly identified from the four large proteomics experiments (115, 122, 170, 171). We compared the statistically significant proteins from each study to highlight commonly identified proteins, which likely reflect high confidence interacting proteins at the inclusion (Fig. 4-1, Table 4-8, Table S4-1, Table S4-9). In support, three of the four high-confidence hits: LRRF1 (115), MYPT1 (38, 117), and 14-3-3β (142) have been previously validated at the inclusion.

We also used this opportunity to compare the limitations of each experimental system. The two APEX2 proximity labeling experiments were directly compared using the same statistical analysis tool, which revealed that different statistical analysis tools can greatly impact the outcome of an individual experimental dataset (Table 4-3, and 5-4 and Table S4-2 and S4-3). We did not apply the G- and *t*-test to our datasets as the exact methods implemented for these analyses were poorly described. However, we did analyze our datasets using increased peptide threshold minimums (Fig. 4-5, Table 4-6, Table S4-7 and Table S4-8). These data indicated that a two-peptide minimum threshold might decrease the overall false positives for our eukaryotic protein dataset (Fig. 4-5, Table S4-8) but did not impact the chlamydial protein dataset (Table 4-6, Table S4-8). Overall, as more molecular tools are developed and adapted to understand the complex interactions at the chlamydial inclusion membrane and to understand host-pathogen interactions at

the bacterial-containing vacuole of other intracellular bacteria, it is important to understand both the limitations and advantages of these different tools. Finally, as a field, it will be important to use statistical analysis tools that allow for efficient and meaningful interpretation of AP-MS data.

Table 4-8. High-confidence proteins commonly identified in all four AP-MS studies at the inclusion membrane

Venny comparison using the reported significant proteins	Venny comparison of significant proteins post-SAINT analysis of Dickinson et al. 24 hpi datasets
LRRF1_HUMAN	LRRF1_HUMAN
MYPT1_HUMAN	MYPT1_HUMAN
TMOD3_HUMAN	TMOD3_HUMAN
1433B_HUMAN	1433B_HUMAN
1433F_HUMAN	
RTN4_HUMAN	
SNX1_HUMAN	

[a] Complete data provided in Table S4-1

[b] Complete data provided in Table S4-9

The proteins that are highlighted were identified in both comparisons

Table adapted from Olson et al. 2020. JProt

Appendix C-Supplementary figures and tables

Figure S4-1. Analysis of APEX2 modifiable target residues of Inc proteins. https://www.sciencedirect.com/science/article/pii/S1874391919303677

Table S4-1. Venny comparison of reported significant proteins from AP-MS studies at the *C. trachomatis* inclusion membrane

Table S4-2. SAINT analysis of Dickinson et al. datasets

Table S4-3. Venny comparison of Dickinson et al. SAINT analyzed datasets with Dickinson et al. reported G- and *t*-test analyzed datasets

Table S4-4. Comparison of SAINT analyzed Dickinson et al. datasets with Dickinson et al. reported RNAi experiments

Table S4-5. CRAPome analysis of Dickinson et al. and Olson et al. significant eukaryotic proteins

Table S4-6. Contaminant proteins identified from streptavidin AP-MS of uninfected HeLa cell lysates

Table S4-7. SAINT analysis of Olson et al. eukaryotic proteins with a two-peptide minimum threshold

Table S4-8. SAINT analysis of Olson et al. *C. trachomatis* L2 proteins with a two-peptide minimum threshold

Chapter 5 - Discussion and Concluding Remarks

We hypothesize that Incs perform two broad functions in the inclusion membrane: (i) to organize the inclusion membrane and (ii) to bind eukaryotic proteins for acquiring nutrients from host cell pathways or for blocking host immune responses. To test this hypothesis, we have adapted the APEX2 proximity labeling system for use in *C. trachomatis* serovar L2 to label the interactions that occur at the inclusion membrane *in vivo* to test the propensity of different Incs to bind eukaryotic and chlamydial proteins. We performed the proximity labeling studies using Incs that may fall within the proposed Inc functional categories: inclusion organization (i.e., IncF) and eukaryotic protein binding (i.e., IncA). BACTH assays supported these functions, as IncF interacted with several Incs, whereas IncA interacted with fewer Incs (105). Importantly, the APEX2 proximity labeling studies are performed in the context of *C. trachomatis* infected cells using Inc-APEX2 fusion proteins that are secreted from *C. trachomatis* L2 transformed with a plasmid that expresses IncF-APEX2, IncA-APEX2, or $IncA_{TM}$-APEX2. Importantly, these fusion proteins localized appropriately to the inclusion membrane, as determined by immunofluorescence (Fig. 3-1) and electron microscopy (Fig. 3-2).

Validation of significant eukaryotic proteins identified using Inc-APEX2 constructs

We demonstrated that a statistically significant eukaryotic protein, LRRF1, localized to the inclusion and interacted with CT226 (Fig. 3-5, Fig. 3-8) (115). Three other eukaryotic proteins, Microtubule-associated protein 1B (MAP1B), Brain acid soluble domain protein 1 (BASP1), and Cystatin B (CYTB), were also identified as statistically significant using each Inc-APEX2 construct (Table S3-2), suggesting the likely recruitment of these proteins to the inclusion. MAP1B has previously been observed to co-localize

with the inclusion membrane (227), so we aimed to determine if BASP1 and CYTB also co-localized with the inclusion. BASP1 belongs to the MARCKS family of proteins, which are known to regulate the actin cytoskeleton and plasma membrane signaling dynamics (255, 256). Given that the actin cytoskeleton is manipulated by numerous chlamydial proteins (128, 129, 131, 134, 252), BASP1 may play a role in actin modification during *C. trachomatis* infection. Cystatin B inhibits cathepsins and typically associates with lysosomes (257), which are known to be a nutrient source for *C. trachomatis* during infection (124). As such, CYTB may also play a role during chlamydial infection.

While we were unable to verify the localization of cystatin B during *C. trachomatis* L2 infection of HeLa cells (data not shown), we detected BASP1 in microdomains at the inclusion membrane at 24 hpi (Fig. 5-1A). A time-course study of BASP1 localization during *C. trachomatis* L2 infection revealed robust BASP1 localization early during infection (8 hpi), which decreased throughout the developmental cycle (Fig 5-1B). BASP1 is detected in the plasma membrane in uninfected HeLa cells, which may suggest that BASP1 is part of the early endocytic vacuole (Fig. 5-1A). Furthermore, chloramphenicol treatment of early inclusions (10 hpi) prevented the loss of BASP1, suggesting loss of BASP1 is due to inclusion modification by chlamydial proteins or at least as a result of inclusion expansion (Fig 5-1B, Cm panel). BASP1 is known to interact with calmodulin and actin, and the phosphorylation of BASP1 by protein kinase C (PKC) causes BASP1 to dissociate from the plasma membrane (258). Interestingly, PKC localizes to the inclusion membrane (259), which may support the loss of BASP1 after phosphorylation by PKC. MARCKS, a PKC substrate in the same family as BASP1 (256), was also identified as SAINT significant in our Inc-APEX2 datasets (BFDR 0.4 for IncF-APEX2 and IncA-APEX2)(Table S3-2). This may support an additional mechanism of actin modification via BASP1, and potentially MARCKS, during the developmental cycle.

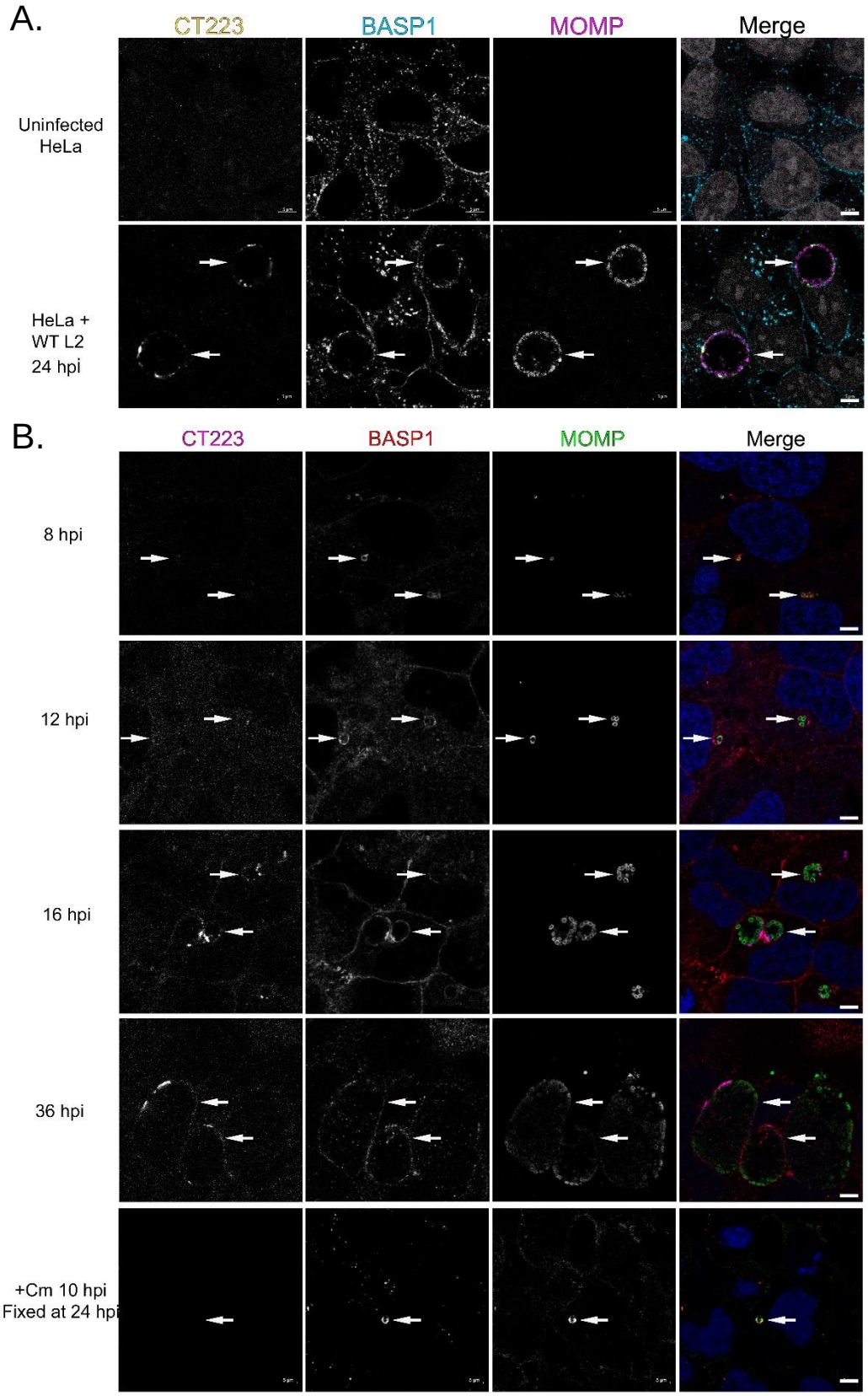
A.
CT223
BASP1
MOMP
Merge
Uninfected HeLa
HeLa + WT L2 24 hpi
B.
CT223
BASP1
MOMP
Merge
8 hpi
12 hpi
16 hpi
36 hpi
+Cm 10 hpi Fixed at 24 hpi

Figure 5-1. BASP1 co-localizes with wild-type *C. trachomatis* L2 inclusions from 8 to 36 hpi during the developmental cycle.

HeLa cells were infected with wild-type *C. trachomatis* L2 or mock-infected, fixed (3.2% formaldehyde and 0.022% glutaraldehyde in DPBS) at the indicated times post-infection (hpi), and stained to visualize A) CT223 (yellow), BASP1 (blue), chlamydiae (MOMP; pink), and DNA (DAPI), or B) CT223 (pink), BASP1 (red), chlamydiae (MOMP; green), and DNA. For chloramphenicol (Cm) treated wells, Cm (35 µg/mL) was added at 10 hpi and coverslips were fixed and stained for immunofluorescence at 24 hpi. Images were obtained using a Zeiss confocal LSM 800 63x with 2x zoom (scale bar =5 µm). Inclusions are denoted by arrows.

Statistically significant eukaryotic proteins unique to individual C. trachomatis L2 IncF-APEX2, IncA-APEX2, or IncA$_{TM}$-APEX2 datasets

Another goal of our APEX2 study was to determine if our Inc-APEX2 constructs biotinylated different proteins, which may suggest distinct protein binding specificity conferred by IncF and IncA based on their function within the inclusion membrane. Consistent with our hypothesis that IncF serves an organizational role in the inclusion membrane, IncF-APEX2 labeled more Inc proteins than IncA-APEX2 (Table 3-1, Table S3-1) and significantly fewer eukaryotic proteins compared to IncA-APEX2. In addition, aside from the four proteins identified using each Inc-APEX2 construct, there was no overlap between IncF-APEX2 and IncA$_{TM}$-APEX2 SAINT significant proteins, which may suggest specificity conferred by IncF-APEX2 compared to IncA$_{TM}$-APEX2 (Fig. 5-2, Table S3-3). However, it also is reasonable that Incs serve both organizational (via transmembrane domains) and eukaryotic protein-binding functions (via their cytosolic C-terminus).

The significant eukaryotic proteins that were unique to the IncF-APEX2 dataset include POTE ankyrin domain family member I (POTEI_HUMAN), 60*S* ribosomal protein L26 (RL26_HUMAN), 60*S* ribosomal protein L26-like 1 (RL26L_HUMAN), 14-3-3 Θ, and 14-3-3 γ (1433T_HUMAN and 1433G_HUMAN, respectively) (BFDR ≤0.05) (Fig. 5-2, Table S3-3). RL26 and POTEI have not been assessed for their localization during *C. trachomatis* infection. RL26 is a component of the large subunit of the eukaryotic ribosome. The function of POTEI is unknown; however, it contains an ankyrin domain with spectrin-like coiled-coil motifs, suggesting functions associated with actin regulation or signal transduction (260, 261). Two 14-3-3 protein isoforms were also unique to IncF-APEX2. This is of interest because IncG is known to bind 14-3-3 β (142), and IncF is

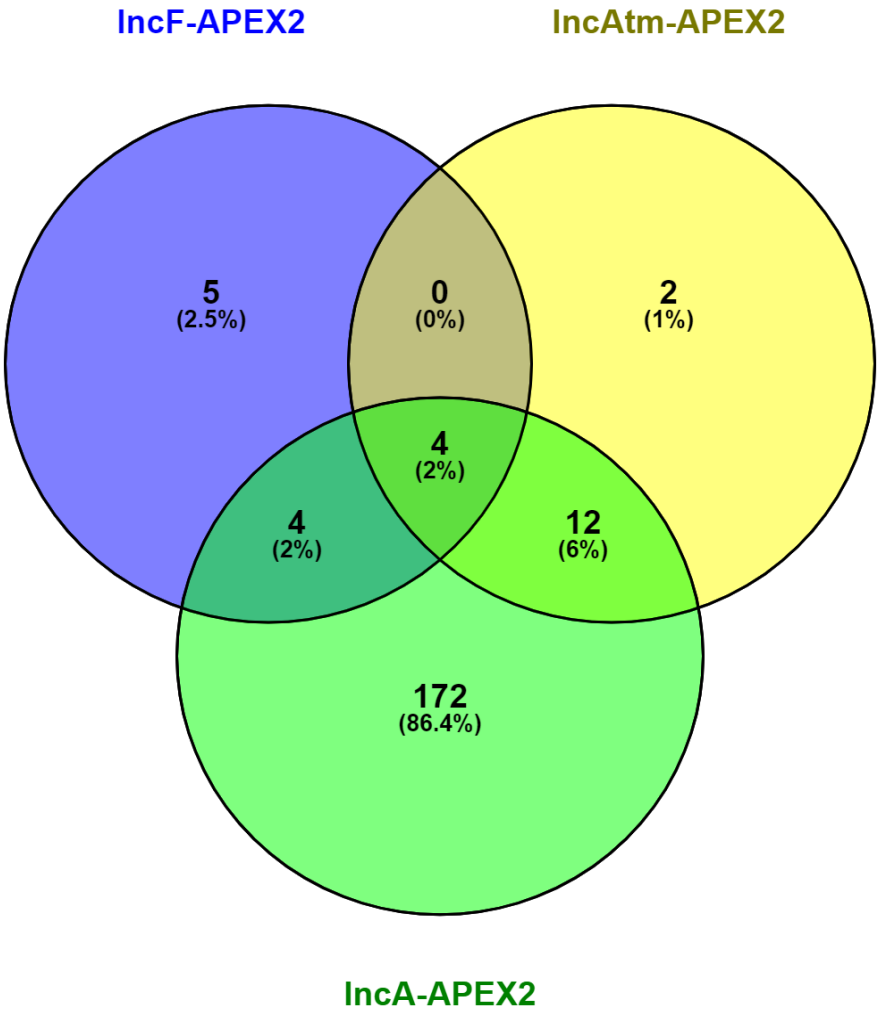

Figure 5-2. Venny comparison of SAINT significant eukaryotic proteins identified using IncF-APEX2, IncA_{TM}-APEX2, and IncA-APEX2 at 24 hpi.

SAINT significant proteins (199 proteins) identified by AP-MS using *C. trachomatis* L2 IncF-APEX2, IncA_{TM}-APEX2, and IncA-APEX2 transformant. The significant proteins were analyzed using Venny to determine which proteins were similarly or uniquely identified proteins between each Inc-APEX2 construct. The total number of proteins as well as the percentage of total is indicated within each overlapping section.

presumed to be encoded within an operon with IncG (44), which may support similar protein functions. The 14-3-3 proteins are adaptor proteins involved in various host cell signaling pathways, including apoptosis, autophagy, and glucose metabolism (262). Each of these functions are important during *C. trachomatis* development; as such, these proteins would be interesting to examine further.

For $IncA_{TM}$-APEX2, the unique SAINT significant proteins included CERT (C43BP_HUMAN) and Sorcin (SORCN_HUMAN) (Fig. 5-2, Table S3-2, and Table S3-3). CERT is recruited to the inclusion by IncD (54, 126), and SORCN is involved in calcium homeostasis and vesicle trafficking (263, 264). By BACTH, IncA interacts with IncD (105), supporting the identification of CERT possibly via interactions between these Incs in the inclusion membrane. The lack of SAINT significant proteins identified for $IncA_{TM}$-APEX2 supports the notion that the C-terminus of IncA provides protein binding specificity. It is important to note that in addition to localizing around the inclusion membrane, full-length IncA has both a long C-terminus and is observed in “fiber-like” extensions in the host cell. Thus, IncA-APEX2 expressed from *C. trachomatis* L2 IncA-APEX2 could label more proteins as a result of the increased area and APEX2 flexibility as APEX2 is tethered to a longer cytosolic C-terminal IncA. We observed biotinylation of IncA-APEX2 positive fibers by super resolution microscopy (Fig. 5-3A), whereas no fibers are detected in *C. trachomatis* $IncA_{TM}$-APEX2 infected cells (Fig. 5-3B). SAINT significant proteins that are unique to IncA-APEX2, including SNX2, SNX3, and SNX5, have been observed on endogenous IncA fibers (171). However, we currently do not understand the major components of these fibers, making speculation about their function difficult. To limit APEX2 labeling as a result of increased flexibility (i.e., large C-terminus), we created a *C. trachomatis* L2 strain transformed with a plasmid that expresses APEX2 “sandwiched” between $IncA_{TM}$ and the IncA C-terminus. We transformed this construct into *Chlamydia*

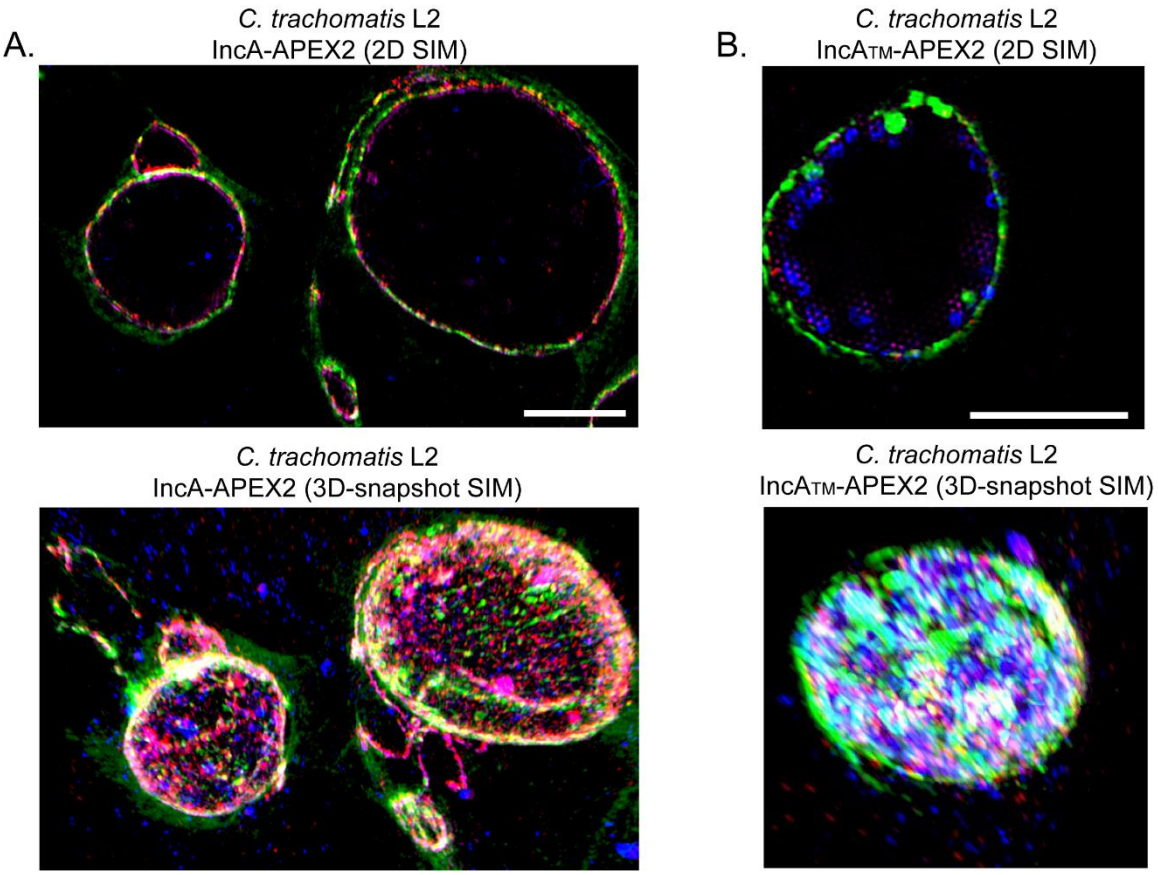

Figure 5-3. Visualization of biotinylated IncA-APEX2 positive fibers in *C. trachomatis* L2 IncA-APEX2 infected HeLa cells using super-resolution microscopy.

HeLa cells were infected with *C. trachomatis* L2 IncA-APEX2 or $IncA_{TM}$-APEX2 transformed strains and induced using 5nM aTc at 7hpi. Biotin-phenol was added at 23.5 hpi, the labeling reaction was performed at 24hpi followed by a quenching/wash solution, and the cells were methanol fixed and stained for immunofluorescence. Biotinylated proteins (Streptavidin-488; green), IncA (pink), IncA-APEX2 (red), and chlamydiae (blue). Coverslips were imaged using Zeiss ELYRA PS.1 Super Resolution Microscope Zeiss with Structured Illumination Microscopy (SIM). Scale bar= 5 µm. Using Zen Blue (Zeiss) A) *C. trachomatis* L2 IncA-APEX2 and B) $IncA_{TM}$-APEX2 inclusions represented as 2D and 3D snapshots.

and confirmed expression, but we have not performed biotinylation studies. If limiting IncA-APEX2 flexibility by sandwiching APEX2 between the hydrophobic and cytosolic domains of IncA does not work, an alternative approach may be to use new *in vivo* labeling methods that surpass the resolution of proximity labeling approaches (~10-20 nm) (189, 193, 209) by labeling direct protein-protein interactions (265, 266).

Examination of Incs that are conserved between Chlamydia species

One issue that commonly arises when assessing the function of Inc-eukaryotic protein-protein interactions is that loss of a single Inc or eukaryotic protein often does not substantially impact chlamydial development (e.g., SNX6 (122) and VAPA (54)). This is typically attributed to redundancy in the *C. trachomatis* effectors that are secreted into, or the host cell pathways that are recruited to, the inclusion membrane. Redundancy of function within Incs might suggest paralogous gene sets, but *inc* genes share little sequence homology (87, 104). Rather, these genes may encode proteins that perform tissue-specific functions that may be apparent using a more physiologically relevant system (i.e., primary cell lines, 3D organoid, or primate models). Alternatively, two different Incs may target different parts of the same pathway to maximize survival. Bioinformatic analyses identified 23 conserved (i.e., core) Incs in five chlamydial species based on the presence of predicted hydrophobic bilobed transmembrane domains: *C. trachomatis* (ocular and STIs), *C. pneumoniae* (community-acquired pneumonia), *C. muridarum* (mouse pathogen), *C. caviae* (guinea pig pathogen), and *C. felis* (feline chlamydiosis) (104). This study also identified divergent Incs potentially indicative of tissue tropism (104). Of the human pathogens, *C. pneumoniae* has the highest number of predicted Incs (92 Incs), compared to *C. trachomatis* with 55 Incs. Regarding animal pathogens, *C. muridarum* (closely related to *C. trachomatis*) has 54 Incs, compared to *C. felis* with 69 and *C. caviae* with 79 predicted Incs (104). Furthermore, the majority of Incs (i.e., 49 Inc

proteins) were similarly identified between *C. muridarum* and *C. trachomatis.* A group of 23 core Incs were detected in all five *Chlamydia* species: CT005, CT006, CT058, CT134, CT179, CT195, CT232 (IncB), CT233 (IncC), CT288, CT324, CT365, CT383, CT440, CT449, CT483, CT484, CT565, CT616, CT618, CT642, CT728, CT788, and CT850. These 23 core Incs likely perform essential functions during chlamydial development, regardless of tissue differences. Unfortunately, the function of only two core Incs has been defined thus far.

CT850 binds dynein light chain one to traffic the early inclusion to the MTOC (123), and CT288 has been suggested to bind the centrosomal protein, CCDC146 (133). A large screen using *C. trachomatis* L2 transformed strains that expressed a predicted Inc fused to a FLAG-tag confirmed that some Incs localized to the inclusion membrane (93). This study also demonstrated that a few predicted Incs localized instead to the bacterial cytosol or bacterial membrane (i.e., CT058, CT195, CT365, CT483, CT484, CT565, CT616, CT642, CT728, and CT788) (93). It's important to note that overexpression systems may fail to secrete proteins or could result in the mislocalization of predicted Incs. However, we have tested variable induction conditions and consistently observed CT483, CT484, and CT788 expressed from *C. trachomatis* L2 transformed strains localized to the bacterial membrane (data not shown). This may suggest that the criteria used to identify candidate *inc* genes are too permissive and that there are fewer core Incs than predicted.

In our evaluation of LRRF1 functions, neither siRNA knockdown of LRRF1 or overexpression significantly impacted *C. trachomatis* growth (Fig. S3-4). While this may support a role for CT226 to sequester LRRF1 to prevent its function, the downstream interactions remain unclear. Consistent with our studies of LRRF1 co-localization with the inclusion of various *Chlamydia* species (Fig. 3-7), CT226 was found to be conserved between *C. trachomatis* and *C. muridarum*, but not *C. pneumoniae*, *C. caviae*, or *C. felis*

(104). Perhaps the function of the interaction between CT226 and LRRF1 is important for survival in infected human macrophages since *C. trachomatis* serovar L2 can infect macrophages and spread to the lymph nodes.

Future Directions

Our meta-analysis revealed that the majority of statistically significant proteins were not shared between the two APEX2 studies (Fig. 4-3 and Fig. 4-4). Both APEX2 studies statistically significant proteins that are known to be recruited to the inclusion membrane (i.e., 14-3-3-β (IncG binding partner), LRRF1 (CT226 binding partner), and MYPT1 (CT228 binding partner) (Table S3-3, Table S4-3). Only our APEX2 study identified CERT (IncD binding partner), DYNLT1 (CT850 binding partner), SNX5 and SNX6 (IncE binding partner). Only Dickinson et al. identified VAPA and VAPB (CT005 binding partner), and neither study identified Arf1 (CT813 binding partner), CEP170 (CT223), or CCDC146 (CT288)(Table S4-3). These data may be indicative of different protein binding specificities and/or different proximal partners conferred by IncB, IncA, and IncF. It is also possible that there are changes in the organization of the inclusion membrane when certain Incs are overexpressed, which may also alter the eukaryotic proteins that are normally recruited to the inclusion during *C. trachomatis* infection. The organization of the inclusion membrane is not well understood (105), and the impact of Inc overexpression on the expression and localization of endogenous Incs has not been studied.

The overexpression of specific Incs from C. trachomatis *L2 alters the organization of the inclusion membrane*

We hypothesize that some Incs organize the inclusion through Inc-Inc interactions, and the overexpression of these Incs alters the organization of the inclusion membrane.

In support, we previously demonstrated the negative impact of the overexpression IncF-APEX2 on chlamydial development using the *C. trachomatis* L2 IncF-APEX2 transformed strain (57). The negative impact is not a result of the large APEX2 tag since these data were recapitulated using a *C. trachomatis* IncF-FLAG transformed strain (Fig 5-4A). The decreased inclusion size may be indicative of an altered inclusion membrane organization. To test our hypothesis, we created additional *C. trachomatis* L2 CT813-FLAG, CT226-FLAG, or CT483-FLAG transformed strains. CT483 is a predicted Inc based on the presence of transmembrane domains, but CT483-FLAG localized to the membrane of chlamydiae (93), so this construct was used as a control for the metabolic burden of inducing Inc-FLAG expression from the transformed strains.

To determine if the expression of additional Incs negatively impacted the inclusion area, *C. trachomatis* L2 transformed strains were induced using various concentrations of anhydrotetracycline (aTc), and the inclusion area was measured. HeLa cells were infected with *C. trachomatis* L2 transformed strains, CT813-FLAG, CT226-FLAG, CT483-FLAG, or wild-type *C. trachomatis* L2 and induced for expression at 7 hours post-infection (hpi) using 5 nM or 20 nM anhydrotetracycline (aTc). Samples were fixed at 36 hpi, stained for immunofluorescence, and the inclusion area was measured using ImageJ. The overexpression of both IncF-FLAG and CT813-FLAG from *C. trachomatis* L2 transformed strains resulted in a significantly decreased inclusion area (Fig. 5-4A). The smaller inclusion area after overexpression of CT813-FLAG and IncF-FLAG, but not CT226-FLAG, may support altered inclusion membrane organization due to the dysregulation of Incs that perform organizational roles.

The overexpression CT813-FLAG and IncF-FLAG also negatively impacted chlamydial development, as indicated by decreased infectious progeny production (Fig. 5-4B). There was a 77-fold decrease in infectious progeny for CT813-FLAG (20 nM aTc) and an 81-fold decrease for IncF-FLAG (20 nM aTc), compared to *C. trachomatis* L2

A.

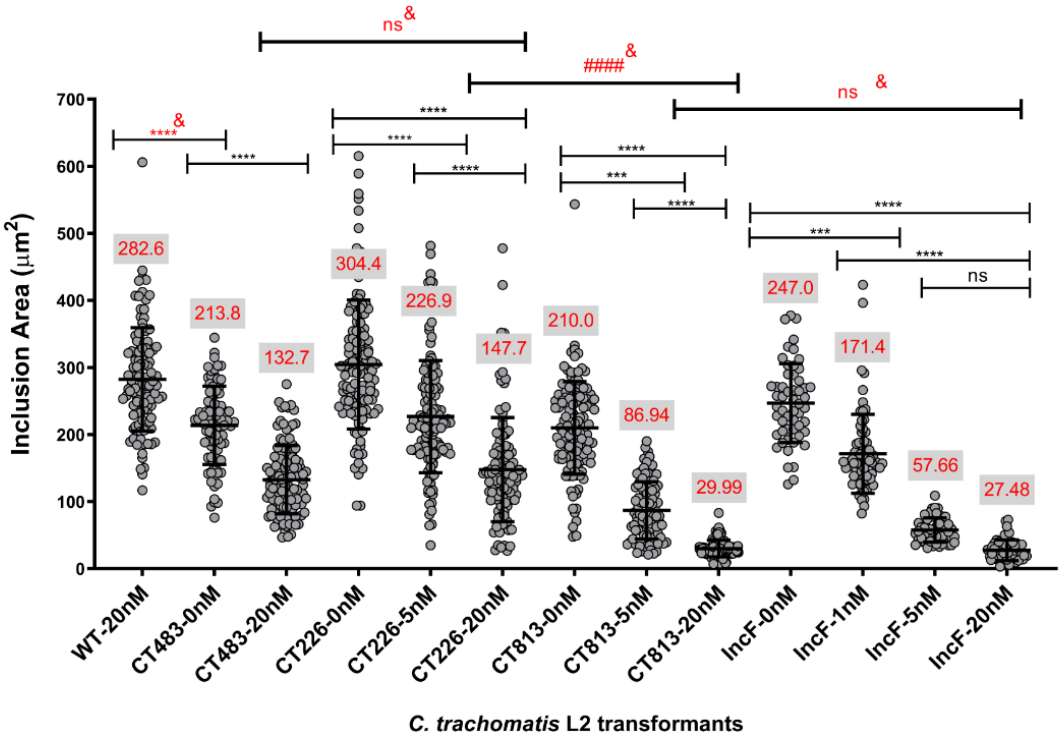
Inclusion Area (μm²)
700
600
500
400
300
200
100
0
282.6
213.8
132.7
304.4
226.9
147.7
210.0
86.94
29.99
247.0
171.4
57.66
27.48
ns
&
####
****
***
WT-20nM
CT483-0nM
CT483-20nM
CT226-0nM
CT226-5nM
CT226-20nM
CT813-0nM
CT813-5nM
CT813-20nM
IncF-0nM
IncF-1nM
IncF-5nM
IncF-20nM
C. trachomatis L2 transformants

B.

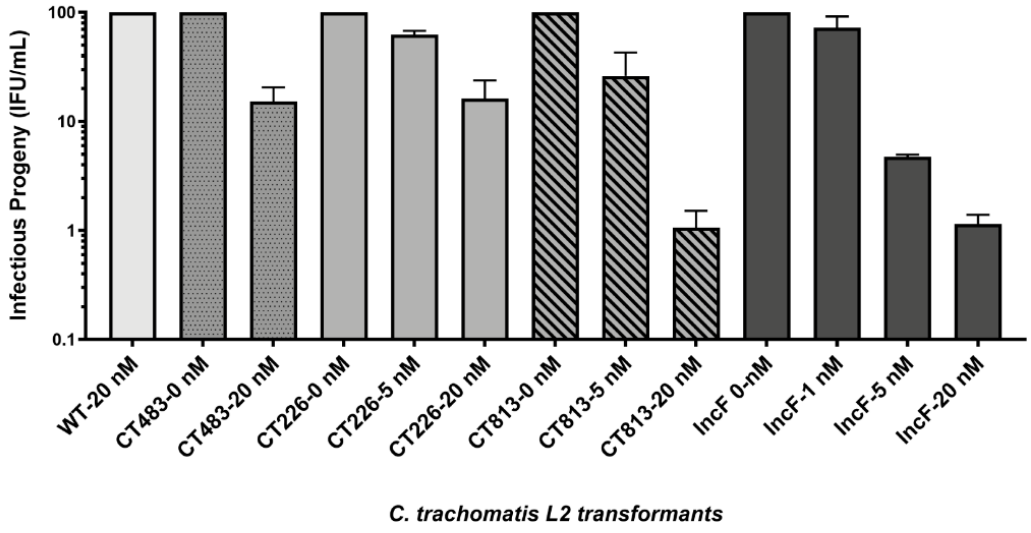
Infectious Progeny (IFU/mL)
100
10
1
0.1
WT-20 nM
CT483-0 nM
CT483-20 nM
CT226-0 nM
CT226-5 nM
CT226-20 nM
CT813-0 nM
CT813-5 nM
CT813-20 nM
IncF 0-nM
IncF-1 nM
IncF-5 nM
IncF-20 nM
C. trachomatis L2 transformants

C.

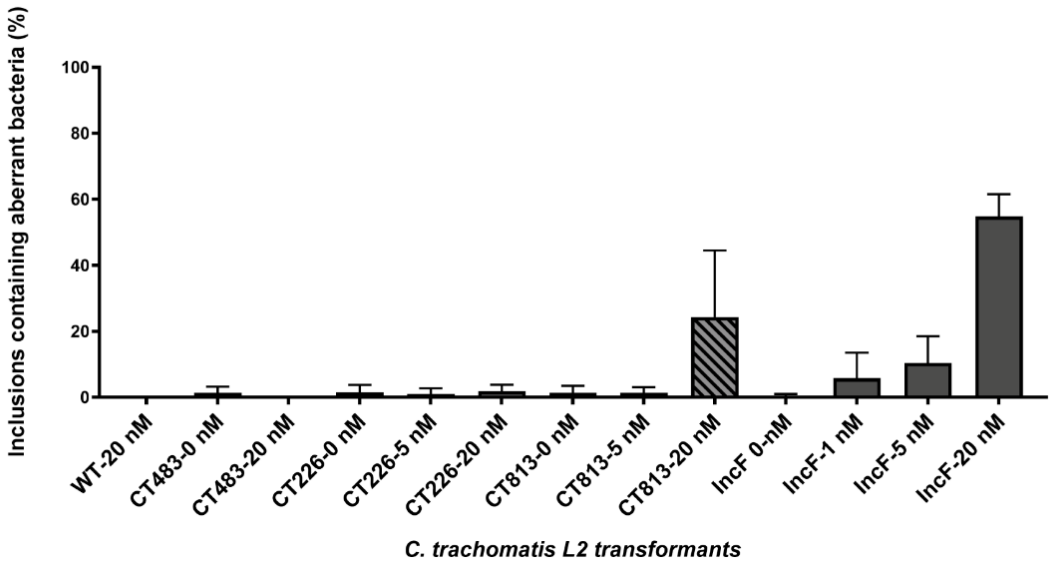

Figure 5-4. Overexpression of CT813-FLAG and IncF-FLAG from *C. trachomatis* L2 transformed strains negatively impacts inclusion growth and progeny production.

A) HeLa cells seeded on coverslips were infected with *C. trachomatis* L2 transformed strains or wild-type L2, and induced at 7 hpi with 1, 5 or 20 nM aTc or not induced. Coverslips were methanol fixed at 36 hpi and stained for immunofluorescence to determine inclusion area. A minimum of 100 inclusions per condition were measured using ImageJ, and inclusion area (μm^2) and standard deviation were plotted using GraphPad Prism 8.4.0. N=3. The mean inclusion area is indicated in red. A one-way ANOVA was applied to test for statistical significance; ******* p≤ 0.001, ******** p≤ 0.0001, **&**(red) indicates a statistical comparison between *C. trachomatis* L2 strains.

B) HeLa cells infected in duplicate with *C. trachomatis* L2 CT813-FLAG, IncF-FLAG, CT226-FLAG, CT483-FLAG transformed strains, or wild-type *C. trachomatis* L2, were induced for expression at 7 hpi using 1nM, 5 nM, or 20 nM aTc. At 36 hpi infected monolayers were lysed, serially diluted, and infected onto a fresh monolayer of HeLa cells (i.e., secondary infection) in media containing penicillin to enumerate infectious progeny (Inclusion Forming Units (IFU)/mL). Infectious progeny (IFU/mL) and standard deviation was plotted using GraphPad Prism 8.4.0. N=3. Only inclusions with wild-type phenotype were enumerated for this assay.

C) Plasmid loss was indicated by inclusions containing aberrant bacteria in media containing penicillin (i.e., sensitivity due to the loss of the plasmid encoded *bla*^{r}). To enumerate the percent of inclusions containing aberrant bacteria, the number of inclusions with aberrant bacteria were divided by the total number of inclusions counted (part B) and standard deviation was plotted using GraphPad Prism 8.4.0. N=3.

CT813-FLAG and IncF-FLAG transformed strains not induced for expression. On the other hand, there was only a 4.6-fold in infectious progeny for CT226-FLAG (20 nM aTc) when overexpressed and a 5-fold decrease in infectious progeny for CT483-FLAG (20 nM aTc) compared to uninduced strains (Fig. 5-4B).

The overexpression of CT813-FLAG and IncF-FLAG from *C. trachomatis* L2 transformed strains is also associated with increased plasmid loss (Fig. 5-4C). During the secondary infection assay, *C. trachomatis* L2 transformed strains were grown in penicillin media to indicate plasmid retention. Samples were fixed and stained for immunofluorescence to enumerate inclusions that contained aberrant chlamydiae. The overexpression of CT813-FLAG and IncF-FLAG from *C. trachomatis* L2 transformed strains (induced in the primary infection using 20 nM aTc) resulted in 25% of CT813-FLAG inclusions and 50% of IncF-FLAG inclusions containing aberrant bacteria (Fig. 5-4C). Plasmid loss could be reduced for *C. trachomatis* L2 IncF-FLAG and CT813-FLAG when lower induction conditions were used in the primary infection (i.e. 1 and 5 nM aTc). In contrast, there was no significant plasmid loss even at the highest induction conditions for *C. trachomatis* L2 CT226-FLAG and CT483-FLAG transformed strains (Fig. 5-4C). These data indicate that the overexpression of CT813-FLAG and IncF-FLAG is not well tolerated by *Chlamydia*. These data also support the importance in the carefully controlled expression of certain Incs, whereby altered expression negatively impacts development.

To determine if decreased inclusion size, infectious progeny, and plasmid loss were a consequence of the altered organization of Inc proteins in the inclusion membrane, we overexpressed the Inc-FLAG constructs from our *C. trachomatis* L2 transformed strains and assessed the localization of endogenous Incs. HeLa cells seeded on coverslips were infected with *C. trachomatis* CT813-FLAG, CT226-FLAG, CT483-FLAG transformed strains, or wild-type L2 and either not induced or induced using 5 or 20 nM aTc at 7 hpi. Coverslips were methanol fixed at 36 hpi and stained for immunofluorescence

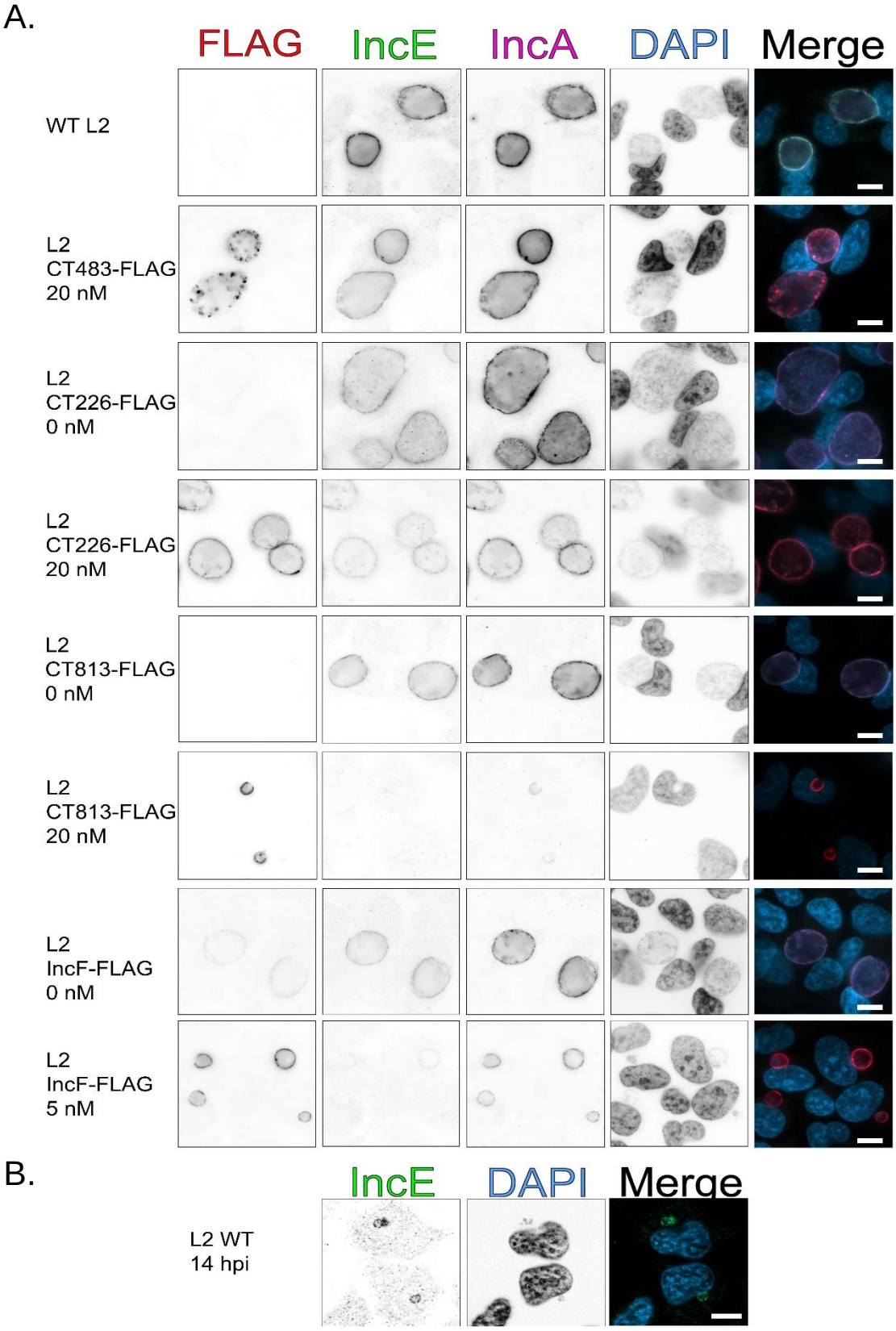
A.
FLAG
IncE
IncA
DAPI
Merge
WT L2
L2 CT483-FLAG 20 nM
L2 CT226-FLAG 0 nM
L2 CT226-FLAG 20 nM
L2 CT813-FLAG 0 nM
L2 CT813-FLAG 20 nM
L2 IncF-FLAG 0 nM
L2 IncF-FLAG 5 nM
B.
IncE
DAPI
Merge
L2 WT 14 hpi

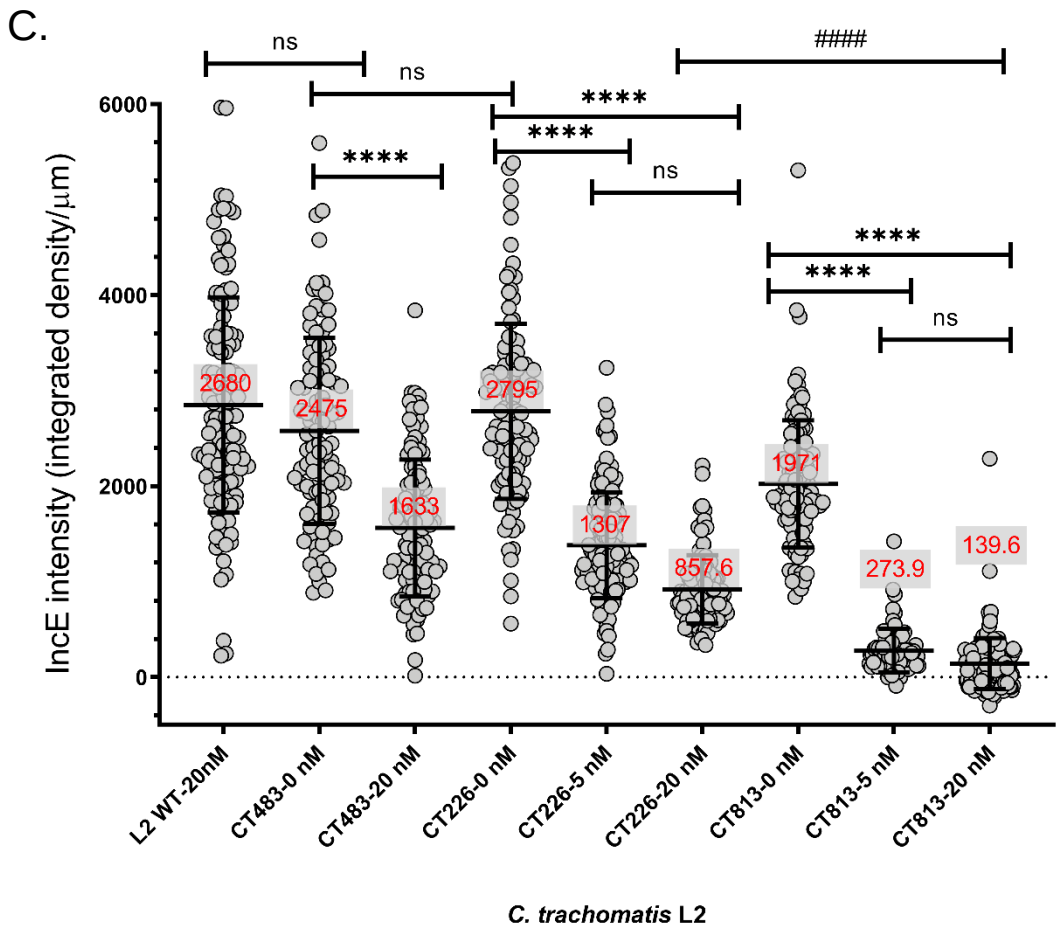

Figure 5-5. The overexpression of CT813-FLAG, but not CT226-FLAG, or CT483-FLAG from C. trachomatis L2 transformed strains results in loss of endogenous IncE.

A) HeLa cells infected with *C. trachomatis* L2 transformed strains or wild-type L2 were induced with 5 or 20 nM aTc, or not induced at 7 hpi. Coverslips were methanol fixed at 36 hpi and stained for immunofluorescence to observe expression of the constructs (FLAG; red), IncE (green), IncA (pink), or DNA (DAPI; blue). Coverslips were imaged using the same exposure for each sample at 63x magnification. Scale bar= 10 µm.

B) *C. trachomatis* L2 infected HeLa cells were fixed at 14 hpi and stained for immunofluorescence to observe IncE (green) and DNA (blue). Coverslips were imaged using the same exposure for each sample at 63x magnification. Scale bar= 10 µm.

C) The intensity of IncE was measured with ImageJ from images in part A. The background integrated density was subtracted from individual images and the intensity (integrated density/µm) and standard deviation were plotted using GraphPad Prism 8.4.0. Samples were analyzed for statistical significance using a one-way ANOVA. A minimum of 80 inclusions were measured for each condition. N=3. The mean integrated density/µm is reported in red for each sample measured. **** $p < 0.0001$ between *C. trachomatis* L2 transformed strains and #### indicates $p < 0.0001$ between *C. trachomatis* L2 transformed strains.

using anti-IncE and anti-IncA antibodies to determine the expression and localization of endogenous Incs. An anti-FLAG antibody was used to detect the expression of each construct. Images were captured using the same exposure for each IncE and IncA. The overexpression of CT813-FLAG and IncF-FLAG from *C. trachomatis* L2 transformed strains results in the loss of detectable IncE in the inclusion membrane (Fig. 5-5A). In contrast, the overexpression of CT226-FLAG did not substantially impact IncE intensity (Fig. 5-5A). Importantly, IncE was detected in the inclusion membrane of small, early (14 hpi) wild-type *C. trachomatis,* which resemble the inclusion area for overexpressed CT813-FLAG and IncF-FLAG (Fig. 5-5B). This indicates that the loss of detectable IncE when CT813-FLAG and IncF-FLAG are overexpressed is not due to smaller inclusions or slower inclusion development.

To quantify the intensity of IncE, the integrated density was measured in ImageJ and normalized to the inclusion perimeter (integrated density/µm). Compared to *C. trachomatis* L2 CT813-FLAG not induced for expression, there was a 7.2-fold and 14.1-fold decrease in IncE intensity when induced using 5 nM and 20 nM aTc, respectively (Fig. 5-5C). For *C. trachomatis* L2 CT226-FLAG induced using 5 nM and 20 nM aTc, the intensity of IncE was decreased 2.1-fold and 3.3-fold, respectively (Fig. 5-6C). These data support our hypothesis that the overexpression of certain Incs alters the localization of endogenous Incs in the inclusion membrane and that altered inclusion organization negatively impacts inclusion development.

We further tested if the loss of IncE localization in the inclusion membrane also impacted the recruitment of a eukaryotic binding partner of IncE, SNX6. HeLa cells were infected with *C. trachomatis* L2 CT813-FLAG, CT226-FLAG, or CT483-FLAG transformed strains, induced for expression at 7 hpi using 5 nM or 20 nM aTc, or not induced, fixed at 30 hpi and then stained to determine the localization of SNX6 (Fig. 5-6). Corresponding to the loss of IncE when CT813-FLAG is overexpressed, increased expression of CT813-

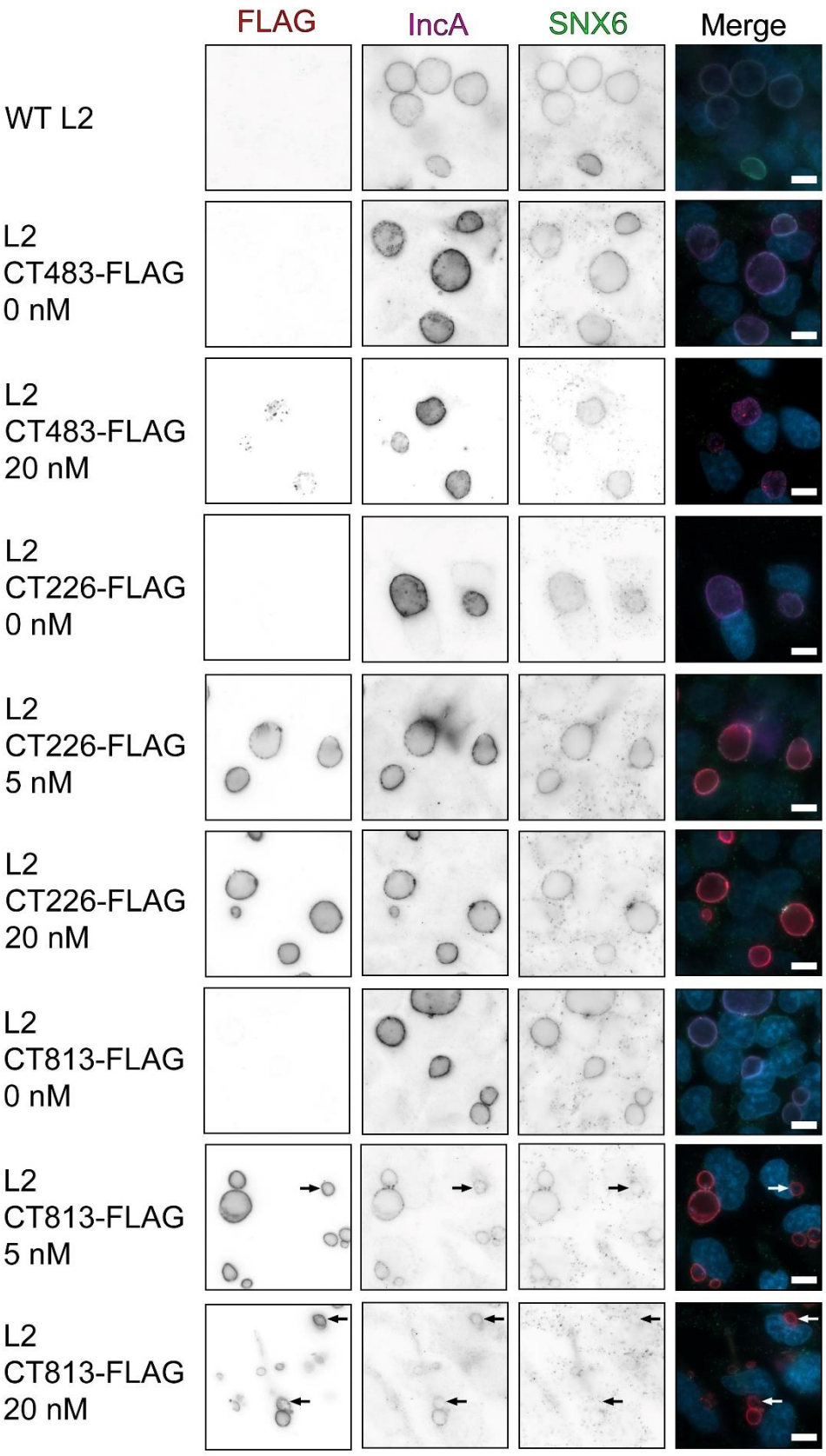
FLAG
IncA
SNX6
Merge
WT L2
L2 CT483-FLAG 0 nM
L2 CT483-FLAG 20 nM
L2 CT226-FLAG 0 nM
L2 CT226-FLAG 5 nM
L2 CT226-FLAG 20 nM
L2 CT813-FLAG 0 nM
L2 CT813-FLAG 5 nM
L2 CT813-FLAG 20 nM

Figure 5-6. Overexpression of CT813-FLAG, but not CT226-FLAG, or CT483-FLAG from *C. trachomatis* L2 transformed strains results in the loss of SNX6 co-localization with the inclusion membrane.

HeLa cells infected with *C. trachomatis* L2 transformed strains or wild-type L2 were induced at 7 hpi with 5 or 20 nM aTc, or not induced. Coverslips were methanol fixed at 30 hpi and stained for immunofluorescence to observe expression of the Inc-FLAG constructs (FLAG; red), SNX6 (green), IncA (pink), or DNA (DAPI; blue). Coverslips were imaged at 63x magnification using the same exposure (scale bar= 10 µm). Arrows indicate *C. trachomatis* L2 CT813-FLAG inclusions that do not have SNX6 co-localized with the inclusion membrane (IncA marker).

FLAG resulted in decreased SNX6 localization at the inclusion (122, 161) (Fig. 5-6). In contrast, SNX6 localization with the inclusion was not impacted by the overexpression of CT226-FLAG or CT483-FLAG from *C. trachomatis* L2 transformed strains (Fig. 5-6). Combined, these data indicate that the overexpression of certain Incs alters the inclusion membrane organization. This may also support the overexpression of different Inc-APEX2 fusion proteins resulting the identification of different proteins in the two APEX2 studies.

We next sought to determine if changes in Inc expression were occurring on the level of transcription or translation. To test this, we analyzed the expression of *incs* during the developmental cycle using our *C. trachomatis* L2 transformed strains and wild-type *C. trachomatis* L2 as a control. HeLa cells were infected with *C. trachomatis* L2 CT813-FLAG, CT226-FLAG, CT483-FLAG transformed strains, or wild-type *C. trachomatis* L2, and either not induced or induced at 7 hpi using 5 nM or 20 nM aTc. At 7, 16, 24, and 36 hpi RNA and DNA were collected. Normalized RNA was reverse transcribed to cDNA, and *inc* expression was measured by quantitative PCR and normalized to genomic DNA (ng cDNA/gDNA). The *C. trachomatis* L2 CT813-FLAG strain induced with 20 nM aTc had reduced detectable genomic DNA (Fig. 5-7A) and plasmid DNA (Fig. 5-7B), which corresponds with the observed decrease in infectious progeny production and increased plasmid loss (Fig. 5-4).

When we performed transcript analyses, the overexpression of CT813-FLAG (20 nM aTc) resulted in reduced transcription of each chlamydial gene that was tested (orange line, 20 nM aTc; Fig. 5-8 to Fig. 5-10), except for the late gene *omcB* (Fig. 5-8B). First assessed early gene expression using *euo,* which is considered a prototypical early gene (102, 106). The overexpression of CT813-FLAG using 20 nM aTc resulted in decreased transcription of *euo*, compared to CT226-FLAG, or CT483-FLAG *C. trachomatis* L2 transformed strains induced for expression, (Fig. 5-8A). Interestingly, increased transcription of a late gene, *omcB* was observed*,* (Fig. 5-8B; lower *omcB* panel), and

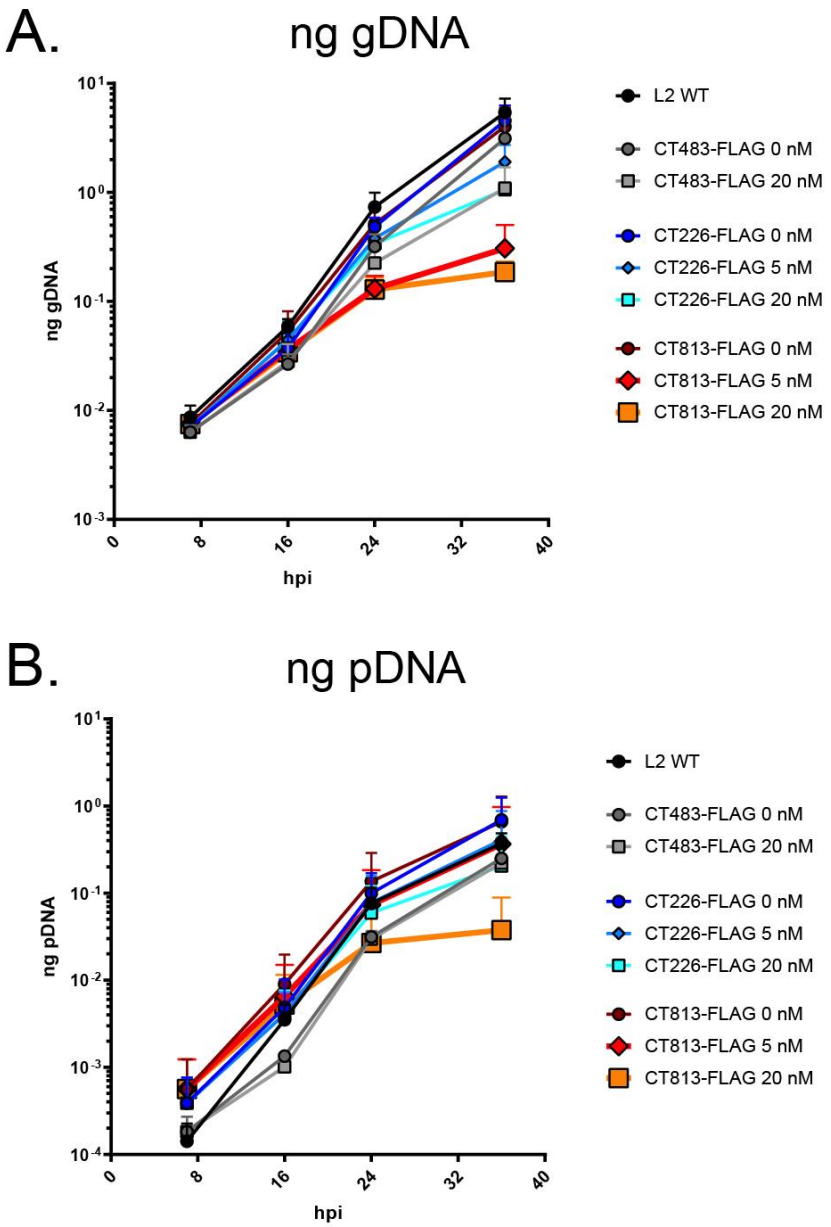

Figure 5-7. *C. trachomatis* L2 genomic DNA and plasmid DNA is reduced when CT813-FLAG is overexpression, but not CT226-FLAG, CT483-FLAG from *C. trachomatis* L2 transformed strains.

HeLa cells were infected with *C. trachomatis* L2 CT813-FLAG, CT226-FLAG, CT483-FLAG transformed strains, or wild-type *C. trachomatis* L2, and either not induced or induced at 7 hpi (5 nM or 20 nM aTc). RNA and DNA were collected from separate wells of a 6-well plate at 7, 16, 24, and 36 hpi. Prior to the collection of nucleic acids, coverslips in each well were fixed and stained for immunofluorescence to confirm expression of the construct. Normalized RNA was reverse transcribed to cDNA, and *inc* expression was measured by quantitative PCR. cDNA (ng) was normalized to genomic DNA (ng) and plotted using GraphPad Prism 8.4.0. N=3. A) genomic DNA, B) plasmid DNA.

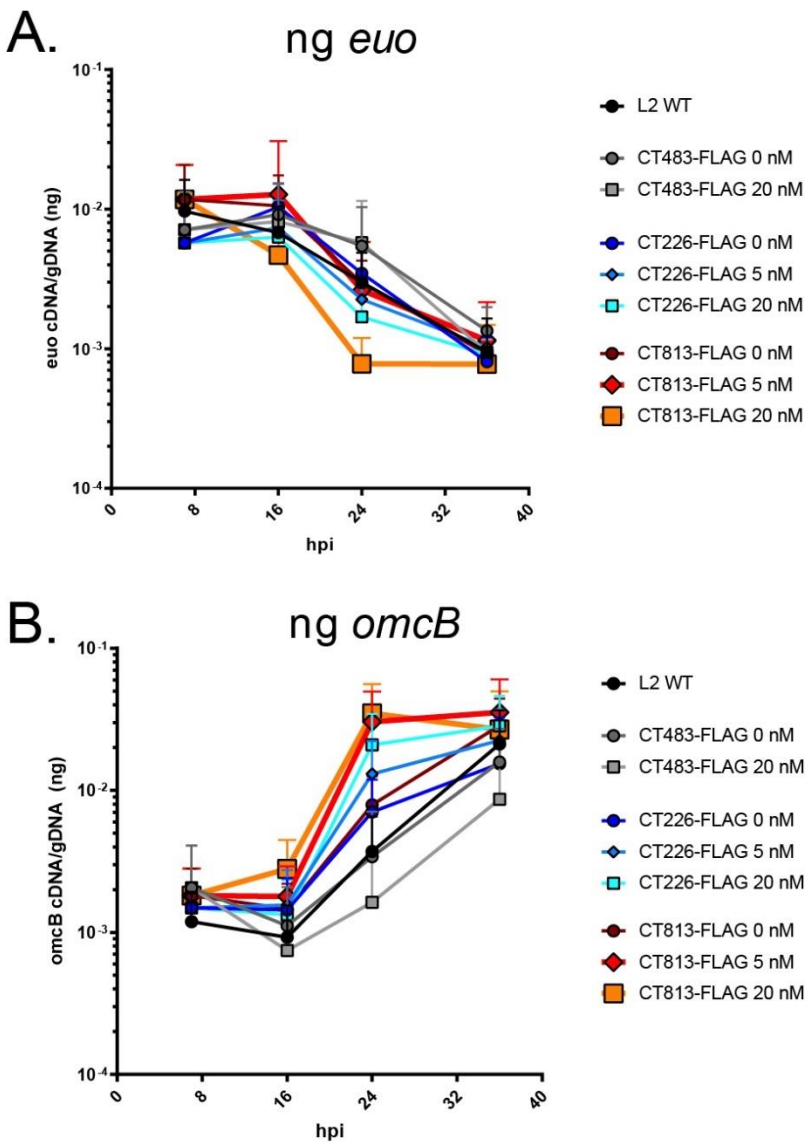

Figure 5-8. *C. trachomatis* L2 *euo* is reduced and *omcB* transcription is increased when CT813-FLAG is overexpressed from *C. trachomatis* L2 CT813-FLAG.

HeLa cells were infected with *C. trachomatis* L2 CT813-FLAG, CT226-FLAG, CT483-FLAG transformed strains, or wild-type *C. trachomatis* L2, and either not induced or induced at 7 hpi (5 nM or 20 nM aTc). RNA and DNA were collected from separate wells of a 6-well plate at 7, 16, 24, and 36 hpi. Prior to collection of nucleic acids, coverslips in each well were fixed and stained for immunofluorescence to confirm construct expression. Normalized RNA was reverse transcribed to cDNA, and *inc* expression was measured by quantitative PCR. cDNA (ng) was normalized to genomic DNA (ng) and plotted using GraphPad Prism 8.4.0. N=3. Transcript profile of the early gene (non-*inc*), early upstream open reading frame (*euo*), and late gene (non-*inc*), outer membrane protein complex B (*omcB*).

increased transcripts were observed when both CT813-FLAG and CT226-FLAG were overexpressed. The reason for this is unknown, but we are currently investigating this phenomenon.

We performed transcript analyses of both early *incs* (Fig. 5-9) and mid-cycle expressed *incs* (Fig. 5-10A). There was reduced transcription of early *incs, incE,* and *incG* when CT813-FLAG was overexpressed (orange line, 20 nM aTc), (Fig. 5-9). We also observed decreased transcription of mid-cycle *incs*, *ct223* and *incA* (Fig. 5-10A). Transcription was not significantly impacted when CT226-FLAG, or CT483-FLAG were overexpressed from *C. trachomatis* L2 transformed strains (Fig. 5-9 and Fig. 5-10A). To determine if this decrease was also observed for genes encoding non-T3SS proteins, we analyzed *clpP2* (Fig. 5-10B). Similar to the transcriptional profile of early and mid-cycle expressed *incs,* the overexpression of CT813-FLAG had decreased transcription of *clpP2* earlier in the developmental cycle (Fig. 5-10B). Reducing the induction conditions for CT813-FLAG moderately diminished the effect on transcription for each gene transcript analyzed (red line, 5 nM aTc). These data indicate that the overexpression of CT813-FLAG from *C. trachomatis* L2 negatively impacts development and that normal expression of early and mid-cycle genes is altered under these conditions.

Collectively, these data demonstrate that the overexpression of certain Incs (i.e., CT813 and IncF) alters the organization of Incs in the inclusion membrane. Furthermore, disrupted inclusion organization negatively impacts chlamydial development, as indicated by smaller inclusions and fewer infectious progeny. In support of our hypothesis that Incs may play different roles in the inclusion membrane, not all Incs negatively impact chlamydial development when overexpressed. We also demonstrated that altered Inc organization negatively impacts the recruitment of at least one eukaryotic protein, SNX6,

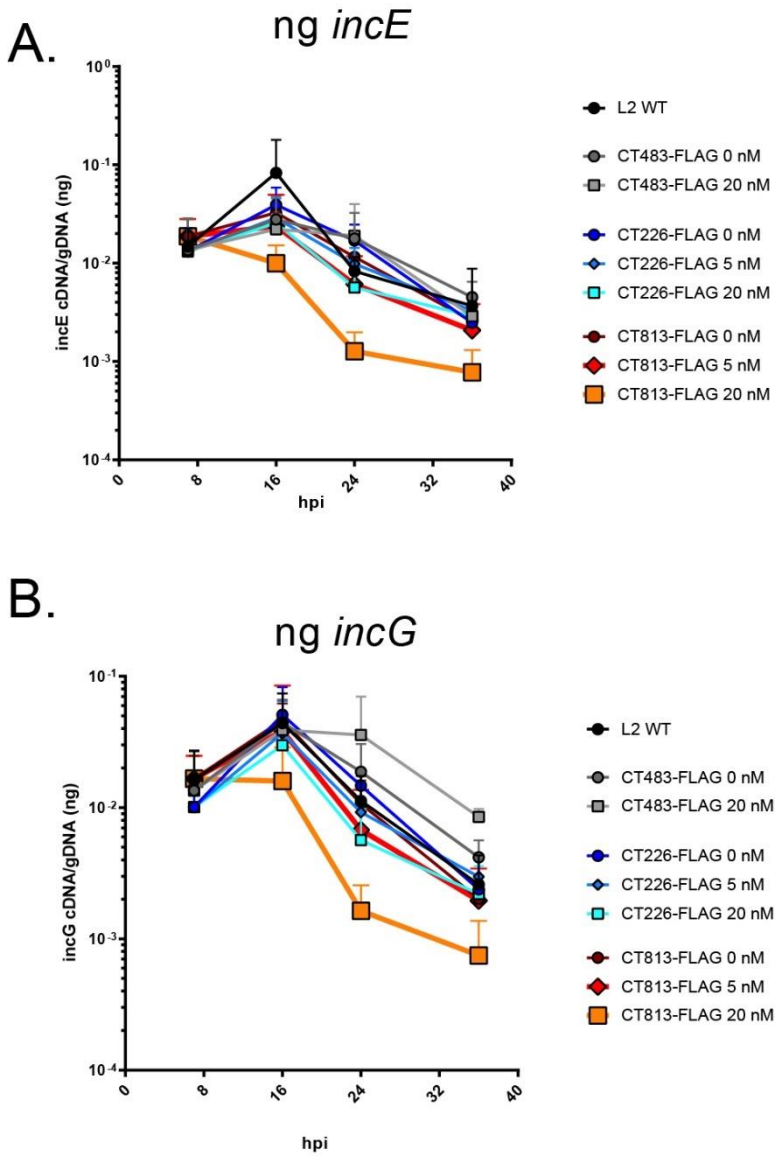

Figure 5-9. Transcription of early expressed *incs* is reduced when CT813-FLAG is overexpressed from *C. trachomatis* L2 CT813-FLAG.

HeLa cells were infected with *C. trachomatis* L2 CT813-FLAG, CT226-FLAG, CT483-FLAG transformed strains, or wild-type *C. trachomatis* L2, and either not induced or induced at 7 hpi (5 nM or 20 nM aTc). RNA and DNA were collected from separate wells of a 6-well plate at 7, 16, 24, and 36 hpi. Prior to collection of nucleic acids, coverslips in each well were fixed and stained for immunofluorescence to confirm construct expression. Normalized RNA was reverse transcribed to cDNA, and *inc* expression was measured by quantitative PCR. cDNA (ng) was normalized to genomic DNA (ng) and plotted using GraphPad Prism 8.4.0. N=3. Transcript profile of the early *incs,* A) *incE* and B) *incG.*

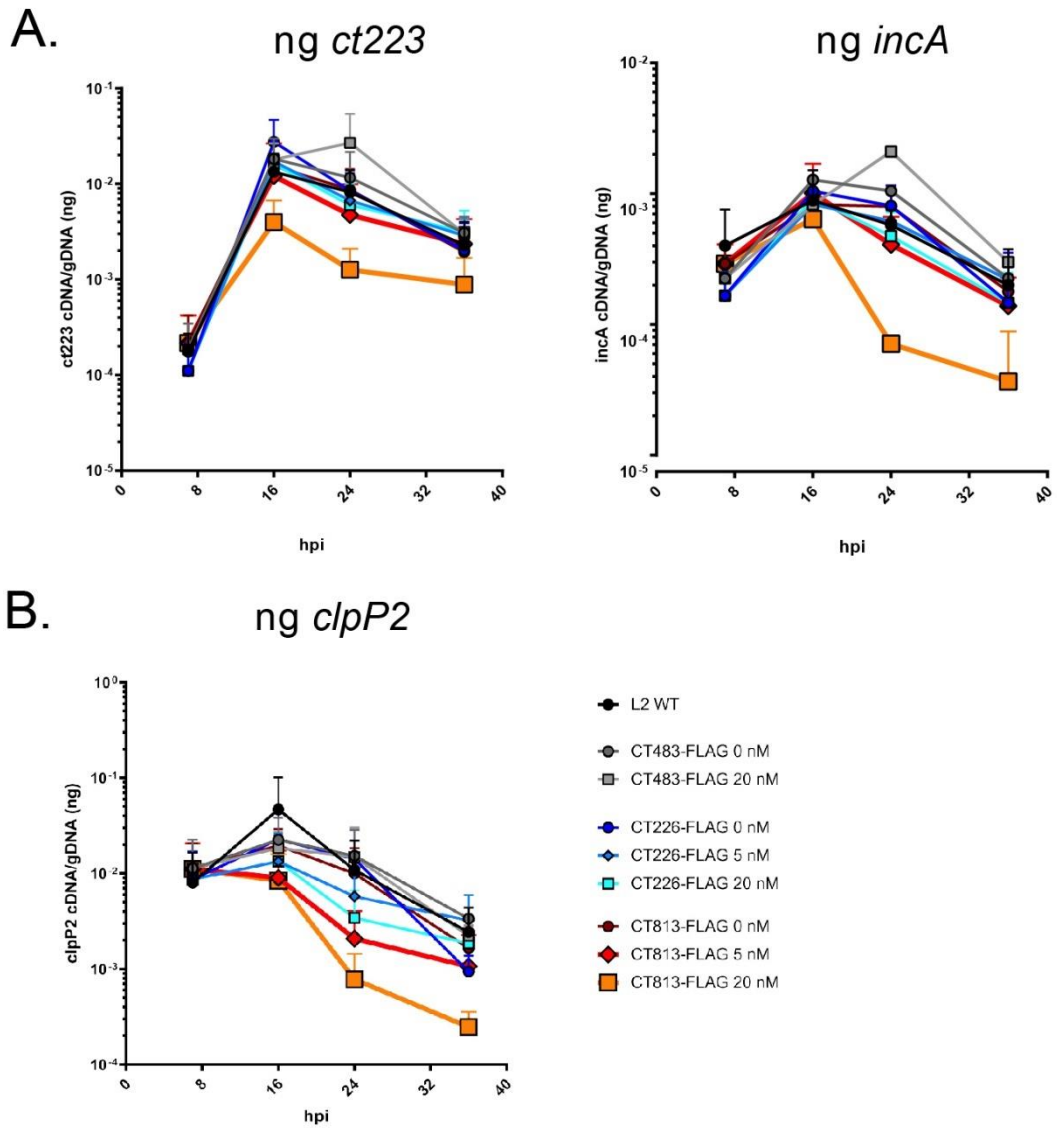

Figure 5-10. Transcription of mid-cycle genes is reduced when CT813-FLAG is overexpressed from *C. trachomatis* L2 CT813-FLAG.

HeLa cells were infected with *C. trachomatis* L2 CT813-FLAG, CT226-FLAG, CT483-FLAG transformed strains, or wild-type *C. trachomatis* L2, and either not induced or induced at 7 hpi (5 nM or 20 nM aTc). RNA and DNA were collected from separate wells of a 6-well plate at 7, 16, 24, and 36 hpi. Prior to collection of nucleic acids, coverslips in each well were fixed and stained for immunofluorescence to confirm construct expression. Normalized RNA was reverse transcribed to cDNA, and *inc* expression was measured by quantitative PCR. cDNA (ng) was normalized to genomic DNA (ng) and plotted using GraphPad Prism 8.4.0. Transcript profile of A) mid-cycle *incs,* ct223 (N=3) and *incA* (N=2) and B) *clpP2* (N=2).

to the inclusion during *C. trachomatis* L2 infection, which highlights the significance of carefully coordinated expression of Incs during infection to promote survival.

Survival strategies of other intracellular bacteria

These APEX2 datasets, in addition to previous reports, indicate that *C. trachomatis* is heavily involved in the modification of host biological pathways during infection of a eukaryotic cell to promote development. Bacteria undergo genome reduction while adapting to intracellular dependence, which is associated with the loss of complete metabolic pathways (267, 268). *Chlamydia,* among other obligate intracellular bacteria, including *Rickettsia, Coxiella*, and the facultative intracellular bacterium *Legionella,* modify the host cell to gain entry, to avoid degradation or pre-mature host cell death, and to obtain the nutrients required for intracellular survival.

Bacterial genome size and disease

Chlamydia has the smallest genome (1.0 Mbp) compared to *Rickettsia, Coxiella, and Legionella. Rickettsia* is an obligate intracellular bacterium that is spread to humans by either the tick (*Dermacentor sp.),* causing Rocky Mountain spotted fever (*R. rickettsii*), or the louse vector (*Pediculus* sp.) causing epidemic typhus (*R. prowazekii*) (267, 269). *Rickettsia prowazekii* has a 1.1 Mbp genome encoding 830 ORFs, the smallest genome of the *Rickettsia* species (267). *Rickettsia* primarily infects endothelial cells. Another obligate intracellular bacterium, *Coxiella*, primarily infects macrophages (270). *Coxiella burnetii*, the causative agent of Q fever, has a 1.995 Mbp genome and encodes approximately 2,134 ORFs and a 37,393-bp plasmid (i.e., QpH1) (271). *C. burnetii* has two morphological forms, the environmentally stable small cell variant (SCV), and the large cell variant (LCV), which is the replicative form. *C. burnetii* has more complete biosynthetic pathways than *Chlamydia,* including enzymes for glycolysis, the electron transport chain,

the pentose phosphate pathway, and the tricarboxylic acid (TCA) cycle (271, 272). As a result, *Chlamydia* relies more on obtaining energy (e.g., ATP) and other nutrients from the host cell than *Coxiella* species (124, 272, 273). Finally, the facultative intracellular bacterium closely related to *Coxiella*, *Legionella pneumophila* (3.36 Mbp genome), is found in freshwater replicating within amoeba (274). *Legionella* has a complete glycolysis pathway, TCA cycle, and pentose phosphate pathway. When contaminated aerosols are inhaled (e.g., from large air conditioning units), *Legionella* infects human alveolar macrophages, causing atypical pneumonia called Legionnaires' disease.

Host cell entry and the intracellular niche

Rickettsia, unlike *Chlamydia,* breaks out from the vacuole into which it is initially internalized. This is elicited by a bacterial phospholipase A2, and *Rickettsia* subsequently replicate in the host cytosol (275). Cytosolic growth is hypothesized to provide *Rickettsia* with greater access to nutrients of the host cell (268). In support, *Rickettsia* is predicted to import over 20 metabolites from the host cell using multiple encoded translocases (268). Unlike *Rickettsia*, *Chlamydia, Coxiella*, and *Legionella* develop within a vacuole after infection of a host cell. Similar to *C. trachomatis* infection of a host cell, *Coxiella* infection requires the re-arrangement of F-actin and Rho GTPases such as RhoA. In addition, Src-family kinases and cortactin also aid in the internalization of *C. burnetii*. *Coxiella* develops within a vacuole, termed the *Coxiella* containing vacuole (CCV) (270). In contrast to the neutral pH of the *C. trachomatis* inclusion, the CCV becomes acidified (pH ~4.5) and is marked by lysosomal markers like cathepsins and LAMP1 (31). *Coxiella* can remain in this acidified vacuole for up to 153 days in cell culture (276). The CCV also fuses with autophagic vesicles, which contribute to the available nutrient pool (277, 278). *Legionella* develops within the *Legionella* containing vacuole (LCV); like *Chlamydia,* the LCV does not fuse with the lysosome. The ER-derived LCV is the intracellular niche harboring the

replicative and infectious developmental forms (279). Intracellular bacteria acquire nutrients from the host cell via transporters, from interactions with proximal organelles (i.e., *Chlamydia*), or by directly fusing with organelles (i.e., *Coxiella*) such as MVBs, lysosomes, and autophagic vesicles (124, 268, 271).

Secreted effectors and interactions with host proteins

Interactions with the host cell vary based on the specific intracellular niche. For example, bacteria that reside within a vacuole during intracellular growth and development need to transport nutrients across the vacuolar membrane to obtain them (i.e., *Chlamydia, Coxiella, Legionella*), which requires additional effector proteins compared to directly acquiring proteins from the cytosol (i.e., *Rickettsia*). Furthermore, intracellular bacteria need to have effectors that adequately defend from different types of eukaryotic cells. For example, macrophages have an increased capacity to destroy invading bacteria compared to non-antigen presenting cells such as epithelial cells. Therefore, bacteria that infect macrophages, such as *Coxiella* and *Legionella* (and *C. trachomatis* L2), must be able to survive this harsh intracellular environment.

Chlamydia utilizes a T3SS to translocate effectors into the inclusion membrane and host cytosol (58, 81, 89), whereby *Rickettsia*, *Coxiella,* and *Legionella* utilize a Type IV secretion system (T4SS; Dot/Icm dependent) secretion system to secrete effectors and promote survival within the host. The *Rickettsia* effector proteins, RickA and Sca2 (functionally mimicking the eukaryotic protein, formin) nucleate actin polymerization (280-282). Actin is utilized by several *Rickettsia* species for motility within the host cytosol and to disseminate into neighboring eukaryotic cells. Some *Rickettsia* species (e.g., *R. parkeri*) that do not have actin motility have been shown to secrete an effector, Sca4, that reduces vinculin associated tension at the plasma membrane to allow dissemination (283).

Coxiella also has a T4SS that is necessary for intracellular replication, CCV expansion, and for secreting effector proteins (279, 284), with over 133 predicted T4SS effectors identified to date (285). Similar to *Chlamydia*, *Coxiella* effectors have been shown to interact with the ER, Golgi, and intracellular trafficking components (e.g., via interactions with SNARE proteins), which is important for intracellular development (279). Many *Coxiella* effectors have coiled-coil regions and eukaryotic-like motifs that are involved in binding eukaryotic proteins. Both *Chlamydia* and *Coxiella* appear to use the clathrin-coated vesicle pathway for optimal development. The *Coxiella* effector, CpvA, interacts with AP2 on clathrin-coated vesicles, while Rab proteins are heavily involved in mediating these interactions during the chlamydial developmental cycle (157). *Coxiella* effectors modify protein kinase A (PKA), which phosphorylates BAD, inhibiting apoptosis. Similarly, *C. trachomatis* IncG binds 14-3-3β, which interacts with BAD and sequestering it from the mitochondria to prevent apoptosis (142, 143).

Legionella encodes over 200 T4SS effectors, with a large number of redundant functions (286). Of significant interest, reticulon-4 (RTN4) is ubiquitinated by a *Legionella* effector, which results in the localization of RTN4 to the LCV early after infection (287). RTN4 is an ER-associated protein that, when localized to the LCV, modified ER tubule dynamics (287). RTN4 was a SAINT significant protein identified using the *C. trachomatis* L2 Inc-APEX2 transformed strains and was identified in all four AP-MS studies (115, 122, 170, 171, 288).

Summary

Although the intracellular niche for each of the bacteria described above differs, there are core requirements for intracellular survival. The differences in growth requirements are related to genome size and adaptation/evolution in different cell types (271). Fundamental requirements for intracellular bacteria include infection of a host cell

(e.g., actin modification), avoiding detection by host (e.g., develop in a vacuole disguised as a host organelle), and acquiring nutrients from the host cell during infection (e.g., molecular mimicry by bacterial proteins to bind eukaryotic proteins (137, 282)). Actin is manipulated to achieve a wide array of functions, from invasion, motility (i.e., *Rickettsia*), and ultimately exit from the host cell. These data are consistent with the large number of cytoskeleton-associated proteins identified in our Inc-APEX2 dataset. In addition, intracellular bacteria target the same eukaryotic biological pathways using uniquely evolved effector proteins that block different parts of a biological pathway. Identifying the various ways that bacteria manipulate or block normal eukaryotic biological pathways will contribute to a greater understanding of the underlying molecular mechanisms of eukaryotic cell biology.

Concluding remarks

This work, using the APEX2 proximity labeling system to identify proximal proteins *in vivo,* has added to the characterization of the *C. trachomatis* L2 inclusion interactome and described previously unreported Inc-eukaryotic protein-protein interactions. These data are consistent with eukaryotic proteins previously reported to be associated with the inclusion, and many of these proteins belong to pathways that are also important for the survival of other intracellular bacteria. These studies generated new experimental questions regarding how the overexpression of some Incs may alter the inclusion membrane organization. We showed that the altered organization of Incs in the inclusion membrane had consequences on the ability of *C. trachomatis* to bind host proteins during infection. These data highlight the importance of the balanced expression of Incs to support normal host cell interactions and overall chlamydial fitness. The information obtained from these studies paves the way for the identification of new proteins interacting with chlamydial effectors during *C. trachomatis* infection. Future studies of Inc-Inc

interactions will provide much needed insight into the organization of Incs in the inclusion membrane. This will help better contextualize our data regarding altered inclusion organization and recruitment of eukaryotic proteins.

REFERENCES

1. Brunham RC, Rey-Ladino J. 2005. Immunology of Chlamydia infection: implications for a Chlamydia trachomatis vaccine. Nat Rev Immunol 5:149-61.

2. de la Maza LM, Zhong G, Brunham RC. 2017. Update on Chlamydia trachomatis Vaccinology. Clinical and Vaccine Immunology 24:e00543-16.

3. CDC. 2017. Sexually Transmitted Disease Surveillance 2017.

4. Darville T, Rours GIJG. 2018. Chlamydia trachomatis, p 908-914.e2. *In* Long SS, Prober CG, Fischer M (ed), Principles and Practice of Pediatric Infectious Diseases (Fifth Edition) doi:https://doi.org/10.1016/B978-0-323-40181-4.00167-5. Elsevier.

5. Mackern-Oberti JP, Motrich RD, Breser ML, Sanchez LR, Cuffini C, Rivero VE. 2013. Chlamydia trachomatis infection of the male genital tract: an update. J Reprod Immunol 100:37-53.

6. Darville T, Hiltke TJ. 2010. Pathogenesis of genital tract disease due to Chlamydia trachomatis. J Infect Dis 201 Suppl 2:S114-25.

7. Lan J, Melgers I, Meijer CJ, Walboomers JM, Roosendaal R, Burger C, Bleker OP, van den Brule AJ. 1995. Prevalence and serovar distribution of asymptomatic cervical Chlamydia trachomatis infections as determined by highly sensitive PCR. Journal of clinical microbiology 33:3194-3197.

8. Sachse K, Bavoil PM, Kaltenboeck B, Stephens RS, Kuo C-C, Rosselló-Móra R, Horn M. 2015. Emendation of the family Chlamydiaceae: Proposal of a single

genus, Chlamydia, to include all currently recognized species. Systematic and Applied Microbiology 38:99-103.

9. Nunes A, Gomes JP. 2014. Evolution, phylogeny, and molecular epidemiology of Chlamydia. Infection, Genetics and Evolution 23:49-64.

10. Bachmann NL, Polkinghorne A, Timms P. 2014. Chlamydia genomics: providing novel insights into chlamydial biology. Trends in Microbiology 22:464-472.

11. Speight KN, Polkinghorne A, Penn R, Boardman W, Timms P, Fraser T, Johnson K, Faull R, Bate S, Woolford L. 2016. PREVALENCE AND PATHOLOGIC FEATURES OF CHLAMYDIA PECORUM INFECTIONS IN SOUTH AUSTRALIAN KOALAS. Journal of Wildlife Diseases 52:301-306, 6.

12. Knittler MR, Sachse K. 2014. Chlamydia psittaci: update on an underestimated zoonotic agent. Pathogens and Disease 73:1-15.

13. Hatch TP, Miceli M, Silverman JA. 1985. Synthesis of protein in host-free reticulate bodies of Chlamydia psittaci and Chlamydia trachomatis. Journal of Bacteriology 162:938-942.

14. Shah SS. 2018. Chlamydophila (Chlamydia) pneumoniae, p 906-908.e2. *In* Long SS, Prober CG, Fischer M (ed), Principles and Practice of Pediatric Infectious Diseases doi:https://doi.org/10.1016/B978-0-323-40181-4.00166-3. Elsevier.

15. Miyashita N, Niki Y, Nakajima M, Fukano H, Matsushima T. 2001. Prevalence of Asymptomatic Infection With Chlamydia pneumoniae in Subjectively Healthy Adults. Chest 119:1416-1419.

16. Al-Younes HM. 2014. High prevalence of Chlamydia pneumoniae infection in an asymptomatic Jordanian population. J Microbiol Immunol Infect 47:412-7.

17. Cui J, Yan W, Xie H, Xu S, Wang Q, Zhang W, Ni A. 2018. A retrospective seroepidemiologic survey of Chlamydia pneumoniae infection in patients in Beijing between 2008 and 2017. PloS one 13:e0206995-e0206995.

18. Burton MJ. 2007. Trachoma: an overview. British Medical Bulletin 84:99-116.

19. Harris SR, Clarke IN, Seth-Smith HMB, Solomon AW, Cutcliffe LT, Marsh P, Skilton RJ, Holland MJ, Mabey D, Peeling RW, Lewis DA, Spratt BG, Unemo M, Persson K, Bjartling C, Brunham R, de Vries HJC, Morré SA, Speksnijder A, Bébéar CM, Clerc M, de Barbeyrac B, Parkhill J, Thomson NR. 2012. Whole-genome analysis of diverse Chlamydia trachomatis strains identifies phylogenetic relationships masked by current clinical typing. Nature genetics 44:413-S1.

20. Morré SA, Rozendaal L, van Valkengoed IG, Boeke AJ, van Voorst Vader PC, Schirm J, de Blok S, van Den Hoek JA, van Doornum GJ, Meijer CJ, van Den Brule AJ. 2000. Urogenital Chlamydia trachomatis serovars in men and women with a symptomatic or asymptomatic infection: an association with clinical manifestations? Journal of clinical microbiology 38:2292-2296.

21. Stephens RS, Kalman S, Lammel C, Fan J, Marathe R, Aravind L, Mitchell W, Olinger L, Tatusov RL, Zhao Q, Koonin EV, Davis RW. 1998. Genome sequence of an obligate intracellular pathogen of humans: Chlamydia trachomatis. Science 282:754-9.

22. Abdelrahman YM, Belland RJ. 2005. The chlamydial developmental cycle. FEMS Microbiol Rev 29:949-59.

23. Hatch TP, Allan I, Pearce JH. 1984. Structural and polypeptide differences between envelopes of infective and reproductive life cycle forms of Chlamydia spp. J Bacteriol 157:13-20.

24. Carabeo RA, Hackstadt T. 2001. Isolation and Characterization of a Mutant Chinese Hamster Ovary Cell Line That Is Resistant to Chlamydia trachomatis Infection at a Novel Step in the Attachment Process. Infection and Immunity 69:5899.

25. Abromaitis S, Stephens RS. 2009. Attachment and Entry of Chlamydia Have Distinct Requirements for Host Protein Disulfide Isomerase. PLOS Pathogens 5:e1000357.

26. Eissenberg LG, Wyrick PB, Davis CH, Rumpp JW. 1983. Chlamydia psittaci elementary body envelopes: ingestion and inhibition of phagolysosome fusion. Infection and immunity 40:741-751.

27. Brinkworth AJ, Malcolm DS, Pedrosa AT, Roguska K, Shahbazian S, Graham JE, Hayward RD, Carabeo RA. 2011. Chlamydia trachomatis Slc1 is a type III secretion chaperone that enhances the translocation of its invasion effector substrate TARP. Mol Microbiol 82:131-44.

28. Clifton DR, Fields KA, Grieshaber SS, Dooley CA, Fischer ER, Mead DJ, Carabeo RA, Hackstadt T. 2004. A chlamydial type III translocated protein is tyrosine-phosphorylated at the site of entry and associated with recruitment of actin. Proc Natl Acad Sci U S A 101:10166-71.

29. Carabeo RA, Grieshaber SS, Fischer E, Hackstadt T. 2002. Chlamydia trachomatis induces remodeling of the actin cytoskeleton during attachment and entry into HeLa cells. Infect Immun 70:3793-803.

30. Hackstadt T, Scidmore MA, Rockey DD. 1995. Lipid metabolism in Chlamydia trachomatis-infected cells: directed trafficking of Golgi-derived sphingolipids to the chlamydial inclusion. Proceedings of the National Academy of Sciences of the United States of America 92:4877-4881.

31. Heinzen RA, Scidmore MA, Rockey DD, Hackstadt T. 1996. Differential interaction with endocytic and exocytic pathways distinguish parasitophorous vacuoles of Coxiella burnetii and Chlamydia trachomatis. Infect Immun 64:796-809.

32. Taraska T, Ward DM, Ajioka RS, Wyrick PB, Davis-Kaplan SR, Davis CH, Kaplan J. 1996. The late chlamydial inclusion membrane is not derived from the endocytic pathway and is relatively deficient in host proteins. Infection and Immunity 64:3713-3727.

33. Moulder JW. 1991. Interaction of chlamydiae and host cells in vitro. Microbiological Reviews 55:143-190.

34. Scidmore MA, Fischer ER, Hackstadt T. 2003. Restricted fusion of Chlamydia trachomatis vesicles with endocytic compartments during the initial stages of infection. Infect Immun 71:973-84.

35. Grieshaber SS, Grieshaber NA, Hackstadt T. 2003. Chlamydia trachomatis uses host cell dynein to traffic to the microtubule-organizing center in a p50 dynamitin-independent process. Journal of Cell Science 116:3793-3802.

36. Abdelrahman Y, Ouellette SP, Belland RJ, Cox JV. 2016. Polarized Cell Division of Chlamydia trachomatis. PLOS Pathogens 12:e1005822.

37. Lee J, Cox JV, Ouellette SP. 2020. Critical Role for the Extended N-Terminus of Chlamydial MreB in Directing Its Membrane Association and Potential Interaction with Divisome Proteins. Journal of Bacteriology doi:10.1128/jb.00034-20:JB.00034-20.

38. Lutter EI, Barger AC, Nair V, Hackstadt T. 2013. Chlamydia trachomatis inclusion membrane protein CT228 recruits elements of the myosin phosphatase pathway to regulate release mechanisms. Cell Rep 3:1921-31.

39. Hybiske K, Stephens RS. 2007. Mechanisms of host cell exit by the intracellular bacterium Chlamydia. Proceedings of the National Academy of Sciences of the United States of America 104:11430-11435.

40. Matsumoto A. 1981. Isolation and electron microscopic observations of intracytoplasmic inclusions containing Chlamydia psittaci. Journal of bacteriology 145:605-612.

41. Heinzen RA, Hackstadt T. 1997. The Chlamydia trachomatis parasitophorous vacuolar membrane is not passively permeable to low-molecular-weight compounds. Infection and immunity 65:1088-1094.

42. Grieshaber S, Swanson JA, Hackstadt T. 2002. Determination of the physical environment within the Chlamydia trachomatis inclusion using ion-selective ratiometric probes. Cellular Microbiology 4:273-283.

43. Rockey DD, Heinzen RA, Hackstadt T. 1995. Cloning and characterization of a Chlamydia psittaci gene coding for a protein localized in the inclusion membrane of infected cells. Molecular Microbiology 15:617-626.

44. Scidmore-Carlson MA, Shaw EI, Dooley CA, Fischer ER, Hackstadt T. 1999. Identification and characterization of a Chlamydia trachomatis early operon encoding four novel inclusion membrane proteins. Mol Microbiol 33:753-65.

45. Weber MM, Lam JL, Dooley CA, Noriea NF, Hansen BT, Hoyt FH, Carmody AB, Sturdevant GL, Hackstadt T. 2017. Absence of Specific Chlamydia trachomatis Inclusion Membrane Proteins Triggers Premature Inclusion Membrane Lysis and Host Cell Death. Cell Rep 19:1406-1417.

46. Hackstadt T, Rockey DD, Heinzen RA, Scidmore MA. 1996. Chlamydia trachomatis interrupts an exocytic pathway to acquire endogenously synthesized sphingomyelin in transit from the Golgi apparatus to the plasma membrane. The EMBO Journal 15:964-977.

47. Moore ER. 2012. Sphingolipid trafficking and purification in Chlamydia trachomatis-infected cells. Current protocols in microbiology CHAPTER:Unit11A.2-Unit11A.2.

48. Moore ER, Fischer ER, Mead DJ, Hackstadt T. 2008. The Chlamydial Inclusion Preferentially Intercepts Basolaterally Directed Sphingomyelin-Containing Exocytic Vacuoles. Traffic (Copenhagen, Denmark) 9:2130-2140.

49. Lippincott-Schwartz J, Yuan LC, Bonifacino JS, Klausner RD. 1989. Rapid redistribution of Golgi proteins into the ER in cells treated with brefeldin A: Evidence for membrane cycling from Golgi to ER. Cell 56:801-813.

50. Carabeo RA, Mead DJ, Hackstadt T. 2003. Golgi-dependent transport of cholesterol to the Chlamydia trachomatis inclusion. Proceedings of the National Academy of Sciences of the United States of America 100:6771-6776.

51. Hatch GM, McClarty G. 1998. Phospholipid Composition of Purified Chlamydia trachomatis Mimics That of the Eucaryotic Host Cell. Infection and Immunity 66:3727.

52. Wylie JL, Hatch GM, McClarty G. 1997. Host cell phospholipids are trafficked to and then modified by Chlamydia trachomatis. Journal of Bacteriology 179:7233.

53. Agaisse H, Derre I. 2014. Expression of the effector protein IncD in Chlamydia trachomatis mediates recruitment of the lipid transfer protein CERT and the endoplasmic reticulum-resident protein VAPB to the inclusion membrane. Infect Immun 82:2037-47.

54. Derre I, Swiss R, Agaisse H. 2011. The lipid transfer protein CERT interacts with the Chlamydia inclusion protein IncD and participates to ER-Chlamydia inclusion membrane contact sites. PLoS Pathog 7:e1002092.

55. Beatty WL. 2008. Late endocytic multivesicular bodies intersect the chlamydial inclusion in the absence of CD63. Infect Immun 76:2872-81.

56. Beatty WL. 2006. Trafficking from CD63-positive late endocytic multivesicular bodies is essential for intracellular development of Chlamydia trachomatis. Journal of Cell Science 119:350-359.

57. Rucks EA, Olson MG, Jorgenson LM, Srinivasan RR, Ouellette SP. 2017. Development of a Proximity Labeling System to Map the Chlamydia trachomatis Inclusion Membrane. Frontiers in Cellular and Infection Microbiology 7:40.

58. Fields KA, Mead DJ, Dooley CA, Hackstadt T. 2003. Chlamydia trachomatis type III secretion: evidence for a functional apparatus during early-cycle development. Mol Microbiol 48:671-83.

59. Moore ER, Ouellette SP. 2014. Reconceptualizing the chlamydial inclusion as a pathogen-specified parasitic organelle: an expanded role for Inc proteins. Front Cell Infect Microbiol 4:157.

60. Chen D, Lei L, Lu C, Flores R, DeLisa MP, Roberts TC, Romesberg FE, Zhong G. 2010. Secretion of the chlamydial virulence factor CPAF requires the Sec-dependent pathway. Microbiology (Reading, England) 156:3031-3040.

61. Chen Y-S, Bastidas RJ, Saka HA, Carpenter VK, Richards KL, Plano GV, Valdivia RH. 2014. The Chlamydia trachomatis Type III Secretion Chaperone Slc1 Engages Multiple Early Effectors, Including TepP, a Tyrosine-phosphorylated Protein Required for the Recruitment of CrkI-II to Nascent Inclusions and Innate Immune Signaling. PLoS Pathogens 10:e1003954.

62. Dai W, Li Z. 2014. Conserved type III secretion system exerts important roles in Chlamydia trachomatis. International Journal of Clinical and Experimental Pathology 7:5404-5414.

63. Ferrell JC, Fields KA. 2016. A working model for the type III secretion mechanism in Chlamydia. Microbes and infection / Institut Pasteur 18:84-92.

64. Hefty PS, Stephens RS. 2007. Chlamydial Type III Secretion System Is Encoded on Ten Operons Preceded by Sigma 70-Like Promoter Elements. Journal of Bacteriology 189:198.

65. Löwer M, Schneider G. 2009. Prediction of Type III Secretion Signals in Genomes of Gram-Negative Bacteria. PLoS ONE 4:e5917.

66. Wehrl W, Brinkmann V, Jungblut PR, Meyer TF, Szczepek AJ. 2004. From the inside out – processing of the Chlamydial autotransporter PmpD and its role in bacterial adhesion and activation of human host cells. Molecular Microbiology 51:319-334.

67. Bavoil PM, Byrne GI. 2014. Analysis of CPAF mutants: new functions, new questions (the ins and outs of a chlamydial protease). Pathog Dis 71:287-91.

68. Chen AL, Johnson KA, Lee JK, Sutterlin C, Tan M. 2012. CPAF: a Chlamydial protease in search of an authentic substrate. PLoS Pathog 8:e1002842.

69. Jorgensen I, Bednar MM, Amin V, Davis BK, Ting JPY, McCafferty DG, Valdivia RH. 2011. The Chlamydia protease CPAF regulates host and bacterial proteins to maintain pathogen vacuole integrity and promote virulence. Cell host & microbe 10:21-32.

70. Pirbhai M, Dong F, Zhong Y, Pan KZ, Zhong G. 2006. The secreted protease factor CPAF is responsible for degrading pro-apoptotic BH3-only proteins in Chlamydia trachomatis-infected cells. J Biol Chem 281:31495-501.

71. Kumar Y, Valdivia RH. 2008. Actin and intermediate filaments stabilize the Chlamydia trachomatis vacuole by forming dynamic structural scaffolds. Cell host & microbe 4:159-169.

72. Johnson KA, Lee JK, Chen AL, Tan M, Sütterlin C. 2015. Induction and inhibition of CPAF activity during analysis of Chlamydia-infected cells. Pathogens and Disease 73:1-8.

73. Patton MJ, McCorrister S, Grant C, Westmacott G, Fariss R, Hu P, Zhao K, Blake M, Whitmire B, Yang C, Caldwell HD, McClarty G. 2016. Chlamydial Protease-Like Activity Factor and Type III Secreted Effectors Cooperate in Inhibition of p65 Nuclear Translocation. mBio 7:e01427-16.

74. Lei L, Qi M, Budrys N, Schenken R, Zhong G. 2011. Localization of Chlamydia trachomatis hypothetical protein CT311 in host cell cytoplasm. Microbial Pathogenesis 51:101-109.

75. Zhong G. 2011. Chlamydia Trachomatis Secretion of Proteases for Manipulating Host Signaling Pathways. Frontiers in Microbiology 2.

76. Betts HJ, Wolf K, Fields KA. 2009. Effector protein modulation of host cells: examples in the Chlamydia spp. arsenal. Curr Opin Microbiol 12:81-7.

77. Engel J. 2004. Tarp and Arp: How Chlamydia induces its own entry. Proceedings of the National Academy of Sciences of the United States of America 101:9947-9948.

78. Thwaites TR, Pedrosa AT, Peacock TP, Carabeo RA. 2015. Vinculin Interacts with the Chlamydia Effector TarP Via a Tripartite Vinculin Binding Domain to

Mediate Actin Recruitment and Assembly at the Plasma Membrane. Frontiers in cellular and infection microbiology 5:88-88.

79. Matsumoto A. 1982. Surface projections of Chlamydia psittaci elementary bodies as revealed by freeze-deep-etching. Journal of bacteriology 151:1040-1042.

80. Matsumoto A, Fujiwara E, Higashi N. 1976. Observations of the surface projections of infectious small cell of Chlamydia psittaci in thin sections. J Electron Microsc (Tokyo) 25:169-70.

81. Hsia RC, Pannekoek Y, Ingerowski E, Bavoil PM. 1997. Type III secretion genes identify a putative virulence locus of Chlamydia. Mol Microbiol 25:351-9.

82. Kalman S, Mitchell W, Marathe R, Lammel C, Fan J, Hyman RW, Olinger L, Grimwood J, Davis RW, Stephens RS. 1999. Comparative genomes of Chlamydia pneumoniae and C. trachomatis. Nat Genet 21:385-9.

83. Peters J, Wilson DP, Myers G, Timms P, Bavoil PM. 2007. Type III secretion a la Chlamydia. Trends Microbiol 15:241-51.

84. Bavoil PM, Hsia R, Ojcius DM. 2000. Closing in on Chlamydia and its intracellular bag of tricks. Microbiology 146 (Pt 11):2723-31.

85. Nans A, Kudryashev M, Saibil HR, Hayward RD. 2015. Structure of a bacterial type III secretion system in contact with a host membrane in situ. Nature Communications 6:10114.

86. Rockey DD, Scidmore MA, Bannantine JP, Brown WJ. 2002. Proteins in the chlamydial inclusion membrane. Microbes and Infection 4:333-340.

87. Bannantine JP, Griffiths RS, Viratyosin W, Brown WJ, Rockey DD. 2000. A secondary structure motif predictive of protein localization to the chlamydial inclusion membrane. Cell Microbiol 2:35-47.

88. Bannantine JP, Stamm WE, Suchland RJ, Rockey DD. 1998. Chlamydia trachomatis IncA Is Localized to the Inclusion Membrane and Is Recognized by Antisera from Infected Humans and Primates. Infection and Immunity 66:6017-6021.

89. Subtil A, Blocker A, Dautry-Varsat A. 2000. Type III secretion system in Chlamydia species: identified members and candidates. Microbes and Infection 2:367-369.

90. Subtil A, Parsot C, Dautry-Varsat A. 2001. Secretion of predicted Inc proteins of Chlamydia pneumoniae by a heterologous type III machinery. Molecular Microbiology 39:792-800.

91. Bauler LD, Hackstadt T. 2014. Expression and Targeting of Secreted Proteins from Chlamydia trachomatis. Journal of Bacteriology 196:1325-1334.

92. Hackstadt T, Scidmore-Carlson MA, Shaw EI, Fischer ER. 1999. The Chlamydia trachomatis IncA protein is required for homotypic vesicle fusion. Cell Microbiol 1:119-30.

93. Weber MM, Bauler LD, Lam J, Hackstadt T. 2015. Expression and localization of predicted inclusion membrane proteins in Chlamydia trachomatis. Infect Immun 83:4710-8.

94. Fischer A, Harrison KS, Ramirez Y, Auer D, Chowdhury SR, Prusty BK, Sauer F, Dimond Z, Kisker C, Hefty PS, Rudel T. 2017. Chlamydia trachomatis-containing vacuole serves as deubiquitination platform to stabilize Mcl-1 and to interfere with host defense. Elife 6.

95. Auer D, Hügelschäffer SD, Fischer AB, Rudel T. 2019. The chlamydial deubiquitinase Cdu1 supports recruitment of Golgi vesicles to the inclusion. Cellular Microbiology 0:e13136.

96. Wang X, Hybiske K, Stephens RS. 2018. Direct visualization of the expression and localization of chlamydial effector proteins within infected host cells. Pathog Dis 76.

97. Vromman F, Perrinet S, Gehre L, Subtil A. 2016. The DUF582 Proteins of Chlamydia trachomatis Bind to Components of the ESCRT Machinery, Which Is Dispensable for Bacterial Growth In vitro. Frontiers in cellular and infection microbiology 6:123-123.

98. Pais SV, Key CE, Borges V, Pereira IS, Gomes JP, Fisher DJ, Mota LJ. 2019. CteG is a Chlamydia trachomatis effector protein that associates with the Golgi complex of infected host cells. Scientific Reports 9:6133.

99. Wolf K, Betts HJ, Chellas-Géry B, Hower S, Linton CN, Fields KA. 2006. Treatment of Chlamydia trachomatis with a small molecule inhibitor of the Yersinia type III secretion system disrupts progression of the chlamydial developmental cycle. Molecular microbiology 61:1543-1555.

100. Triboulet S, Subtil A. 2019. Make It a Sweet Home: Responses of Chlamydia trachomatis to the Challenges of an Intravacuolar Lifestyle. Microbiol Spectr 7.

101. Li Z, Chen C, Chen D, Wu Y, Zhong Y, Zhong G. 2008. Characterization of Fifty Putative Inclusion Membrane Proteins Encoded in the Chlamydia trachomatis Genome. Infection and Immunity 76:2746-2757.

102. Shaw EI, Dooley CA, Fischer ER, Scidmore MA, Fields KA, Hackstadt T. 2000. Three temporal classes of gene expression during the Chlamydia trachomatis developmental cycle. Molecular Microbiology 37:913-925.

103. Dehoux P, Flores R, Dauga C, Zhong G, Subtil A. 2011. Multi-genome identification and characterization of chlamydiae-specific type III secretion substrates: the Inc proteins. BMC Genomics 12:109.

104. Lutter EI, Martens C, Hackstadt T. 2012. Evolution and Conservation of Predicted Inclusion Membrane Proteins in Chlamydiae. Comparative and Functional Genomics 2012:362104.

105. Gauliard E, Ouellette SP, Rueden KJ, Ladant D. 2015. Characterization of interactions between inclusion membrane proteins from Chlamydia trachomatis. Front Cell Infect Microbiol 5:13.

106. Belland RJ, Zhong G, Crane DD, Hogan D, Sturdevant D, Sharma J, Beatty WL, Caldwell HD. 2003. Genomic transcriptional profiling of the developmental cycle of Chlamydia trachomatis. Proceedings of the National Academy of Sciences 100:8478.

107. Rockey DD, Rosquist JL. 1994. Protein antigens of Chlamydia psittaci present in infected cells but not detected in the infectious elementary body. Infect Immun 62:106-12.

108. Rockey DD. 1997. Chlamydia psittaci IncA is phosphorylated by the host cell and is exposed on the cytoplasmic face of the developing inclusion. Molecular microbiology 24:217-228.

109. Johnson CM, Fisher DJ. 2013. Site-Specific, Insertional Inactivation of incA in Chlamydia trachomatis Using a Group II Intron. PLoS ONE 8:e83989.

110. Ronzone E, Paumet F. 2013. Two Coiled-Coil Domains of Chlamydia trachomatis IncA Affect Membrane Fusion Events during Infection. PLoS ONE 8:e69769.

111. Ronzone E, Wesolowski J, Bauler LD, Bhardwaj A, Hackstadt T, Paumet F. 2014. An α-Helical Core Encodes the Dual Functions of the Chlamydial Protein IncA. The Journal of Biological Chemistry 289:33469-33480.

112. Weber MM, Noriea NF, Bauler LD, Lam JL, Sager J, Wesolowski J, Paumet F, Hackstadt T. 2016. A Functional Core of IncA Is Required for Chlamydia trachomatis Inclusion Fusion. J Bacteriol 198:1347-55.

113. Cingolani G, McCauley M, Lobley A, Bryer AJ, Wesolowski J, Greco DL, Lokareddy RK, Ronzone E, Perilla JR, Paumet F. 2019. Structural basis for the homotypic fusion of chlamydial inclusions by the SNARE-like protein IncA. Nature Communications 10:2747.

114. Mital J, Miller NJ, Fischer ER, Hackstadt T. 2010. Specific chlamydial inclusion membrane proteins associate with active Src family kinases in microdomains that interact with the host microtubule network. Cellular microbiology 12:1235-1249.

115. Olson MG, Widner RE, Jorgenson LM, Lawrence A, Lagundzin D, Woods NT, Ouellette SP, Rucks EA. 2019. Proximity Labeling to Map Host-Pathogen Interactions at the Membrane of a Bacteria Containing Vacuole in Chlamydia trachomatis Infected Human Cells. Infect Immun 87.

116. Wang Y, Kahane S, Cutcliffe LT, Skilton RJ, Lambden PR, Clarke IN. 2011. Development of a transformation system for Chlamydia trachomatis: restoration of glycogen biosynthesis by acquisition of a plasmid shuttle vector. PLoS Pathog 7:e1002258.

117. Shaw JH, Key CE, Snider TA, Sah P, Shaw EI, Fisher DJ, Lutter EI. 2018. Genetic Inactivation of Chlamydia trachomatis Inclusion Membrane Protein CT228 Alters MYPT1 Recruitment, Extrusion Production, and Longevity of Infection. Frontiers in Cellular and Infection Microbiology 8.

118. McKuen MJ, Mueller KE, Bae YS, Fields KA. 2017. Fluorescence-Reported Allelic Exchange Mutagenesis Reveals a Role for Chlamydia trachomatis TmeA in Invasion That Is Independent of Host AHNAK. Infection and immunity 85:e00640-17.

119. Mueller KE, Wolf, K., Fields K. A. . 2016. Gene Deletion by Fluorescence-Reported Allelic Exchange Mutagenesis in Chlamydia trachomatis. mBio Jan 19;7(1):e01817-15. doi: 10.1128/mBio.01817-15.

120. Mueller KE, Wolf K, Fields KA. 2017. Chlamydia trachomatis transformation and allelic exchange mutagenesis. Current protocols in microbiology 45:11A.3.1-11A.3.15.

121. Ouellette SP. 2018. Feasibility of a Conditional Knockout System for Chlamydia Based on CRISPR Interference. Frontiers in Cellular and Infection Microbiology 8:59.

122. Mirrashidi KM, Elwell CA, Verschueren E, Johnson JR, Frando A, Von Dollen J, Rosenberg O, Gulbahce N, Jang G, Johnson T, Jager S, Gopalakrishnan AM, Sherry J, Dunn JD, Olive A, Penn B, Shales M, Starnbach MN, Derre I, Valdivia R, Krogan NJ, Engel J. 2015. Global Mapping of the Inc-Human Interactome Reveals that Retromer Restricts Chlamydia Infection. Cell host & microbe 18:109-121.

123. Mital J, Lutter EI, Barger AC, Dooley CA, Hackstadt T. 2015. Chlamydia trachomatis inclusion membrane protein CT850 interacts with the dynein light chain DYNLT1 (Tctex1). Biochemical and biophysical research communications 462:165-170.

124. Ouellette SP, Dorsey FC, Moshiach S, Cleveland JL, Carabeo RA. 2011. Chlamydia Species-Dependent Differences in the Growth Requirement for Lysosomes. PLOS ONE 6:e16783.

125. Banhart S, Schäfer EK, Gensch J-M, Heuer D. 2019. Sphingolipid Metabolism and Transport in Chlamydia trachomatis and Chlamydia psittaci Infections. Frontiers in cell and developmental biology 7:223-223.

126. Elwell CA, Jiang S, Kim JH, Lee A, Wittmann T, Hanada K, Melancon P, Engel JN. 2011. Chlamydia trachomatis co-opts GBF1 and CERT to acquire host sphingomyelin for distinct roles during intracellular development. PLoS Pathog 7:e1002198.

127. Sixt BS, Bastidas RJ, Finethy R, Baxter RM, Carpenter VK, Kroemer G, Coers J, Valdivia RH. 2017. The Chlamydia trachomatis Inclusion Membrane Protein CpoS Counteracts STING-Mediated Cellular Surveillance and Suicide Programs. Cell host & microbe 21:113-121.

128. Wesolowski J, Weber MM, Nawrotek A, Dooley CA, Calderon M, St Croix CM, Hackstadt T, Cherfils J, Paumet F. 2017. Chlamydia Hijacks ARF GTPases To Coordinate Microtubule Posttranslational Modifications and Golgi Complex Positioning. MBio 8.

129. Wesolowski J, Paumet F. 2017. Taking control: reorganization of the host cytoskeleton by Chlamydia. F1000Research 6:2058.

130. Kokes M, Dunn Joe D, Granek Joshua A, Nguyen Bidong D, Barker Jeffrey R, Valdivia Raphael H, Bastidas Robert J. 2015. Integrating Chemical Mutagenesis and Whole-Genome Sequencing as a Platform for Forward and Reverse Genetic Analysis of Chlamydia. Cell Host & Microbe 17:716-725.

131. Clausen JD, Christiansen G, Holst HU, Birkelund S. 1997. Chlamydia trachomatis utilizes the host cell microtubule network during early events of infection. Mol Microbiol 25:441-9.

132. Al-Zeer MA, Al-Younes HM, Kerr M, Abu-Lubad M, Gonzalez E, Brinkmann V, Meyer TF. 2014. Chlamydia trachomatis remodels stable microtubules to coordinate Golgi stack recruitment to the chlamydial inclusion surface. Mol Microbiol 94:1285-97.

133. Almeida F, Luis MP, Pereira IS, Pais SV, Mota LJ. 2018. The Human Centrosomal Protein CCDC146 Binds Chlamydia trachomatis Inclusion

Membrane Protein CT288 and Is Recruited to the Periphery of the Chlamydia-Containing Vacuole. Front Cell Infect Microbiol 8:254.

134. Dumoux M, Menny A, Delacour D, Hayward RD. 2015. A Chlamydia effector recruits CEP170 to reprogram host microtubule organization. Journal of cell science 128:3420-3434.

135. Sakamoto T, Uezu A, Kawauchi S, Kuramoto T, Makino K, Umeda K, Araki N, Baba H, Nakanishi H. 2008. Mass spectrometric analysis of microtubule co-sedimented proteins from rat brain. Genes to Cells 13:295-312.

136. Rejman Lipinski A, Heymann J, Meissner C, Karlas A, Brinkmann V, Meyer TF, Heuer D. 2009. Rab6 and Rab11 regulate Chlamydia trachomatis development and golgin-84-dependent Golgi fragmentation. PLoS pathogens 5:e1000615-e1000615.

137. Stanhope R, Flora E, Bayne C, Derré I. 2017. IncV, a FFAT motif-containing Chlamydia protein, tethers the endoplasmic reticulum to the pathogen-containing vacuole. Proceedings of the National Academy of Sciences 114:12039-12044.

138. Radhakrishnan GK, Splitter GA. 2012. Modulation of host microtubule dynamics by pathogenic bacteria. Biomolecular concepts 3:571-580.

139. Krachler AM, Woolery AR, Orth K. 2011. Manipulation of kinase signaling by bacterial pathogens. The Journal of cell biology 195:1083-1092.

140. Nguyen PH, Lutter EI, Hackstadt T. 2018. Chlamydia trachomatis inclusion membrane protein MrcA interacts with the inositol 1,4,5-trisphosphate receptor type 3 (ITPR3) to regulate extrusion formation. PLoS Pathog 14:e1006911.

141. Agaisse H, Derre I. 2015. STIM1 Is a Novel Component of ER-Chlamydia trachomatis Inclusion Membrane Contact Sites. PLoS One 10:e0125671.

142. Scidmore MA, Hackstadt T. 2001. Mammalian 14-3-3β associates with the Chlamydia trachomatis inclusion membrane via its interaction with IncG. Molecular Microbiology 39:1638-1650.

143. Verbeke P, Welter-Stahl L, Ying S, Hansen J, Häcker G, Darville T, Ojcius DM. 2006. Recruitment of BAD by the Chlamydia trachomatis Vacuole Correlates with Host-Cell Survival. PLOS Pathogens 2:e45.

144. Paumet F, Wesolowski J, Garcia-Diaz A, Delevoye C, Aulner N, Shuman HA, Subtil A, Rothman JE. 2009. Intracellular bacteria encode inhibitory SNARE-like proteins. PLoS One 4:e7375.

145. Delevoye C, Nilges M, Dehoux P, Paumet F, Perrinet S, Dautry-Varsat A, Subtil A. 2008. SNARE Protein Mimicry by an Intracellular Bacterium. PLOS Pathogens 4:e1000022.

146. Lucas AL, Ouellette SP, Kabeiseman EJ, Cichos KH, Rucks EA. 2015. The trans-Golgi SNARE syntaxin 10 is required for optimal development of Chlamydia trachomatis. Front Cell Infect Microbiol 5:68.

147. Hong W, Lev S. 2014. Tethering the assembly of SNARE complexes. Trends in Cell Biology 24:35-43.

148. Kabeiseman EJ, Cichos K, Hackstadt T, Lucas A, Moore ER. 2013. Vesicle-associated membrane protein 4 and syntaxin 6 interactions at the chlamydial inclusion. Infection and immunity 81:3326-3337.

149. Moore ER, Mead DJ, Dooley CA, Sager J, Hackstadt T. 2011. The trans-Golgi SNARE syntaxin 6 is recruited to the chlamydial inclusion membrane. Microbiology 157:830-8.

150. Moorhead AR, Rzomp KA, Scidmore MA. 2007. The Rab6 effector Bicaudal D1 associates with Chlamydia trachomatis inclusions in a biovar-specific manner. Infection and immunity 75:781-791.

151. Rzomp KA, Moorhead AR, Scidmore MA. 2006. The GTPase Rab4 Interacts with Chlamydia trachomatis Inclusion Membrane Protein CT229. Infection and Immunity 74:5362.

152. Damiani MT, Gambarte Tudela J, Capmany A. 2014. Targeting eukaryotic Rab proteins: a smart strategy for chlamydial survival and replication. Cell Microbiol 16:1329-38.

153. Leiva N, Capmany A, Damiani MT. 2013. Rab11-Family of Interacting Protein 2 associates with chlamydial inclusions through its Rab-binding domain and promotes bacterial multiplication. Cellular Microbiology 15:114-129.

154. Capmany A, Leiva N, Damiani MT. 2011. Golgi-associated Rab14, a new regulator for Chlamydia trachomatis infection outcome. Commun Integr Biol 4:590-3.

155. Gambarte Tudela J, Capmany A, Romao M, Quintero C, Miserey-Lenkei S, Raposo G, Goud B, Damiani MT. 2015. The late endocytic Rab39a GTPase regulates the interaction between multivesicular bodies and chlamydial inclusions. Journal of Cell Science 128:3068.

156. Rzomp KA, Scholtes LD, Briggs BJ, Whittaker GR, Scidmore MA. 2003. Rab GTPases are recruited to chlamydial inclusions in both a species-dependent and species-independent manner. Infect Immun 71:5855-70.

157. Faris R, Merling M, Andersen SE, Dooley CA, Hackstadt T, Weber MM. 2019. Chlamydia trachomatis CT229 Subverts Rab GTPase-Dependent CCV Trafficking Pathways to Promote Chlamydial Infection. Cell Rep 26:3380-3390.e5.

158. Dobbs N, Burnaevskiy N, Chen D, Gonugunta VK, Alto NM, Yan N. 2015. STING Activation by Translocation from the ER Is Associated with Infection and Autoinflammatory Disease. Cell host & microbe 18:157-168.

159. Gonugunta VK, Sakai T, Pokatayev V, Yang K, Wu J, Dobbs N, Yan N. 2017. Trafficking-Mediated STING Degradation Requires Sorting to Acidified Endolysosomes and Can Be Targeted to Enhance Anti-tumor Response. Cell Rep 21:3234-3242.

160. Moorhead AM, Jung J-Y, Smirnov A, Kaufer S, Scidmore MA. 2010. Multiple Host Proteins That Function in Phosphatidylinositol-4-Phosphate Metabolism Are Recruited to the Chlamydial Inclusion. Infection and Immunity 78:1990.

161. Paul B, Kim HS, Kerr MC, Huston WM, Teasdale RD, Collins BM. 2017. Structural basis for the hijacking of endosomal sorting nexin proteins by Chlamydia trachomatis. Elife 6.

162. van Ooij C, Apodaca G, Engel J. 1997. Characterization of the Chlamydia trachomatis vacuole and its interaction with the host endocytic pathway in HeLa cells. Infection and immunity 65:758-766.

163. Karimova G, Pidoux J, Ullmann A, Ladant D. 1998. A bacterial two-hybrid system based on a reconstituted signal transduction pathway. Proc Natl Acad Sci U S A 95:5752-6.

164. Karimova G, Ullmann A, Ladant D. 2000. A bacterial two-hybrid system that exploits a cAMP signaling cascade in Escherichia coli. Methods Enzymol 328:59-73.

165. Ouellette SP, Karimova G, Davi M, Ladant D. 2017. Analysis of Membrane Protein Interactions with a Bacterial Adenylate Cyclase-Based Two-Hybrid (BACTH) Technique. Curr Protoc Mol Biol 118:20.12.1-20.12.24.

166. Suchland RJ, Rockey DD, Bannantine JP, Stamm WE. 2000. Isolates of Chlamydia trachomatis That Occupy Nonfusogenic Inclusions Lack IncA, a Protein Localized to the Inclusion Membrane. Infection and Immunity 68:360-367.

167. Roux KJ, Kim DI, Raida M, Burke B. 2012. A promiscuous biotin ligase fusion protein identifies proximal and interacting proteins in mammalian cells. J Cell Biol 196:801-10.

168. Martell JD, Deerinck TJ, Sancak Y, Poulos TL, Mootha VK, Sosinsky GE, Ellisman MH, Ting AY. 2012. Engineered ascorbate peroxidase as a genetically encoded reporter for electron microscopy. Nat Biotechnol 30:1143-8.

169. Olson MG, Jorgenson LM, Widner RE, Rucks EA. 2019. Proximity Labeling of the Chlamydia trachomatis Inclusion Membrane. Methods Mol Biol 2042:245-278.

170. Dickinson MS, Anderson LN, Webb-Robertson B-JM, Hansen JR, Smith RD, Wright AT, Hybiske K. 2019. Proximity-dependent proteomics of the Chlamydia trachomatis inclusion membrane reveals functional interactions with endoplasmic reticulum exit sites. PLOS Pathogens 15:e1007698.

171. Aeberhard L, Banhart S, Fischer M, Jehmlich N, Rose L, Koch S, Laue M, Renard BY, Schmidt F, Heuer D. 2015. The Proteome of the Isolated Chlamydia trachomatis Containing Vacuole Reveals a Complex Trafficking Platform Enriched for Retromer Components. PLOS Pathogens 11:e1004883.

172. Muschiol S, Bailey L, Gylfe A, Sundin C, Hultenby K, Bergstrom S, Elofsson M, Wolf-Watz H, Normark S, Henriques-Normark B. 2006. A small-molecule inhibitor of type III secretion inhibits different stages of the infectious cycle of Chlamydia trachomatis. Proc Natl Acad Sci U S A 103:14566-71.

173. Saka HA, Thompson JW, Chen Y-S, Kumar Y, Dubois LG, Moseley MA, Valdivia RH. 2011. Quantitative proteomics reveals metabolic and pathogenic properties of *Chlamydia trachomatis* developmental forms. Mol Microbiol 82:1185-1203.

174. Weber MM, Faris R. 2018. Subversion of the Endocytic and Secretory Pathways by Bacterial Effector Proteins. Front Cell Dev Biol 6:1.

175. Lane MD, Rominger KL, Young DL, Lynen F. 1964. THE ENZYMATIC SYNTHESIS OF HOLOTRANSCARBOXYLASE FROM APOTRANSCARBOXYLASE AND (+)-BIOTIN. II. INVESTIGATION OF THE REACTION MECHANISM. J Biol Chem 239:2865-71.

176. Beckett D, Kovaleva E, Schatz PJ. 1999. A minimal peptide substrate in biotin holoenzyme synthetase-catalyzed biotinylation. Protein Sci 8:921-9.

177. Kwon K, Beckett D. 2000. Function of a conserved sequence motif in biotin holoenzyme synthetases. Protein Sci 9:1530-9.

178. Choi-Rhee E, Schulman H, Cronan JE. 2004. Promiscuous protein biotinylation by Escherichia coli biotin protein ligase. Protein Sci 13:3043-50.

179. Green NM. 1963. AVIDIN. 1. THE USE OF (14-C)BIOTIN FOR KINETIC STUDIES AND FOR ASSAY. Biochem J 89:585-91.

180. Firat-Karalar EN, Rauniyar N, Yates JR, 3rd, Stearns T. 2014. Proximity interactions among centrosome components identify regulators of centriole duplication. Curr Biol 24:664-70.

181. Firat-Karalar EN, Stearns T. 2015. Probing mammalian centrosome structure using BioID proximity-dependent biotinylation. Methods Cell Biol 129:153-70.

182. Bareja A, Hodgkinson CP, Soderblom E, Waitt G, Dzau VJ. 2018. The proximity-labeling technique BioID identifies sorting nexin 6 as a member of the insulin-like growth factor 1 (IGF1)-IGF1 receptor pathway. J Biol Chem 293:6449-6459.

183. Mousnier A, Schroeder GN, Stoneham CA, So EC, Garnett JA, Yu L, Matthews SJ, Choudhary JS, Hartland EL, Frankel G. 2014. A new method to determine in vivo interactomes reveals binding of the Legionella pneumophila effector PieE to multiple rab GTPases. MBio 5.

184. Chen AL, Kim EW, Toh JY, Vashisht AA, Rashoff AQ, Van C, Huang AS, Moon AS, Bell HN, Bentolila LA, Wohlschlegel JA, Bradley PJ. 2015. Novel components of the Toxoplasma inner membrane complex revealed by BioID. MBio 6:e02357-14.

185. Morriswood B, Havlicek K, Demmel L, Yavuz S, Sealey-Cardona M, Vidilaseris K, Anrather D, Kostan J, Djinovic-Carugo K, Roux KJ, Warren G. 2013. Novel bilobe components in Trypanosoma brucei identified using proximity-dependent biotinylation. Eukaryot Cell 12:356-67.

186. Schnider CB, Bausch-Fluck D, Bruhlmann F, Heussler VT, Burda PC. 2018. BioID Reveals Novel Proteins of the Plasmodium Parasitophorous Vacuole Membrane. mSphere 3.

187. Schopp IM, Bethune J. 2018. Split-BioID - Proteomic Analysis of Context-specific Protein Complexes in Their Native Cellular Environment. J Vis Exp doi:10.3791/57479.

188. Chojnowski A, Sobota RM, Ong PF, Xie W, Wong X, Dreesen O, Burke B, Stewart CL. 2018. 2C-BioID: An Advanced Two Component BioID System for Precision Mapping of Protein Interactomes. iScience 10:40-52.

189. Lam SS, Martell JD, Kamer KJ, Deerinck TJ, Ellisman MH, Mootha VK, Ting AY. 2015. Directed evolution of APEX2 for electron microscopy and proximity labeling. Nat Meth 12:51-54.

190. Connolly CN, Futter CE, Gibson A, Hopkins CR, Cutler DF. 1994. Transport into and out of the Golgi complex studied by transfecting cells with cDNAs encoding horseradish peroxidase. J Cell Biol 127:641-52.

191. Li J, Wang Y, Chiu SL, Cline HT. 2010. Membrane targeted horseradish peroxidase as a marker for correlative fluorescence and electron microscopy studies. Front Neural Circuits 4:6.

192. Hopkins C, Gibson A, Stinchcombe J, Futter C. 2000. Chimeric molecules employing horseradish peroxidase as reporter enzyme for protein localization in the electron microscope. Methods Enzymol 327:35-45.

193. Rhee HW, Zou P, Udeshi ND, Martell JD, Mootha VK, Carr SA, Ting AY. 2013. Proteomic mapping of mitochondria in living cells via spatially restricted enzymatic tagging. Science 339:1328-1331.

194. Mandelman D, Schwarz FP, Li H, Poulos TL. 1998. The role of quaternary interactions on the stability and activity of ascorbate peroxidase. Protein Sci 7:2089-98.

195. Khan AA, Quigley JG. 2011. Control of intracellular heme levels: heme transporters and heme oxygenases. Biochimica et biophysica acta 1813:668-682.

196. Lee S-Y, Kang M-G, Park J-S, Lee G, Ting Alice Y, Rhee H-W. 2016. APEX Fingerprinting Reveals the Subcellular Localization of Proteins of Interest. Cell Reports 15:1837-1847.

197. Lobingier BT, Huttenhain R, Eichel K, Miller KB, Ting AY, von Zastrow M, Krogan NJ. 2017. An Approach to Spatiotemporally Resolve Protein Interaction Networks in Living Cells. Cell 169:350-360.e12.

198. Santin YG, Doan T, Lebrun R, Espinosa L, Journet L, Cascales E. 2018. In vivo TssA proximity labelling during type VI secretion biogenesis reveals TagA as a protein that stops and holds the sheath. Nature Microbiology doi:10.1038/s41564-018-0234-3.

199. Kabeiseman EJ, Cichos KH, Moore ER. 2014. The eukaryotic signal sequence, YGRL, targets the chlamydial inclusion. Frontiers in cellular and infection microbiology 4:129-129.

200. Watson RT, Pessin JE. 2000. Functional cooperation of two independent targeting domains in syntaxin 6 is required for its efficient localization in the *trans*-golgi network of 3T3L1 adipocytes. J Biol Chem 275:1261-1268.

201. Mojica SA, Hovis KM, Frieman MB, Tran B, Hsia R-c, Ravel J, Jenkins-Houk C, Wilson KL, Bavoil PM. 2015. SINC, a type III secreted protein of Chlamydia psittaci, targets the inner nuclear membrane of infected cells and uninfected neighbors. Molecular biology of the cell 26:1918-1934.

202. Fields KA, McCormack R, de Armas LR, Podack ER. 2013. Perforin-2 restricts growth of Chlamydia trachomatis in macrophages. Infect Immun 81:3045-54.

203. Papageorgiou DN, Demmers J, Strouboulis J. 2013. NP-40 reduces contamination by endogenous biotinylated carboxylases during purification of biotin tagged nuclear proteins. Protein Expr Purif 89:80-3.

204. Hollinshead M, Sanderson J, Vaux DJ. 1997. Anti-biotin antibodies offer superior organelle-specific labeling of mitochondria over avidin or streptavidin. J Histochem Cytochem 45:1053-7.

205. Rodriguez P, Braun H, Kolodziej KE, de Boer E, Campbell J, Bonte E, Grosveld F, Philipsen S, Strouboulis J. 2006. Isolation of Transcription Factor Complexes by In Vivo Biotinylation Tagging and Direct Binding to Streptavidin Beads, p 305-323. *In* Bina M (ed), Gene Mapping, Discovery, and Expression: Methods and Protocols doi:10.1385/1-59745-097-9:305. Humana Press, Totowa, NJ.

206. de Boer E, Rodriguez P, Bonte E, Krijgsveld J, Katsantoni E, Heck A, Grosveld F, Strouboulis J. 2003. Efficient biotinylation and single-step purification of tagged transcription factors in mammalian cells and transgenic mice. Proc Natl Acad Sci U S A 100:7480-5.

207. Choi H, Larsen B, Lin Z-Y, Breitkreutz A, Mellacheruvu D, Fermin D, Qin ZS, Tyers M, Gingras A-C, Nesvizhskii AI. 2011. SAINT: Probabilistic Scoring of Affinity Purification - Mass Spectrometry Data. Nature methods 8:70-73.

208. Webb-Robertson BJ, Matzke MM, Datta S, Payne SH, Kang J, Bramer LM, Nicora CD, Shukla AK, Metz TO, Rodland KD, Smith RD, Tardiff MF, McDermott JE, Pounds JG, Waters KM. 2014. Bayesian proteoform modeling improves protein quantification of global proteomic measurements. Mol Cell Proteomics 13:3639-46.

209. Martell JD, Deerinck TJ, Lam SS, Ellisman MH, Ting AY. 2017. Electron microscopy using the genetically encoded APEX2 tag in cultured mammalian cells. Nature Protocols 12:1792.

210. Wickstrum J, Sammons LR, Restivo KN, Hefty PS. 2013. Conditional gene expression in Chlamydia trachomatis using the tet system. PLoS One 8:e76743.

211. Mueller KE, Fields KA. 2015. Application of beta-lactamase reporter fusions as an indicator of effector protein secretion during infections with the obligate intracellular pathogen Chlamydia trachomatis. PLoS One 10:e0135295.

212. Willingham MC. 1999. Fluorescence Labeling of Surface Antigens of Attached or Suspended Tissue-Culture Cells, p 113-119. *In* Javois LC (ed),

Immunocytochemical Methods and Protocols doi:10.1385/1-59259-213-9:113. Humana Press, Totowa, NJ.

213. Kurien BT, Scofield RH. 2015. Western blotting: an introduction. Methods Mol Biol 1312:17-30.

214. Kokes M, Valdivia RH. 2015. Differential Translocation of Host Cellular Materials into the Chlamydia trachomatis Inclusion Lumen during Chemical Fixation. PLoS One 10:e0139153.

215. Caldwell HD, Kromhout J, Schachter J. 1981. Purification and partial characterization of the major outer membrane protein of Chlamydia trachomatis. Infect Immun 31:1161-76.

216. Scidmore MA. 2005. Cultivation and Laboratory Maintenance of Chlamydia trachomatis. Curr Protoc Microbiol Chapter 11:Unit 11A.1.

217. Furness G, Graham DM, Reeve P. 1960. The titration of trachoma and inclusion blennorrhoea viruses in cell cultures. J Gen Microbiol 23:613-9.

218. Matsumoto A, Izutsu H, Miyashita N, Ohuchi M. 1998. Plaque formation by and plaque cloning of Chlamydia trachomatis biovar trachoma. Journal of clinical microbiology 36:3013-3019.

219. Han Y, Derré I. 2017. A Co-infection Model System and the Use of Chimeric Proteins to Study Chlamydia Inclusion Proteins Interaction. Frontiers in cellular and infection microbiology 7:79-79.

220. Lotia S, Montojo J, Dong Y, Bader GD, Pico AR. 2013. Cytoscape app store. Bioinformatics 29:1350-1.

221. Ouellette SP, Rueden KJ, Gauliard E, Persons L, de Boer PA, Ladant D. 2014. Analysis of MreB interactors in Chlamydia reveals a RodZ homolog but fails to detect an interaction with MraY. Front Microbiol 5:279.

222. Ouellette SP, Rueden KJ, AbdelRahman YM, Cox JV, Belland RJ. 2015. Identification and Partial Characterization of Potential FtsL and FtsQ Homologs of Chlamydia. Front Microbiol 6:1264.

223. Olson MG, Goldammer M, Gauliard E, Ladant D, Ouellette SP. 2018. A Bacterial Adenylate Cyclase-Based Two-Hybrid System Compatible with Gateway® Cloning, p 75-96. *In* Oñate-Sánchez L (ed), Two-Hybrid Systems: Methods and Protocols doi:10.1007/978-1-4939-7871-7_6. Springer New York, New York, NY.

224. Athappilly FK, Hendrickson WA. 1995. Structure of the biotinyl domain of acetyl-coenzyme A carboxylase determined by MAD phasing. Structure 3:1407-1419.

225. Fisher DJ, Fernández RE, Adams NE, Maurelli AT. 2012. Uptake of Biotin by Chlamydia Spp. through the Use of a Bacterial Transporter (BioY) and a Host-Cell Transporter (SMVT). PLoS ONE 7:e46052.

226. Swaney DL, Wenger CD, Coon JJ. 2010. Value of using multiple proteases for large-scale mass spectrometry-based proteomics. Journal of proteome research 9:1323-1329.

227. Al-Younes HM, Al-Zeer MA, Khalil H, Gussmann J, Karlas A, Machuy N, Brinkmann V, Braun PR, Meyer TF. 2011. Autophagy-independent function of MAP-LC3 during intracellular propagation of Chlamydia trachomatis. Autophagy 7:814-28.

228. Dai P, Jeong SY, Yu Y, Leng T, Wu W, Xie L, Chen X. 2009. Modulation of TLR Signaling by Multiple MyD88-Interacting Partners Including Leucine-Rich Repeat Fli-I-Interacting Proteins. The Journal of Immunology 182:3450.

229. Yang P, An H, Liu X, Wen M, Zheng Y, Rui Y, Cao X. 2010. The cytosolic nucleic acid sensor LRRFIP1 mediates the production of type I interferon via a beta-catenin-dependent pathway. Nat Immunol 11:487-94.

230. Bagashev A, Fitzgerald MC, LaRosa DF, Rose PP, Cherry S, Johnson AC, Sullivan KE. 2010. Leucine-Rich Repeat (in Flightless I) Interacting Protein-1 Regulates a Rapid Type I Interferon Response. Journal of Interferon & Cytokine Research 30:843-852.

231. Nguyen JB, Modis Y. 2013. Crystal structure of the dimeric coiled-coil domain of the cytosolic nucleic acid sensor LRRFIP1. Journal of Structural Biology 181:82-88.

232. Labbe P, Faure E, Lecointe S, Le Scouarnec S, Kyndt F, Marrec M, Le Tourneau T, Offmann B, Duplaa C, Zaffran S, Schott JJ, Merot J. 2017. The alternatively spliced LRRFIP1 Isoform-1 is a key regulator of the Wnt/beta-catenin transcription pathway. Biochim Biophys Acta 1864:1142-1152.

233. Ivashkiv LB, Donlin LT. 2014. Regulation of type I interferon responses. Nature reviews Immunology 14:36-49.

234. Fong KS, de Couet HG. 1999. Novel proteins interacting with the leucine-rich repeat domain of human flightless-I identified by the yeast two-hybrid system. Genomics 58:146-57.

235. Lee Y-H, Stallcup MR. 2006. Interplay of Fli-I and FLAP1 for regulation of beta-catenin dependent transcription. Nucleic acids research 34:5052-5059.

236. Battesti A, Bouveret E. 2012. The bacterial two-hybrid system based on adenylate cyclase reconstitution in Escherichia coli. Methods 58:325-34.

237. Karimova G, Dautin N, Ladant D. 2005. Interaction network among Escherichia coli membrane proteins involved in cell division as revealed by bacterial two-hybrid analysis. J Bacteriol 187:2233-43.

238. Alzhanov DT, Weeks SK, Burnett JR, Rockey DD. 2009. Cytokinesis is blocked in mammalian cells transfected with Chlamydia trachomatis gene CT223. BMC microbiology 9:2-2.

239. Suchland RJ, Rockey DD, Weeks SK, Alzhanov DT, Stamm WE. 2005. Development of Secondary Inclusions in Cells Infected by Chlamydia trachomatis. Infection and Immunity 73:3954-3962.

240. Mital J, Miller NJ, Dorward DW, Dooley CA, Hackstadt T. 2013. Role for Chlamydial Inclusion Membrane Proteins in Inclusion Membrane Structure and Biogenesis. PLOS ONE 8:e63426.

241. Heinecke NL, Pratt BS, Vaisar T, Becker L. 2010. PepC: proteomics software for identifying differentially expressed proteins based on spectral counting. Bioinformatics (Oxford, England) 26:1574-1575.

242. Skarra DV, Goudreault M, Choi H, Mullin M, Nesvizhskii AI, Gingras A-C, Honkanen RE. 2011. Label-free quantitative proteomics and SAINT analysis

enable interactome mapping for the human Ser/Thr protein phosphatase 5. PROTEOMICS 11:1508-1516.

243. Meysman P, Titeca K, Eyckerman S, Tavernier J, Goethals B, Martens L, Valkenborg D, Laukens K. 2017. Protein complex analysis: From raw protein lists to protein interaction networks. Mass Spectrometry Reviews 36:600-614.

244. Chin E, Kirker K, Zuck M, James G, Hybiske K. 2012. Actin recruitment to the Chlamydia inclusion is spatiotemporally regulated by a mechanism that requires host and bacterial factors. PloS one 7:e46949-e46949.

245. Volceanov L, Herbst K, Biniossek M, Schilling O, Haller D, Nölke T, Subbarayal P, Rudel T, Zieger B, Häcker G. 2014. Septins Arrange F-Actin-Containing Fibers on the Chlamydia trachomatis Inclusion and Are Required for Normal Release of the Inclusion by Extrusion. mBio 5:e01802-14.

246. Gunderson FF, Cianciotto NP. 2013. The CRISPR-associated gene cas2 of Legionella pneumophila is required for intracellular infection of amoebae. MBio 4:e00074-13.

247. Ouellette SP, Gauliard E, Antosova Z, Ladant D. 2014. A Gateway((R)) -compatible bacterial adenylate cyclase-based two-hybrid system. Environ Microbiol Rep 6:259-67.

248. Oliveros JC. 2007-2015. Venny. An interactive tool for comparing lists with Venn's diagrams. https://bioinfogp.cnb.csic.es/tools/venny/index.html. Accessed

249. Mellacheruvu D, Wright Z, Couzens AL, Lambert JP, St-Denis NA, Li T, Miteva YV, Hauri S, Sardiu ME, Low TY, Halim VA, Bagshaw RD, Hubner NC, Al-Hakim

A, Bouchard A, Faubert D, Fermin D, Dunham WH, Goudreault M, Lin ZY, Badillo BG, Pawson T, Durocher D, Coulombe B, Aebersold R, Superti-Furga G, Colinge J, Heck AJ, Choi H, Gstaiger M, Mohammed S, Cristea IM, Bennett KL, Washburn MP, Raught B, Ewing RM, Gingras AC, Nesvizhskii AI. 2013. The CRAPome: a contaminant repository for affinity purification-mass spectrometry data. Nat Methods 10:730-6.

250. Wang CLA, Coluccio LM. 2010. New insights into the regulation of the actin cytoskeleton by tropomyosin. International review of cell and molecular biology 281:91-128.

251. Pathan-Chhatbar S, Taft MH, Reindl T, Hundt N, Latham SL, Manstein DJ. 2018. Three mammalian tropomyosin isoforms have different regulatory effects on nonmuscle myosin-2B and filamentous β-actin in vitro. The Journal of biological chemistry 293:863-875.

252. Fawaz FS, van Ooij C, Homola E, Mutka SC, Engel JN. 1997. Infection with Chlamydia trachomatis alters the tyrosine phosphorylation and/or localization of several host cell proteins including cortactin. Infect Immun 65:5301-8.

253. Gupta N, Pevzner PA. 2009. False discovery rates of protein identifications: a strike against the two-peptide rule. Journal of proteome research 8:4173-4181.

254. Bagag A, Jault J-M, Sidahmed-Adrar N, Réfrégiers M, Giuliani A, Le Naour F. 2013. Characterization of Hydrophobic Peptides in the Presence of Detergent by Photoionization Mass Spectrometry. PLOS ONE 8:e79033.

255. Zakharov VV, Mosevitsky MI. 2010. Oligomeric structure of brain abundant proteins GAP-43 and BASP1. Journal of Structural Biology 170:470-483.

256. Laux T, Fukami K, Thelen M, Golub T, Frey D, Caroni P. 2000. GAP43, MARCKS, and CAP23 modulate PI(4,5)P(2) at plasmalemmal rafts, and regulate cell cortex actin dynamics through a common mechanism. The Journal of cell biology 149:1455-1472.

257. Rivera LE, Colon K, Cantres-Rosario YM, Zenon FM, Melendez LM. 2014. Macrophage derived cystatin B/cathepsin B in HIV replication and neuropathogenesis. Current HIV research 12:111-120.

258. Hartl M, Schneider R. 2019. A Unique Family of Neuronal Signaling Proteins Implicated in Oncogenesis and Tumor Suppression. Frontiers in Oncology 9.

259. Sah P, Nelson NH, Shaw JH, Lutter EI. 2019. Chlamydia trachomatis recruits protein kinase C during infection. Pathogens and Disease 77.

260. Hahn Y, Bera TK, Pastan IH, Lee B. 2006. Duplication and extensive remodeling shaped POTE family genes encoding proteins containing ankyrin repeat and coiled coil domains. Gene 366:238-245.

261. Mosavi LK, Cammett TJ, Desrosiers DC, Peng Z-y. 2004. The ankyrin repeat as molecular architecture for protein recognition. Protein Science 13:1435-1448.

262. Pennington KL, Chan TY, Torres MP, Andersen JL. 2018. The dynamic and stress-adaptive signaling hub of 14-3-3: emerging mechanisms of regulation and context-dependent protein–protein interactions. Oncogene 37:5587-5604.

263. Ilari A, Fiorillo A, Poser E, Lalioti VS, Sundell GN, Ivarsson Y, Genovese I, Colotti G. 2015. Structural basis of Sorcin-mediated calcium-dependent signal transduction. Scientific Reports 5:16828.

264. Lalioti VS, Ilari A, O'Connell DJ, Poser E, Sandoval IV, Colotti G. 2014. Sorcin Links Calcium Signaling to Vesicle Trafficking, Regulates Polo-Like Kinase 1 and Is Necessary for Mitosis. PLOS ONE 9:e85438.

265. Hill ZB, Pollock SB, Zhuang M, Wells JA. 2016. Direct Proximity Tagging of Small Molecule Protein Targets Using an Engineered NEDD8 Ligase. J Am Chem Soc 138:13123-13126.

266. Liu Q, Zheng J, Sun W, Huo Y, Zhang L, Hao P, Wang H, Zhuang M. 2018. A proximity-tagging system to identify membrane protein-protein interactions. Nat Methods doi:10.1038/s41592-018-0100-5.

267. Diop A, Raoult D, Fournier P-E. 2018. Rickettsial genomics and the paradigm of genome reduction associated with increased virulence. Microbes and Infection 20:401-409.

268. Driscoll TP, Verhoeve VI, Guillotte ML, Lehman SS, Rennoll SA, Beier-Sexton M, Rahman MS, Azad AF, Gillespie JJ. 2017. Wholly Rickettsia! Reconstructed Metabolic Profile of the Quintessential Bacterial Parasite of Eukaryotic Cells. mBio 8.

269. Palmer GH, Noh SM. 2012. Rickettsial entry into host cells: finding the keys to unlock the doors. Infection and immunity 80:3746-3747.

270. Larson CL, Martinez E, Beare PA, Jeffrey B, Heinzen RA, Bonazzi M. 2016. Right on Q: genetics begin to unravel Coxiella burnetii host cell interactions. Future Microbiol 11:919-39.

271. Seshadri R, Paulsen IT, Eisen JA, Read TD, Nelson KE, Nelson WC, Ward NL, Tettelin H, Davidsen TM, Beanan MJ, Deboy RT, Daugherty SC, Brinkac LM, Madupu R, Dodson RJ, Khouri HM, Lee KH, Carty HA, Scanlan D, Heinzen RA, Thompson HA, Samuel JE, Fraser CM, Heidelberg JF. 2003. Complete genome sequence of the Q-fever pathogen Coxiella burnetii. Proc Natl Acad Sci U S A 100:5455-60.

272. Omsland A, Sager J, Nair V, Sturdevant DE, Hackstadt T. 2012. Developmental stage-specific metabolic and transcriptional activity of Chlamydia trachomatis in an axenic medium. Proc Natl Acad Sci U S A 109:19781-5.

273. Fisher DJ, Fernández RE, Maurelli AT. 2013. Chlamydia trachomatis Transports NAD via the Npt1 ATP/ADP Translocase. Journal of Bacteriology 195:3381-3386.

274. Amaro F, Gilbert JA, Owens S, Trimble W, Shuman HA. 2012. Whole-Genome Sequence of the Human Pathogen Legionella pneumophila Serogroup 12 Strain 570-CO-H. Journal of Bacteriology 194:1613.

275. Walker DH, Feng HM, Popov VL. 2001. Rickettsial phospholipase A2 as a pathogenic mechanism in a model of cell injury by typhus and spotted fever group rickettsiae. Am J Trop Med Hyg 65:936-42.

276. Maurin M, Benoliel AM, Bongrand P, Raoult D. 1992. Phagolysosomes of Coxiella burnetii-infected cell lines maintain an acidic pH during persistent infection. Infect Immun 60:5013-6.

277. Newton HJ, Kohler LJ, McDonough JA, Temoche-Diaz M, Crabill E, Hartland EL, Roy CR. 2014. A screen of Coxiella burnetii mutants reveals important roles for

Dot/Icm effectors and host autophagy in vacuole biogenesis. PLoS Pathog 10:e1004286.

278. Beron W, Gutierrez MG, Rabinovitch M, Colombo MI. 2002. Coxiella burnetii localizes in a Rab7-labeled compartment with autophagic characteristics. Infect Immun 70:5816-21.

279. Carey KL, Newton HJ, Luhrmann A, Roy CR. 2011. The Coxiella burnetii Dot/Icm system delivers a unique repertoire of type IV effectors into host cells and is required for intracellular replication. PLoS Pathog 7:e1002056.

280. Rennoll-Bankert KE, Rahman MS, Gillespie JJ, Guillotte ML, Kaur SJ, Lehman SS, Beier-Sexton M, Azad AF. 2015. Which Way In? The RalF Arf-GEF Orchestrates Rickettsia Host Cell Invasion. PLoS Pathog 11:e1005115.

281. Heinzen RA, Hayes SF, Peacock MG, Hackstadt T. 1993. Directional actin polymerization associated with spotted fever group Rickettsia infection of Vero cells. Infect Immun 61:1926-35.

282. Alqassim SS, Lee IG, Dominguez R. 2019. Rickettsia Sca2 Recruits Two Actin Subunits for Nucleation but Lacks WH2 Domains. Biophys J 116:540-550.

283. Lamason RL, Bastounis E, Kafai NM, Serrano R, Del Álamo JC, Theriot JA, Welch MD. 2016. Rickettsia Sca4 Reduces Vinculin-Mediated Intercellular Tension to Promote Spread. Cell 167:670-683.e10.

284. Howe D, Melnicakova J, Barak I, Heinzen RA. 2003. Maturation of the Coxiella burnetii parasitophorous vacuole requires bacterial protein synthesis but not replication. Cell Microbiol 5:469-80.

285. Qiu J, Luo ZQ. 2017. Legionella and Coxiella effectors: strength in diversity and activity. Nat Rev Microbiol 15:591-605.

286. Burstein D, Zusman T, Degtyar E, Viner R, Segal G, Pupko T. 2009. Genome-scale identification of Legionella pneumophila effectors using a machine learning approach. PLoS Pathog 5:e1000508.

287. Kotewicz KM, Ramabhadran V, Sjoblom N, Vogel JP, Haenssler E, Zhang M, Behringer J, Scheck RA, Isberg RR. 2017. A Single Legionella Effector Catalyzes a Multistep Ubiquitination Pathway to Rearrange Tubular Endoplasmic Reticulum for Replication. Cell Host & Microbe 21:169-181.

288. Olson MG, Ouellette SP, Rucks EA. 2020. A meta-analysis of affinity purification-mass spectrometry experimental systems used to identify eukaryotic and chlamydial proteins at the Chlamydia trachomatis inclusion membrane. Journal of Proteomics 212:103595.